National Library of Canada
Bibliothèque nationale du Canada

Canadian Theses Service
Service des thèses canadiennes

Ottawa, Canada
K1A 0N4

NOTICE

The quality of this microform is heavily dependent upon the quality of the original thesis submitted for microfilming. Every effort has been made to ensure the highest quality of reproduction possible.

If pages are missing, contact the university which granted the degree.

Some pages may have indistinct print especially if the original pages were typed with a poor typewriter ribbon or if the university sent us an inferior photocopy.

Reproduction in full or in part of this microform is governed by the Canadian Copyright Act, R.S.C. 1970, c. C-30, and subsequent amendments.

AVIS

La qualité de cette microforme dépend grandement de la qualité de la thèse soumise au microfilmage. Nous avons tout fait pour assurer une qualité supérieure de reproduction.

S'il manque des pages, veuillez communiquer avec l'université qui a conféré le grade.

La qualité d'impression de certaines pages peut laisser à désirer, surtout si les pages originales ont été dactylographiées à l'aide d'un ruban usé ou si l'université nous a fait parvenir une photocopie de qualité inférieure.

La reproduction, même partielle, de cette microforme est soumise à la Loi canadienne sur le droit d'auteur, SRC 1970, c. C-30, et ses amendements subséquents.

Canada

A Deuterium NMR Analysis of the Structure, Order, and Motions of a Diunsaturated Acyl Chain in a Model Bilayer

by

John Edward Baenziger

Thesis submitted to the School of Graduate Studies, University of Ottawa in partial fulfillment of the requirements for the Degree of Doctor of Philosophy in Biochemistry

© John Baenziger, Ottawa, Canada, 1989

National Library of Canada
Bibliothèque nationale du Canada

Canadian Theses Service
Service des thèses canadiennes

Ottawa, Canada
K1A 0N4

The author has granted an irrevocable non-exclusive licence allowing the National Library of Canada to reproduce, loan, distribute or sell copies of his/her thesis by any means and in any form or format, making this thesis available to interested persons.

The author retains ownership of the copyright in his/her thesis. Neither the thesis nor substantial extracts from it may be printed or otherwise reproduced without his/her permission.

L'auteur a accordé une licence irrévocable et non exclusive permettant à la Bibliothèque nationale du Canada de reproduire, prêter, distribuer ou vendre des copies de sa thèse de quelque manière et sous quelque forme que ce soit pour mettre des exemplaires de cette thèse à la disposition des personnes intéressées.

L'auteur conserve la propriété du droit d'auteur qui protège sa thèse. Ni la thèse ni des extraits substantiels de celle-ci ne doivent être imprimés ou autrement reproduits sans son autorisation.

ISBN 0-315-60087-X

Canada

UNIVERSITÉ D'OTTAWA
UNIVERSITY OF OTTAWA

© John Baenziger, Ottawa, 1989

a ma compagne et mon épouse, Donna

What one man can devise, another can understand. All it takes, simply enough, is the ardent desire and firm intention to learn.

Acknowledgements

I would like to thank each of my three co-supervisors Dr. Ian C.P. Smith, Dr. Harold C. Jarrell, and Dr. Robin J. Hill for their help, encouragement and friendship over the past four years. Each has lent their own expertise to the project and has greatly increased the quality of the work described in the following pages. It has been a privilege to work with and learn from such distinguished scientists.

I am also grateful for the opportunity to work along side so many distinguished (and soon to be distinguished) people at the NRCC. Special thanks to Dr. David Siminovitch for informative seminars on deuterium NMR theory and to fellow students Michèle Auger, Beatrice Winsborrow, Laura Stewart, Myrna Monck, Gerald Stelmack, Sylvain Lareau, Eva Princz, Marie-Rose van Calsteron, Paul Berti, and Cindy Hutnick for their friendship and for making my stay at the NRC an exciting and educational experience. I am especially grateful to my lab partner Beatrice Winsborrow for her advice and patience over the last two years.

I would like to thank Jack and Michael Vandenhoff for the manufacture of numerous glass NMR tubes and glass laboratory equipment, Fred Cooper for running samples on the GC-MS and for assistance in the interpretation of the GC-MS results, and Sylvain Lareau for expert advice and assistance with the HPLC. I am also grateful to the Natural Sciences and Engineering Research Council (NSERC) and the Ontario Government (OGS) for financial support, and to the guest-worker program at the National Research Council of Canada for allowing me the privilege of working in the laboratories of the NRCC.

Finally, I would like to acknowledge the support, love, and patience of my wife and family over the past four and one half years.

Abstract

Deuterium NMR spectroscopy has been used extensively to investigate the average structural and associated dynamical properties of saturated and monounsaturated acyl chains in both model and biological membranes. Unfortunately, due to a requirement for specifically labelled (deuteriated) fatty acids and difficulties in the synthesis of labelled polyunsaturated compounds, the technique has not been applied to acyl chains containing more than one double bond. In order to gain a better understanding of the physico-chemical properties and thus the biological function of polyunsaturated acyl chains in membranes, a procedure for the biosynthesis and subsequent isolation of a series of specifically deuteriated *cis, cis*-octadeca-6,9-dienoic acids ($18{:}2^{\Delta 6,9}$, referred to as isolinoleic acid) was developed and the structural and motional properties of the diunsaturated acyl chain in model bilayers were examined by ^{2}H NMR spectroscopy.

An unsaturated fatty acid auxotroph of *Tetrahymena* was grown with an oleic acid supplement under a variety of conditions in order to determine the optimal conditions for uptake and conversion of the supplement into isolinoleic acid. A series of eleven-litre cultures were then supplemented with oleic acid deuteriated at one of ten different positions along the chain and the corresponding deuteriated isolinoleic acids isolated and purified by argentation chromatography and HPLC. GC and TLC showed that each fatty acid preparation is greater than 95 % pure and a GC-MS analysis of the fragmentation pattern of the *O*-(trimethylsilyl) derivative of the isolinoleate ethyl ester labelled at the C_9-C_{10} positions confirmed that the fatty acid is 18 carbons in length and contains two double bonds located at the C_6-C_7 and the C_9-C_{10} positions. The location and level of deuteriation of each labelled fatty acid was also determined by ^{13}C NMR and by comparison of the ^{13}C spectra and the retention times of the various fatty acid methyl esters on GC to those of the

C_9-C_{10} labelled sample, the structure of each fatty acid was established. Approximately 100 milligrams of isolinoleic acid were isolated per culture and the fatty acids were deuteriated, on average, to a level of 30 %.

The deuteriated isolinoleic acid were esterified to form 1-palmitoyl-2-isolinoleoyl-*sn*-glycero-3-phosphocholine (PiLPC) and ^2H NMR spectra of aqueous dispersions of each were acquired over a temperature range of 1 °C to 40 °C. The line shapes of the various powder spectra are characteristic of lipids undergoing axially symmetric motions in the bilayer and the temperature dependences of the quadrupolar splittings indicate that the acyl chain becomes more disordered and that several of the segments change their average orientation with respect to the bilayer normal, with increasing temperature. The observed splittings for the C_8 methylene segment also collapse to zero at 15 °C indicating that, on average, the methylene unit adopts one of four possible orientations whereby both C-^2H bonds are at the magic angle (54.7°) with respect to the bilayer normal.

Acquiring spectra of oriented multibilayers of [$^2H_2$-8']-PiLPC with proton decoupling narrowed the line widths of the deuterium signals sufficiently to allow a direct measurement of the ^2H-^2H dipolar coupling between the two C_8 geminal deuterons and with this additional parameter the average orientation and the associated ordering tensor of the C_8 methylene unit were defined. Based on this orientation and the ratios of the quadrupolar splitting for the two deuterons attached to each double bond, the average orientations and molecular order parameters, S_{mol}, for the C_6-C_7 and the C_9-C_{10} double bonds were also calculated. The resulting conformation for the 1,4-pentadiene unit of the isolinoleoyl chain appears to be inconsistent with the angle iron/helical structures proposed for highly unsaturated acyl chains by Applegate & Glomset ((1986), *J. Lipid Res.* **27**, 658-680) and would likely disrupt the parallel packing of the chain in the lipid bilayer.

However, it was proposed that the linoleoyl chain undergoes a two-site jump between angle iron/helical conformations and that the calculations reflect the average of the two conformations as opposed to each individual state. Low temperature spectra are consistent with the acyl chain adopting an angle iron/helical structure in the gel state (where the jump motion is frozen) and thus provide further support to the jump model.

The molecular order parameters determined for the C_8 methylene unit and the C_6-C_7 and C_9-C_{10} double bonds are consistent with the two-site jump model and indicate that the ordering profile of the diunsaturate differs substantially from those of saturated and monounsaturated acyl chains. At 40°C, the S_{mol} value of the C_6-C_7 double bond is either 0.55 or 0.71 (two possible solutions), indicating restricted motion, whereas the S_{mol} values for the C_8 methylene unit and the C_9-C_{10} double bond are 0.15 and 0.08, respectively, indicating considerable motional freedom. The chain therefore is substantially more ordered than saturates and monounsaturates at the C_6-C_7 segment, but the jump motion, which occurs mainly by rotations about the C_7-C_8 and the C_8-C_9 single bonds, leads to large amplitudes of motion for the C_8 and the C_9-C_{10} segments and consequently a dramatic disordering of the chain at the C_8 position. However, the apparent disordering arises from a specific jump as opposed to the random motions generally associated with the disordering of saturates and monounsaturates. The motions of the diunsaturated chain clearly differ from those of both saturates and monounsaturates.

The work presented in the thesis clearly demonstrates that it is possible to use a biological organism to produce specifically deuteriated polyunsaturated fatty acids and that the fatty acids can be isolated in sufficient quantities and at a high enough level of purity for NMR investigations. The work also demostrates the utility of using oriented multibilayers and ^2H NMR spectroscopy for obtaining detailed information on the structural and

motional properties of polyunsaturated acyl chains in membranes. The analysis led to a two-site jump model describing the motions of the isolinoleoyl chain, and the model is consistent with the proposed angle iron or helical structures proposed for polyunsaturated acyl chains in the bilayer. In addition, the two site jump would likely not occur in chains containing three or more double bonds thus suggesting that highly unsaturated acyl chains exhibit a high degree of order for the length of the chain. This contrasts the accepted concept that polyunsaturation plays a "fluidizing" role in membranes and suggests that the hydrophobic interior of membranes rich in polyunsaturates is not highly "fluid" or flexible as is generally thought. Clearly, analyses of highly unsaturated lipids using the approach described in this thesis are required in order to obtain a complete understanding of the role of polyunsaturation in biological membranes.

Résumé

Un auxotrophe de l' organisme, *Tetrahymena*, ayant besoin d' acides gras non saturés, a été cultivé dans différentes conditions afin d' obtenir un rendement optimal pour transformer les suppléments de l' acide oléique ($18:1^{\Delta 9}$) en acide isolinoléique ($18:2^{\Delta 6,9}$). Ensuite, plusiers cultures ont été enrichies avec l' acide oléique deutérié à une des dix positions de la chaine et les acides isolinoléique deuteriés à la meme position ont été isolés. La GC et la TLC ont démontré que tous les acides sont purs. De plus, la GC-MS a démontré que l ' acide isolinoléique deutérié aux positions C_9 et C_{10} est une chaine de 18 carbones contenant 4 carbones non saturés aux positions C_6-C_7 et C_9-C_{10}. Pour chaque acide isolinoléique, la position et le pourcentage de deutériation ont été déterminés avec la RMN du ^{13}C. En général, cent milligrammes de l' acide isolinoléique ont été isolés par culture, et les acides sont deutériés à moyen de 35 %.

Les acides isolinoléique sont estériés en 1-palmitoyl-*sn*-glycero-3-phosphocholine et les spectres RMN cu ^2H de dispersions aqueuses de 1-palmitoyl-2-isonlinoleoyl-*sn*-glycero-3-phosphocholine (PiLPC) ont été mesurés. les spectres sont caractéristiques de lipides ayant des mouvements à symétrie axiale et isl suggèrent que l' orientation de plusieurs segments carbonés changent avec la température. Les couplages quadrupolaires du segment C_8 sont orientés à "l' angle magique" (54.7°) par rapport à la normal de la bicouche. De plus, lorsque les spectre orientés de [$^2H_2$-8']-PiLPC sont mesurés avec découplages dipolaires entre les deux deutérons du segment C_8. Avec cette information, les orientations des segments C_6-C_7, C_8, et C_9-C_{10} ont été déterminées. La structure de l'

acide n' est pas conforme aux structures proposées pour les acides polyinsaturés et n' est pas compatible avec une orientation parallèle des chaines dans les bicouches lipidiques. Toutefois, il est proposé que la chaine exécute un saut entre deux conformations conformes aux structures proposées et que les résultats réflètent la moyenne des deux conformations plutot que chacune des conformation.

Les paramètres d' ordre, S_{mol}, pour les trois segments ont aussi été déterminés, et le profil d' ordre contraste avec les profils d' ordre déterminés pour les acides saturés et monoinsaturés. La chaine a une paramètre d' ordre assez élevé pour le segment C_6-C_7 tandis que les segments C_8 et C_9-C_{10} sont très désordonnés. Ainsi, le saut entre deux conformations, tel que décrit plus haut, est peut-etre le mouvement duquel résultent les faibles paramètres d' ordre. Si tel est le cas, il est proposé qu' une chaine ayant plusieurs liaisons doubles, ne peut exécuter ce saut et, donc, aura des paramètres d' ordre très élevés pour toute la chaine. Ainsi, les acides polyinsaturés sont peut-etre rigides et non fluides comme on croit généralement.

Le travail présenté dans cette thèse démontre qu' il est possible de synthétiser des acides gras polyunsaturés deutériés par des organismes biologiques, et que la RMN du ^2H est une très bonne méthode pour examiner les propriétés physique des lipides dans les membraanes. Les résultats suggèrent que les lipides polyinsaturés ne sont pas fluides ou flexibles comme on croit généralement. De plus, en utilisant les techniques développées ici, il est possible d' obtenir beaucoup d' information sur les propriétés physiques des

acides gras polyinsaturés et éventuellement, d' en comprendre le role dans les tissus biologiques.

Table of Contents

	page number
Acknowledgements	iv
Abstract (English)	vi
Abstract (French)	x
Table of Contents	xiv
List of Tables	xxiii
List of Figures	xxv
Abbreviations	xxxi

Chapter 1

General Introduction 1

The Biological Membrane 3

Unsaturation in Biological Systems 6

Biosynthesis and Classification
of Unsaturated Fatty Acids.....6

The Distribution of Unsaturated Lipids and
Their Effects on Tissue Function.....7

**The Role of Unsaturation
in Membrane Function.....15**

Membrane "Fluidity".....15

Effects of Unsaturation on the
"Fluidity" of Biological Membranes.....16

Temperature Acclimation Studies with *Tetrahymena*.....16

Membrane Enrichment and Mammalian Membranes. 16

The Effects of Unsaturation on the "Fluidity"
of Model Membrane Systems: Biophysical Studies.....17

Differential Scanning Calorimetry (DSC). 17

Phospholipid Surface Area Measurements. 21

Fluorescence Polarization. 21

Electron Spin Resonance (ESR) 23

Nuclear Magnetic Resonance Spectroscopy (NMR). 24

Computer Modeling Studies of DHA.....28

Summary and Conclusions.....31

Chapter 2

Deuterium and Phosphorus NMR Theory and Applications.....33

Theory 35

Deuterium NMR Spectroscopy 35

The Magnetic Hamiltonian, H_M.....37

Quadrupolar Hamiltonian, H_Q. 39

Dipolar Hamiltonian, H_D. 45

Phosphorus NMR Spectroscopy 47

Applications 50

Deuterium NMR Spectroscopy 50

Phosphorus NMR Spectroscopy 56

Summary and Thesis Goals 57

Chapter 3

Biosynthesis of a Series of Specifically Deuteriated Isolinoleic Acids.....59

Introduction 62

Materials and Methods.....65

Feasibility of a Biological Approach 65

Culture Conditions. 65

Effect of Supplement Concentration. 66

Effect of Growth Temperature. 66

Cell Density Measurements. 66

Gas-Chromatography (GC). 67

Uptake of [1-^{14}C] Oleic Acid. 67

High Performance Liquid Chromatography (HPLC).....68

Liquid-Scintillation Counting.....69

Argentation Chromatography.....60

Characterization of the Deuteriated Products.....70

Culture Conditions.....70

Purification. 71

Analysis of Purity. 72

Identification of the Number and Location

of the Double Bonds. 72

Identification of the Sites of Deuteration. 72

Oxidation. 73

Results **74**

Feasibility of a Biological Approach 74

Optimization of Growth Conditions. 74

Purification of Isolinoleic Acid. 79

Characterization of the Deuteriated Products 81

Discussion **95**

Summary and Conclusions **102**

Chapter 4

Aqueous Dispersions of 1-Palmitoyl-2-Isolinoleoyl Phosphatidylcholine **103**

Introduction **106**

Materials and Methods **107**

Sample Preparation 107

Esterification to Lyso PC 107

Acyl Chain Migration 109

Aqueous Dispersions 109

NMR Spectroscopy 109

Deuterium NMR Spectroscopy 109

Phosphorous NMR 111

Results **112**

The Liquid Crystalline Phase 112

Quadrupolar Splittings Versus Temperature 112

Conformation of the Isolinoleoyl Chain in the Liquid-Crystalline Phase 124

Order Parameter Profile 131

The Gel Phase 136

Gel to Liquid-Crystal Transition Temperature 136

Conformation of Isolinoleic Acid in the Gel Phase 140

Spectral Simulations and Acyl Chain Migration 144

Discussion **149**

Conformation of the Isolinoleoyl Chain 149

Ordering of the Isolinoleoyl Chain 153

1-Isolinoleoyl-2-Palmitoyl PC (iLPPC) and Acyl Chain Migration 155

Summary and Conclusions 157

Chapter 5

Oriented Multibilayers of 1-Palmitoyl-2-Isolinoleoyl Phosphatidylcholine 159

Introduction 161

Materials and Methods.....162

Oriented Multibilayers. 162

NMR Spectroscopy. 162

Results.....163

[$^2H_2$-8']-PiLPC. 163

[$^2H_2$ -9',10']-PiLPC. 182

Discussion.....184

Summary and Conclusions 187

Chapter 6

General Summary and Conclusions 188

Appendices 206

Appendix 1:

Alkenyl Bond Angles and Torsion Angles of the 1,4-Pentadiene Unit of Linoleic Acid 208

Appendix 2:

Orientations of the C_6-C_7 Double Bonds in the Liquid Crystalline Phase 209

Double Bond Orientations 209

Sensitivity of the Calculations to the Angle ψ 216

Sensitivity of the Calculation to the Double Bond Torsion Angles 216

Appendix 3:

Orientations of the Isolinoleoyl Chain in the Gel Phase 222

Angle Iron Conformation 222

C_7 Deuteron 222

C_8 Methylene Deuterons 223

C_9-C_{10} Double Bond 224

Linoleic Acid Crystal Structure 228

Appendix 4:

Calculation of the Orientation and Order Matrix for the C_8 Methylene Segment in the Liquid Crystalline Phase 231

List of Tables

Table 1.1 The Major Fatty Acids In Retinal Rod Outer Segments Isolated from the Frog, Rat, and Bull1 10

Table 2.1 Properties of the Deuterium Nucleus 51

Table 3.1 Effect of the Supplement ($18:1^{\Delta 9}$) on Cell Growth and and Isolinoleic Acid Producition 75

Table 3.2 Effect of Culture Temperature on Cell Growth and Isolinoleic Acid Production 76

Table 3.3 Uptake of [1-^{14}C] Oleic Acid from the Culture Medium by RH179E1 78

Table 3.4 The Yield, Purity, and Level of Deuteriation of the Purified Isolinoleic Acids 84

Table 3.5 A quantitative summary of the fragmentation pattern and level of deuteriation of the *O*-TMS derivative of the ethyl ester of [$^2H_2$-9,10]-$18:2^{\Delta 6,9}$ 87

Table 3.7 Resonance Assignments in the ^{13}C NMR Spectrum of Isolinoleic Acid 90

Table 4.1 Comparison of the spectral widths observed for PiLPC in the gel phase and those calculated based upon the average conformation defined for the chain at 15 °C, the conformation proposed by Applegate & Glomset, and a conformation consistent with the crystal structure of linoleic acid ($18:2^{\Delta 9,12}$) 143

Table 4.2. Comparison of the relative intensities of the ^{2}H signals arising from iLPPC to the amount of acyl chain migration in the samples 146

Table 5.1. Summary of the tensor components and Euler angles resulting from diagonalization of the ordering matrices for PiLPC and iLPPC 178

Table A2.1. Orientation of the C_6-C_7 Double Bond 214

Table A2.2. Orientation of the C_9-C_{10} Double Bond 215

Table A2.3. Orientation of the C_6-C_7 Double Bond at 15°C: Sensitivity to Variations in the Angles ψ_6 and ψ_7 217

Table A2.4. Orientation of the C_9-C_{10} Double Bond at 15°C. Sensitivity to Variations in the Angles ψ_9 and ψ_{10} 219

Table A2.5. Effect of the torsion angle on the calculated orientation of the C_9-C_{10} double bond 220

Table A3.1. Maximum spectral widths for the deuteriated segments of the isolinoleoyl chain calculated assuming an angle iron/helical conformation 225

Table A3.2. Maximum spectral widths for the deuteriated segments of the isolinoleoyl chain calculated assuming a conformation consistent with the crystal structure of linoleic acid. 229

List of Figures

Figure 1.1. A schematic diagram of the gross structural features of the biological membrane as described by the "fluid-mosaic model" of Singer & Nicolson (1972)..... 4

Figure 1.2. Chemical structures of the most common unsaturated fatty acids in mammalian cell membranes..... 8

Figure 1.3. Distribution of polyunsaturated fatty acids in the phosphatidyl-ethanolamine fraction isolated from the a) liver, and b) grey matter of 45 different species..... 13

Figure 1.4. A schematic diagram of some molecular membrane probes. Abbreviations are as follows..... 18

Figure 1.5. The gel-to-liquid crystal transition temperatures of phosphatidyl-choline bilayers as a function of the number of double bonds. 20

Figure 1.6. Deuterium NMR spectrum of an aqueous dispersion of 1-palmitoyl-2-(vinyl perdeuteriated) docosahexaenoyl PC at 25 °C..... 27

Figure 1.7. A comparison of the crystal structure of linoleic acid (Ernst et al., 1979) with the proposed structure of docosahexaenoyl chains in lipid bilayers (Applegate & Glomset, 1986). 30

Figure 2.1. Effect of Zeemzn, Quadrupolar, and Dipolar interactions on the energy levels and the NMR spectrum of a quadrupolar spin = 1 nucleus..... 38

Figure 2.2. Origin of the deuterium NMR "powder spectrum"..... 44

Figure 2.3. Phosphorus NMR spectra arising from the various motional states of a phosphodiester group of a phospholipid. 49

Figure 2.4. A comparison of the S_{CD} bond order parameter profiles obtained from A) synthetic lipids and B) biological lipid mixtures..... 52

Figure 2.5. A) A comparison of the molecular order parameters, S_{mol}, for the sn-1 and sn-2 chains in the phospholipid POPC. A comparison of the deuterium bond order parameters, S_{CD}, of the palmitoyl and oleoyl chains of POPC 55

Figure 3.1. Desaturation pathway of 18-carbon fatty acids in *Tetrahymena*.. 63

Figure 3.2. Comparison of the HPLC chromatograms of teh phenacyl esters fromed from teh free fatty acids of *T. thermophila*. The chromatogram in **a)** is before and **b)** after argentation chromatography..... 80

Figure 3.3. Comparison of the GC chromatograms for free fatty acid methyl esters isolated from RH179E1. The chromatogram in **a)** is the total cellular free fatty acids, wheras the chromatogram in **b)** shows the pure isolinoleic acid.. 82

Figure 3.4 The expected fragmentation pattern for the *O*-TMS derivative of the deuteriated ethyl ester of isolinoleic acid..... 85

Figure 3.5. A quantitative summary of the fragmentation pattern and level of deuteriation of the *O*-TMS derivative of the ethyl ester of [$^2H_2$-9',10'] - PiLPC. 87

Figure 3.6. A portion of the ^{13}C NMR spectrum of isolinoleic acid deuteriated at both the C_9 and C_{10}positions showing the alkene (127-132 ppm) and methylene resonances (20-36 ppm)..... 88

Figure 3.7. A portion of the ^{13}C NMR spectrum of isolinoleic acid deuteriated at the C_6 position..... 91

Figure 3.8. High resolution ^2H NMR spectrum of the [^2H-6']-18:2$^{\Delta 6,9}$ preparation isolated from cultures of RH179E1 supplemented with [$^2H_2$-6']-18:1$^{\Delta 9}$..... 93

Figure 3.9. Comparison of **a)** the protocol used by Conner et al. (1984) to synthesize radiolabelled isolinoleic acid and **b)** the protocol developed here for the biosynthesis of deuteriated isolinoleic acids..... 97

Figure 4.1. 1-palmitoyl-2-isolinoleoyl phosphatidylcholine (PiLPC). 113

Figure 4.2. ^2H powder spectra of PiLPC deuteriated at the indicated postion of the isolinoleoyl chain.Figure 4.6. 114

Figure 4.3. Depaked spectra of PiLPC deuteriated at the indicated positions of the isolinoleoyl chain.Figure 4.7. 116

Figure 4.4. **a)** A phosphorus spectrum of [$^2H_2$-8']-PiLPC acquired as indicated under Materials and Methods on a Bruker MSL-300 spectrometer operating at 121.497 MHz. **b)** An expanded view of the ^2H powder spectrum of [$^2H_2$-8']-PiLPC recorded as indicated in Figure 4.2 at 30 °C..... 118

Figure 4.5. **a)** Proton-decoupled ^2H NMR spectra of acqueous dispersions of [$^2H_2$-8']-PiLPC acquired on a Bruker MSL-300 spectrometer operating at 46.064 MHz. **b)** The oriented sample spectra arising from dePaking the spectra shown in **a)**..... 120

Figure 4.6. A summary of the values of the quadrupolar splittings for each deuteriated position of the isolinoleoyl chain of PiLPC as a function of temperature..... 122

Figure 4.7. A summary of the relative changes in the quadrupolar splittings for each deuteriated position of the isolinoleoyl chain of PiLPC as a function of temperature..... 123

Figure 4.8. The proposed orientations of the C_8 methylene segment at 15 °C..... 125

Figure 4.9. The jump model proposed for the motions of the α,4-pentadiene segment of the isolinoleoyl chain of PiLPC..... 129

Figure 4.10. The average conformation of the 1,4-pentadiene segment of the isolinoleoyl chain of PiLPC in the liquid crystalline phase at 15 °C..... 130

Figure 4.11. A plot of the bond order parameter, S_{CD}, versus labelled position for the isolinoleoyl chain of PiLPC..... 133

Figure 4.12. a) A plot of the molecular order parameter versus reduced temperature (Tred = [Tobs- Tc]/Tc and Tc = -15 °C) for the C_6-C_7, the C_8, and the C_9-C_{10} segments of the isolinoleoyl chain of PiLPC. 134

Figure 4.13. ^2H spectra of aqueous dispersions of [2H2-5']-PiLPC acquired with a recycle time of **a)** 5 x T1 and **b)** 10 x T1..... 135

Figure 4.14. ^2H spectra of acqueous dispersions of [^2H-7']-PiLPC acquired from 25 °C down to -25°C. 137

Figure 4.15. Temperature dependence of the Δ_2 parameter for the ^2H NMR spectra of [^2H-2-7']-PiLPC..... 139

Figure 4.16. Temperature dependence of the second moment, M_2, for the ^2H NMR spectra of [^2H-2-7']-PiLPC..... 139

Figure 4.17. Spectra of PiLPC acquired at the center of the phase transition temperature, -15 °C..... 141

Figure 4.18. Simulations of the powder and the dePaked spectra obtained from aqueous dispersions of **a)** [$^2H_2$-14']-PiLPC (1 °C) and **b)** [$^2H_2$-5']-PiLPC (30 °C). 145

Figure 4.19. **a)** Summary of the values of the quadrupolar splittings for each deuteriated position of the isolinoleoyl chain of iLPPC and for the C_6 position of the linoleoyl chain of PLPC (C_6*). **b)** Plot of the S_{CD} bond order parameter as a function of the labelled position along the isolinoleoyl chain of iLPPC, at 30 °C. 147

Figure 5.1. Phosphorus spectra of oriented multibilayers of [$^2H_2$-8']-PiLPC acquired with the sample oriented at an angle of **a)** 90° and **b)** 0° with respect to the magnetic field direction..... 164

Figure 5.2. ^2H spectra of oriented multibilayers of [$^2H_2$-8']-PiLPC acquired **a)** without, and **b)** with proton decoupling..... 165

Figure 5.3. ^2H spectra of oriented multibilayers of [$^2H_2$-8']-PiLPC acquired with proton decoupling as a function of temperature..... 166

Figure 5.4. A plot of the temperature dependences of the quadrupolar splittings opbtained from spectra of oriented multibilayers of [$^2H_2$-8']-PiLPC at 25 °C..... 167

Figure 5.5. ^2H spectra of oriented multibilayers of [$^2H_2$-8']-PiLPC acquired as a function of the angle betweeen the normal to the glass plates (bilayer normal) and the magnetic field direction, H_o..... 170

Figure 5.6. a) Plot of the quadrupolar splittings of [$^2H_2$-8']-PiLPC and [$^2H_2$-8]-iLPPC versus the angle between the bilayer normal and the magnetic field direction (the doubletss corresponding to iLPPC have the same splittings as the doublet with larger splitting of PiLPC). b) Plot of the quadrupolar splittings as a function of $(3Cos^2\theta - 1)/2$, where θ is the angle between the bilayer normal and the magnetic field direction 171

Figure 5.7. Resolution enhancement of the spectrum of [$^2H_2$-8']-PiLPC acquired at 40 °C with the sample oriented such that the bilayer normal is parllel to H_o. 172

Figure 5.8. Sensitivity of the simulations of the spectrum of [$^2H_2$-8']-PiLPC (40 °C) to the signs of the quadrupolar splittings and the dipolar coupling. 174

Figure 5.9. Simulations of the spectrum of [$^2H_2$-8']-PiLPC (40 °C) acquired at both the 90° and 0° orientations. 175

Figure 5.10. Orientation of the C_8 methylene unit of PiLPC at 40 °C as determined in Appendix 4..... 177

Figure 5.11. Simulations of the proton-coupled and proton-decoupled spectra of oriented multibilayers of [$^2H_2$-8']-PiLPC acquired at 25 °C..... 180

Figure 5.12. ^2H spectra of oriented multibilayers of [$^2H_2$-9',10']-PiLPC acquired a) with proton decoupling, and b) without proton decoupling..... 181

Figure 5.13. Phosphorus spectra of oriented multibilayers of [$^2H_2$-9',10']-PiLPC acquired as a function of temperature..... 183

Figure 6.1 Comparison of the bond order parameter, S_{CD}, and the molecular order parameter, S_{mol}, profiles for saturated, monounsaturated, and diunsaturated fatty acyl chains..... 192

Figure A1.1. Bond angles of the 1,4-pentadiene segment of linoleic acid as determined by X-ray crystallography (Ernst & Sheldrick, 1979). 208

Figure A2.1. The X-Y-Z axis systems attached to the C_6-C_7 and the C_9-C_{10} double bonds. 210

Figure A2.2. The two coordinate transformations performed to calculate the geometric factors for each double bond given any orientation of each consistent with the specified orientation of the C_8 methylene segment..... 212

Figure A2.3. A schematic representation of the effect of the torsion angle on the calculated orientation of the C_9-C_{10} double bond. 220

Figure A3.1. The X-Y-Z axis system attached to the C_8 methylene segment. 224

Figure A3.2. The X-Y-Z axis system attached to the C_9-C_{10} double bond..... 224

Figure A4.1. The cartesian coordinate system attached to the C_8 methylene segment in Appendix 4. 231

Abbreviations

BHT,	butylated hydroxytoluene
BSA,	bovine serum albumin
CSA,	chemical shift anisotropy
DAPC,	1,2-di-*cis,cis,cis,cis*-eicosa-5,8,11,14-tetraenoyl-*sn*-glycero-3-phosphocholine
DCC,	N,N'-dicyclohexylcarbodiimide
DHA,	*cis,cis,cis,cis,cis,cis*-4,7,10,13,16,19-docosahexaenoic acid
DMAP,	4-dimethylaminopyridine
DMPC,	1,2-ditetradecanoyl-*sn*-glycero-3-phosphocholine
DOPC,	1,2-di-*cis*-octadec-9-enoyl-*sn*-glycero-3-phosphocholine
DPA,	*cis,cis,cis,cis,cis*-5,8,11,14,17-eicosapentaenoic acid
DPH,	1,6-diphenyl-1,3,5-hexatriene
DPPA,	1,2-dihexadecanoyl-*sn*-glycero-3-phosphatidic acid
DPPC,	1,2-dihexadecanoyl-*sn*-glycero-3-phosphocholine
DPPS,	1,2-dihexadecanoyl-*sn*-glycero-3-phosphoserine

DLPC,	1,2-di-*cis,cis*-octadeca-9,12-dienoyl-*sn*-glycero-3-phosphocholine
DMPC,	1,2-ditetreadecanoyl-*sn*-glycero-3-phosphocholine
DSC,	Differential Scanning Calorimetry
EDTA,	ethylenediamine tetraacetic acid
ESR,	Electron Spin Resonance
FAA,	fatty acid anhydride
FID	free induction decay
GC,	gas chromatography
GC-MS,	gas chromatography coupled to mass spectrometry
HPLC,	high performance liquid chromatography
iLPPC,	1-*cis,cis*-octadeca-6,9-dienoyl-2-hexadecanoyl-*sn*-glycero-3-phosphocholine
NMR,	nuclear magnetic resonance
NS,	nitroxide stearic acid
O-TMS,	*O*-(trimethylsilyl)
PC,	*sn*-glycero-3-phosphocholine
PE,	*sn*-glycero-3-phosphoethanolamine

PNE, 0.15 M phosphate, 0.45 M NaCl, 3 mM EDTA

PS, *sn*-glycero-3-phosphoserine

PDhPC, 1-hexadecanoyl-2-*cis,cis,cis,cis,cis,cis*-docosa-4,7,10,13,16,19-*sn*-glycero-3-phosphocholine

PiLPC, 1-hexadecanoyl-2-*cis,cis*-octadeca-6,9-dienoyl-*sn*-glycero-3-phosphocholine

PLPC, 1-hexadecanoyl-2-*cis,cis*-octadeca-9,12-dienoyl-*sn*-glycero-3-phosphocholine

POPC, 1-hexadecanoyl-2-*cis*-octadec-9-enoyl-*sn*-glycero-3-phosphocholine

rf radiofrequency

S_{CD}, carbon-deuterium bond order parameter

S_{geo}, geometric factor

S_{mol}, molecular order parameter

T_c, gel-to-liquid crystal transition temperature

TMA-DPH, trimethylamine 1,6-diphenyl-1,3,5-hexatriene

T_{obs}, observe temperature

TLC, thin-layer chromatography

T_{red}, reduced temperature, $(T_{red} = T_{obs} - T_c)/T_c$

T_1, spin-lattice relaxation time

T_2, spin-spin relaxation time

Chapter 1

General Introduction

Chapter 1

General Introduction 1

The Biological Membrane 3

Unsaturation in Biological Systems 6

Biosynthesis and Classification of Unsaturated Fatty Acids 6

The Distribution of Unsaturated Lipids and Their Effects on Tissue Function 7

The Role of Unsaturation in Membrane Function **15**

Membrane "Fluidity" 15

Effects of Unsaturation on the "Fluidity" of Biological Membranes 16

Temperature Acclimation Studies with Tetrahymena 16

Membrane Enrichment and Mammalian Membranes. 16

The Effects of Unsaturation on the "Fluidity" of Model Membrane Systems: Biophysical Studies 17

Differential Scanning Calorimetry (DSC). 17

Phospholipid Surface Area Measurements. 21

Fluorescence Polarization. 21

Electron Spin Resonance (ESR) 23

Nuclear Magnetic Resonance Spectroscopy (NMR). 24

Computer Modeling Studies of DHA 28

Summary and Conclusions **31**

The Biological Membrane

The basic unit of life is the cell and the existence and survival of any cell is dependent upon the presence and proper function of its membranes. Membranes define the cell and its internal organelles and provide a selectively permeable barrier between the intracellular and extracellular environments. They are also the site of considerable biochemical activity (for example; oxidative phosphorylation, photosynthesis, nerve transmission, etc.) and are intimately involved in cellular phenomena such as cell division.

The multi-functional aspect of biological membranes arises as a consequence of their composition and structure. They are a complex mixture of lipid, protein, and carbohydrate organized in a two-dimensional fluid such as described by the "fluid-mosaic model" of Singer and Nicolson (1972). The lipids form a bilayer with their non-polar hydrocarbon regions extended towards the interior and their polar headgroups exposed to the external, aqueous environment (Figure 1.1). Proteins are located within the lipid matrix either spanning it completely or facing one side only and the carbohydrate portion is found covalently bound to both lipid and protein, usually on the surface of the cell.

The lipid bilayer is the basic structural feature of all biological membranes and bilayers are composed of a wide variety of lipids. Phospholipid, neutral lipid and glycolipid are common and within each class there is considerable variation in the length and degree of unsaturation of the acyl chains, the nature of th head groups, etc. All lipids are amphiphilic and are capable of forming bilayers in aqueous solution. Their structural variations, however, have been shown to affect bilayer phase transition temperatures and

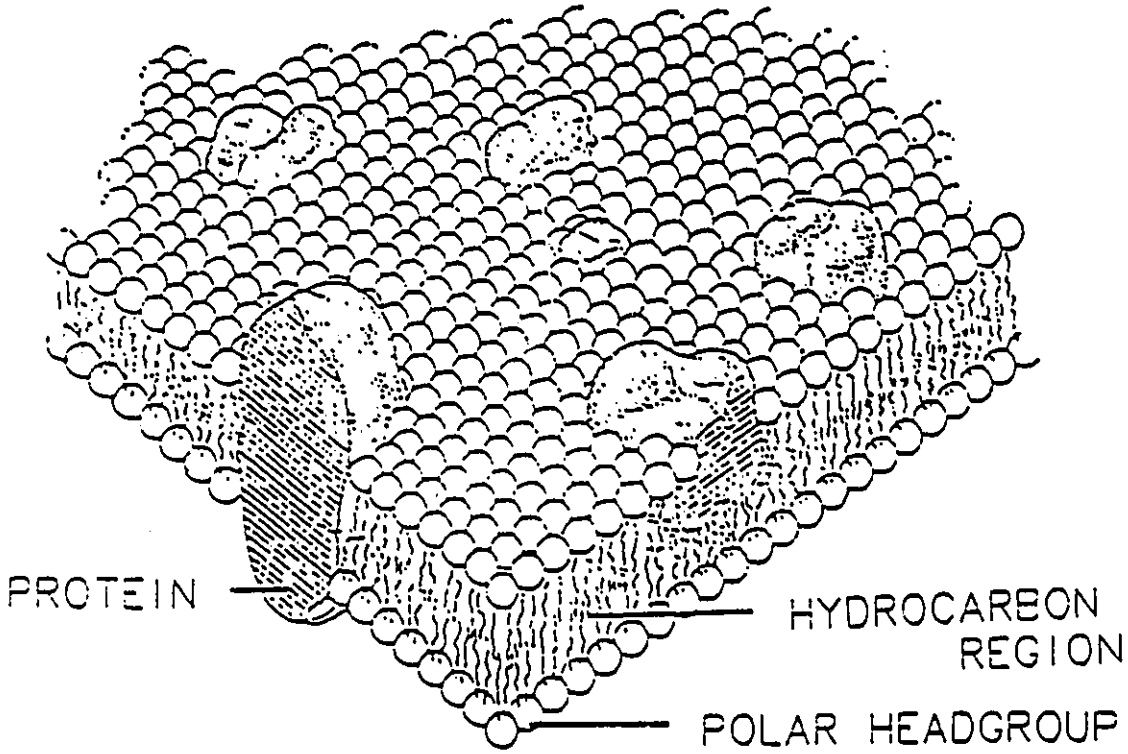

Figure 1.1. A schematic diagram of the gross structural features of the biological membrane as described by the "fluid-mosaic model" of Singer & Nicolson (1972)

lateral phase separations, and in turn the activity of membrane bound enzymes and membrane permeability, etc. (Stubbs & Smith, 1984; Boggs, 1984; Sandermann, 1978). Lipids therefore play a functional role in maintaining or perhaps even modulating the physical properties of the bilayer (often referred to as the bilayer "fluidity") so that proper membrane functions can occur.

Polyunsaturated lipids are common in mammals and there is considerable interest in their biological function. In order to understand their contribution to membrane function, however, investigations of their physico-chemical properties in lipid bilayers are essential. Here, the average structural properties and associated molecular dynamics of a lipid containing an eighteen-carbon, diunsaturated acyl chain ($18:2^{\Delta 6,9}$, isolinoleic acid) will be examined by ^{2}H and ^{31}P NMR spectroscopy in an attempt to gain insight into the role of polyunsaturates in membranes. To put the work into perspective, a brief review of some of the biochemical and physico-chemical properties of polyunsaturated lipids, as they pertain to membrane function, will first be presented.

Unsaturation in Biological Systems

Biosynthesis and Classification of Unsaturated Fatty Acids

Unsaturated fatty acyl chains are found in essentially all eukaryotic membranes and they are classified into three groups according to the location of the double bond closest to the terminal methyl of the chain. In mammals, each group is synthesized from a specific eighteen carbon unsaturated fatty acid as shown below:

18:3 ω-3 -> 18:4 ω-3 -> 20:4 ω-3 -> 20:5 ω-3 -> 22:5 ω-3 -> **22:6 ω-3**

18:2 ω-6 -> 18:3 ω-6 -> 20:3 ω-6 -> **20:4 ω-6** -> 22:4 ω-6 -> 22:5 ω-6

18:1 ω-9 -> *18:2 ω-9* -> 20:2 ω-9 -> 20:3 ω-9 -> 22:3 ω-9 -> 22:4 ω-9

The ω-3 or n-3 series is derived from α-linolenic acid ($18:3^{\Delta 9,12,15}$ or 18:3 ω-3) and all derivatives in the series contain a double bond at the third carbon from the terminal methyl of the chain. The ω-6 and ω-9 series are synthesized from linoleic ($18:2^{\Delta 9,12}$ or 18:2 ω-6) and oleic acid ($18:1^{\Delta 9}$ or 18:1 ω-9), respectively, and their closest double bonds are found 6 and 9 carbons from their respective chain termini.

The microsomal enzyme complex responsible for the desaturation and elongation of all three eighteen carbon precursors has a preference for the ω-3 and ω-6 fatty acids (ω-3 > ω-6 >> ω-9). As a result, high levels of the ω-3 and ω-6 polyunsaturates are found in

mammalian tissues whereas the ω-9 polyunsaturates are rare. Both α-linolenic and linoleic acid, however, must be obtained from the diet and in times of dietary stress, oleic acid, which can be synthesized "de novo", is metabolized to form polyunsaturated ω-9 fatty acids (Tinoco et al., 1978). The most common unsaturates in mammalian systems are designated, above, in bold face and their structures are shown in Figure 1.2. The fatty acyl chain studied in this thesis is in italics.*

The Distribution of Unsaturated Lipids and Their Effects on Tissue Function

Much of the current interest in the biological effects of polyunsaturated lipids was catalyzed by research which focused on understanding both the role of lipid diversity and the need for membranes whose fatty acyl chain compositions are characteristic of individual organs and organelles. Studies of the distribution of fatty acyl chains revealed that long chain saturates and monounsaturates are generally found in membranes of low metabolic activity, such as myelin, whereas highly unsaturated acyl chains are often found in membranes of high metabolic activity, such as mitochondria (Fleischer & Rouser, 1965). The results also showed that despite the wide spectrum of polyunsaturates synthesized by

* Both the "ω-X" and the "ΔY, Z" notations are common in the literature and each has its advantages and disadvantages. In this chapter the "ω-X" notation will be used to emphasize the metabolic relations of the fatty acids but in the following chapters the ΔY, Z notation will be used to emphasize the structural relations of the fatty acids.

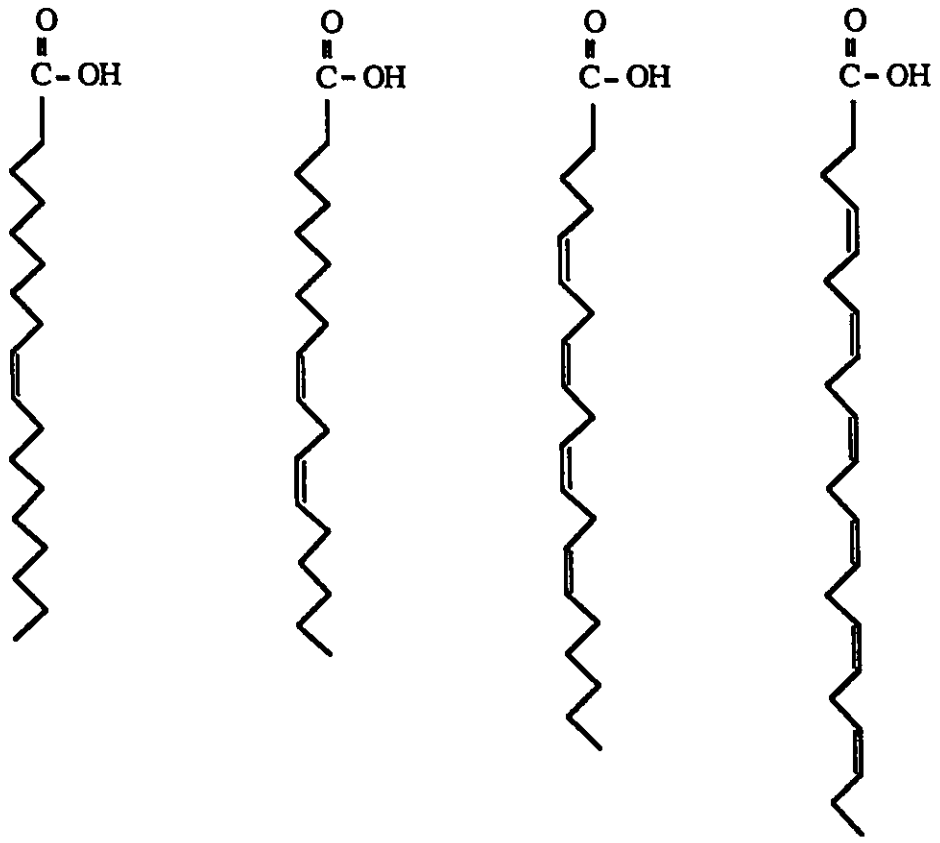

Oleic Acid	Linoleic Acid	Arachidonic Acid	Docosahexaenoic Acid
$18{:}1^{\Delta 9}$	$18{:}2^{\Delta 9,12}$	$20{:}4^{\Delta 5,8,11,14}$	$22{:}^{\Delta 4,7,10,13,16,19}$
18:1 ω-9	18:1 ω-6	20:4 ω-6	22:6 ω-3

Figure 1.2. Chemical structures of the most common unsaturated fatty acids in mammalian cell membranes. From left to right: oleic, linoleic, arachidonic, and docosahexaenoic acid.

mammals, only two, arachidonic (20:4 ω-6) and docosahexaenoic acid (22:6 ω-3; referred to as DHA), are generally found at high levels in most tissues (Tinoco et al., 1978). These patterns suggest a passive, structural role for saturates and a more dynamic, functional role for polyunsaturates. They also suggest that both arachidonic acid and DHA perform a "specific" function in cell membranes.

Arachidonic acid is a precursor for the synthesis of a number of compounds involved in cell regulatory processes (for example, prostaglandins, leukotrienes, etc.; Granstrom & Hedqvest, 1982). Its "specific" role may therefore be in the initiation of such metabolic events and most research focuses on this aspect to explain the high levels of arachidonic acid in membranes. In contrast, DHA is the end product of the ω-3 desaturation pathway and is not converted into additional, biologically important compounds (Tinoco et al., 1978). Its "specific" function is generally attributed to an important role in membrane structure and function and its biological effects are therefore of particular interest to an understanding of the role of unsaturation in membranes.

In most tissues DHA is found at low levels but in the retina it makes up 15 % - 25 % of the fatty acyl chains and is further enriched in the specialized and functionally active region of the tissue, the rod outer segment, where it comprises 45 % - 50 % of the acyl chains (Stone et al., 1979; Miljanich et al., 1979; Drenthe et al., 1981). The high levels of DHA are well conserved in the frog, rat, and bull (Table 1.1), and are strongly maintained in times of dietary stress. For example, rats fed an ω-3 fatty acid deficient diet quickly lose the DHA from most tissues but after ten weeks the levels in the retina are only reduced to 8 % of normal (Anderson & Maude, 1972; Futterman et al., 1971). In fact, rats must be

Table 1.1

The Major Fatty Acids In Retinal Rod Outer Segments
Isolated from the Frog, Rat, and Bull[1]

Fatty Acids	Frog[2]	Rat[2]	Bull[2]
16:0	14.3	9.8	16.3
18.0	13.8	24.3	20.2
18:1 ω-9	4.2	3.8	4.7
20:4 ω-6	2.6	5.3	3.6
22:6 ω-3	46.9	43.3	47.1
% Polyunsaturates	68.0	63.2	59.4

[1] data was taken from Dratz & Deese (1986) and derived from Stone et al. (1979).

[2] mol %

maintained on an ω-3 fatty acid free diet for two generations in order to deplete the levels of DHA by 50 % (Tinoco et al., 1978; Benolken et al., 1973).

The effect of ω-3 fatty acid deprivation on rod outer segment function has also been assessed, and the results show that even a minor decrease in the levels of DHA can have significant effects. For example, rats maintained for forty days on either a fat free diet or the same diet supplemented with oleic (ω-9), linoleic (ω-6), or α-linolenic (ω-3) acids show variations in their response to an electroretinogram which measures the currents generated by the retina in response to illumination. Retinas from animals supplemented with α-linolenic acid exhibit a strong response while those from animals supplemented with oleic acid or those fed a fat free diet show a relatively weak response. Retinas obtained from rats fed a linoleic acid rich diet also exhibit a strong response, the strength of which is reduced relative to retinas from the ω-3 supplemented animals (Wheeler et al., 1975). A correlation between the ability of an animal to synthesize and maintain high levels of DHA in its tissues (and to a lessor extent ω-6 polyunsaturates), and proper retinal function therefore exists.

Rhesus monkeys have also been tested for the effects of ω-3 fatty acid deprivation on visual function. The visual acuity of animals fed either an ω-3 fatty acid deficient or an ω-3 rich diet were determined and the deficient animals were less successful in the test than their counterparts who were fed the normal diets (Neuringer et al., 1984). Again the presence of DHA is correlated with superior visual or retinal function.

Cerebral grey matter is another tissue where DHA seems to play an important role. It makes up 15 - 25 % of the fatty acyl chains in this tissue and is concentrated in the brain synaptic endings and vesicles to a level of approximately 35 % (Cotman et al., 1969;

Breckenridge et al., 1970). The grey matter from 45 species varying from marine fish to the zebra also shows consistent levels of all polyunsaturates with especially high levels of DHA, despite the fact that in the liver of the same animals wide variations in the levels of all polyunsaturates exist (see Figure 3 and Crawford et al., 1977). The fatty acyl chain distribution in the liver depends upon the diets of the particular animals (which vary considerably in this study) but it appears that a specific mechanism operates to control the levels of all polyunsaturates in the nerves of each animal. DHA is strongly retained by nerve tissue and studies have shown that ω-3 fatty acid deficient rats have less neuromotor development and an impaired learning ability in a simple Y-maze test (Lamptey & Walker, 1976). The results therefore suggest an important function for DHA in nerves although the learning impairment may be due to the effects of DHA on vision and not on synaptic transmission.

The high content, specific incorporation, strong retention, and physiological effects of ω-3 fatty acid deprivation clearly illustrate that DHA plays an important role in the membranes of the retina and nerve. DHA, however, is abundant in many other organs such as the liver, heart, testes, muscle etc., and although its effects in these tissues are not as well documented, in some it is strongly retained in times of dietary stress and in others, physiological effects of an ω-3 fatty acid deficiency have been demonstrated (Tinoco et al., 1978; Salem et al., 1986). The effect of DHA on membrane function is therefore important in many mammalian tissues.

There is also evidence that the role of DHA in tissue function is the result of a general effect of polyunsaturates on membranes as opposed to a specific effect of this one fatty acid. For example, in the PE fraction of rat muscle after one generation of ω-3 fatty acid deficiency, the levels of DHA drop from 36 % to 1.5 % whereas the levels of 22:5 ω-6

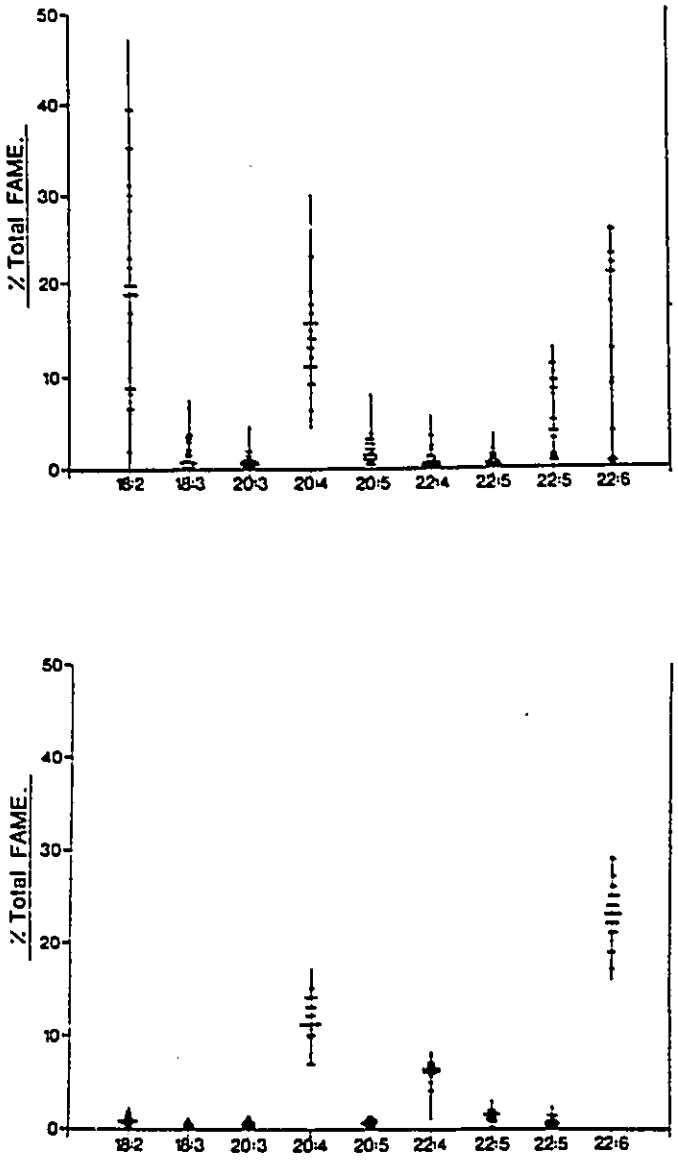

Figure 1.3. Distribution of polyunsaturated fatty acids in the phosphatidyl-ethanolamine fraction isolated from the a) liver, and b) grey matter of 45 different species. The animals varied from marine fish to the wild zebra (Crawford et al., 1977)

(docosapentaenoic acid; DPA) increase from 2 % to 25% (Tinoco et al., 1978). DPA is only found at high levels in mammalian cells in times of dietary stress and at such times it replaces DHA in almost all tissues (Stubbs & Smith, 1984). The electroretinogram experiments, discussed above, show that retinas from animals supplemented with linoleic acid (they therefore have the ability to produce DPA) have a strong response, although not quite as strong as those from ω-3 fat supplemented animals. DPA can therefore replace DHA and to a slightly reduced degree perform its function in membranes. Experiments performed with cells in tissue culture also show that an increase in the levels of linoleic or arachidonic acid in the cell membranes has a dramatic effect upon membrane transport and the activity of membrane bound enzymes (Spector & Yorek, 1985; and references within). Therefore, all polyunsaturated lipids have important effects on membrane function.

DHA is the most unsaturated fatty acid in mammalian tissue and represents the extreme effects of unsaturation on membrane function. Research has therefore often focused on describing the effects of DHA on mammalian tissues in an attempt to gain a general understanding of the role of unsaturation in membranes and the results clearly indicate that a correlation between the presence of DHA and proper tissue function in the retina and nerve exists. Other unsaturated fatty acyl chains clearly have important effects, but the results presented here for DHA illustrate the biological importance of polyunsaturates and show that there is a need for experiments to determine their role in membrane function.

The Role of Unsaturation in Membrane Function

Membrane "Fluidity"

One of the basic postulates of the "fluid-mosaic model" of Singer and Nicolson is that biological membranes are "fluid". The concept of a "fluid" bilayer arose from experiments which showed that membrane components are free to diffuse laterally in the membrane (Frye & Edidin, 1970) and undergo a variety of anisotropic motions such as rapid rotation about their long axes (Brown, 1972; Pone, 1972). It is now generally accepted that membranes also exhibit different degrees of "fluidity" ranging from the solid-like gel phase, where motions are slow and of small amplitude (high order), to the solution-like liquid-crystalline phase, where motions are fast and relatively unrestricted (low order). The degree of "fluidity" is generally characterized by both the "order" and dynamics (rates of motion; Seelig & Seelig, 1977a) of the membrane components and is largely determined by the lipid composition of the membrane. Membrane "fluidity" is thought to play an important role in the maintenance of proper membrane function (see Lands & Davis, 1984 and others in the same volume).

Effects of Unsaturation on the "Fluidity" of Biological Membranes

Temperature Acclimation Studies with Tetrahymena. A correlation between the degree of unsaturation and the "fluidity" of a membrane has been suggested from a variety of biochemical studies. For example, when the protozoan *Tetrahymena* is grown at 40 °C and then shifted to 15 °C, the organism dramatically increases the proportion of 18:3 ω-6 (its major polyunsaturate) and decreases the levels of saturates in its membranes (Ramesha & Thompson, 1983; Ramesha & Thompson, 1982; Muruyama et al., 1982; Dickens & Thompson, 1981; Kasai et al., 1976; Nozawa et al., 1974). In other words, in response to a rigidifying stress, *Tetrahymena* increases the unsaturation of its membranes and this increase is correlated with an increase in membrane "fluidity" as measured by the fluorescence polarization of the probe 1,6-diphenyl-1,3,5-hexatriene (DPH; see below).

Membrane Enrichment and Mammalian Membranes. Others have shown that enriching mammalian cell membranes with polyunsaturated fatty acids affects both membrane transport and the activity of membrane bound enzymes (see Spector & Yorek for a review) and that these effects are correlated with an increase in "fluidity" as judged by both fluorescence polarization and electron spin resonance spectroscopy (ESR; see Spector & Yorek for a review). ESR studies have shown that myelin membranes (high content of saturates and monounsaturates) are more "rigid" than synaptosomal plasma membranes or synaptic vesicles (both have a high content of DHA; Viret & Leterrier, 1976; Chin & Goldstein, 1977), a ^{13}C NMR analysis of rod outer segments has revealed long T_1 values

for the methylene carbons of DHA indicating considerable motional freedom (Millet et al., 1973), and fluorescence polarization of the probe, trans-parinaric acid, indicates that an increasing DHA content of PC subfractions from rod outer segments is correlated with increasing "fluidity" of liposomes (Miljanich et al., 1979). Several experimental techniques therefore indicate that an increase in the proportion of unsaturated lipids as well as an increase in the degree of unsaturation of individual acyl chains are both correlated with increased "fluidity".

The Effects of Unsaturation on the "Fluidity" of Model Membrane Systems: Biophysical Studies

Studies performed with biological systems are very useful but due to the complexity of structures found in biological membranes, a clear understanding of membrane "fluidity" is difficult to obtain. To gain a more quantitative and qualitative measure, the physico-chemical properties of simple model systems containing unsaturated acyl chains have been analyzed by a variety of physical techniques which differ in the type and detail of the information that can be obtained, and also in the requirement or lack of requirement for "reporter groups" (see Figure 1.4 for a schematic diagram of some common reporter groups). These techniques will be discussed in terms of the effects of polyunsaturation on membrane "fluidity".

Differential Scanning Calorimetry (DSC). Differentiial Scanning Calorimetry is a noninvasive technique used to measure the gel-to-liquid crystal transition temperature (T_c) of membranes and it has been applied to model systems composed of a variety of polyunsaturates. Based on statistical mechanical theories it has been shown that,

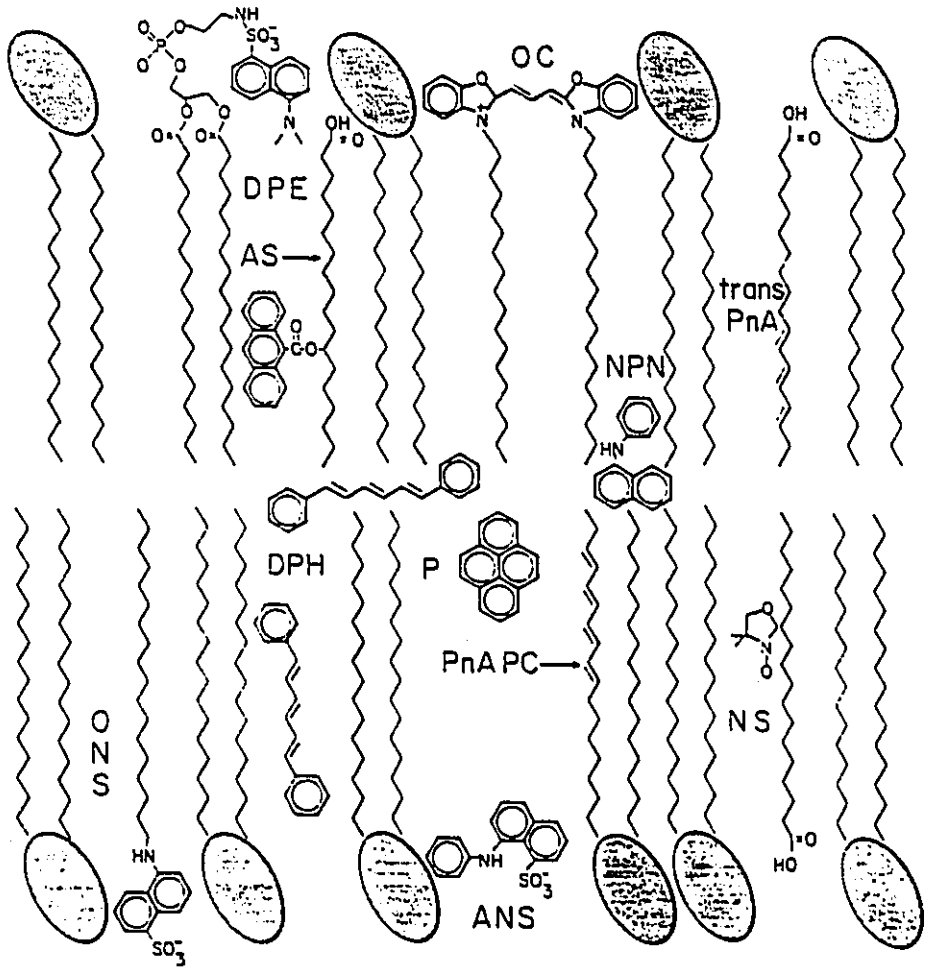

Figure 1.4. A schematic diagram of some molecular membrane probes. Abbreviations are as follows. From left to right: DPE: dansyl phosphatidylethanolamine; AS: anthroyl stearic acid; OC: octadecyl carbocyanine; trans PnA: all-trans parinaric acid. In the center of the bilayer: DPH: diphenylhexatriene; P: Perylene; NPN: N-phenylnapthylamine. Lower monolayer: ONS: octadecyl naphthylamine sulfocholine, NS: nitroxide stearic acid. The probe trimethylamine diphenylhexatriene (TMA-DPH) is not shown but occupies a position parallel to the bilayer normal with the trimethylamine group at the acqueous interface. Figure from Dratz & Deese (1986).

in general, the lower the transition temperature the more disordered is a compound at a given temperature in the liquid state (Seelig & Seelig, 1977a). Therefore, a low gel-to-liquid crystal transition temperature should, in general, correlate with increased membrane "fluidity".

DSC has shown that bilayers composed of phosphatidylcholines with two stearoyl chains are in the gel state at physiological temperatures, but the introduction of oleic acid (one double bond) into the *sn*-2 position causes a disordering of the gel phase and leads to a dramatic decrease of 50 °C in the transition temperature of the bilayer. As shown in Figure 1.5, introduction of a second double bond into the *sn*-2 chain causes a further decrease in T_C, but lecithins with 3-6 double bonds actually have increased transition temperatures (Coolbear et al, 1983). In fact, the transition temperature of 1-palmitoyl-2-palmitoleoyl PC (one double bond) is very close to that of 1-palmitoyl-2-docosahexaenoyl PC (PDhPC; six double bonds; Deese et al., 1981). Based on the statistical mechanical argument presented above, a "fluidizing" effect can be argued for lipids of low unsaturation relative to saturates, but highly unsaturated lecithins appear to be less "fluidizing" then their diunsaturated counterparts. The important effects of DHA on membranes (as discussed under "The Distribution of Unsaturated Lipids and Their Effects on Tissue Function") therefore cannot be explained by an effect on the membrane "fluidity" as measured by this technique and therefore additional properties of the acyl chains must be reponsible for their important biological effects.

DSC has also shown that the number of double bonds in a fatty acyl chain is not the only factor affecting the transition temperature of lipids. A series of lecithins containing two eighteen carbon monounsaturated acyl chains with the double bond at each possible carbon have been examined and the results show that when the double bond is at the centre

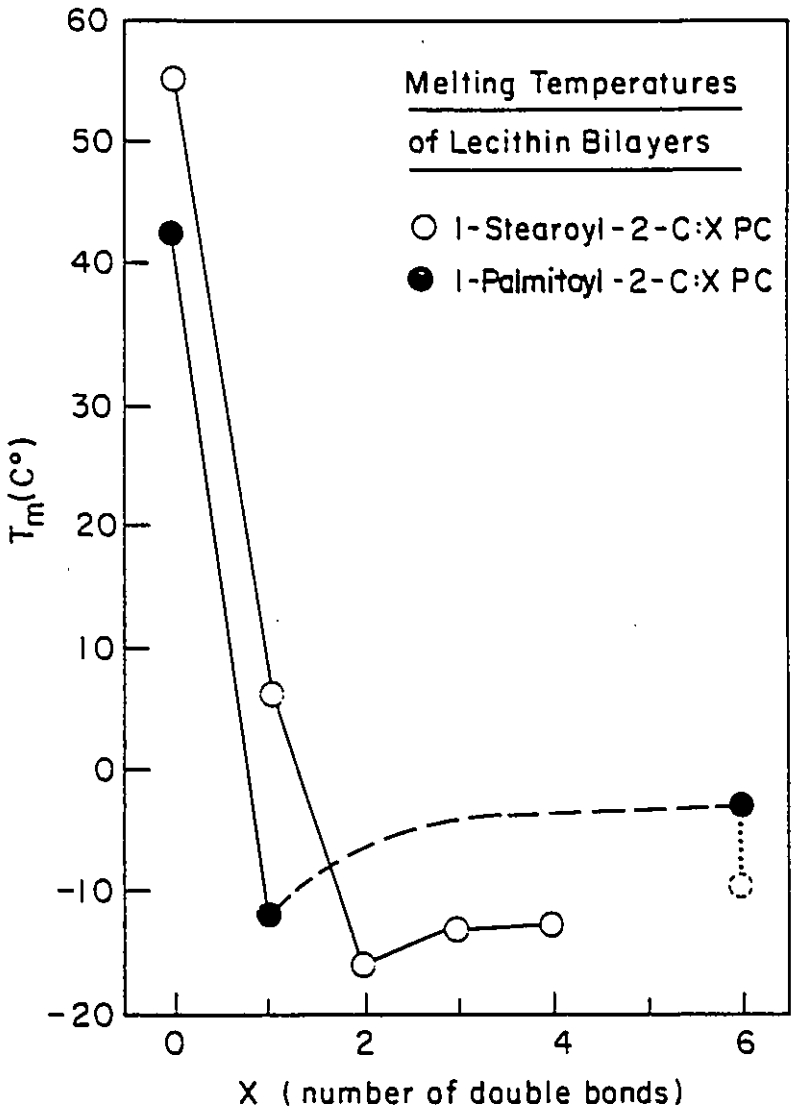

Figure 1.5. The gel-to-liquid crystal transition temperatures of phosphatidylcholine bilayers as a function of the number of double bonds. The 1-stearoyl-2-C:X PC data was obtained by differential scanning calorimetry (Coolbear et al., 1983) and the 1-palmitoyl-2-C:X PC data was obtained by NMR (Deese et al., 1981). From Dratz & Deese (1986).

of the chains (carbons nine to ten) the transition temperature is 60 °C lower than when it is close to the methyl or carboxyl termini (Barton & Gunstone, 1975). A similar situation is also observed when the melting temperatures of unesterified mono, di, and tri-unsaturated fatty acids are examined (Gunstone & Ismail, 1967; Christie & Holman, 1967). If the melting temperature data can be extrapolated to bilayers composed of phospholipids with the same acyl chains (as it can for the monounsaturates) then the position of the double bonds in di and tri-unsaturated lecithens will also have an effect on the transition temperatures of the lipids. The correlation between membrane "fluidity" and the number of double bonds in a membrane is therefore not as simple and straightforward as was generally thought.

Phospholipid Surface Area Measurements. Lipid monolayers have been used to study the effects of unsaturation on the surface area of phospholipids. At a given temperature and lateral pressure the surface area of a lecithin with two saturated chains is relatively low, however, the introduction of one double bond into the *sn*-2 fatty acyl chain dramatically increases the surface area of the phospholipid (Evans & Tinoco, 1978). In parallel with the DSC data, however, the effects of additional double bonds are minimal and in fact the results indicate that DHA adopts a very compact structure. The surface area of unsaturated phospholipids therefore does not provide insight into the effects of highly unsaturated fatty acyl chains on membranes.

Fluorescence Polarization. Another technique which has been used to investigate the physico-chemical properties of unsaturated lipids in membranes is fluorescence polarization. In steady state fluorescence, a probe is placed in a membrane

and is excited with plane polarized light. If the probe does not move (slow motions) before it fluoresces the emission is highly polarized whereas if the probe does move (fast motions) the emission is weakly polarized. Results have generally been interpreted in terms of the microviscosity of the system which can be calculated using the Perrin equation and hydrocarbons of known viscosity as a calibration standard (Shinitzky & Barenholtz, 1974; Dratz & Deese, 1986). Unfortunately, the Perrin equation assumes that the probe undergos isotropic motions (as it would in solution) and it has been shown that reference hydrocarbons of very similar viscosities yield widely different polarization values (Hare & Lussan, 1977). Membrane microviscosity is therefore not a well defined parameter and many of the conclusions from the fluorescence measurements quoted above, are questionable.

Time-resolved fluorescence depolarization measurements can also be performed and the conclusions derived from these studies are more reliable (Wolber & Hudson, 1981). The results are generally interpreted in terms of the molecular order and dynamics of the probe which are thought to reflect the same properties of the lipid environment. As discussed above, if the membrane is ordered its components undergo motions of small amplitude whereas if it is disordered the lipids undergo motions of large amplitude (ie. motions are less restricted) and according to the generally accepted definition, a membrane of high "fluidity" should be relatively disordered and should also undergo fast motions.

Both steady state and time resolved fluorescence have been used to study the motions of the probe DPH in model membranes composed of a series of lecithins with their *sn*-2 position acyl chain ranging in degree of unsaturation from zero to four double bonds. The results indicate that there is no change in the motional cone angle (average order), essentially no change in the wobbling diffusion constant (rate of motion), and no change in

the steady state anisotropy (relates to both) of the probe upon increasing unsaturation (Stubbs et al., 1981). It therefore appears that unsaturation has very little effect on the motions of DPH and thus on membrane "fluidity". The study, however, has been criticized because significant amounts of DPH align themselves parallel to the bilayer surface (ie. at the centre of the bilayer) and it is not apparent whether this affects the data, and because the data was interpreted using a wobbling-in-cone model (Deinem et al., 1988). It is also not clear whether a rigid molecule, such as DPH, can detect subtle differences between the motions of different unsaturates.

In another study, angle-resolved fluorescence depolarization measurements of DPH and the probe 1-[4-(trimethylammonio)phenyl]-6-phenyl-1,3,5-hexatriene (TMA-DPH) were made in bilayers composed of dimyristoyl PC (DMPC), 1-palmitoyl-2-oleoyl PC, (POPC) and dilinoleoyl PC (DLPC). The results were interpreted using a rotational diffusion model and the conclusions of this study were that in bilayers of increasing unsaturation (up to four double bonds in DLPC) the ordering of the system decreased as did the rates of probe motion (Deinum et al., 1988). As with the previous work, this study does not provide the expected results based on the accepted concept of "fluidity" but to a certain extent the interpretations of the results are model dependent and therefore are not conclusive. In addition, the phase transition temperatures were not accounted for in the comparison of results for the different lipids (see reduced temperature below and in Chapter 2 under "Applications").

Electron Spin Resonance (ESR). ESR has also been used to investigate membrane "fluidity" but in general studies have focused on biological systems as opposed to model membranes (Hsung at al., 1974; Huang et al., 1974). In one study, however, bilayer mixtures of 1-stearoyl-2-oleoyl PS and 1-stearoyl-2-docosahexaenoyl PS purified

from brain were examined and it was concluded that increasing the proportion of the DHA containing lipid in the membrane increases the "fluidity" of the system (Salem et al., 1986). However, the experiments were performed at temperatures where some of the membranes should be in the gel state while others should be in the liquid crystalline state and the distinction between the two was not made in the interpretation of the results. The technique also requires the use of a bulky probe, and it has been shown that probes can change in conformation according to their environment (Taylor & Smith, 1982). The conclusions drawn from the study, therefore, may not be justified.

Nuclear Magnetic Resonance Spectroscopy (NMR). In recent years, investigators have turned to NMR spectroscopy in order to obtain more detailed information on the motions of polyunsaturated lipids in bilayers. Deuterium NMR is generally the method of choice because information on the ordering, the structure, and the dynamics of the lipids themselves (as opposed to the same properties of a probe in a membrane) can be obtained. The technique has provided a detailed description of the ordering of lipids in membranes as will be discussed in more detail in Chapter 2. Here, experiments that have attempted to apply the technique to understanding the effects of polyunsaturation on membranes will be described.

Salmon et al. (1987) examined the effects of unsaturation by comparing ^2H NMR spectra from aqueous dispersions of dipalmitoyl PC (DPPC) and 1-palmitoyl-2-docosahexaenoyl PC (PDhPC) with the deuterium labels located on the palmitoyl chains. At the same temperature, each position along the palmitoyl chain had a smaller quadrupolar splitting in PDhPC than in DPPC and the plateau region of high order (see Chapter 2) was reduced in length for PDhPC. The quadrupolar splittings are related to the ordering of the system and a small value corresponds to a low degree of order. At the same reduced

temperature (T_{red}), however, the palmitoyl chain of PDhPC appears to be more ordered than it is in DPPC (see Chapter 2 for a thorough discussion of ordering and reduced temperatures). It was concluded that the interactions of the two chains in DPPC are significantly different than the interactions of the palmitoyl and docosahexaenoyl chains in PDhPC but no insight into how they are different was gained.

Paddy et al. (1985) performed a similar study varying the *sn*-2 fatty acyl chain in lecithins perdeuteriated along the sn-1 palmitoyl chain and their results were similar to those of Salmon et al. (1987). At the same reduced temperature the palmitoyl chain was more ordered in PDhPC than in DPPC but the ordering was slightly less than in 1-palmitoyl-2-palmitoleoyl PC. T_1-spin lattice relaxation measurements were also recorded and one possible interpretation of the results is that, at the same reduced temperature, fast motions are more predominant for the unsaturated lipids than for the saturated lipids. Little difference, however, was noted between the monounsaturate and the hexaunsaturate.

A different approach was used by Yeagle & Frye (1987) to examine the ordering of polyunsaturated lipids. Using dioleoyl PC (DOPC) deuteriated at the nine and ten positions of each chain as a probe, the motional order of model bilayers composed of DMPC, DPPC, POPC, DLPC, and diarachidonoyl PC (DAPC) were examined. The spectra for the highly unsaturated systems generally were broadened, possibly due to an increase in the intensity of low frequency motions, and indicate that there is relatively little difference in the motional order of the probe in bilayers of increasing unsaturation. The results, however, are unusual because almost no change in the spectra or the ordering of the probe is observed between the saturated system, which should be in the gel state, and the unsaturated systems, which should be in the liquid crystalline state and in other systems the spectra of oleoyl chains are dramatically different in the two states. The physical

properties of the probe itself (which contains two unsaturated chains) are also not well characterized nor are its properties upon mixing with other lipids. The results presented here may therefore arise because the probe is self-associating in the bilayer and thus forming its own micro-environment.

The rates of motion in similar model systems were also examined (Yeagle & Frye, 1987) using ^{13}C NMR and magic angle spinning. The results showed, in agreement with others, that the rates of motion are relatively slow at positions along the acyl chains in the plateau region of high order but increase towards the interior of the bilayer. The rates of motion of the highly unsaturated lipids (diarachidonoyl PC), however, were not significantly different when compared to saturated systems. Unfortunately the measurement temperatures were not given and therefore it is difficult to compare the results. In addition, the conclusions are limited to motions on time scales within one or 2 orders of magnitude of the Larmor frequency (37.7 MHz) and therefore the results do not tell the whole story. For example, the relaxation data could arise because the long axis rotation rate of the lipids (or another motion) does not change significantly from one system to another, whereas the rate of a different motion, that occurs on different time scale, may change significantly.

One spectrum of an aqueous dispersion of PDhPC deuteriated at each alkene carbon of the docosahexaenoyl chain has been published and is shown in Figure 1.6 (Dratz & Deese, 1986). A detailed analysis of the ordering of the polyunsaturate was not presented but it was suggested that the spectrum is consistent with the hypothesis that the fatty acid adopts a helical conformation in the bilayer. As discussed below it has been suggested by others that this conformation is responsible for the effects of polyunsaturates on membranes (Applegate & Glomset, 1986).

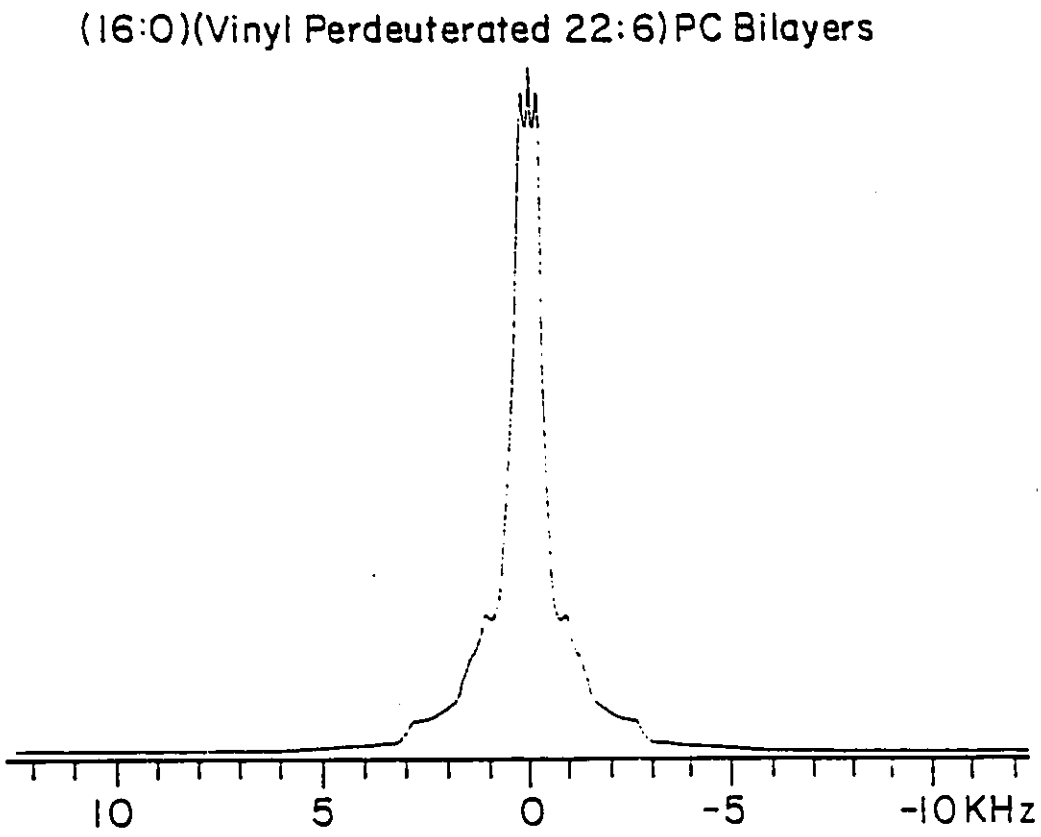

Figure 1.6. Deuterium NMR spectrum of an aqueous dispersion of 1-palmitoyl-2-(vinyl perdeuteriated) docosahexaenoyl PC at 25 °C. The spectrum was obtained at 55 MHz on a Nicolet NT-360 spectrometer by Dratz & Deese (1986).

Computer Modeling Studies of DHA

In essentially all polyunsaturated fatty acids found in nature the double bonds are separated from each other by individual methylene units. The fatty acids can therefore be visualized as consisting of repeating propene segments (bold face) or overlapping 1,4-pentadiene units (indicated by the lines) as shown below:

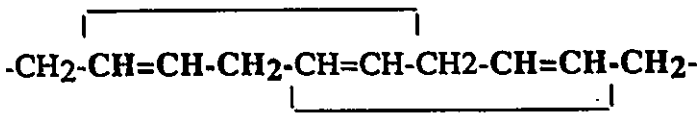

The chemical structure shown here is very succeptible to oxidation and the degree of succeptibility increases with an increasing number of double bonds (Whitting et al., 1961; Porter, 1986). Highly unsaturated lipids are therefore potentially very dangerous to mammalian systems and it seems unlikely that a requirement for such large quantities of lipids, with this particular configuration, would evolve unless the configuration imparted important properties onto the fatty acyl chains.

Applegate and Glomset (1986) developed a computer modeling program to investigate the structural properties of polyunsaturated fatty acids and they showed, in agreement with experimental data, that this pentadiene unit has a particular low energy conformation consistent with the crystal structure of linoleic acid ($18:2^{\Delta 9,12}$) shown in Figure A1.1 (Appendix 1). In this conformation, the two double bond directions are essentially parallel and the double bond planes are at 90^{o} with respect to each other.

Assuming this conformation for each pentadiene unit, the program then calculated the low energy conformations of a 19 carbon chain with 6 double bonds, and two structures consistent with the parallel packing constraints of a bilayer, were the result (see Figure 1.7 for one of the structures). It was suggested that these two structures, a helix and an angle-iron, had unique packing properties in membranes and were responsible for the important effects of polyunsaturates on membrane function (NB. in both the angle iron and helical conformations, the double bonds are parallel to the bilayer normal. The fatty acid studied in this thesis does not have enough double bonds to distinguish between the two and therefore in future discussions the two conformations will be collectively referred to as the angle iron/helical conformation).

The existence of such structural properties for polyunsaturated acyl chains has not been investigated experimentally. The only structural work that has been performed is an X-ray crystallographic study of linoleic acid (18:2 ω-6 or 18:2$^{\Delta 9,12}$) and the results confirm the existence of the conformation proposed above for the 1,4-pentadiene unit, however, the crystal structure of the fatty acid was such that the long axis of the molecule is not oriented parallel to either double bond direction as shown in Figure 1.7. The presence of additional double bonds in the chain, however, may lead to the type of structures proposed by Applegate and Glomset (1986).

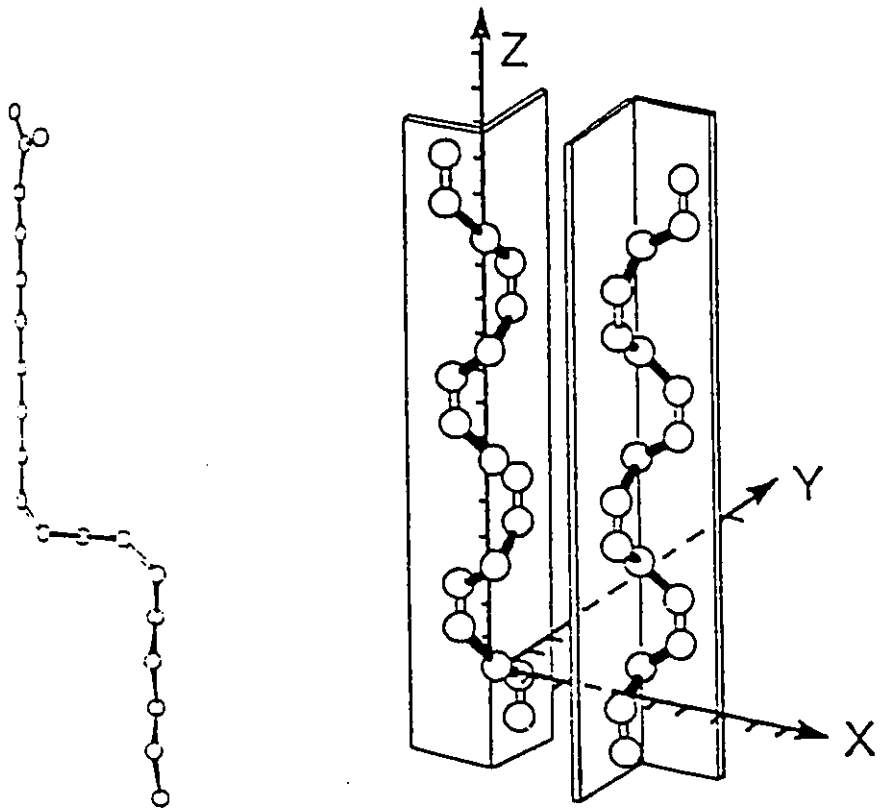

Figure 1.7. A comparison of the crystal structure of linoleic acid (Ernst et al., 1979) with the proposed angle iron structure of docosahexaenoyl chains in lipid bilayers (Applegate & Glomset, 1986).

Summary and Conclusions

It is generally assumed that the role of polyunsaturation in mammalian systems is to maintain membranes in a state of high "fluidity" so that proper membrane function can occur. This hypothesis arose from DSC data which showed that lipids containing a monounsaturated acyl chain have a much lower T_c than the same lipid with two saturated chains and by extrapolating the data it is often suggested that increasing the unsaturation further (ie more than one double bonds) causes a further decrease in T_c and thus an increase the "fluidity" of the system. As shown above (see Differential Scanning Calorimetry), however, this extrapolation is false and therefore the "fluidity" argument cannot be used to explain the important effects of highly unsaturated lipids, such as DHA, on membrane function.

Other techniques, such as fluorescence polarization, ESR, and NMR have also been used to examine the effects of unsaturation on membrane order and dynamics but these techniques have provided contradictory and often confusing results. The only concrete conclusion that can be made is that definitive work in this area is necessary. In addition, the existence of unique structures, such as those proposed by Applegate and Glomset (1986), and their effect on membrane function must be investigated to determine whether it is the overlapping 1,4-pentadiene unit which imparts onto polyunsaturates their unique effects.

The goal of this thesis was to obtain more detailed information on the physico-chemical properties of polyunsaturated fatty acyl chains in membranes by NMR and thus obtain a better understanding of the effects of polyunsaturation on biological membranes.

The thesis is divided into six chapters as follows: Chapter 2 describes the techniques of deuterium and phosphorus NMR spectroscopy and the type of information that can be obtained using both techniques. A more detailed outline of the goals of the thesis can also be found in this chapter under the section entitled "Summary and Thesis Goals". Chapter 3 describes the experiments that were performed in order to synthesize the deuteriated diunsaturated fatty acid, isolinoleic acid ($18:2^{\Delta 6,9}$) which is the focus of the NMR work presented in later chapters. The bulk of the NMR experiments are presented in Chapter 4 and Chapter 5 describes NMR experiments on oriented bilayers of the lipid which were necessary for the interpretation of the NMR data presented in Chapter 4. Finally, a summary and brief discussion of the results will be presented in Chapter 6.

Chapter 2

Deuterium and Phosphorus NMR: Theory and Applications

Chapter 2

Deuterium and Phosphorus NMR Theory and Applications.....33

Theory 35

Deuterium NMR Spectroscopy 35

The Magnetic Hamiltonian, H_M. 37

Quadrupolar Hamiltonian, H_Q. 39

Dipolar Hamiltonian, H_D. 45

Phosphorus NMR Spectroscopy 47

Applications 50

Deuterium NMR Spectroscopy 50

Phosphorus NMR Spectroscopy 56

Summary and Thesis Goals 57

Theory

Deuterium NMR Spectroscopy

Deuterium NMR spectroscopy is a technique that can provide detailed information about the structural and dynamical properties of polyunsaturated lipids. Interpretation of deuterium NMR spectra in terms of molecular order parameters and acyl chain structure, however, requires the use of quantum-mechanical theory and therefore, a brief review of quantum mechanics, from an NMR perspective, is essential for an understanding of the work presented in this and subsequent chapters. A review also provides the opportunity to highlight the assumptions inherent in the analysis and to point out both the potential and the drawbacks of the technique.

Atomic nuclei that possess both spin angular momentum and a magnetic moment assume discrete spin energy levels called "stationary states" (ie. the energy is quantized) in an external magnetic field (H_0). If a radiofrequency (rf) field is then applied whose frequency satisfies the Bohr condition,

$$\Delta E = h\upsilon \qquad (1)$$

where ΔE is the energy between two stationary states, h is Planck's constant, and υ is the frequency of the radiation; energy is absorbed and a transition between the two states is induced. This phenomenon is referred to as "magnetic resonance" and its detection and interpretation is the basis of any NMR experiment.

The utility of NMR spectroscopy arises because the NMR active nuclei within a sample not only interact with the applied magnetic field, as discussed above, but also with each other and with electrons and electric field gradients (for spin > 1/2 nuclei) within the sample. The magnitudes of these additional, local interactions depend upon the nature (for example their spin quantum numbers, I, etc.) and the number of interacting magnetic moments, the distance between the interacting moments, and orientational and motional effects. These local interactions are also relatively weak but they do affect the number and the energies of the stationary states that a given nucleus can attain and thus the energies or frequencies of its NMR transitions. NMR spectra therefore contain information on both the structural and dynamic properties of nuclei.

Interpretation of NMR spectra can be a difficult process and requires use of the spin Hamiltonian, $\boldsymbol{H}$ (Abragam, 1961). The Hamiltonian is a mathematical expression that describes all of the magnetic interactions discussed above and is used to predict the energy levels of the stationary states of a system of nuclei via the Schrodinger equation:

$$\boldsymbol{H}\,|\alpha\rangle = E\,|\alpha\rangle \qquad (2)$$

where $|\alpha\rangle$ is a wave function used to describe the stationary state and E is the energy of the state $|\alpha\rangle$. If the frequencies of all NMR transitions in a spectrum can be predicted from the Schrodinger equation, the resonance frequencies can be related to physical parameters such as structure and dynamics via the Hamiltonian.

The Hamiltonian is usually broken up into a number of terms, each describing a specific type of magnetic interaction, so that individual interactions can be dealt with

separately. To interpret deuterium NMR spectra in terms of the average structure and the molecular order of membrane lipids, three terms will be considered:

$$H = H_M + H_Q + H_D \quad (3)$$

where H_M is the magnetic Hamiltonian, H_Q is the quadrupolar Hamiltonian, and H_D is the dipolar Hamiltonian.

The Magnetic Hamiltonian, H_M. The interaction of a nuclear magnetic moment with an applied magnetic field is called the Zeeman interaction and is described by the magnetic Hamiltonian, H_M. A consequence of the Zeeman interaction is that a deuterium nuclear spin (which has a spin quantum number of 1) can assume one of three different energy levels or stationary states in a magnetic field. The energy of each state can be calculated from the Schrodinger equation and both of the allowed NMR transitions between states have the same energy (Figure 2.1) and therefore the same transition frequency (ie. they are degenerate):

$$\upsilon = gB_NH_o \quad (4)$$

where g is the so-called g-factor and B_N is the nuclear magneton (Harris, 1984). From this equation the Larmor (resonance) frequency at any field strength can be calculated and for

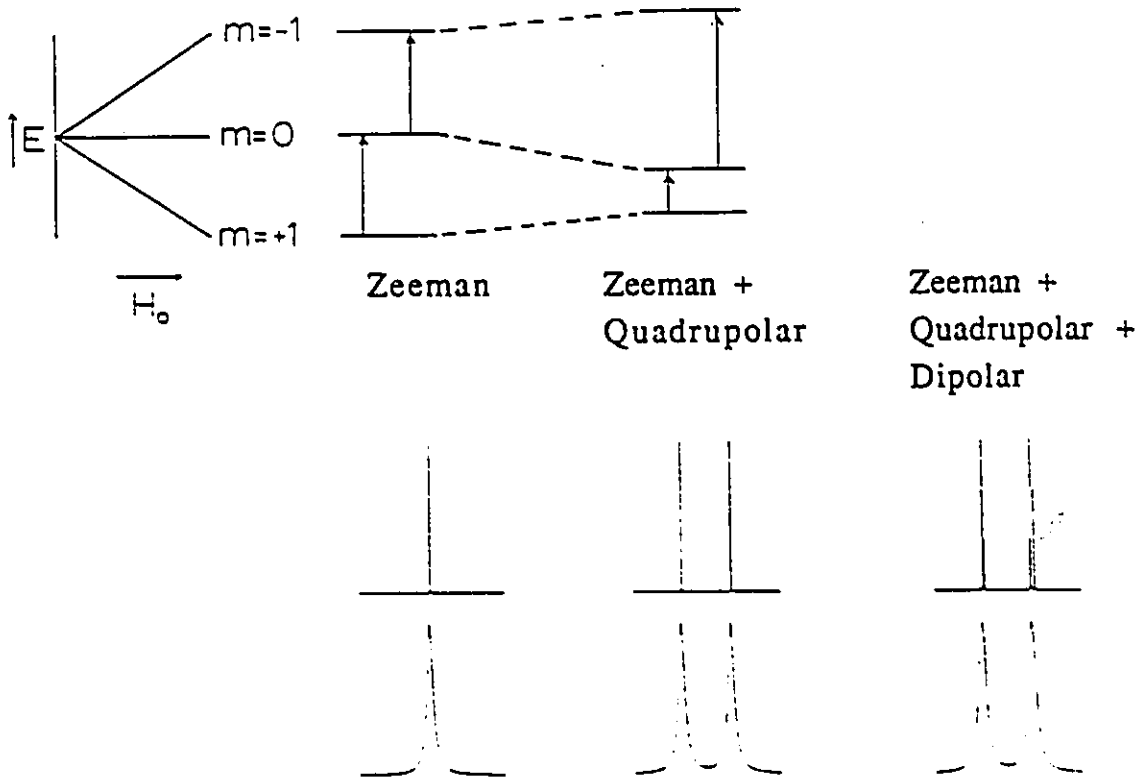

Figure 2.1. Effect of Zeeman, Quadrupolar, and Dipolar interactions on the energy levels and the NMR spectrum of a quadrupolar spin = 1 nucleus. Transitions between energy levels (stationary states) give rise to NMR resonance lines which in practice are broadened into Lorentzian peaks due to relaxation effects. An energy level diagram including dipolar interactions is not shown because the number of energy levels depends upon the number of interacting nuclei and even with two dipolar coupled nuclei the diagram becomes quite complex. The spectrum is for two dipolar coupled quadrupolar spin = 1 nuclei each with an equivalent quadrupolar interaction. In this case the spins undergo 12 transitions which result in a spectrum consisting of 6 resonance lines (some transitions are degenerate). In practice, dipolar interactions generally lead to a slight broadening of the peaks.

the work presented here, where both a 7.03 Tesla and a 4.69 Tesla magnet are used, the resonance frequencies are 46.064 MHz and 30.700 MHz, respectively.

Quadrupolar Hamiltonian, H_Q. Due to an unsymmetrical charge distribution, the deuterium nucleus possesses a quadrupole moment that interacts with the electronic environment surrounding the nucleus (the electric field gradient, efg). This quadrupolar interaction is mathematically defined by the Quadrupolar Hamiltonian and its net effect is a perturbation of the Zeeman energy levels (ie. the energies of the stationary states) so that the two allowed NMR transitions are no longer degenerate. Most spectra therefore consist of a doublet, instead of one peak (see Figure 2.1). The separation between the two peaks of the doublet, the quadrupolar splitting ($\Delta\upsilon_Q$), can be interpreted in terms of the average structure and ordering of lipids in membranes.

The mathematical formulation of the quadrupolar Hamiltonian shows that the strength of the interaction (and thus the size of the splitting, $\Delta\upsilon_Q$) depends on both the orientation of the dominant axis of the electric field gradient (the V_{zz} term of the efg tensor, see Seelig, 1977) with respect to the magnetic field and the amplitudes of motion of the deuterium nucleus (assuming that the electric field gradient is axially symmetric - which it is for deuterium in C-^{2}H bonds: see Seelig, 1977). For example, if the V_{zz} term of a deuterium nucleus attached to a rigid molecule is aligned parallel to H_o, then the splitting is at its maximum whereas at any other orientation the value is scaled by $(3\text{Cos}^2\,\theta - 1)/2$, where θ is the angle between V_{zz} and H_o. Molecular motion averages the quadrupolar interaction and also reduces the size of the quadrupolar splitting. A rigid deuterium nucleus will therefore give rise to a large quadrupolar splitting but as the amplitudes of motion of the nucleus increase, the size of the splitting will decrease as well.

For deuterium covalently bound to a carbon atom (such as for a deuteriated methylene segment in a lipid acyl chain) the V_{zz} term is coincident with the C-^{2}H bond direction, so in fact the value of the quadrupolar splitting can be related to the average orientation of the C-^{2}H bond and the amplitudes of fluctuation of the C-^{2}H bond about this orientation. The added characteristic of a membrane is that lipids undergo fast axially symmetric motions (for example, rotation) about the bilayer normal. These fast motions average the quadrupolar interaction in such a way that all the orientational effects are referred to the bilayer normal (in addition to the magnetic field direction). The strength of the quadrupolar interaction for membrane lipids therefore depends on three parameters: 1) the average orientation of the C-^{2}H bond with respect to the bilayer normal, 2) the orientation of the bilayer normal with respect to the magnetic field direction (see below), and 3) the ordering (amplitudes of motion) of the C-^{2}H segment.

Following the approach of Seelig (1977), the Schrodinger equation can be solved to yield the following expression:

$$\Delta\upsilon_Q = \frac{3}{2}\frac{eQ}{h} V^{(2,0)} \qquad (5)$$

where e is the elementary charge, Q is the the quadrupolar moment (Table 2.1), and $V^{(2,0)}$ is an irreducible tensor element of the electric field gradient tensor. The mathematical definition of the term $V^{(2,0)}$ depends upon the information that is desired and its derivation is described in detail in Seelig (1977).

In the simplest case, definition of $V^{(2,0)}$ leads to the following expression for the value of the quadrupolar splitting:

$$\Delta\upsilon_Q = \frac{3}{2}\frac{e^2qQ}{h} S_{CD}\left(\frac{3\mathrm{Cos}^2\theta - 1}{2}\right) \qquad (6)$$

where e^2qQ/h is the quadrupolar coupling constant (170 kHz for a methylene unit), θ is the angle between the bilayer normal and the magnetic field direction, and S_{CD} is the carbon-deuterium bond order parameter defined as follows:

$$S_{CD} = \left(\frac{3\mathrm{Cos}^2\beta - 1}{2}\right)\overline{\left(\frac{3\mathrm{Cos}^2\alpha - 1}{2}\right)} \qquad (7)$$

The term involving the angle α is called S_{mol}, the molecular order parameter, and it is a quantitative measure of the amplitudes of fluctuation of the C-^{2}H bond about its average orientation and reflects motions averaged over the time scale of $1/\upsilon_Q$ (10^{-5} - 10^{-6} sec; the line denotes a time average). The term involving the angle β is a geometric factor (referred to here as S_{geo}) which describes the average orientation of the C-^{2}H bond with respect to the bilayer normal. Equations 6 and 7 are valid for any deuteriated lipid undergoing axially symmetric motion (ordering) about the bilayer normal but both assume that the electric field gradient at the nucleus is axially symmetric (see Seelig, 1977). This assumption is found to be true for deuterium covalently bound to carbon atoms.

Based on experimental data it is generally accepted that the average conformation of a saturated chain is the all-*trans* state (Higgs & Mackay, 1977; Smith et al., 1979) and in this conformation the angle between both C-^{2}H bonds of each methylene segment and the bilayer normal is 90°. The geometrical term, S_{geo}, for each methylene segment can therefore be defined (ie. $\beta = 90°$) and the quadrupolar splittings interpreted in terms of the molecular order, S_{mol} of each segment. Introduction of a *cis* unsaturated double bond into a saturated chain, however, prevents the chain from assuming the all-*trans* conformation (Seelig & Waespe-Sarcevic, 1978) and the average orientation of each methylene segment assumed above, is no longer valid. In this situation, the quadrupolar splittings cannot be interpreted in terms of either molecular order paramters, S_{mol}, or the geometry of the segments, S_{geo} and additional information must be obtained in order to say something concrete about either the average orientation of the units or their amplitudes of motion (Seelig & Waespe-Sarcevic, 1978; Dufourc et al., 1983; Taylor et al., 1981). One must therefore resort to other techniques such as the measurement of deuteron-deuteron dipolar couplings as described under "Dipolar Hamiltonian" and in Chapter 5 to solve the problem.

One not only wants to know the average orientation of the individual C-^{2}H bonds with respect to the bilayer normal (ie. S_{geo}), but more importantly the average orientation of the methylene or alkene segments to which the deuterium atoms are covalently bound. This is because a methylene or alkene unit may be able to adopt several orientations with respect to the bilayer consistent with one specific orientation of a C-^{2}H bond (see for example in Chapter 4) and therefore difinition of S_{geo} may still create ambiguity in the results. To define the orientation of the segment one must derive a different expression for the term $V^{(2,0)}$ (equation 5) and this leads to an expression for the quadrupolar splitting that contains additional mathematical terms or unknowns. The result is that for a rigid unit such as a

double bond or a methylene segment, three independent observables are generally required to completely define the orientation of the segment and its molecular order parameter, S_{mol} (assuming axially symmetric motion). This problem will be discussed further in Chapter 5.

One final complicating factor, in the analysis of deuterium spectra, arises due to the dependence of the quadrupolar splitting on the orientation of the bilayer normal with respect to the magnetic field direction, H_0. Lipid dispersion assume spherical aggregate structures (ie. liposomes) and all possible orientations of the microdomains within each liposome occur. The result is an NMR spectrum consisting of a summation of individual doublets called a "powder spectrum" (Figure 2.2) where the separation between the two most intense peaks represents the splitting for the $\theta = 90^o$ orientation. The spectra, however, can be deconvoluted by a process called dePakeing (Bloom et al., 1980; Sternin et al., 1983) which reduces the powder spectrum to that of an oriented sample with the bilayer normal at an angle of $\theta = 90^o$ with respect to the magnetic field direction. The process of dePakeing provides an accurate estimation of the splitting for the 90^o orientation but does lead to a decrease in the signal to noise ratio of the spectrum.

A better feeling for the equations presented above can be obtained if one considers a lipid with saturated acyl chains containing one deuteriated methylene segment. If the deuteriated acyl chain adopts the all-*trans* conformation and the lipid undergoes fast axial rotation, the value of the quadrupolar splitting is described by equations 6 and 7 and is equal to 64 kHz. In this case both β and θ are 90^o and the value of S_{mol} is equal to 1.0 (ie. the chain is completely ordered). If we then allow the lipid to undergo additional whole body motions or segmental motions arising from trans-gauche isomerization about carbon-carbon bonds, the quadrupolar interaction will be averaged to a smaller value and the quadrupolar splitting will therefore be reduced. As the amplitudes of the motions increase,

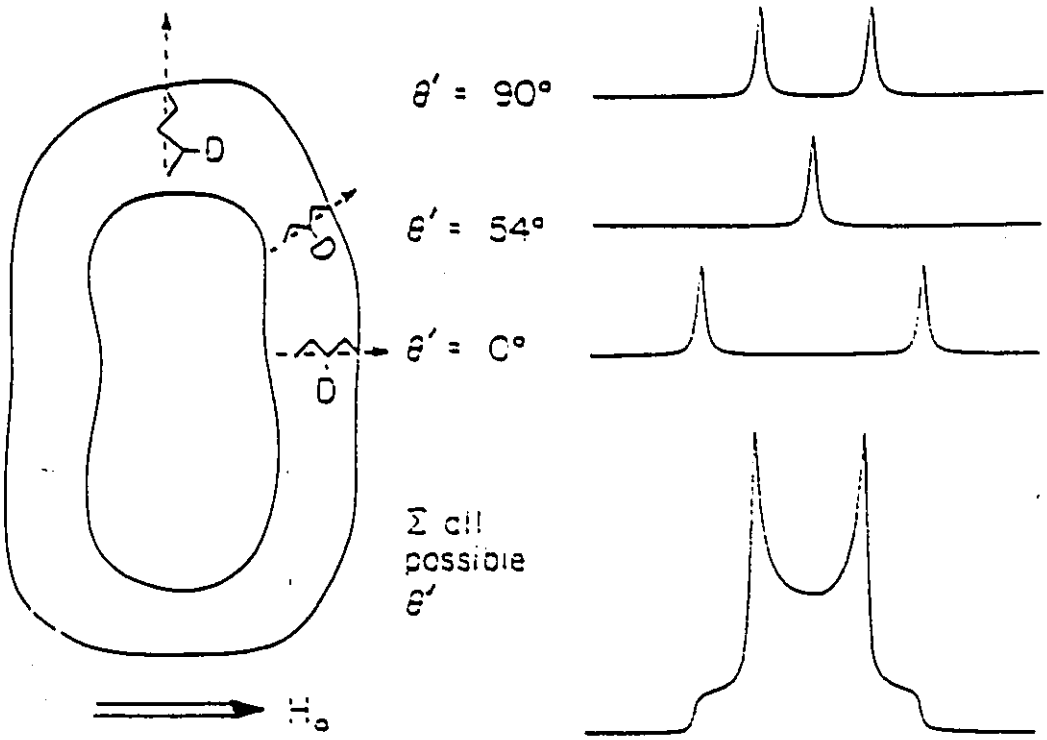

Figure 2.2. Origin of the deuterium NMR "powder spectrum". The deuteriated lipid is undergoing fast axially symmetric motion (eg. rotation) about the bilayer normal and therefore the size of the quadrupolar splitting is scaled by a dependence upon the angle between the bilayer normal and the magnetic field direction, H_o. All possible angles exist for a spherical liposome and each orientation gives rise to a doublet. The sum total of all the doublets gives rise to the "powder" spectrum.

the size of the splitting will decrease further and the lipid segment is said to become increasingly disordered. In the extreme case where the amplitudes of motion are unrestricted (ie. isotropic motion in solutions) the quadrupolar interaction is averaged to zero and both the splitting and the molecular order parameter, S_{mol}, are reduced to zero.

Most deuterium NMR analyses of membranes have focused on determining the ordering of lipids, as indicated under "Applications", but for the analysis of polyunsaturates both the orientation and molecular order of the chains are of interest. If the orientation of each alkene and methylene segment can be determined, then the data can be interpreted in terms of the structure of the chain which can be related to the unique structures proposed in Chapter 1. The molecular ordering of the chain will also give insight into the "rigidity" of the lipids and thus their role in modulating membrane "fluidity".

Dipolar Hamiltonian, H_D. The dipolar Hamiltonian, H_D defines the dipolar interactions between all of the nuclear magnetic moments within a sample and the effect of these interactions is to perturb the Zeeman energy levels in a fashion similar to the effects of the quadrupolar interaction (see Figure 2.1). For a specifically deuteriated methylene segment of a lipid, interactions between the two deuterons of the segment and between each deuteron and neighbouring protons occur so that in principle a complex spectrum should result (ie. a large number of peaks). Because the magnitude of these interactions are small (maximum 4 kHz) relative to the quadrupolar (maximum 250 kHz) and Zeeman (46 MHz at 7 Tesla) interactions, the usual effect, however, is that the two peaks of the quadrupolar doublet are broadened as opposed to being split into number of resonances whose separation is very small (see Figure 2.1).

As will be shown, acquiring spectra of oriented samples with proton decoupling allows one to access the geminal deuteron-deuteron dipolar coupling of a deuteriated methylene segment and the magnitude of this interaction is related to structural information by solving the Schrodinger equation. The result is the following expression (Jarrell et al., 1987; Emsley & Lindon, 1975):

$$D_{DD} = \frac{-\gamma_D^2 h}{4\pi r^3} S_{mol} \left(\frac{3\mathrm{Cos}^2\alpha - 1}{2}\right)\left(\frac{3\mathrm{Cos}^2\theta - 1}{2}\right) \qquad (8)$$

where γ_D is the deuteron magnetogyric ratio, r is the internuclear distance, α is the angle between between the ^2H-^2H internuclear vector and the motional axis (bilayer normal), and θ is the angle between the bilayer normal and the magnetic field. The sum total of all the proton-deuteron interactions can also be accessed and the magnitude of each individual interaction is defined as (Jarrell et al., 1987; Emsley & Lindon, 1975):

$$D_{HD} = \frac{-\gamma_D \gamma_H h}{8\pi} S_{mol} \left(\frac{3\mathrm{Cos}^2\alpha - 1}{r_{HD}^3}\right)\left(\frac{3\mathrm{Cos}^2\theta - 1}{2}\right) \qquad (9)$$

where the symbols are defined in an analogous way to the above equation.

From each equation it can be seen that both interactions depend upon the distance between the interacting nuclei, the orientation of the internuclear vector, and on the ordering

of the segment of interest. In principle they can therefore provide detailed information on lipid structure and as will be shown, can aid in the interpretation of the quadrupolar splittings in terms of the ordering of lipid acyl chains.

Deuterium NMR relaxation times (T_1 and T_2) can also provide detailed information on acyl chain motions and dynamics but due to lack of space these measurements will not be included in the thesis.

Phosphorus NMR Spectroscopy

The majority of the work performed in this thesis involves the use of deuterium NMR, however, important information will be obtained using phosphorous NMR spectroscopy. Phosphorous NMR is used extensively to study lipid bilayers and the spectra can be interpreted in terms of the amplitudes of motion at the headgroup of phospholipids.

The chemical shift of a rigid phosphate group is dependent upon the orientation of the phosphate with respect to the magnetic field direction of the NMR spectrometer. The chemical shielding along the three principle directions are arbitrarily denoted σ_{11}, σ_{22}, and σ_{33} which correspond to the three pricipal components of the chemical shielding tensor describing the Zeeman interaction between the phosphate and the magnetic field.

In a randomly oriented sample, all possible orientations of the phosphate group with respect to H_o occur and the NMR spectrum therefore consists of superposition of resonances with all possible chemical shifts. The result is a powder pattern such as shown in Figure 2.3a (Smith & Ekiel, 1984). In a membrane, fast axial rotation of the

phospholipid leads to partial averaging of the shielding tensor to yield motionally averaged principal components $\sigma_{\perp} = \sigma_{11}$ and $\sigma_{\parallel} = (\sigma_{22} + \sigma_{33})/2$ and the result is a spectrum such as shown in Figure 2.3b. This spectrum is characteristic of lipids organized in multilamellar dispersions and the width of the spectrum is defined as the chemical shift anisotropy, CSA ($CSA = \sigma_{\perp} - \sigma_{\parallel}$). If the lipids undergo further motions, such as whole body wobbling, the chemical shielding tensor is averaged further and the values of $\sigma_{\perp}$ and $\sigma_{\parallel}$ are reduced. The result is a spectrum (Figure 2.3c) with the same line shape as in Figure 2.3b, but with a reduced line width and thus a reduced CSA. The width of the spectrum or size of the CSA is therefore proportional to the degree of order at the phosphate group. In the extreme case of completely disordered motion (ie. isotropic tumbling in solution), the shielding tensor is completely averaged and the spectrum consists of a single resonance with a chemical shift given by the shielding component $\sigma_{iso} = (\sigma_{\perp} + 2\sigma_{\parallel})/3$.

Figure 2.3

Phosphorus NMR spectra arising from the various motional states of a phosphodiester group of a phospholipid. **a)** a static phosphodiester; **b)** an ordered phosphodiester undergoing rapid long axis rotation, and **c)** a disordered phosphodiester.

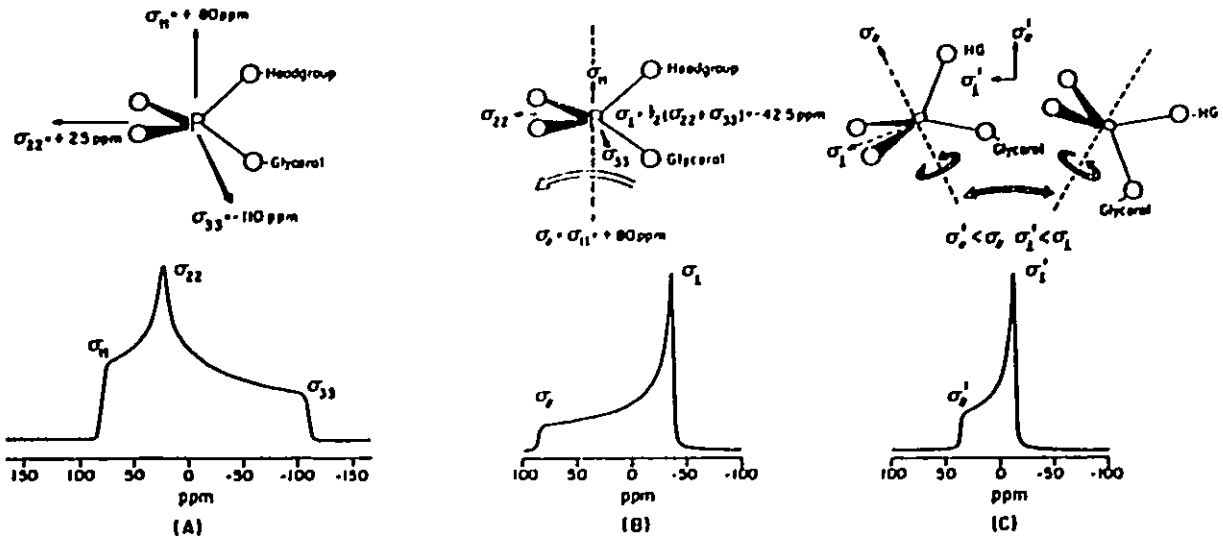
Headgroup
Glycerol
ppm
(A)
(B)
(C)

Applications

Deuterium NMR Spectroscopy

As discussed above, deuterium NMR spectroscopy can provide detailed information on the structural and dynamic properties of lipids in membranes, but due to the low sensitivity (ie. a low γ) and natural abundance of deuterium (see Table 2.1), deuteriated lipids are required. This is an advantage in that one can monitor specific regions of a molecule without background interference by labelling the desired carbon atoms but can be a disadvantage because the synthesis of deuteriated compounds is often difficult and/or time consuming and therefore one is limited to studying lipids (in this case fatty acyl chains) that are readily obtainable in deuteriated form.

Specifically deuteriated saturated and monounsaturated fatty acids have been synthesized and studies of these acyl chains have provided considerable insight into the structure and dynamics of membranes. A variety of saturated lipids have been examined, and qualitatively they all yield the same results. The acyl chains exhibit a constant and high level of order (ie. low amplitudes of motion) for each of the first 8 -10 carbons but become increasingly disordered (large amplitudes of motion) towards their methyl termini (Figure 2.4 and references in the figure caption). The region of high order is called the "plateau" region and, based on statistical-mechanical calculations, its existence is thought to arise as a result of lateral pressure at the headgroup region. A decrease in the lateral pressure should shorten the plateau region and decrease the order parameters, S_{mol}, of each segment,

Table 2.1

Properties of the Deuterium Nucleus[1]

Nuclear Spin	1
Natural Abundance	0.015 %
Sensitivity[2] Relative to ^{1}H	0.965 %
Receptivity[3]	1.45×10^{-6}
Quadrupolar Moment	2.73×10^{-31}

[1] data from Smith & Mantsch (1982)

[2] for equal number of spins

[3] sensitivity relative to protons at natural abundance

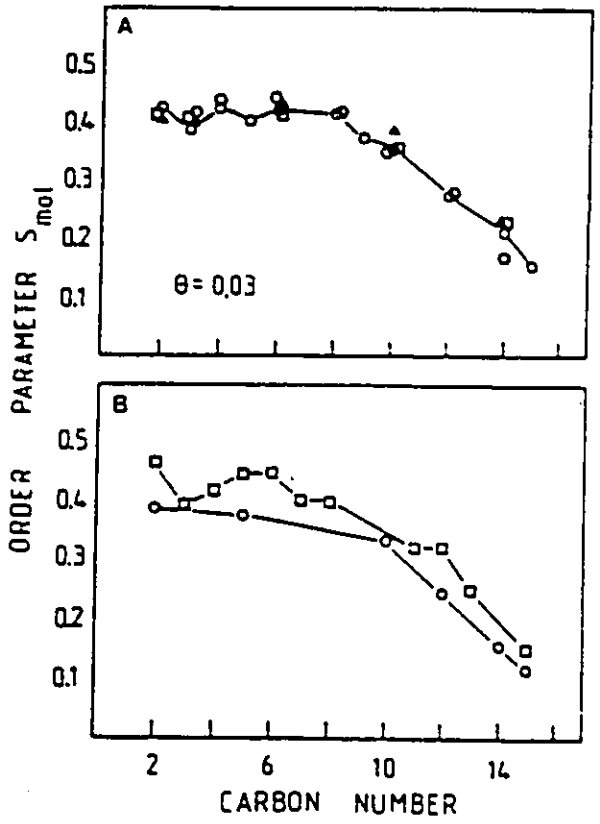

Figure 2.4. A comparison of the order profiles obtained from A) synthetic lipids and B) biological lipid mixtures. A) "o": DPPC (Seelig & Seelig, 1974); "o"; DMPC (Oldfield et al., 1978); "□": DPPS (Seelig & Browning, 1978); and "Δ": DPPA (Browning, unpublished work). B) "o": palmitoyl chains in *A. laidlawii* (Stockton et al., 1977); and "□": palmitoyl chains in *E.coli* (Gally et al., 1980). All data are plotted for the same reduced temperature, $T_{red} = 0.03$.

whereas an increase in pressure should increase both the size of the plateau region and the order parameters.

Quantitatively the order parameter profiles of saturated acyl chains vary from one membrane system to another at any given temperature. When compared at the same reduced temperature ($T_{red} = (T - T_c)/T_c$), however, the order profiles for the acyl chains of different lipids (eg. DPPC, DMPC, DPPS, and DPFA) have remarkably similar values (Figure 8, Seelig & Browning, 1978; Browning, 1981). The use of reduced temperatures allows comparison of the ordering of different systems in the same thermodynamic state and therefore removes the effect of proximity to the gel-to-liquid phase transition temperature from the comparison. The significance is that the values of the order parameters, S_{mol}, for an acyl chain in a biological membrane (where a distinct transition can be defined) are similar to the values of the pure lipids at the same reduced temperature (see Figure 2.4) and therefore with the use of reduced temperatures one can compare the molecular order data obtained from two different lipids in different systems, as if they were in the same membrane. This is particularly important when analyzing the data obtained from polyunsaturated systems because, as shown in Chapter 1 (see "Differential Scanning Calorimetry, DSC"), the unique role of polyunsaturates can not be explained by an increase in "fluidity" arising from the decrease in the gel-to-liquid crystal transition temperature of the lipid. Reduced temperatures allow one to look for additional physico-chemical properties beyond the effect of the transition temperature.

Introduction of a *cis* double bond into a bilayer has also been investigated. The double bond introduces a rigid element into an otherwise flexible hydrocarbon chain and prevents the chain from assuming the all-*trans* configuration (Seelig & Seelig, 1977; Seelig & Waespe-Šarčević, 1978; Rance et al., 1980). In bilayers of POPC labeled along the

oleoyl chain, the double bond causes a large drop in the measured $\Delta\upsilon_Q$ and the calculated S_{CD} order parameters, in the plateau region (Figure 2.5a). It can, however, be shown that the low values of S_{CD} for methylene segments in the region of the double bond is caused by a difference in the average orientation of the segments (ie. S_{geo}) in the region of the double bond as opposed to a difference in the amplitudes of motion (S_{mol}). When the orientational effect is defined (ie. the angle β and thus S_{geo}) the order parameters, S_{mol}, are similar to those for saturated chains (Figure 2.5b). Again there is a plateau region of high order which decreases towards the centre of the bilayer. The double bond therefore appears to undergo the same amplitudes of motion as methylene segments at this position in the bilayer.

Comparison of the palmitoyl and oleoyl chains of POPC also reveals that the absolute values of the order parameters are similar for both the saturated and unsaturated chains although the double bond has a slight rigidifying effect on the saturate. At the same temperature the calculated order parameters for the palmitoyl chain of POPC are also slightly less than for palmitoyl chains in DPPC but at the same reduced temperatures the palmitoyl chains of DPPC are actually less ordered than in POPC. In a biological system containing both species one would therefore expect the POPC lipid to be slightly more ordered than DPPC but the presence of POPC would also have an effect on the phase transition of the membrane (ie. it would drop).

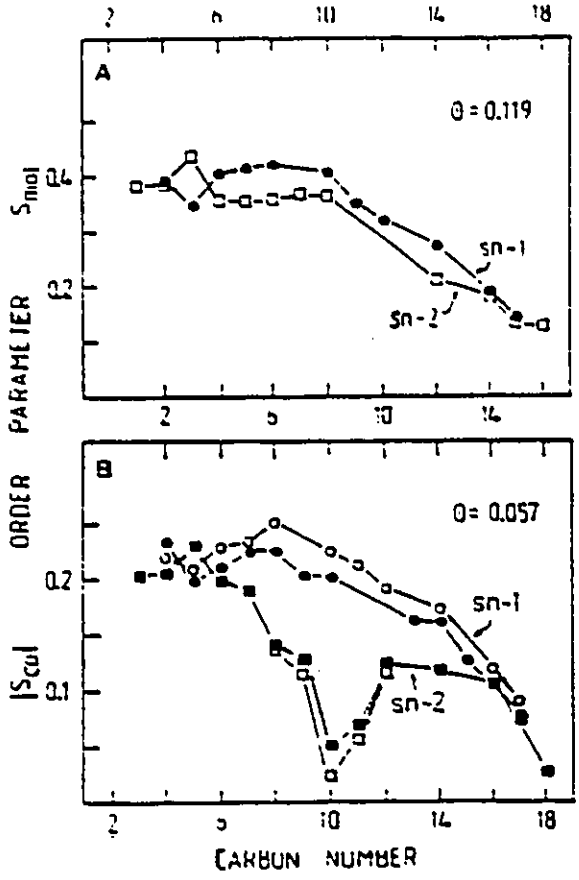

Figure 2.5. A) A comparison of the molecular order parameters, S_{mol}, for the *sn*-1 (o) and *sn*-2 (□) chains in the phospholipid POPC. The data for the *sn*-1 chain are from Seelig & Seelig (1977). The S_{mol} values for the C_8, C_9, and C_{10} position of the *sn*-2 chain are from Seelig & Waesp-Šarčevič (1978) while those for the remaining positions are from membranes of *A. laidlawii* enriched with deuteriated oleic acid (Rance et al., 1980). B) A comparison of the deuterium bond order parameters, S_{CD}, for the palmitoyl (o) and oleoyl (□) chains of POPC (Seelig & Seelig, 1977a, Seelig &Waespe-Šarčevič, 1978; open symbols) and from the membranes of *A. laidlawii* enriched with palmitoyl (Stockton et al., 1977) and oleoyl (Rance et al., 1980) chains. All the data is plotted at the same reduced temperature and the numbering of the *sn*-2 chain has been shifted relative to that of the *sn*-1 chain to account for the staggered conformation of the two chains (Browning, 1981). Figure from Browning, 1981.

Phosphorus NMR Spectroscopy

Phosphorus NMR has been used to investigate the amplitudes of motion at the headgroup region of a number of phospholipids under a variety of different physical conditions and it has also been used to investigate the polymorphism of lipid structures. The work presented in this thesis will be restricted to the former type of analysis. In general the chemical shift anisotropies measured for lipids are fairly constant from one type of lipid to another (in lamellar structures) and are generally in the range of 45 - 50 ppm (Smith & Ekiel, 1984; Hemminga & Cullis, 1982).

Summary and Thesis Goals

From the results presented in Chapter 1 it was concluded that polyunsaturated lipids play an important role in mammalian membranes and that more detailed experiments are required to obtain an understanding of their effect on membrane structure and dynamics. From the discussion presented in this chapter it is clear that, in principle, deuterium NMR spectroscopy can provide information on the structure and the amplitudes of lipid motions and that application of the technique to an analysis of polyunsaturated acyl chains would be extremely informative. Unfortunately, deuteriated compounds are required and this requirement has delayed attempts to study polyunsaturated acyl chains.

Some researchers have resorted to the use of specifically deuteriated lipid probes or to the use of perdeuteriated saturated chains in order to examine the bulk effects of polyunsaturation on membranes (Chapter 1) but the results have not been particularly enlightening. In only one case (other than the work presented here) has a labeled polyunsaturated chain been examined and this study involved a mixed-acid lecithin containing one vinyl perdeuteriated docosahexaenoyl chain. The only published result from this work (so far) is the spectrum shown in Figure 1.6 and it is clear that both the assignment of resonances to individual positions (there are 12 deuteriated sites) and the definition of the orientational versus the ordering effects on the values of the quadrupolar splittings will be very difficult to obtain. Perdeuteriated polyunsaturated lipids clearly do not provide the opportunity to perform a detailed analyses such as has been performed for the saturated and monounsaturated acyl chains. Specifically deuteriated polyunsaturated acyl chains are required.

The goals of this thesis are therefore 1) to develop a procedure for the synthesis of a polyunsaturated fatty acid specifically deuteriated at selected positions along the chain, and 2) to produce and use these deuteriated compounds to study the physico-chemical properties of polyunsaturated acyl chains in model bilayers by deuterium NMR. In the next chapter of the thesis (Chapters 3) a protocol for the biosynthesis of a series of specifically deuteriated isolinoleic acids ($18{:}2^{\Delta 6,9}$) using the protozoan *Tetrahymena* will be presented. In the remaining chapters, the results from a detailed ^2H NMR analysis of the physico-chemical properties of this diunsaturate in model bilayers will be examined and the following questions addressed:

1) Does this diunsaturated acyl chain adopt a conformation consistent with the computer modeling study of Applegate and Glomset (1986)?

2) Does the molecular ordering of the diunsaturated lipid differ from saturated and monounsaturated lipid? In particular, how does the presence of two double bonds affect the order profile and thus the existence of the "plateau" region in the diunsaturated acyl chain?

3) What can the answers to the first three questions tell us about the physico-chemical properties of highly unsaturated lipids such as docosahexaenoic acid?

Chapter 3

Biosynthesis of a Series of Specifically Deuteriated Isolinoleic Acids

---

Chapter 3

Biosynthesis of a Series of Specifically Deuteriated Isolinoleic Acids.....59

Introduction 62

Materials and Methods.....65

Feasibility of a Biological Approach 65

Culture Conditions. 65

Effect of Supplement Concentration. 66
Effect of Growth Temperature. 66
Cell Density Measurements. 66
Gas-Chromatography (GC). 67
Uptake of [1-^{14}C] Oleic Acid. 67
High Performance Liquid Chromatography (HPLC). 68
Liquid-Scintillation Counting. 69
Argentation Chromatography. 60

Characterization of the Deuteriated Products 70

Culture Conditions. 70
Purification. 71
Analysis of Purity. 72
Identification of the Number and Location of the Double Bonds. 72
Identification of the Sites of Deuteration. 72
Oxidation. 73

Results **74**

Feasibility of a Biological Approach 74

Optimization of Growth Conditions. 74
Purification of Isolinoleic Acid. 79

Characterization of the Deuteriated Products 81

Discussion **95**

Summary and Conclusions **102**

Introduction

The chemical synthesis of any fatty acid specifically deuteriated at each individual position along the chain is very difficult and time consuming and the synthesis of specifically deuteriated polyunsaturated fatty acids is complicated further by the ease of oxidation (and thus degradation) of the fatty acids. Consequently, at the commencement of this thesis there were no protocols available for the synthesis of any specifically deuteriated polyunsaturated fatty acids. A series of specifically labelled oleic acids (monounsaturated), however, had been synthesized (Tulloch, 1979) and it was proposed that a biological organism could introduce additional double bonds into the oleic acids thus producing specifically deuteriated polyunsaturated compounds.

The protozoan *Tetrahymena* shares with bacteria an ease of culture but as a eukaryote has the capacity to form highly unsaturated lipids (Figure 3.1) and is therefore an ideal choice for a biosynthetic "factory". An unsaturated fatty acid auxotroph, strain RH179E1 (Hill et al., 1983), which has limited capacity to form unsaturated compounds because it lacks Δ9 and Δ12 desaturase activity (see Figure 3.1 and Hill et al., 1983), is also available and, when supplemented with oleic acid, it incorporates and converts the supplement into the Δ6,9 isomer of linoleic acid, *cis,cis*-octadeca-6,9-dienoic acid (hereafter referred to as isolinoleic acid; Hill et al., 1983; Conner et al., 1984). With the use of deuteriated oleic acid supplements it was therefore hypothesized that a series of specifically deuteriated isolinoleic acids could be produced.

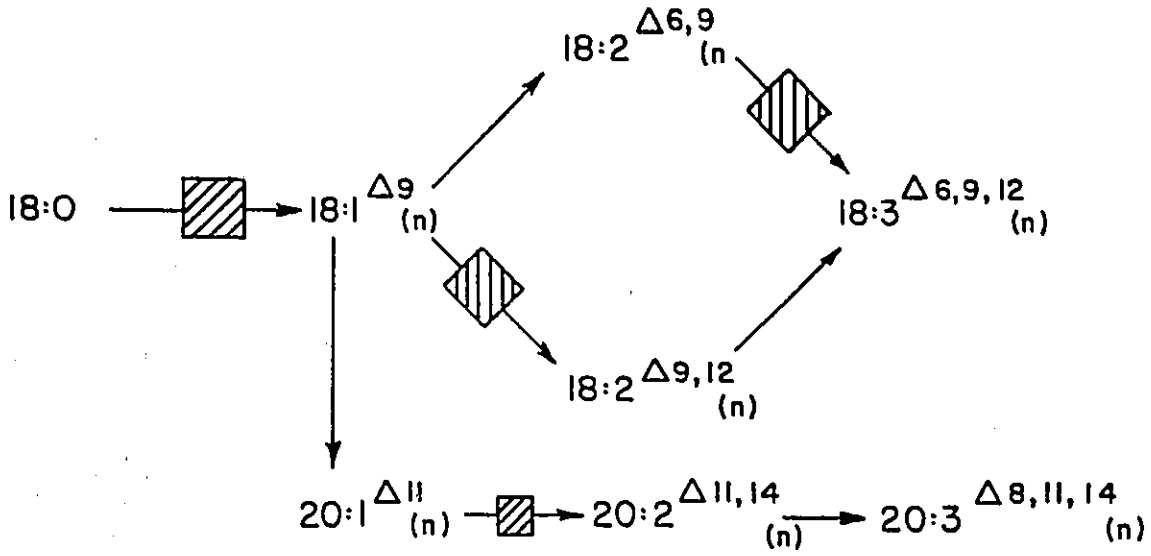

Figure 3.1. Desaturation pathway of 18-carbon fatty acids in *Tetrahymena* . Hatched boxes represent steps in the pathway that are blocked in the mutant, RH179E1, due to deficiences in the Δ9 and Δ12 desaturase enzymes.

This chapter is divided into two sections, each dealing with a different aspect of the biosynthesis of deuteriated isolinoleic acid. The first section, entitled "Feasibility of a Biological Approach" describes the experiments performed to determine the viability of a biosynthetic approach, and also presents experiments performed to optimize the conditions for maximum isolinoleic acid production. The final protocol is described in the second section entitled "Characterization of the Deuteriated Products". A detailed chemical analysis of the deuteriated fatty acids is also presented in this section and the results clearly illustrate that specifically deuteriated isolinoleic acids can be produced for NMR analysis via a biosynthetic route.

Materials and Methods

Feasibility of a Biological Approach

Culture Conditions. The mutant, *Tetrahymena thermophila* (RH179E1), was grown in a medium consisting of bacteriological peptone (1.0% w/v; Oxoid L37), yeast extract (0.1% w/v; Oxoid L21), and $FeCl_3$ added to a concentration of 36 *u*m. Stock cultures of approximately 10 mls were maintained at room temperature in 30 ml covered test tubes by transfering, with a sterile pipette, 4-5 drops of media from a culture of high cell density into fresh media. The transfers were performed each week in order to maintain stock cultures of vigorously growing cells.

Cultures were supplemented with oleic acid as follows: the culture medium was autoclaved for 15 minutes and then after cooling, 41 mg/litre of α-tocopherol (Sigma), 80 mg/litre of both penicillin and streptomycin (Sigma), and fatty acid free bovine serum albumin and oleic acid at a ratio of 40:1 (w/w; both from Sigma), were added. The free fatty acid and α-tocopherol were added as solutions in 95 % ethanol, and the BSA and antibiotics were sterile filtered before addition. All cultures were mixed for 1-2 hours in order to complex the fatty acid with BSA and were then innoculated with either a fresh stock culture of RH179E1 (1-2 weeks old) or as indicated in the text.

Cultures of the wild type strain, *Tetrahymena thermophila* Chx-2/Chx-2 (cysens IV), were grown without a supplement in the peptone/yeast extract medium described above for RH179E1. The cells were harvested, the lipid extracted and saponified (see

below), and the resulting total cellular free fatty acid preparations were used as a lipid source to develop and test the isolation procedures.

Effect of Supplement Concentration. To determine the effect of the supplement concentration on cell growth and isolinoleic acid production, RH179E1 was grown with unlabelled oleic acid at concentrations of 2.5 mg/litre, 5 mg/litre, 10 mg/litre, and 25 mg/litre. One litre cultures in three litre Fernbauch flask were grown at 30 °C to late log phase (approximately twenty four hours) at which time the final cell densities were determined and the cells harvested by centrifugation. The resulting cell pellets were lyophilized, the total lipid was extracted with warm $CHCl_3/CH_3OH$ (2:1, v/v), and the levels of isolinoleic acid determined by GC (see below).

Effect of Growth Temperature. The effect of growth temperature on cell growth and isolinoleic acid production was determined by growing100 ml cultures in 500 ml Erlenmeyer flasks at 15 °C, 20 °C, 25 °C, 30 °C, and 37 °C. Each culture was supplemented at a concentration of 5 mg/litre and was innoculated with an equal portion of a vigorous 100 ml culture to ensure that all started at approximately the same cell density. Growth rates were determined by measuring the cell densities every 3-4 hours, and the amount of isolinoleic acid in each culture was measured by harvesting the cultures at late log phase and then analyzing their fatty acid content by GC.

Cell Density Measurements. For each culture, two 2.0-ml samples were taken with a glass pippete and each was fixed with 2 mls of a 2% formaldehyde solution. Both samples were then diluted with 16 mls of 0.4 % NaCl, and each was counted five times with a counting volume of 0.5 mls on a Coulter Counter (Coulter Electronic Ltd.). The counting parameters were set as follows: a lower threshold of 1.7, an upper threshold

of 99.99, and a current of 120, and the reported cell densities are the average of all ten measurements (ie. two samples, five determinations each).

Gas-Chromatography (GC). Fatty acid methyl esters were prepared by either refluxing the cell extracts in 4.5 mls of methanolic HCL (acetyl chloride 1:16, v/v) for 45 minutes or by the method of Morrison & Smith (1964) using BF_3. For the latter, the reaction was carried out at 100 °C for 5 minutes in methanol/hexane (3:1, v/v) rather than in pure methanol and in both procedures the solutions were cooled with the addition of one ml of H_2O and extracted with hexane. Samples were concentrated and injected into an HP5710A gas chromatograph (Hewlett Packard) equipped with a 30 m x 0.75 mm i.d. Supelcowax 10 column (Supelco), an HP3380A integrator, and a flame ionization detector. Heptadecanoic acid was used as an internal standard.

Both methylation procedures gave similar results when samples were analyzed by GC but the BF_3 method is more time-efficient and therefore was used exclusively in later work.

Uptake of [1-^{14}C] Oleic Acid. In order to confirm that the oleic acid supplements were in fact taken up by the cells and converted into isolinoleic acid, a 100 ml culture of RH179E1 was grown with [1-^{14}C] - oleic acid (Amersham). The culture was set up in a small, glass enclosed fermentor at 30 °C and was bubbled with air and stirred with a magnetic stirrer. The culture was supplemented with 1.0 mg of "cold" oleic acid and 10 µg of [1-^{14}C] - oleic acid (specific activity 201 µC/mg) to produce a final supplement concentration of 10.1 mg/litre, and the fermentor was innoculated with RH179E1 to an initial density of approximately 20,000 cells/ml.

Every 2-3 hours, two 2.0-ml samples were removed to count the cell density and two 1.4-ml samples were taken to determine the content of [1-^{14}C] - oleic acid left in the medium and the amount taken up by the cells. The 1.4 ml samples were cooled on ice for five minutes, centrifuged in an Eppendorf centrifuge (model 5415) and the remaining supernatants removed for counting (counts remaining in medium). The cell pellets were resuspending in PNE (0.15 M phosphate, 0.45 M NaCl, 3 mM EDTA at pH 7.15), pelleted, and then solubilized by heating at 60 °C for 24 hours in a mixture of 200 µl 30 % H_2O_2 and 100 ul of 80 % $HClO_4$. A small portion of each solubilized pellet (100 µl) was then placed in a scintillation vial with 100 µl of ascorbic acid (to reduce quenching), and the mixture was counted by scintillation counting (counts taken up by cell; Rutledge et al., 1984).

When the culture reached late log phase, the remaining medium was harvested and freeze-dried as usual. The lipid was extracted three times with warm $CHCl_3/CH_3OH$, and after evaporation of the solvent, was dissolved in 10 % KOH in CH_3OH/H_2O 80:20 (v/v). This mixture was saponified at 75 °C for 45 minutes and after acidification with concentrated HCl, the free fatty acids were extracted with hexane and then analyzed by HPLC.

High Performance Liquid Chromatography (HPLC). Phenacyl esters of the [1-^{14}C] - labelled free fatty acids were formed to enhance the detection of the fatty acids at 254 nm on the HPLC (Borch, 1975). The free fatty acids were mixed with one ml of both a 10 mg/ml solution of triethylamine in acetone, and a 12mg/ml solution of phenacyl bromide in acetone. The reaction was left at room temperature overnight and injected directly into the HPLC.

The sample was applied to a 5.0 μ, C18 reverse phase "radial pak" column (Waters) using a Z-module radial compression unit (Waters). The HPLC consisted of two pumps (both model 510), an automatic gradient controller (model 680), a data module (plotter, model 730), and a multiple wave length detector (model 490, all from Waters) and the column was eluted at 2.0 mls/min with a gradient running from acetonitrile/water 80:20 (v/v) to pure acetonitrile in 30 minutes (both solvents were HPLC grade). The oleic, isolinoleic, and γ-linolenic phenacyl ester peaks were collected and counted for radioactivity.

Phenacyl esters of the free fatty acids derived from the wild type cells were also prepared as described above but were run on a 19 mm x 150 mm μBondapak C18 reverse-phase column (part 088500, Waters). The column was eluted at 8 mls/min with a gradient running from CH_3CN/H_2O 80:20 (v/v) to pure CH_3CN in 45 minutes, and different peaks were collected. Each peak fraction was dried down under a stream of argon and was methylated and analyzed by GC.

Liquid-Scintillation Counting. Samples were dried under argon and then dissolved in ten mls of "scintiverse" scintillation cocktail. Each was shaken, the radiation counts determined on a Beckman Liquid Scintillation Counter for ten minutes, and the cpm (counts per minute) converted into dpms (disintegrations per minute) using a quench curve and the external ratio method. The quench curves consisted of [1-^{14}C]-oleic acid with increasing amounts of either the growth medium (bacterilogical peptone/yeast extract/$FeCl_3$) or the solubilization solution (H_2O_2/ $HClO_4$/ ascorbic acid) as quenchers.

Argentation Chromatography. Total cellular free fatty acids were run on a small one gram Bio-Sil (Bio-Rad) column impregnated with 25% $AgNO_3$ (w/w). The $AgNO_3$/Bio-Sil was prepared in advance by evaporating an aqueous solution of the two

components on a rotovaporator and was maintained in the oven at 110 °C. The columns were eluted with solvent systems containing mixtures of either benzene and petroleum ether (Ferguson et al., 1975) or methanol and diethyl ether. The various eluates from the columns were collected in round-bottomed flasks, dried under a stream of argon, and analyzed by GC.

Characterization of the Deuteriated Products

Culture Conditions. For each deuteriated isolinoleic acid, a fourteen-litre New Brunswick Microferm fermenter containing 11 litres of media was autoclaved and, after cooling, was supplemented with 100 mg of oleic acid (deuteriated at the corresponding position), 420 mg of α-tocopherol, 4 g of fatty acid free BSA, and 400 mg of both penicillin and streptomycin. All were added to the medium as described in the previous chapter and the oleic acid was complexed to the BSA by rapid stirring for at least 1 hour. The medium was subsequently innoculated with a dense 100 ml culture of RH179E1 prepared a day in advance by innoculating 100 mls of media with a 10 ml stock culture and all were monitored for contamination by visual inspection.

Each eleven litre culture was grown to late log phase at 30 °C with aeration at 3.5 $L.min^{-1}$ and vane rotation at 30 rpm. When the cell density reached approximately 600,000 cells/ml the medium was cooled on ice to 10 °C and the cells harvested by continous-flow centrifugation on a Sorvall RC2-B centrifuge. The resultant cell pellets were transfered to a round-bottomed flask and lyophilized.

Purification. The cellular lipid was extracted from the freeze-dried cellular material with $CHCl_3/CH_3OH$ (2:1 v/v) and the mixture was heated at 55 °C for 15 min, filtered and the extraction repeated twice. After evaporation of the solvent the remaining lipid was saponified and the free fatty acids isolated as indicated in the previous section (Feasibility of a Biological Approach). The free fatty acids, in hexane, were then placed in two, 2-dram vials, cooled at -20 °C and centrifuged at 5000 rpm to precipitate insoluble cellular material. The supernatants were removed and the centrifugation procedure repeated.

After concentrating the hexane, each sample was applied to a column consisting of five grams of Bio-Sil impregnated with $AgNO_3$ (25%, w/v). The column was eluted with 100 mls of hexane followed by 100 mls of diethyl ether (both solvents contained acetic acid at a level of 0.5% (v/v)) and column fractions were collected in 2-dram vials pregassed with argon. The fractions containing $18:2^{\Delta 6,9}$ were identified by thin-layer chromatography (TLC) on $AgNO_3$ impregnated TLC plates. These were prepared, just before use, by dipping silica gel 60 plates (BDH) in a solution of 10% $AgNO_3/H_2O$ (w/v). After drying, the procedure was repeated and the plates were activated at 110 °C for three minutes. The plates were then spotted and chromatographed in a solvent consisting of hexane/diethyl ether/acetic acid (75:25:10, v/v/v) and the spots were visualized by charring with a solution of 70% H_2SO_4 saturated with K_2CrO_7 (Skipski & Barclay, 1969) and the appropriate fractions pooled.

The final purification step was performed by HPLC using a 19 mm x 150 mm μBondapak C18 reverse-phase column (part 088500, Waters). The free fatty acids were passed through a Sep-Pak C18 Cartridge (Waters) and were injected directly into the HPLC. The column was eluted isocratically at 8 mls/min and several injections were

required to purify the entire sample. The appropriate fraction, from each injection, was collected in a flask gassed with argon and after the bulk of the solvent was evaporated, the pure product was extracted with hexane. The hexane solution was subsequently washed three times with H_2O to remove any H_3PO_4.

Analysis of Purity. Each isolated fatty acid and its methyl ester were analyzed for purity by TLC and gas chromatography (GC), respectively. TLC was performed on silica gel 60 plates (BDH) using both a non-polar (hexane/diethyl ether/acetic acid 90:10:1 (v/v)) and a polar ($CHCl_3/CH_3COH/H_2O$ 65:25:4 (v/v)) solvent, and the chromatograms were charred with a solution of 10% $CuSO_4$ (w/v) in 8% H_3PO_4 (v/v; Bitman & Wood, 1982). The methyl esters of the fatty acid were prepared by the method of Morrison and Smith (1964) and analyzed as described in the previous section.

Identification of the Number and Location of the Double Bonds. To identify the number and location of the double bonds in the purified "isolinoleic acid", the *O*-TMS derivatives of both the methyl and ethyl esters of one sample (labelled at the C_9 and C_{10} positions) were analyzed by GC-MS. The ethyl ester was prepared by refluxing the fatty acid for 45 minutes in ethanolic HCl (acetyl chloride/ethanol, 1:16 v/v) and the *O*-TMS derivatives were prepared by the method of Schmitz and Egge (1979) except that the silylation step was performed with a premixed silylation reagent, Tri-Sil (Pierce). Both derivatives were run on an HP5095 GC-MS system, operating in the electron impact mode at 15 eV. The system was equipped with a 25 m X 0.75 mm i.d. OV-17 capillary column.

Identification of the Sites of Deuteration. The specific sites and extent of deuteriation of all samples were established (in conjunction with the GC-MS data, for the C_9-C_{10} labelled sample) by ^{13}C NMR analysis. The samples were run on a Bruker MSL-300 spectrometer operating at 75.5 MHz. Spectra were acquired using the Waltz-16

decoupling sequence (Shaka et al., 1983) at a power level of either 1.3 W or 6 W, a 90° pulse length of 9.5 μs (for ^{13}C), and a recycle time of 5 s.

High resolution ^{2}H NMR spectra of the isolinoleic acids deuteriated at the C_6 and the C_7 positions were also recorded. The spectra were acquired over a sweep width of 5,000 Hz on the Bruker MSL-300 spectrometer operating at 46.064 MHz, with a 90° - τ - acquire pulse sequence, 90° pulses of 4.5 μs, and a recycle time of 2 s.

Oxidation. Several precautions were taken to prevent oxidation of the fatty acids. Solvents were bubbled with argon before use and contained the antioxidant, butylated hydroxytoluene (BHT), at a level of approximately 0.01% (w/v). All columns and reaction flasks were gassed with argon, column fractions were collected in Teflon-capped vials presaturated with argon, and samples were stored under argon at -20 °C. Wherever possible, all other manipulations were also performed under an argon atmosphere.

Results

Feasibility of a Biological Approach

Optimization of Growth Conditions. Varying the concentration of the oleic acid supplement in the culture medium had no affect on the growth of RH179E1, but did affect the ability of the organism to produce isolinoleic acid. Within the concentration range tested, all of the one litre cultures reached log phase after about 24 hours, and all grew to a cell density of approximately 200, 000 cells/ml (Table 3.1). The amount of isolinoleic acid in the cells, however, increased with increasing supplement concentration, although the effect was relatively minor above 5 mg/litre. At 5 mg/litre, conversion of the supplement into isolinoleic acid was the most effecient and therefore this concentration was used in the subsequent experiment.

In contrast, the culture temperature had a large effect on both the growth rate of *Tetrahymena* and the production of isolinoleic acid (Table 3.2). Cell generation times were calculated by fitting the cell density versus time data to an exponential growth curve and the results indicate that cells grow much faster at 30 °C than at other temperatures. At 25 °C and 30 °C, the cultures also grow to a much higher cell density than they do at other temperatures and at 15 °C the cultures did not grow at all. The optimal growth temperature was therefore concluded to be 30 °C.

Table 3.1

Effect of the Supplement ($18:1^{\Delta 9}$) Concentration
on Cell Growth and and Isolinoleic Acid Production

	Amount[1] Produced per Concentration of Supplement (mg/ml)			
Fatty Acid	2.5	5.0	10.0	25.0
$18:1^{\Delta 9}$	1.2	2.2	2.3	3.9
$18:2^{\Delta 6,9}$	1.0	1.7	2.0	2.3
$18:3^{\Delta 6,9,12}$	-	-	0.9	0.7
Final Cell Cell Density[2]	1.9×10^5	1.7×10^5	1.9×10^5	1.9×10^5

[1] in milligrams

[2] in cells per millilitre

Table 3.2

Effect of Culture Temperature on
Cell Growth and Isolinoleic Acid Production

Fatty Acid	Culture Temperature	15 °C [2]	20 °C	25 °C	30 °C	37 °C
		Percentage Composition (%)[1]				
$18:1^{\Delta 9}$		ND	21	17	12	10
$18:2^{\Delta 6,9}$		ND	14	16	22	11
$18:3^{\Delta 6,9,12}$		ND	20	24	22	14
Generation Time [3]		Slow	10.6	5.1	3.8	4.5
Final Cell Density[4]		Low	4.6×10^5	9.3×10^5	9.5×10^5	4.0×10^5

[1] each value is the average of at least two cultures and represents the precentage of the total cellular fatty acids

[2] the cells did not grow at 15 °C

[3] time for the culture to double, in hours

[4] cells per millilitre; at 20 °C the cells were not at late log phase when harvested.

The optimal temperature for isolinoleic acid production was also found to be 30 °C. At the higher temperature, 37 °C, the major unsaturated fatty acids in RH179E1 (see Table 3.2) make up only 34 % of the total fatty acids, whereas in cultures grown between 20 °C and 30 °C the same unsaturates make up approximately 56 % of the total. Isolinoleic acid is the major unsaturate and represents 22 % of the total cellular fatty acids in cultures grown at 30 °C; in comparison, it represents only 14 and 16 % of the fatty acids in growths at 20°C and 25°C, respectively, and oleic and γ-linolenic acid ($18:3^{\Delta 6,9,12}$) are dominant.

The uptake and conversion of the supplement into isolinoleic acid was monitored in a culture grown with [1-^{14}C] - oleic acid. The supplement concentration for this study was 10 mg/litre and after 28 hours, 85 % of the oleic acid supplement was removed from the medium (Table 3.3). The amount of oleic acid retained by the organism was measured by counting either the solubilized cell pellets or the extracted lipid (after harvesting the cells), and the results indicate that after 28 hours between 30% and 50% of the label remains in the cells (Table 3.3). Either a large percentage of the radiolabeled oleic acid is therefore metabolized and given of as [^{14}C] - CO_2 or perhaps quenching during the scintillation counting is not adequately accounted for by the quench curves (see Discussion).

The lipid extract was saponified, derivatized and run on the HPLC, and fractions corresponding to oleic, isolinoleic, and γ-linolenic acid were collected and counted. Only a small proportion of the radioactivity was recovered in these three fatty acids, but the distribution of the label amongst the three was in a ratio of 5:7:1, respectively. Only 1% of the added oleic acid was converted into isolinoleic acid as measured by this experiment (Table 3.3).

Table 3.3

Uptake of [1-^{14}C] Oleic Acid from the Culture Medium by RH179E1

	Initial	Final	Percentage Uptake (%)
DPM in solution	4.2×10^6	6.7×10^5	84.0
DPM in solubilized Cell Pellets	-	1.3×10^6	31.0
DPM in Lipid Extract	-	2.0×10^6	46.4
Fatty Acids:			
$18:1^{\Delta 9}$	-	3.6×10^4	0.9
$18:2^{\Delta 6,9}$	-	5.2×10^4	1.2
$18:3^{\Delta 6,9,12}$	-	7.4×10^3	0.2
		Ratio: 5:7:1	
Cell Density[1]	2.6×10^4	7.1×10^5	

[1] in cells per millilitre

Purification of Isolinoleic Acid. The wild type strain of *T. thermophila* can grow without an unsaturated fatty acid supplement and produces several polyunsaturated fatty acids (Figure 3.1). Cultures of the wild type therefore were grown, harvested, and the total cellular fatty acids used as a lipid source for the developement of the purification procedures. The organism, however, produces a large number of unsaturates including three diunsaturates, isolinoleic, linoleic and cilienic acid ($18:2^{\Delta 6,11}$) in the following molar ratio: 1:7:3, respectively (Conner et al., 1984). Isolation of isolinoleic acid from the total cellular lipids of the wild type strain was in fact more difficult than the isolation of isolinoleic acid from the lipids of strain RH179E1 which has a limited capacity for unsaturated fatty acid production.

When the phenacyl esters of the total cellular fatty acids from the wild type are run on the HPLC, a complex pattern of overlapping peaks results (Figure 3.2a). Several of these peaks were collected and analyzed by GC and it was shown that the peaks corresponding to the three diunsaturates also contain a variety of other saturated fatty acids. In addition, approxmately 150 mgs of lipid were applied to the column and only 30 % of the fatty acids were actually recovered. The phenacylation reaction was therefore monitored by thin-layer chromatography (TLC) which showed that, under the specified conditions, a substantial portion of the free fatty acids were not derivatized and therefore were lost on the column. In order to avoid the phenacylation step, conditions for the separation of lipids as free fatty acids were developed (see "Characterization of the Deuteriated Products" under Materials and Methods).

The total cellular free fatty acid preparations were run on a $AgNO_3$/Biosil column in an attempt to separate the saturated and unsaturated fatty acid fractions and thus augment the purification obtained by HPLC. Separation on a similar column had been achieved by

Figure 3.2.

Comparison of the HPLC chromatograms of the phenacyl esters formed from the free fatty acids of *T.thermophila*. The chromatogram in **a)** is before and **b)** after argentation chromatography. Peaks are identified as **1:** $18{:}3^{\Delta 6,9,12}$, **2:** $18{:}2^{\Delta 9,12}$, **3:** $18{:}2^{\Delta 6,9}$ and $18{:}2^{\Delta 6,11}$, and **4:** $18{:}1^{\Delta 9}$. For more details see Materials and Methods (NB. the timescales of the two runs are not exactly comparable)..

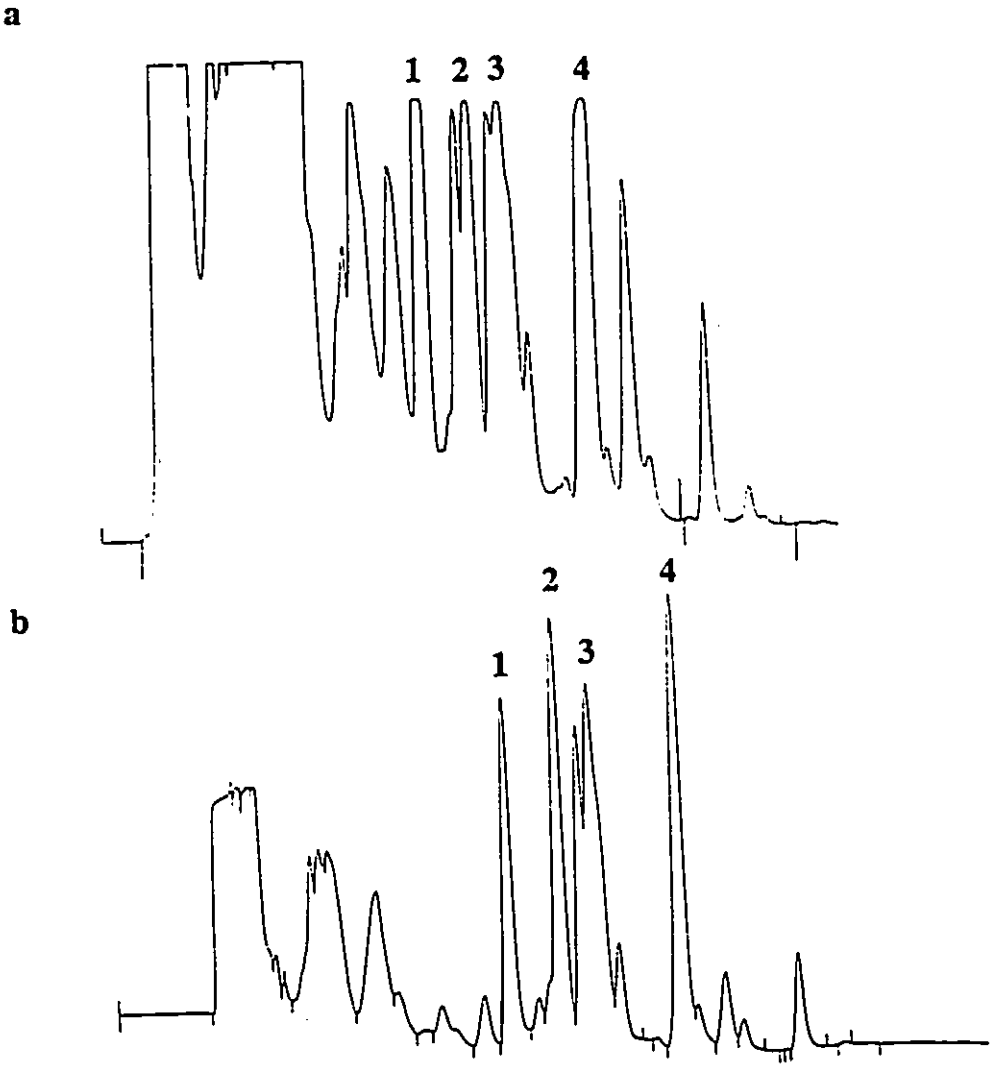
a
1
2
3
4
b
1
2
3
4

eluting with solutions of increasing benzene concentration in petroleum ether (Conner et al., 1984) but our attempts were not met with success. A variety of different mixtures of benzene/petroleum ether as well as a continuous gradient of the two were unsuccessful in effecting a separation, and it was also found that a considerable amount of the unsaturated fatty acids was not eluted with the 100 % benzene solution. Addition of acetic acid to the solvents, however, improved the separation. Elution with petroleum ether and acetic acid removes most of the saturates from the column while retaining the unsaturates and a mixture of methanol/ethyl ether was found to elute the unsaturated fatty acids in quantitative yields. The combination of Argentation chromatography and HPLC was therefore successful in purifying the isolinoleic acid from the other cellular fatty acids (Figure 3.2b and Figure 3.3).

Characterization of the Deuteriated Products

The protocol presented under "Materials and Methods" allows for the production and purification of one deuteriated isolinoleic acid per culture. A series of 11 L cultures of RH179E1 were therefore grown, each with an oleic acid supplement specifically deuteriated at a different position, and a series of isolinoleic acids labeled at each of the C_4, C_5, C_6, C_7, C_8, C_9-C_{10}, C_{11}, C_{14}, or C_{18} position was produced. The cells were harvested, the deuteriated fatty acids isolated and purified, and each fatty acid was analyzed by several techniques to ensure the purity of the preparation and to establish its chemical structure.

Figure 3.3.

Comparison of the GC chromatograms for fatty acid methyl esters isolated from RH179E1. The chromatogram in **a)** is the total cellular free fatty acids, whereas the chromatogram in **b)** shows the pure isolinoleic acid isolated by the protocol described under Materials and Methods and summarized in Figure 3.9. The fatty acid methyl esters are designated as follows: **1**: isolinoleic acid, $18:2^{\Delta 6,9}$, and **2**: heptadecanoic acid, 17:0 (the internal standard). The peak identified by the asterisks, "*", corresponds to BHT.

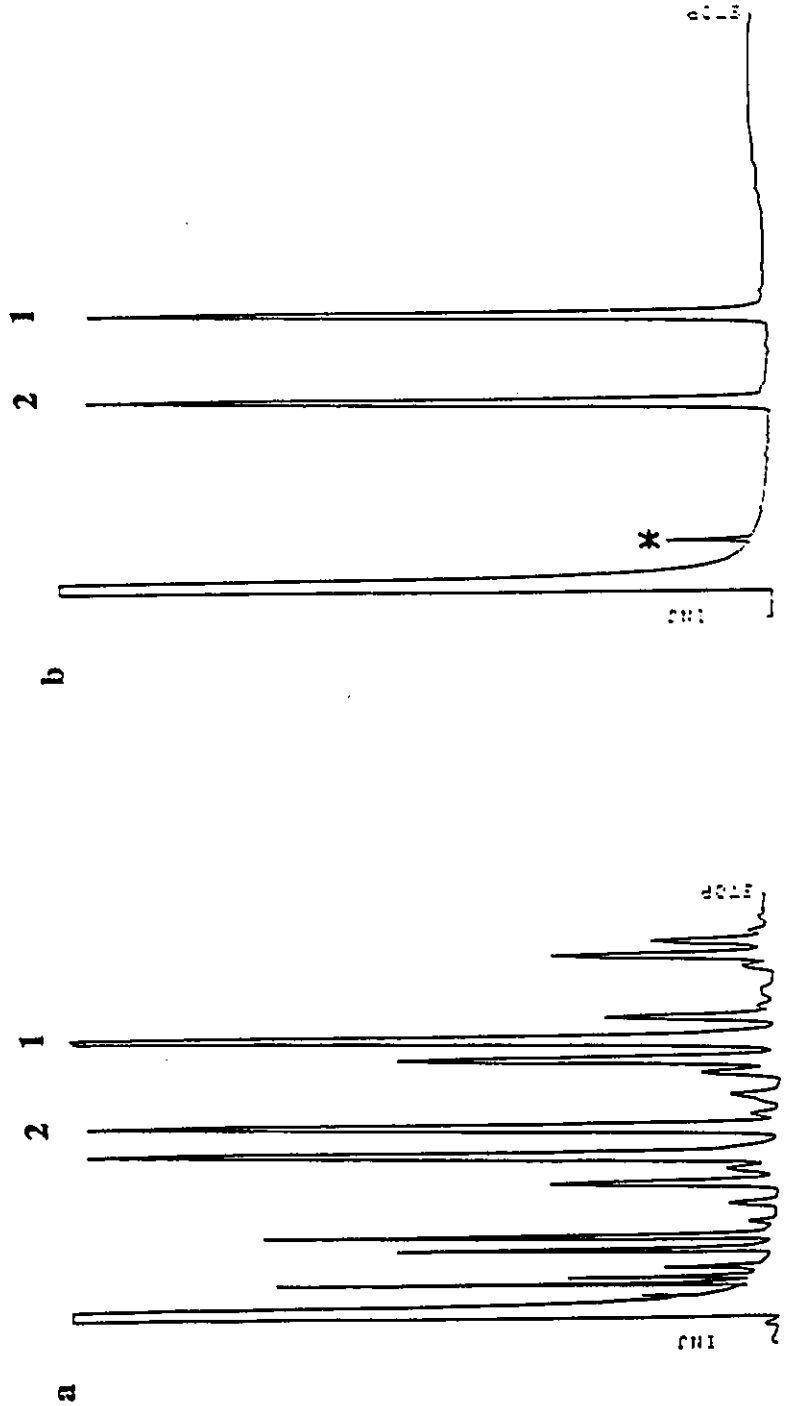
1
2
*
b
1
2
a

The fatty acid preprarations were analyzed for purity by TLC in two solvents of different polarity and in all cases resulted in only one spot having the same Rf as a free fatty acid standard. GC analysis of the methyl ester of each fatty acid also showed that most preparations were greater than 99% pure (see Figure 3.3 and Table 3.4) and each had the same retention time relative to the internal standard indicating that for all preparations the same fatty acid was isolated (ie. $18{:}2^{\Delta 6,9}$, see below).

The *O*-TMS derivatives of both the ethyl and methyl ester of the C_9-C_{10} labelled sample (produced for GC-MS analysis, see below) were resolved into two peaks on the GC-MS capillary column. For both derivatives, the two peaks had identical mass spectra and therefore were attributed to the two diasteriomers formed during derivatization, as opposed to the lack of purity of the sample. The addition of osmium tetroxide to each individual double bond is syn, but with respect to each other both syn and anti addition are possible. Although formation of such diasteriomers has not previously been reported, most early GC-MS work was performed with packed columns, and we found that our packed column (6 ft X 1/16 in. id., SP 2300/2310, Supelco) was unable to resolve the two peaks (not shown).

To establish conclusively the structure of the isolated fatty acid, the *O*-TMS methyl ester derivative of the C_9-C_{10} labelled isolinoleic acid was examined by GC-MS. Under electron impact the derivative fragments in a relatively simple pattern (see Figure 3.4 and Dommes et al., 1976) that allows one to deduce the length of the lipid acyl chain, the number and location of double bonds, and the location of any deuterium labels in the molecule.

Table 3.4

The Yield, Purity, and Level of Deuteriation
of the Purified Isolinoleic Acids

Site of Deuteriation	Yield (mg)[1]	Purity (%)[2]	Deuteriation (%)[3]
C_4	78	96.5	26
C_5	111	98.9	30
C_6	75	99.2	~ 5
C_7	98	> 99.5	38
C_8	75	99.0	28
C_9-C_{10}	101	99.5	35
C_{11}	105	> 99.5	ND[4]
C_{14}	138	99.6	35
C_{18}	120	99.5	21

[1] determined by GC with 17:0 as an internal standard

[2] represents the purity of the sample relative to other free fatty acids as determined by GC. Samples were also examined by TLC under two different solvent conditions (see Materials and Methods)

[3] determined by ^{13}C NMR for all samples except the sample deuteriated at the C_{11} position. The C_9-C_{10} labelled sample was also analyzed by GC-MS

[4] not determined

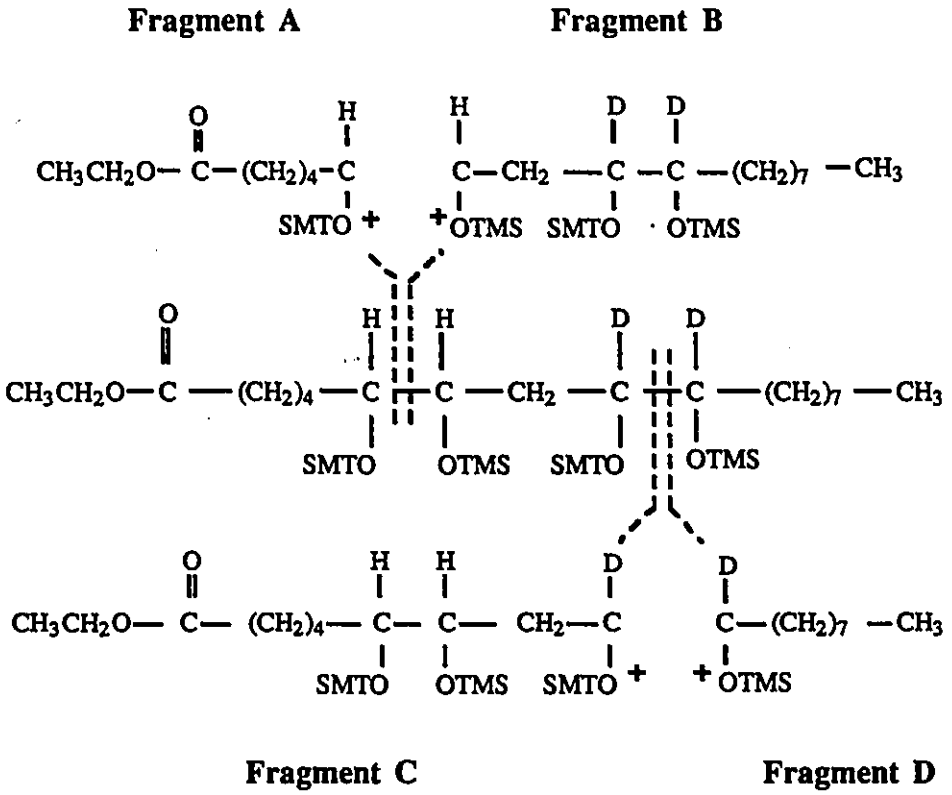

Figure 3.4 The expected fragmentation pattern for the *O*-TMS derivative of the deuteriated ethyl ester of isolinoleic acid. Upon electron impact, four major fragments are formed and these are designated Fragments **A, B, C,** and **D.** These will also break down further to form fragments such as **B-90,** or **C-180** which refer to the fragments **B** and **C** with the additional loss of one or two HOTMS groups, respectively. The deuterium atoms are designated in the chemical structures as "D".

The mass spectrum of the methyl ester was difficult to analyze due to overlapping diagnostic fragments so the ethyl ester derivative was examined (Figure 3.5, and Table 3.5). All the major diagnostic peaks expected for a derivatized, Δ6,9-diunsaturated, 18 carbon fatty acid ethyl ester are found; however, one peak of high molecular weight (fragment **C**) is only present at low intensity due to excessive breakdown to smaller fragments. The fragmentation patterns for all other 18-carbon straight chain, diunsaturated ethyl esters were also predicted, and none are compatible with the observed spectrum. Only the proposed structure of the fatty acid ($18{:}2^{\Delta 6,9}$) is therefore compatible with our results.

Analysis of the mass spectrum for isotope shifts indicates that the C_9-C_{10} labelled fatty acid is deuteriated at two sites with one deuterium found on the fragment from carbons C_{10}-C_{18} and the other on the fragment from carbons C_7-C_9. By comparing the intensities of fragments with and without deuterium isotope shifts (after taking into account the natural abundance of the various elements) the level of deuteriation was also estimated to be between 32 and 35%. In addition, fragments containing both deuterium sites (fragments **B**, **B**-90, **B**-180) only had isotope shifts of 2 mass units and therefore the two labels must appear simultaneously in the same molecule.

The ^{13}C NMR spectrum of the C_9-C_{10} labelled sample also supports the proposed structure of the isolated fatty acid (Figure 3.6). The presence of two double bonds is indicated by the four alkene resonances (127-130 ppm) and the reduction in the intensities of two of these indicates that the corresponding carbon atoms are deuteriated. Comparison of the peak intensities of the deuteriated and non-deuteriated alkene resonances indicates, in agreement with the GC-MS data, that the level of deuteriation is 35%.

Figure 3.5.

GC-MS analysis of the *O*-TMS derivative of the fatty acid ethyl ester of isolinoleic acid deuteriated at the C_9-C_{10} positions. Diagnostic fragments are labelled by the convention of Schmitz & Egge (1979) as shown in Figure 3.4. A quantitative summary is shown below in Table 3.5

Table 3.5

A quantitative summary of the fragmentation pattern and level of deuteriation of the *O*-TMS derivative of the ethyl ester of [$^2H_2$-9,10]-18:2$^{\Delta 6,9}$.

Figure 3.5.

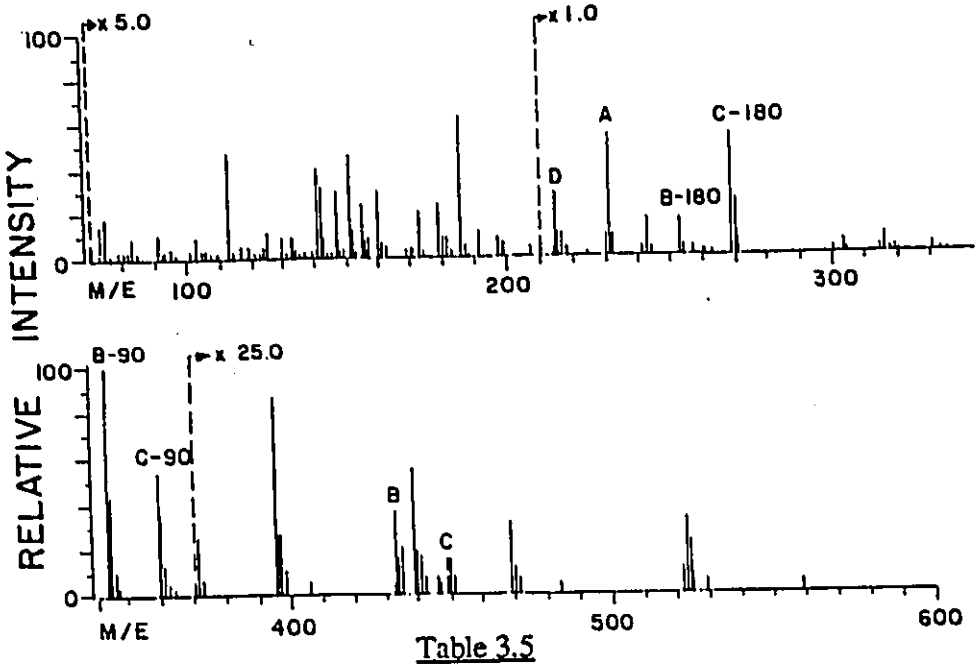

Table 3.5

Fragment	Molecular Weight of Fragment	Relative Abundance	Molecular Weight with Isotope Shift	Relative Abundance	Percentage Deuteriation[1]
A	231	54	—	—	—
C	449	0.7	450	0.7	NC[2]
C-90	359	54	360	37	33%
C-180	269	53	270	25	NC
B	433	1.5	435	0.9	NC
B-90	343	100	345	42	30%
B-180	253	17	255	6	NC
D	215	30	216	12	27%

[1] Determined after the natural abundance of the isotopes were accounted for.

[2] NC: not calculated.

Figure 3.6.

A portion of the ^{13}C NMR spectrum of isolinoleic acid deuteriated at both the C_9 and C_{10} positions showing the alkene (127-132 ppm) and methylene resonances (20-36 ppm). The spectrum was acquired as indicated under Materials and Methods with a sweep width of 15152 Hz, 8K data points, and for 8698 scans. The Free Induciton Decay (FID) was zero filled to 32K points and Fourier transformed with 4 Hz line broadening. The "*" labels peaks that correspond to the antioxidant, BHT.

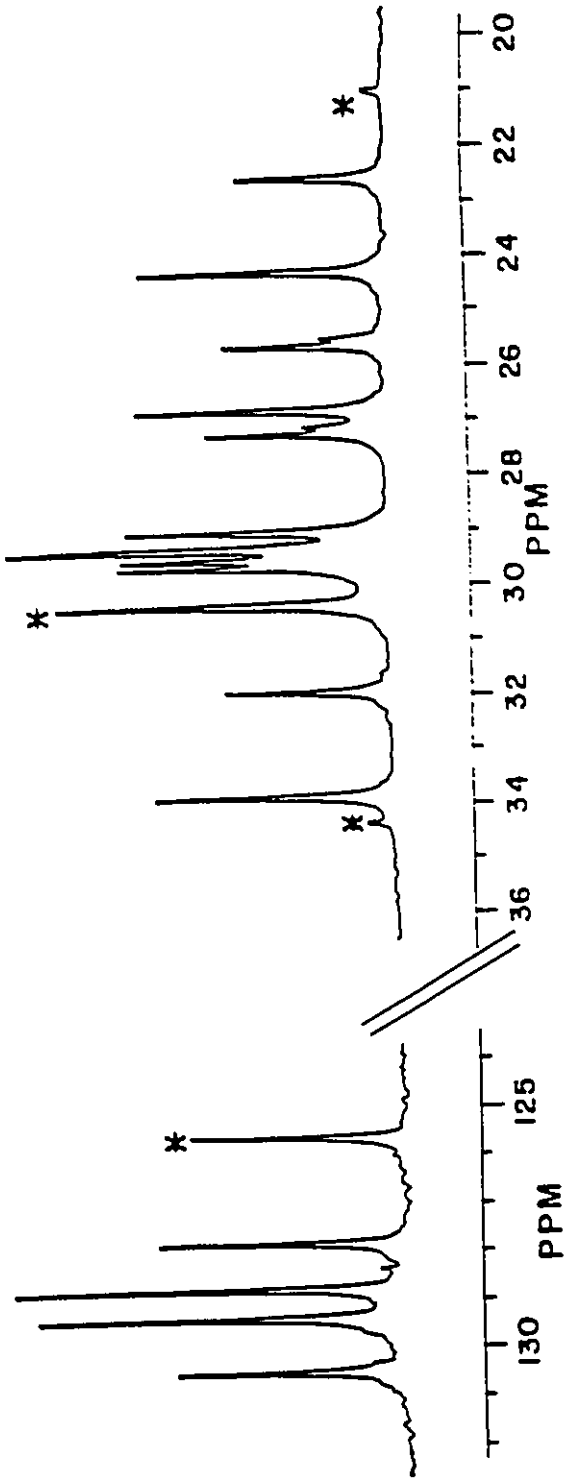
*
*
*
*
20
22
24
26
28
30
32
34
36
PPM
125
130
PPM

Resonances from two methylene carbons (25.5 and 27.1 ppm) are shifted by 0.1 ppm upfield due to the location of these carbons adjacent to deuteriated carbons (only 35% of the intensity is shifted because 35% of the sample is deuteriated). Two of the fatty acid's carbon atoms are deuteriated (GC-MS), and therefore, since only two methylene groups show this β-shift, the sites of deuteriation must be located either on adjacent carbons or on the two terminal carbons of the chain (the methyl and carboxyl carbons). The only possibility is that the two sites are adjacent and are located on one of the two double bonds. When this information is combined with the GC-MS data it can be concluded that the fatty acid is deuteriated at positions C_9 and C_{10}.

^{13}C NMR spectra were recorded for all but one of the deuteriated isolinoleic acid samples and in all cases the spectra were essentially identical to the spectrum of the C_9-C_{10} labelled sample thus confirming the structure of each isolated fatty acid (ie. $18{:}2^{\Delta 6,9}$). By analyzing each of the spectra for β-shifted resonances and for resonances of reduced intensity (both due to the presence of the deuterium labels, see above), essentially all of the ^{13}C resonances in the spectrum were assigned (Table 3.6) and all the sites of deuteriation were established. In all cases, the expected ^{2}H-labelled isolinoleic was produced and scrambling of the ^{2}H label did not occur (see discussion).

The yields of the deuteriated fatty acids were generally between 100 and 130 mgs of isolinoleic acid per culture (as judged by GC with 17:0 as an internal standard) and by measuring the percentage of the resonances in the respective ^{13}C NMR spectra undergoing the β-shifts, the level(s) of deuteriation of each was established to be, on average, 30% (see Table 3.4). The culture supplemented with [$^{2}H_2$-6]-oleic acid, however, yielded only 60 mg of product (NB. a second culture was grown and with similar yields) and, as shown in Figure 3.7, the isolinoleic acid is only deuteriated to a level of approximately 5%

Table 3.6

Resonance Assignments in the ^{13}C NMR Spectrum of Isolinoleic Acid

Carbon	Chemical Shift[1]	Calculated Shift[2]	Carbon	Chemical Shift	Calculated Shift
C_1	ND[3]		C_{10}	130.4	130.3
C_2	33.8*	34.1	C_{11}	27.3	27.3
C_3	24.3	24.4	C_{12}	29.7	29.8
C_4	29.0	29.2	C_{13}	29.3	29.4
C_5	26.8	26.9	C_{14}	29.5	29.6
C_6	129.3	129.3	C_{15}	29.3	29.4
C_7	128.7	128.8	C_{16}	31.9	32.1
C_8	25.7	25.7	C_{17}	22.7	22.8
C_9	127.7	127.9	C_{18}	14.1	14.1

[1] in ppm

[2] calculated as described in Gunstone et al., 1977

3 not determined; outside frequency range of spectrum

* assignment determined by comparison to data for linoleic acid ($18:2^{\Delta 9,12}$)

Figure 3.7.

A portion of the ^{13}C NMR spectrum of isolinoleic acid deuteriated at the 6 position. The spectrum was acquired and processed as described in Figure 16 except with only 2 Hz line broadening and zero filling to 16K data points. The cross (+) indicates the resonance arising from the β-shift (ie. due to the presence of a deuterium atom on the adjacent carbon), the arrows (↓) indicate resonances that correspond to linoleic acid ($18:2^{\Delta 9,12}$ or 18:2 ω-6), and the star (*) indicates resonances corresponding to BHT. The resonances in the spectrum assigned to linoleic acid are tabulated (inset) and compared to the expected resonances for linoleic acid (Batchelor et al., 1974). Some of the expected peaks for linoleic acid overlap with the resonances of isolinoleic acid and therefore were not observed on the spectrum.

^{13}C Resonances of Linoleic Acid

Carbon Number	Predicted Frequency	Observed Frequency
C1	180.2	
C2	34.3	34.4
C3	24.9	24.9
C4	29.3	
C5	29.3	
C6	29.3	
C7	29.8	
C8	27.4	
C9	130.1	130.2
C10	128.4	128.4
C11	25.9	
C12	128.4	128.1
C13	130.3	130.4
C14	27.4	
C15	29.6	
C16	31.8	31.7
C17	22.8	
C18	14.1	

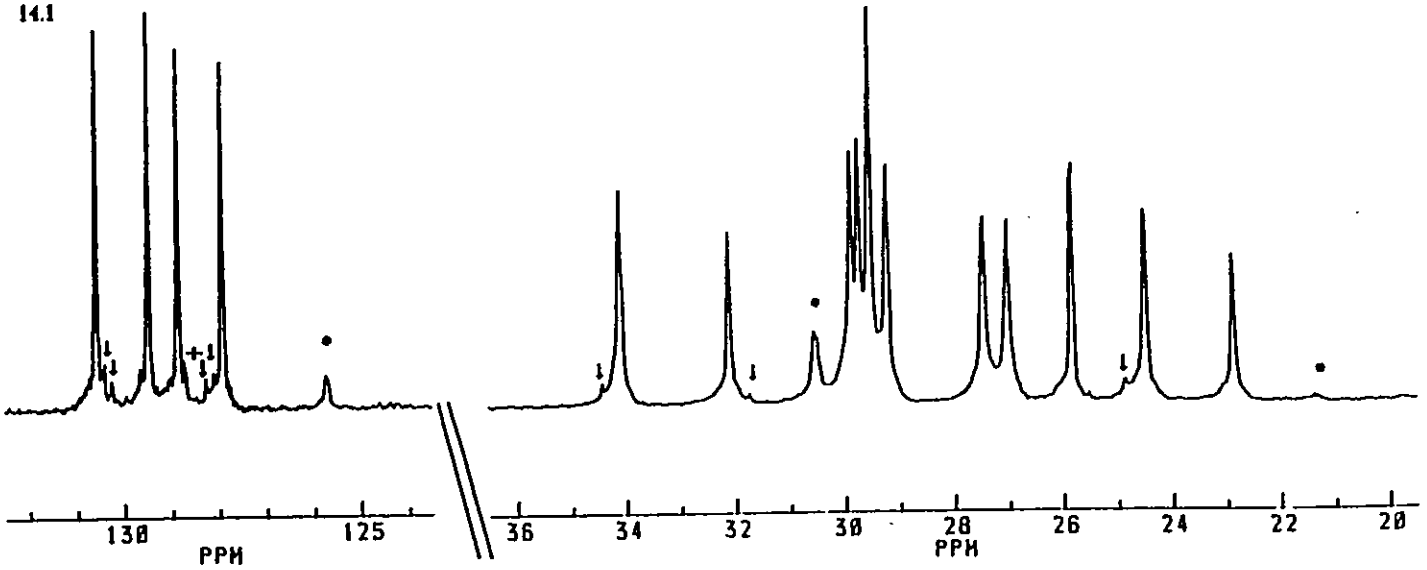

(ie. the β-shifted peak for the C_7 position is approximately 5% of the intensity of the nonshifted peak and the β-shifted peak for the C_5 position is not observed due to its low intensity). Several resonances of minor intensity whose chemical shifts correspond to those for linoleic acid ($18:2^{\Delta 9,12}$) are also present in the ^{13}C NMR spectrum and the GC tracing for this preparation shows a small shoulder on the isolinoleate methyl ester peak whose retention time corresponds to that for the linoleate ester. It therefore appears that the preparation contains some linoleic acid.

A high resolution ^2H NMR spectrum of the [^2H-6]-isolinoleic acid preparation was also recorded and the results shown in Figure 3.8 indicate that the linoleic acid in the sample is deuteriated. The ^2H NMR spectrum consists of two resonances (other than the internal standard C^2HCl_3) at 1.4 ppm and 5.3 ppm which correspond to ^2H atoms covalently attached to methylene and alkene carbons, respectively, and both are of approximately equal intensity. The strength of the ^2H signal from the [$^2H_2$-6]-$18:2^{\Delta 9,12}$ is at first suprising given that it makes up only 2-3 % of the sample, however, the linoleic acid is labelled with two deuterons as opposed to the isolinoleic acid which has only one deuterium label. Assuming a high level of deuteriation of the linoleic acid and given the low level of deuteriation of the isolinoleic acid, one would expect the ^2H spectrum to consist of two resonances of approximately equal intensity and thus the spectrum is consistent with the existence of linoleic acid in the sample and with the assignment of the two ^2H resonances to deuteriated isolinoleic and linoleic acid (NB. the fatty acids were esterified to form PiLPC (see Chapter 4), the unesterified material rerun on the HPLC to remove side products and reagents, and then the high resolution ^{13}C and ^2H NMR spectra were acquired. The sample of PiLPC used in Chapter 4 therefore contains a slightly higher percentage of [$^2H_2$-6]-linoleic acid, ~ 7.5 %).

Figure 3.8.

High resolution ^{2}H NMR spectrum of the [^{2}H-6]-18:2$^{\Delta 6,9}$ preparation isolated from cultures of RH179E1 supplemented with [$^{2}H_{2}$-6]-18:1$^{\Delta 9}$.

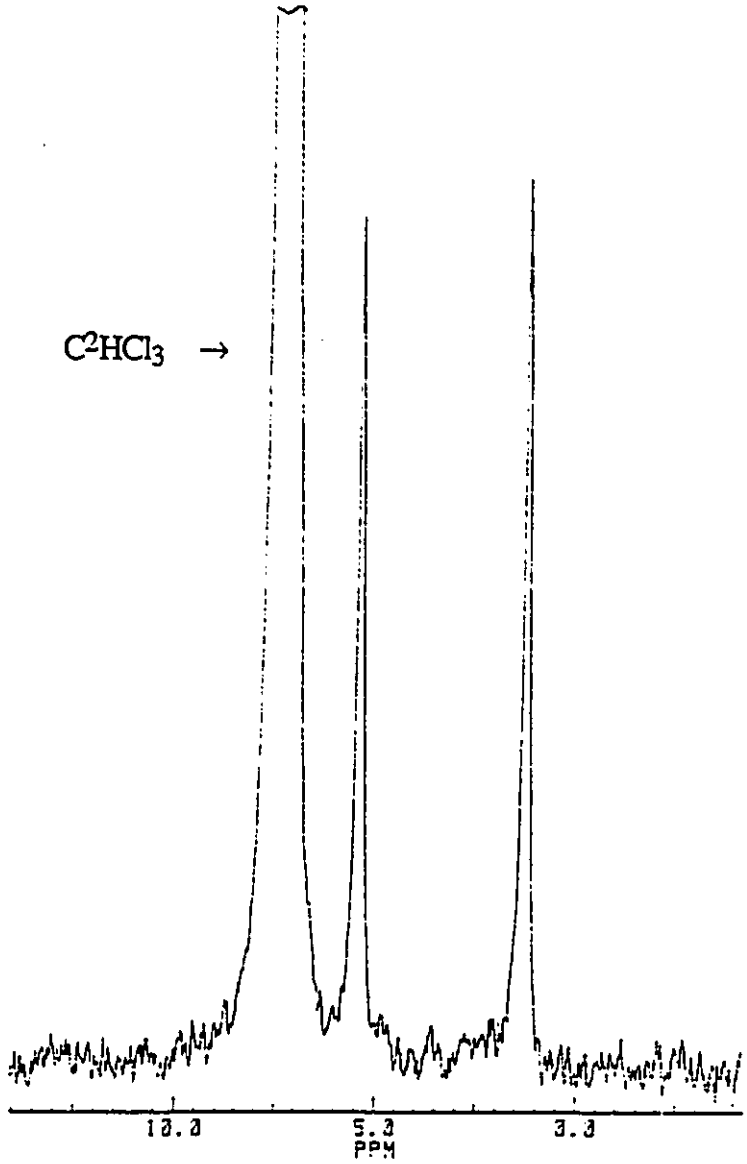
C^2HCl_3 →
10.0
5.0
PPM
3.0

Desaturation of the C_6 deuteriated oleic acid precursor to form [^{2}H-6]-isolinoleic is likely inhibited by an isotope effect, and even though the activity of the Δ12 desaturase enzyme is low, the enzyme would not be affected by the deuterium labels at the C_6 position and therefore could produce small amounts of deuteriated linoleic acid. Since a similar isotope effect could also occur with the isolinoleic acid produced in cells supplemented with [$^2H_2$-7]-oleic acid, the fatty acid preparation was examined for the presence of linoleic acid deuteriated at the C_7 position. The high resolution ^{2}H spectrum of [^{2}H-7]-isolinoleic acid (not shown) contained only one resonance corresponding to a deuterium atom covalently attached to an alkene carbon and therefore it can be concluded that the preparation does not contain significant quantities of C_7 deuteriated linoleic acid. In addition, the relatively high levels of deuteriation of the [^{2}H-7]-isolinoleic acid suggest that desaturation at the C_7 carbon is not affected by the presence of the deuterium labels (see Discussion).

Discussion

The concept of using a biological organism to introduce a double bond into a deuteriated fatty acid precursor and thus produce specifically deuteriated diunsaturated fatty acids is relatively simple, but in practice such an approach is very difficult and requires considerable preliminary experimentation. For example, one must first ensure that the organism will not only ingest the fatty acid supplement but will also convert a large percentage into the desired product. It was also of particular importance to optimize the culture conditions for isolinoleic acid production (eg. growth temperature, supplement concentration, etc.) because the deuteriated oleic acid precursors are expensive and time consuming to synthesize.

If the production of deuteriated isolinoleic acids is feasible, one must also address the problem of product purification. Even the mutant, RH179E1, contains a complex mixture of fatty acids in its membranes (see Figure 3.1) and isolation of isolinoleic acid from the other cellular lipids is difficult (see Figure 3.2); especially on a preparative scale. Common isolation procedures therefore had to be adapted to handle large quantities of lipid and to yield products of very high purity.

Finally, given the nature of the work it was also important to define precisely the structures of the compounds isolated for the NMR studies. The number of carbons and the location of the double bonds in the fatty acid had to be defined, and the location of the deuterium labels had to be specified. This was of particular importance given that the organism could possibly metabolize the oleic acid supplements into either CO_2 or acetate and reincorporate the deuterium labelled compounds back into other labelled fatty acids, or

during the desaturation of the C_6-C_7 carbons it could remove a deuterium label from one carbon and attach it covalently to another. Both situations would not only lead to loss of the labelled fatty acid precursors but would also lead to ambiguous results in the subsequent deuterium NMR analyses.

A protocol developed by Conner et al. (1984) to examine the desaturation pathways in *Tetrahymena* (see Figure 3.9) was used as a basis for the work performed in this chapter. In this experiment, the mutant was supplemented with radiolabeled oleic acid and radiolabeled isolinoleic acid was isolated by HPLC. However, this protocol was developed for the production of very small quantities with no attempt to maximize the uptake and conversion of the supplement. The protocol had therefore to be altered in order to optimize the yields of deuteriated isolinoleic acid.

The conditions used to obtain maximum isolinoleic acid production were determined by culturing *Tetrahymena* at different temperatures and at different supplement concentrations. It was originally hypothesized that at low temperatures (eg. 15 °C) the organism would require more unsaturated lipids in its membranes and therefore would produce more isolinoleic acid. The organism, however, grows faster at higher temperatures (eg. 30 °C) which might offset a less stringent requirement for unsaturated lipids. The cultures revealed that RH179E1 not only grows best at 30 °C , but at this temperature it also produces more isolinoleic acid then at all other temperatures tested. A temperature of 30 °C was therefore chosen as optimum for isolinoleic acid production.

A supplement concentration of 5 mg/litre was originally found to result in maximum conversion of the supplement into isolinoleic acid, but the cultures used to determine this value were grown to a maximum cell density of approximately 2 x 10^5 cells/ml. When the mutant is cultured in smaller volumes and/or in vessels with better oxygenation the cells

Figure 3.9.

Comparison of **a)** the protocol used by Conner et al. (1984) to synthesize radiolabelled isolinoleic acid and **b)** the protocol developed here for the biosynthesis of deuteriated isolinoleic acids.

a

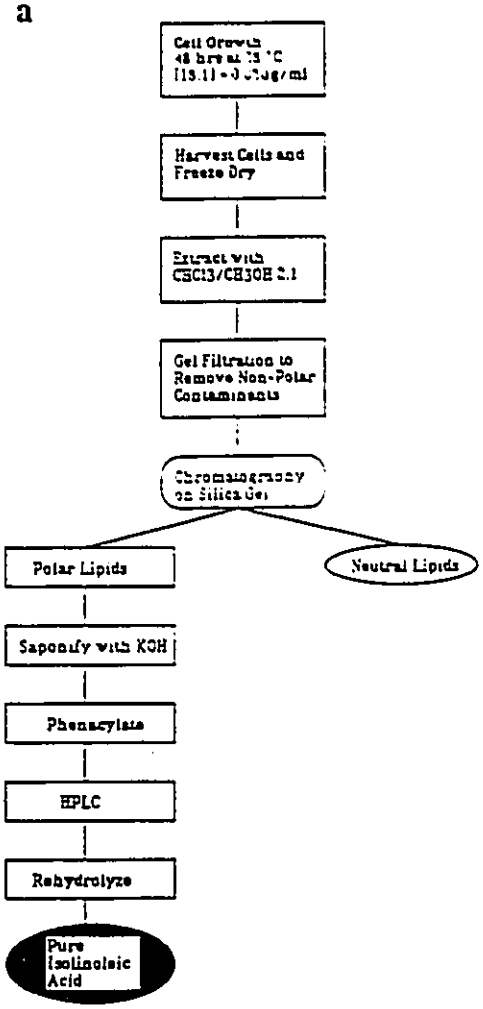
Harvest Cells and Freeze Dry
Extract with CHCl3/CH3OH 2:1
Gel Filtration to Remove Non-Polar Contaminants
Polar Lipids
Neutral Lipids
Saponify with KOH
Phenacylate
HPLC
Rehydrolyze
Pure Isolinoleic Acid

b

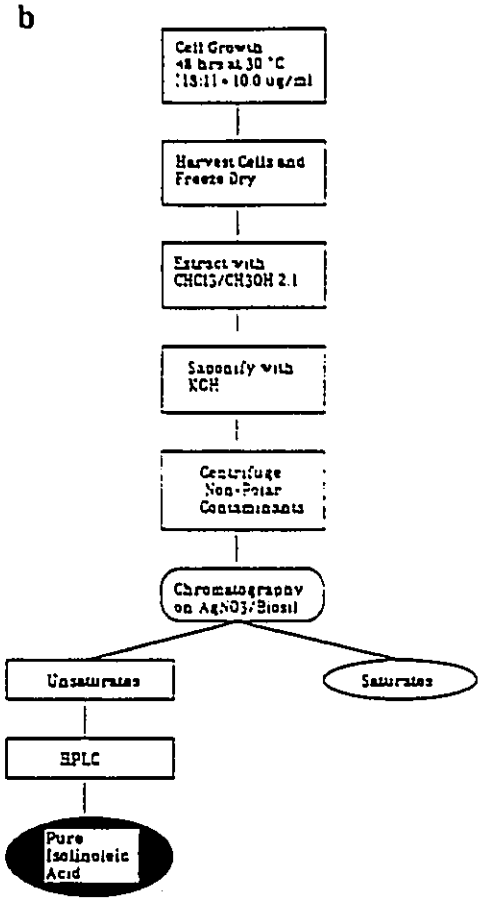
Harvest Cells and Freeze Dry
Extract with CHCl3/CH3OH 2:1
Saponify with KOH
Centrifuge Non-Polar Contaminants
Unsaturates
Saturates
HPLC
Pure Isolinoleic Acid

generally grow to densities approaching 1 x 10^6 cells/ml. Oxygenation is therefore an important factor in determining cell growth and with better oxygenation (and therefore increased cell growth) it was thought that a supplement concentration of 10 mg/litre would be more suitable.

In the culture grown with radioactively labelled oleic acid at a concentration of 10 mg/litre, the cells ingest 85 % of the fatty acid supplement from the medium after 28 hours indicating that the supplement concentration is appropriate. Unfortunately, a much smaller proportion of the label was accounted for in the cell pellets and the cell lipid after 28 hours, and only 1 % of the total label added to the culture was counted in isolinoleic acid. There are several reasons why the values reported here are low, 1) under the conditions used, the phenacylation reaction was not quantitative and therefore resulted in a considerable loss of labelled isolinoleic acid on the HPLC column; 2) the extraction and saponification of the freeze dried cell material was also found to be only approximately 80 % efficient (data not shown) and, given the small quantities, it is likely that additional lipid was lost due to adheration to the vessel walls; and 3) uptake of the fatty acid in the cell pellets corresponds closely to the the loss of label from the medium, although the counts are not as high. This suggests that compounds in the cell pellets may interfere with the scintillation counting process and thus may prevent an accurate quantitation of the label in the cells. It is also supported by the fact that the measured uptake, as determined for the $CHCl_3/CH_3OH$ extract, is almost double the uptake determined in the solubilized cell pellets. Therefore, a much greater proportion of the lipid was likely taken up by the cell and converted into isolinoleic acid than was indicated by the cpm values. To test whether sufficient quantities of deuteriated isolinoleic acid could be produced, a culture was supplemented with [$^2H_2$-9,10]-oleic acid and enough product was formed for NMR analysis as discussed below.

Several changes were made to the purification protocol developed by Conner et al. (1984) to examine desaturation pathways in *Tetrahymena* (see Figure 6). Separation of the nonpolar lipids from the polar cellular constituents, which was performed by a time-consuming Sephadex column, as well as the separation of the polar and neutral lipids, were eliminated. Instead the $CHCl_3/CH_3OH$ extracts were saponified directly and centrifuged to remove non-lipid contaminants. Phenacylation of the free fatty acids for HPLC was also time consuming, required rehydrolysis of the product after HPLC, and resulted in significant losses of lipid. With the large quantities of lipid handled it was found that the free fatty acids could easily be detected at 205 nm thus eliminating the need for phenacylated derivatives (Aveldano et al., 1983).

The HPLC, unfortunately was not able to purify the isolinoleic acid to the desired extent, so it was decided to use argentation chromatography to augment the technique. Solvent conditions were developed and the $AgNO_3$/Bio-Sil column was found to be effective in the separation of unsaturated fatty acids from the saturates. Petroleum ether was eventually replaced by hexane because they have similar dielectric constants and therefore perform equally well on the column (Pierce, 1984). HPLC grade hexane is easily obtained and was used in order to avoid distillation of petroleum ether. The methanol/ether mixture used to elute the unsaturates from the column was also eliminated because it dissolved the $AgNO_3$/Biosil which subsequently caused problems on the HPLC. Straight diethyl ether was found to be effective. Finally, to improve the efficiency of the column and to improve its capacity, the column size was increased to 5 grams and lipids were collected in 8 ml fractions instead of in bulk quantities.

To clearly esatablish the viability of the biosynthetic approach, an 11 litre culture of RH179E1 was supplemented with oleic acid deuteriated at the C_9 and C_{10} positions. The

cells were harvested, the isolinoleic acid isolated, and analysis of the product showed that the isolated fatty acid is pure and has 18 carbons and two double bonds located in the 6 and 9 positions. Approximately 100 mgs was isolated and it was found to be deuteriated at the expected positions (carbons 9 and 10) to a level of 35 %. Approximately 35 mgs of deuteriated product were produced. The results therefore indicate that the protozoan converts the deuteriated oleic acid supplement into isolinoleic acid in sufficient quantities for NMR (see the following chapters) and that the isolation procedures are sufficient to yield products of high purity. In addition, they also show that the isolated fatty acid has the proposed structure (ie. $18{:}2^{\Delta 6,9}$) and that the deuterium labels were not scrambled significantly to other positions.

Isolinoleic acid labelled at each of the C_4, C_5, C_6, C_7, C_8, C_{11}, C_{14}, and C_{18} positions was produced, purified to a level greater than 95 % pure and the yields, in general, were more than 100 mg of fatty acid per culture (except for , most noteably, the C_6 labeled isolinoleic acid, see below). The structure of each was established by comparison of its retention time on the GC and by its ^{13}C NMR to that of the C_9-C_{10} labelled sample. Again the levels of deuteriation were found to be approximately 30 %, at the expected positions, and scrambling of the deuterium labels was not observed.

The yields from cultures supplemented with [$^2H_2$-6]-oleic acid were much lower than average and the isolated isolinoleic acid was deuteriated to a level of less than 5%. For this supplement, the organism must remove one of the deuterium labels in order to desaturate at the C_6-C_7 position and the low yields may therefore reflect an inhibition of the desaturation process due to an isotope effect. In contrast, the sample prepared from cultures supplemented with [$^2H_2$-7]-oleic acid was isolated in good yields with a reasonable level of deuteriation. It therefore appears that the desaturase enzyme is able to

remove the C_7 deuteron with relative ease, whereas removal of the C_6 deuteron is difficult. These results might help provide insight into the mechanism of action of the desaturase enzymes but the research required is beyond the scope of this thesis.

The low levels of deuteriation, in general, were suprising because in defined media RH179E1 cannot synthesize unsaturated fatty acids (Hill et al., 1983). It was expected that the ability of the organisms to synthesize isolinoleic acid would be entirely dependent upon the supplement, which is deuteriated to a level greater than 95 %. The cells, however, were grown in a peptone medium from which they may acquire a precursor for the synthesis of unlabelled $18{:}2^{\Delta 6,9}$. This is supported by the fact that RH179E1 can survive in peptone without a supplement and is able to synthesize both $18{:}2^{\Delta 9,12}$ and $18{:}3^{\Delta 6,9,12}$ (unpublished results, and Chapter 5).

For most cultures 30 to 40 mgs of deuteriated isolinoleic acid were purified and, as will be illustrated in the following chapters, this is sufficient to perform extensive ^2H NMR analyses. For some experiments, however, higher levels of deuteriation would have been beneficial and to achieve this, cultures could be grown in a defined medium which should both increase the level of deuteriation and increase the yields of the product. In addition, cells could be grown in the presence of biotin which inhibits fatty acid synthesis. The protozoan would therefore be entirely dependent upon the supplement for the production of fatty acids and would likely incorporate much larger quantities of the deuteriated oleic acid and also produce more deuteriated isolinoleic acid.

Summary and Conclusions

The work presented in this chapter demonstrates the viability of a biological approach to the synthesis of specifically deuteriated polyunsaturated fatty acids. The techniques for converting specifically deuteriated oleic acid ($18:1^{\Delta 9}$) into the corresponding specifically deuteriated isolinoleic acid ($18:2^{\Delta 6,9}$) have been developed and at present,this is the only route available for the synthesis of a series of specifically deuteriated polyunsaturated fatty acids (ie. deuteriated at several positions along the chain).

Similar biosynthetic procedures could also be used to produce an extensive series of specifically deuteriated polyunsaturated fatty acids. For example, the deuteriated isolinoleic acids could be introduced into the normal strain of *Tetrahymena* and would be converted into the the corresponding deuteriated γ-linolenic acids ($18:3^{\Delta 6,9,12}$). In addition, the deuteriated γ-linolenic acids could be reintroduced into the mutant and specifically deuteriated ciliary membrane vesicles could also be isolated. The deuterium NMR analysis of the physico-chemical properties of a wide range of polyunsaturated fatty acids in both model and eukaryotic membranes is therefore possible.

Chapter 4

Aqueous Dispersions of 1-Palmitoyl-2-Isolinoleoyl Phosphatidylcholine

---

Chapter 4

Aqueous Dispersions of 1-Palmitoyl-2-Isolinoleoyl Phosphatidylcholine 103

Introduction 106

Materials and Methods 107

Sample Preparation 107

Esterification to Lyso PC 107

Acyl Chain Migration. 109

Aqueous Dispersions.. 109

NMR Spectroscopy 109

Deuterium NMR Spectroscopy. 109

Phosphorous NMR. 111

Results **112**

The Liquid Crystalline Phase 112

Quadrupolar Splittings Versus Temperature. 112

Conformation of the Isolinoleoyl Chain
in the Liquid-Crystalline Phase. 124

Order Parameter Profile 131

The Gel Phase 136

Gel to Liquid-Crystal Transition Temperature. 136

Conformation of Isolinoleic Acid in the Gel Phase 140

Spectral Simulations and Acyl Chain Migration. 144

Discussion **149**

Conformation of the Isolinoleoyl Chain 149

Ordering of the Isolinoleoyl Chain 153

1-Isolinoleoyl-2-Palmitoyl PC (iLPPC)
and Acyl Chain Migration 155

Summary and Conclusions 157

Introduction

The synthesis of a series of specifically deuteriated fatty acids (Chapters 3) is the first step in a deuterium NMR investigation of lipid acyl chain structure and ordering. The next step involves esterification of the deuteriated fatty acids to form the desired phospholipid, organization of the phospholipids into a form suitable for NMR analysis, and finally, acquisition and interpretation of the deuterium NMR spectra. In this chapter, a protocol for the esterification of the deuteriated isolinoleic acids to 1-palmitoyl lysoPC will be described, and the results from a subsequent investigation of the structure and ordering of the isolinoleoyl chain in aqueous dispersions of 1-palmitoyl-2-isolinoleoyl phosphatidylcholine will be presented.

Materials and Methods

Sample Preparation

Esterification to Lyso PC. Each of the deuteriated fatty acids was esterified to 1-palmitoyl lyso phosphatidylcholine (lyso PC) by the method of Perly et al. (1984). The esterification process involves two separate reactions as shown below:

$$\text{Fatty Acid (18:2)} + \text{DCC} \xrightarrow{CHCl_3} \text{Fatty Acid Anhydride (FAA)}$$

$$\text{FAA} + \text{(16:0) Lyso PC} \xrightarrow[DMAP]{CHCl_3} \text{(16:0) (18:2) PC} + \text{Fatty Acid}$$

and, due to the presence of the fatty acid anhydride, both are very sensitive to the presence of H_2O.

Each fatty acid preparation (in $CHCl_3$) was dried under a stream of argon, frozen, lyophilized to remove any moisture, and then dissolved in $CHCl_3$ which had previously been refluxed over P_2O_5 for approximately one hour and distilled (again to remove any moisture or alcohol from the solvent). Dicyclohexylcarbodiimide (DCC; 0.7 equivalents) was then added to the fatty acid solution and the reaction left stirring overnight, under argon, in the dark.

1-Palmitoyl lyso PC (0.5 Molar equivalents; Sigma) was dissolved in H_2O, frozen and lyophilized overnight until dry (to remove alcohol from the sample). The lyso PC used for all isolinoleic acid preparations was taken from the same vial and TLC and GC analysis showed that the compound was pure and that the the *sn*-1 fatty acid was > 99.5 % palmitic acid.

The reaction to form the fatty acid anhydride (FAA) was analyzed for completion by TLC in a solvent system consisting of hexane/ether/acetic acid 90:10:1 (v/v/v). When complete, the lyso PC was removed from the lyophilizer and placed for a couple of hours under vacuum in a desiccator with $CaCl_2$ to remove all moisture. The FAA solution was then filtered through a small celite column into the lyso PC and 0.5 molar equivalents of dimethylaminopyridine (DMAP) were added. The reaction was stirred for two to three hours in the dark and stopped by addition of cold 0.9 % KCl (w/v) in 1N HCl. After a thorough mixing, the upper aqueous phase (which contains the catalyst, DMAP) was discarded and the remaining lipid solution (lower phase) was washed three times with CH_3OH/H_2O 1:1 (v/v) to remove any remaining acid. The sample was then concentrated under argon, lyophilized, and dissolved in $CHCl_3$ for purification by column chromatography.

The product was purified on a 5 g Bio-Sil column with elution of the unesterified material with 100 mL of $CHCl_3$ and the pure product with $CHCl_3/CH_3OH/H_2O$ (45:25:2.5 v/v). Both solvents were bubbled with argon before use and lacked BHT to prevent contamination of the final product with the antioxidant. Fractions were collected in 2-dram vials under a stream of argon, and a portion of each was spotted on a Silica-gel 60 plate and chromatographed in a solvent containing $CHCl_3/CH_3OH/H_2O$ (65:25:4 v/v). The plates were charred as described previously and the fractions containing pure PiLPC pooled. The

product was then rechromatographed (in the same solvent system) to ensure the purity of the sample and in some cases the chromatograms were also charred with Dragendorff's reagent (Kates, 1969) to test whether all of the DMAP was removed from the sample (it elutes with PC on both the Bio-Sil column and the TLC plates, but is extracted from the sample prior to the column with dilute HCl; see above).

Acyl Chain Migration. A small portion of each sample was also analyzed for acyl chain migration. In each case, the phospholipid was treated with phospholipase A_2 (*Crotalus adamanteus*, Keough & Davis, 1979) and the fatty acids liberated from the *sn*-2 position were identified by GC.

Aqueous Dispersions. The purified 1-palmitoyl-2-isolinoleoyl PC was dried under a stream of argon, lyophilized to remove traces of $CHCl_3$, and then dispersed in excess deuterium-depleted H_2O (samples contained at most 35 mgs of lipid in 200 µl of H_2O). The samples were subjected to, on the average, five freeze-thaw-vortex cycles to ensure complete dispersion of the lipid and to ensure a relatively uniform vesicle size. After several freeze-thaw-vortex cycles, lipids generally form multilamellar vesicles ranging in size from roughly 0.05 µm to 10 µm in diameter (Hope et al., 1986).

NMR Spectroscopy

Deuterium NMR Spectroscopy. Most of the deuterium NMR spectra were recorded on a 200-MHz custom-built spectrometer operating at 30.700 MHz. Spectra were acquired using a modified quadrupolar echo pulse sequence (Rance et al., 1980):

$$90_x - \tau_1 - 90_y - \tau_2 - \text{acquire} \qquad (10)$$

with full phase cycling of the radiofrequency pulses. The 90° pulse lengths were generally 2.3 μs in length (5-mm solenoid coil) and the echo pulse spacing (τ_1) was 60 μs. The pulse sequence was repeated at most every 100 ms (always > 5 x T_1), and the spectra were generally acquired with a sweep width of 100 kHz, except where indicated.

Spectra indicative of the liquid-crystalline state were acquired over a temperature range of 1 °C to 40 °C; the temperature was monitored and maintained to within ± 0.5 °C with a custom-built variable temperature unit. The gel state spectra were acquired over a temperature range of -25 °C to 0 °C. Low temperatures were achieved by boiling off liquid nitrogen and passing the resulting vapour through the NMR probe.

Deuterium NMR spectra were also acquired on a Bruker MSL-300 spectrometer operating at 46.064 MHz with the quadrupolar echo sequence described above, and 90° pulse lengths of approximately 4.6 μs (10 mm coil) in length. Spectra (where indicated) were acquired with Waltz-16 decoupling (Shaka et al., 1983) during acquisition of the free induction decay (FID). The decoupling was performed with 90° pulses of 60 μs at a decoupler power of 6 watts. The time of decoupling (the acquisition time) was never allowed to exceed 2% of the recycle time in order to prevent heating of the sample.

The deuterium NMR spectra were analyzed on a Nicolet 1280 data processor. The FIDs were left shifted to the top of the echo before Fourier Transformation of the trailing edge and the transformed spectra were then dePaked by the method of Bloom et al. (1981) to give the 90° oriented sample spectra. The quadrupolar splittings for each sample were measured from the dePaked spectra which facilitates an accurate determination of the

splittings as the spectra are free from the convolution operation defining the powder pattern (Seelig, 1977).

Phosphorus NMR. Phosphorus NMR spectra were acquired on the MSL-300 spectrometer operating at a frequency of 121.497 MHz using the Hahn spin-echo:

$$90^{\circ}_{x} - \tau_1 - 180^{\circ}_{y} - \tau_2 - \text{acquire} \qquad (11)$$

with full phase cycling of the radiofrequency pulses (Rance & Bird, 1983; Fukishima & Roeder, 1981; Hahn 1950) and Waltz-16 decoupling (Shaka et al., 1983). Pulse spacings were 50 μs, the 90° phosphorus pulses were 5-6 μs in length and the recycle time was 2.5 seconds. The decoupler power was set at 6 watts with proton 90° pulses of 65 μs. The spectra were acquired at ambient temperature, approximately 25 °C.

Results

The Liquid Crystalline Phase

Quadrupolar Splittings Versus Temperature. The nine deuteriated isolinoleic acids were esterified to form 1-palmitoyl-2-isolinoleoyl phosphatidylcholine (PiLPC, Figure 4.1), and after purification the lipid was dispersed in deuterium-depleted H_2O. The samples were then subjected to several freeze-thaw-vortex cycles until each was a homogeneous milky white solution, sealed under argon in 5 mm NMR tubes, and spectra were acquired over a range of 1 °C to 40 °C. A representative spectrum for each dispersion, at 30 °C, is shown in Figure 4.2.

All but one of the samples ([$^2H_2$-8]-PiLPC, see below) gave deuterium "powder pattern" spectra indicative of lipids undergoing fast axially symmetric motions ($>10^5$ s^{-1}) in the bilayer (see Figure 2.2, Chapter 2). Several of the spectra, however, consist of at least two overlapping powder patterns as can be clearly seen in those recorded from PiLPC deuteriated at the C_6 and the C_9-C_{10} positions. In the case of [^{2}H-6']-PiLPC, the "second" splitting was assigned to a small amount of highly deuteriated 1-palmitoyl-2-linoleoyl phosphatidylcholine ([$^2H_2$-6']-PLPC; see Chapter 3) and, based upon the intensities of the two powder patterns (determined by spectral simulations and integrating the dePaked spectra) relative to the intensities of the two peaks in the high resolution spectrum of the sample, the larger of the splittings was assigned to [$^2H_2$-6']-PLPC.

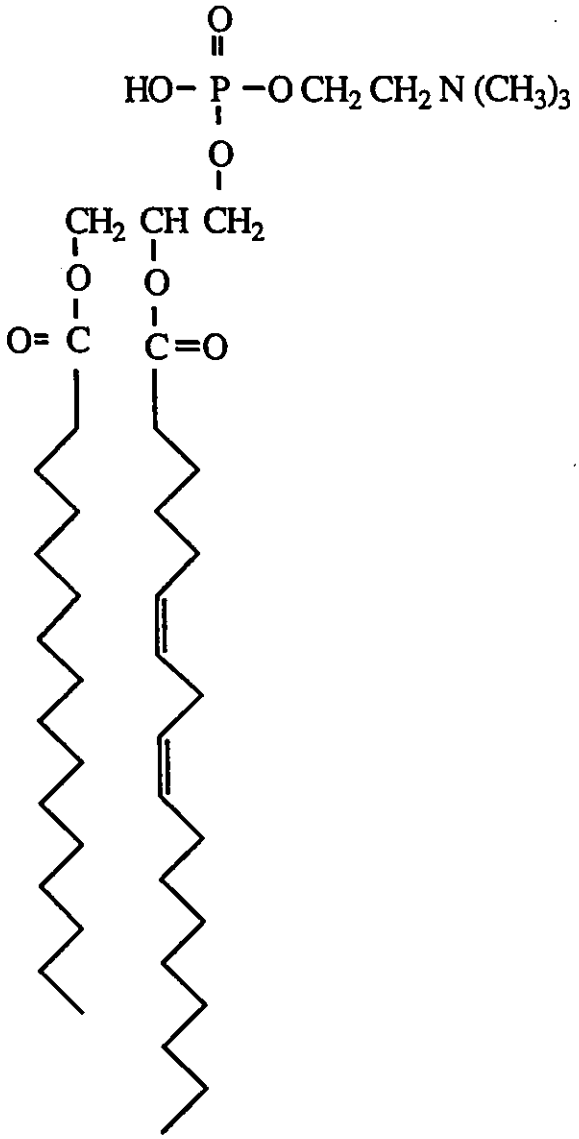

Figure 4.1. 1-palmitoyl-2-isolinoleoyl phosphatidylcholine (PiLPC). The remainder of the work presented in this thesis is focused on PiLPC deuteriated at 10 individual positions along the isolinoleoyl chain.

Figure 4.2.

^2H powder spectra of PiLPC deuteriated at the indicated postion of the isolinoleoyl chain. All were acquired at 37.0 MHz on a home-built spectrometer at 30 °C (see "Deuterium NMR Spectroscopy" under Materials and Methods) and for presentation purposes were folded about the center of the powder to increase the signal to noise ratio by a factor of $\sqrt{2}$. The arrows indicate peaks arising from iLPPC.

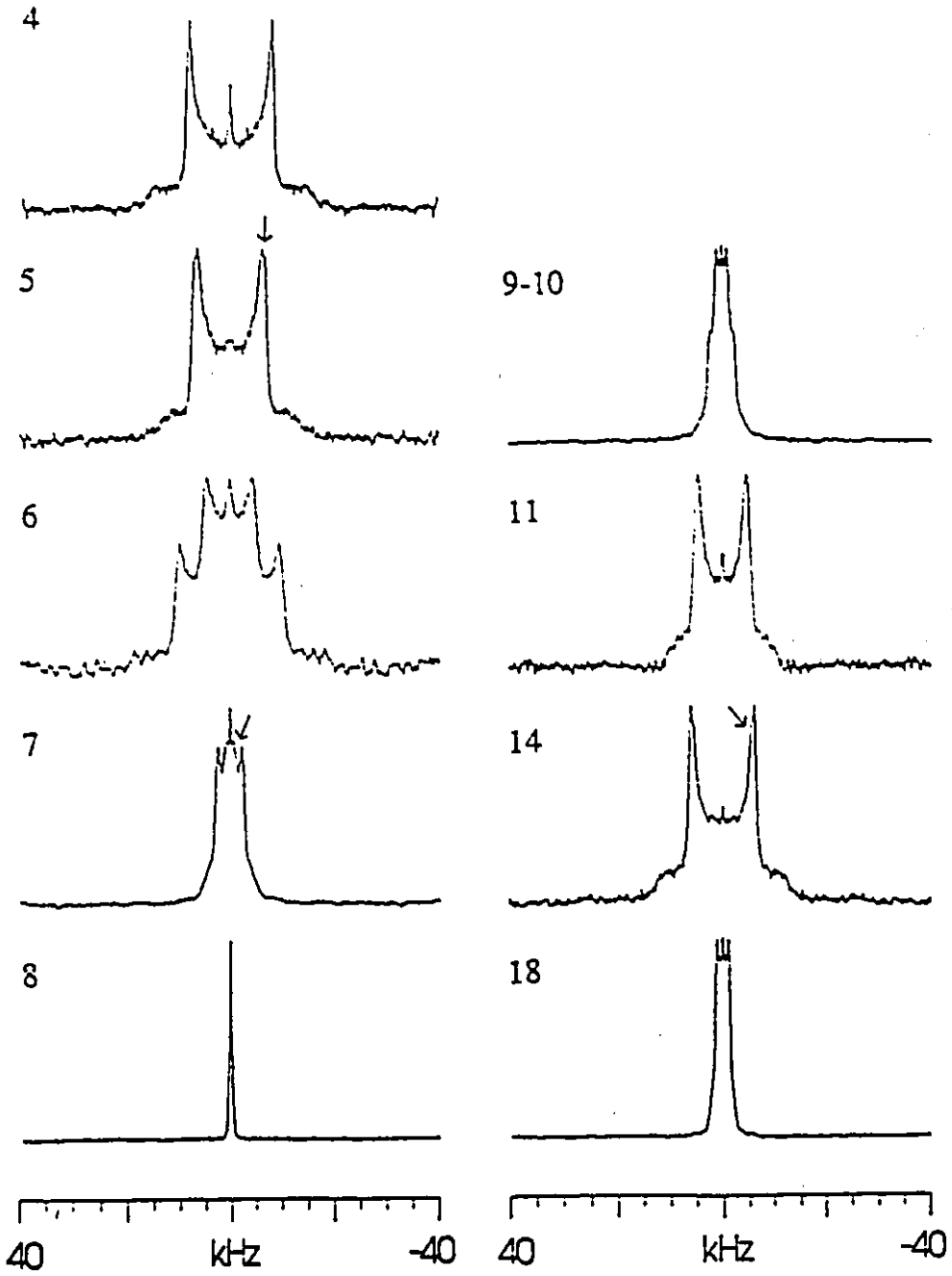
4
5
9-10
6
11
7
14
8
18
40
kHz
-40
40
kHz
-40

The two overlapping powder spectra observed for the dispersions of [$^2H_2$-9,10]-PiLPC are thought to arise due to inequivalence of the two deuterium atoms attached to the C_9 and the C_{10} carbon atoms of the double bond. It is possible that both the C_9 and C_{10} deuterons have the same S_{geo} and S_{mol} and that the two splittings arise from two, long lived, inequivalent lipid conformations. However; the two powder patterns are of approximately equal intensity (as determined by integration of the dePaked spectra and by simulating the powder spectra) and their relative intensities do not change with increasing temperature. If two inequivalent acyl chain conformations were responsible, one would expect that the relative proportions of the two powder patterns to change with temperature and that the two adjacent methylene segments would each yield spectra consisting of two quadrupolar powder patterns of equal intensity. Only one pattern is clearly evident for the C_{11} deuterons and although two major patterns are observed for the C_8 deuterons (see below), by the same arguement one would expect two powder patterns of equal intensity for the C_7 segment and clearly this is not the case. In Chapter 5 it will also be shown that the two major splittings for the C_8 methylene segment arise due to the inequivalence of the two C_8 deuterons. The evidence therefore confirms that the additional splittings arise due to inequivalence of the C_9 and C_{10} deuterons as is observed for the C_9-C_{10} double bond of the oleoyl chain in aqueous dispersions of POPC (Seelig & Waespe-Sarcevic, 1978).

The dePaked spectra (Figure 4.3) reveal that the powder spectra of PiLPC deuteriated at the 5, 7 and 14 positions also consist of two overlapping powder patterns. However, for all three positions the second powder pattern represents only a small proportion of the total signal. The value of its quadrupolar splitting is very close to that measured for the most intense powder pattern and therefore the additional signal was assigned to the presence of 1-isolinoleoyl-2-palmitoyl PC (iLPPC) formed by acyl chain

Figure 4.3.

Depaked spectra of PiLPC deuteriated at the indicated positions of the isolinoleoyl chain. Spectra were acquired as indicated in Figure 4.2 and were dePaked by the method of Bloom et al. (1981). All spectra, except those recorded from [^{2}H-6']-PiLPC, were analyzed without folding but the folded spectra are presented here for consistency.

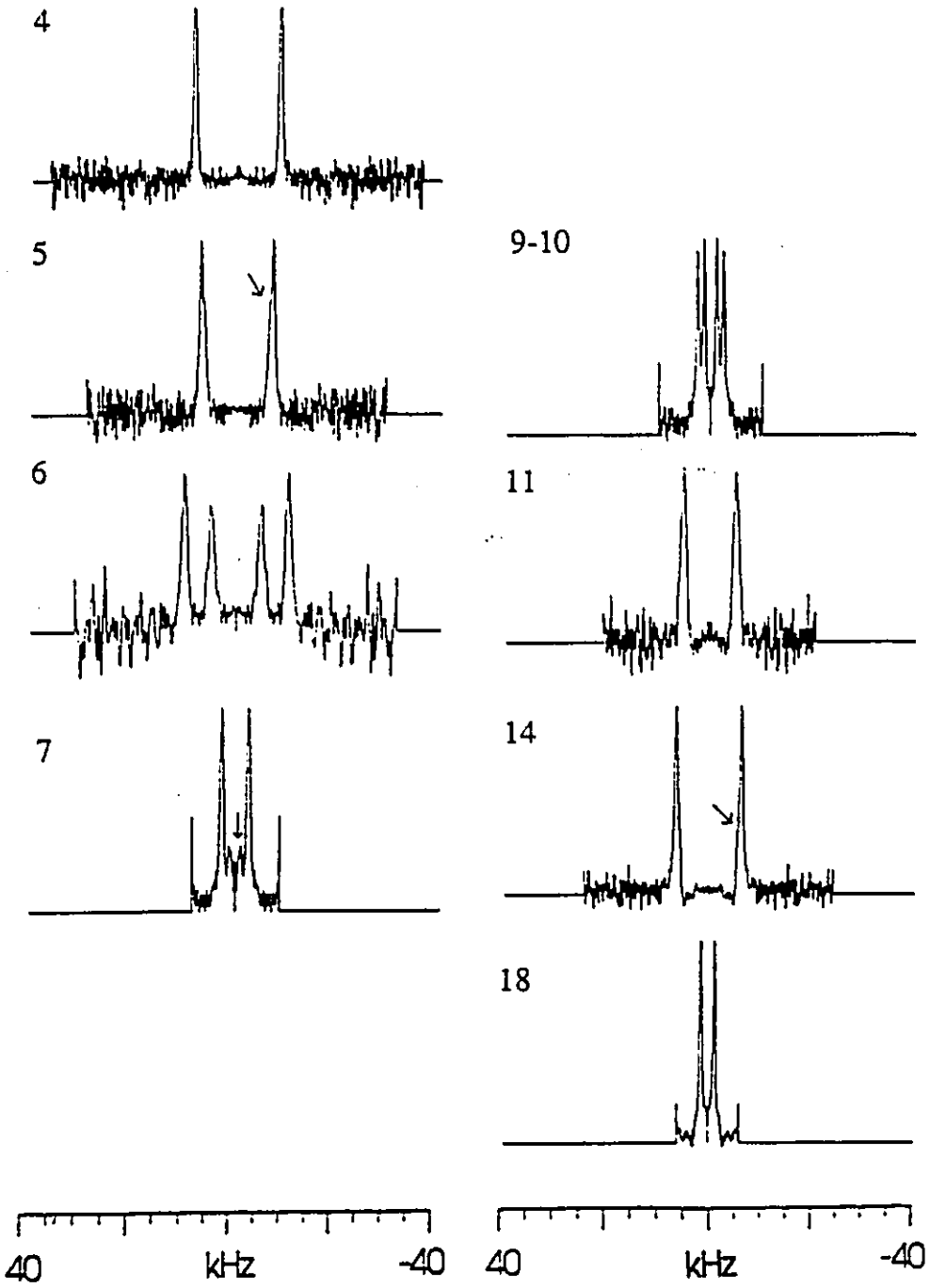
4
5
6
7
9-10
11
14
18
40
kHz
-40
40
kHz
-40

migration during the esterification procedure. The origin of these additional splittings and their effect upon the results presented in this chapter will be discussed in more detail below under "Spectral Simulations and Acyl Chain Migration ".

The spectra of PiLPC, labelled at the 8 position consist of a single narrow peak and are suggestive of lipids organized in small vesicles or micelles which undergo fast isotropic tumbling in solution. The sample, however, formed a homogeneous milky white solution characteristic of lipids organized in large multilamellar vesicles, and additional freeze-thaw-vortex cycles had no affect on the shape or width of the spectra. A phosphorus spectrum was also recorded and the result (Figure 4.4a) is a broad phosphorus powder pattern indicative of lipids undergoing fast axially symmetric motions in large multilamellar vesicles. It can therefore be concluded that the gross structural organization of the lipid is not the cause of the narrow spectra or the unusual line shape. In addition, the chemical shift anisotropy (CSA; width of the phosphorus powder pattern, see Chapter 2) is approximately 48 ppm which is comparable to those that have been measured for other lipids in multilamellar dispersions. The amplitudes of motions in the headgroup region of PiLPC are therefore similar those occuring in the headgroup region of completely saturated lipids.

Narrow, single line deuterium spectra can also arise if either the molecular order parameter, S_{mol}, or the geometric order parameter, S_{geo}, is equal to zero. In either case, the quadrupolar splitting would be reduced to zero and the deuterium NMR spectra would consist of a single, narrow, Lorentzian line. However, the spectrum of [$^2H_2$-8']-PiLPC at 30 °C is approximately 2 kHz in width (Figure 4.4b) and the line shape is not Lorentzian indicating that the quadrupolar splitting is not reduced to zero and that the unusual line shape must arise from other effects such as poor digital resolution, T_2 effects (Rance et al.,

Figure 4.4.

a) A phosphorus spectrum of [$^2H_2$-8']-PiLPC acquired as indicated under Materials and Methods on a Bruker MSL-30′ spectrometer operating at 121. MHz. **b)** An expanded view of the ^2H powder spectrum of [$^2H_2$-8']-PiLPC recorded as indicated in Figure 4.2 at 30 °C.

a

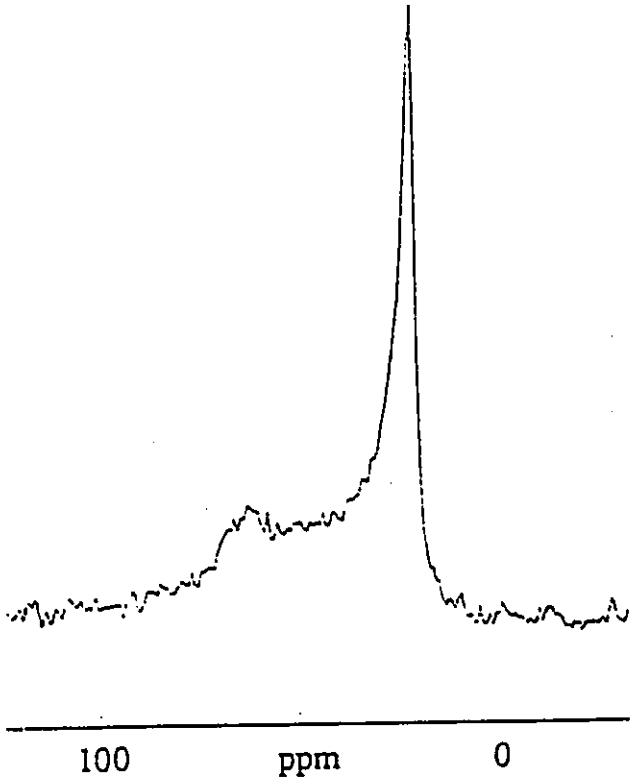

b

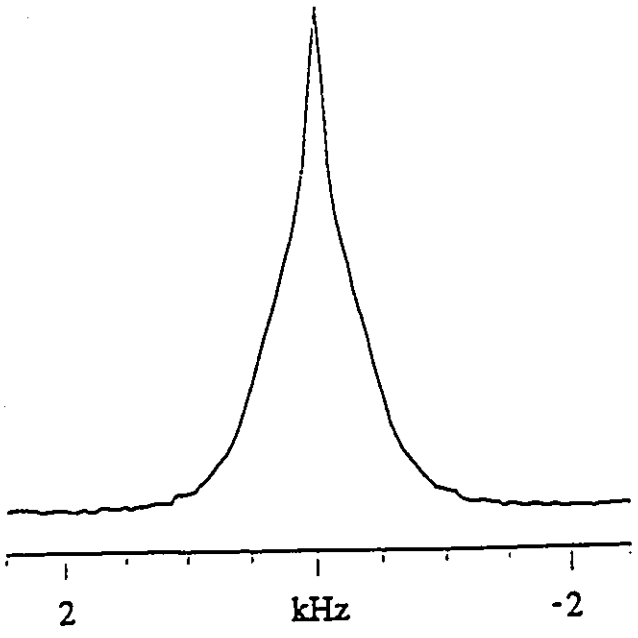

1981), axially asymmetric motion, or line broadening due to dipolar interactions. Spectra were acquired with increased digital resolution and with varied pulse spacings (τ_1), and neither had an effect on the spectral line shape. Acquiring spectra with proton decoupling finally resolved the uncertainty and, as shown in Figure 4.5a, spectra with quadrupolar powder pattern line shapes were observed. The proton-decoupled spectra confirm that the C_8 methylene segment undergoes axially symmetric motions within the bilayer and consist of two major overlapping powder patterns. A third signal which is also evident at some temperatures (40 °C, for example) was attributed to the presence of deuteriated iLPPC in the sample (see Spectral Simulations and Acyl Chain Migration ; below).

Previous work has suggested that proton-deuterium dipolar couplings have no effect on deuterium powder spectra (Seelig & Seelig, 1974). However, for the C_8 methylene unit these couplings are clearly large enough to cause severe distortions of the quadrupolar powder pattern line shape. In Chapter 5, it will also be shown that proton-decoupling can lead to spectra where the deuterium-deuterium dipolar couplings are directly measured, and that this additional information makes it possible to interpret the deuterium NMR data unambiguously in terms of both the orientation and ordering of the methylene segment (see below). Simulation of the deuterium-deuterium dipolar-coupled spectra also provides strong evidence that the two major powder patterns observed for the C_8 methylene segment arise due to inequivalence of the two C_8 deuterons as opposed to the existence of two inequivalent lipid conformations, as discussed above.

The powder spectra were dePaked by the method of Bloom et al. (1981) to yield the 90^o-oriented sample spectra from which the values of the quadrupolar splittings were determined (Figure 4.3 and 4.5b). The splittings for each deuteriated segment are plotted, as a function of temperature, in Figure 4.6 and most decrease in value with increasing

Figure 4.5.

a) Proton-decoupled ^2H NMR spectra of acqueous dispersions of [$^2H_2$-8']-PiLPC acquired on a Bruker MSL-300 spectrometer operating at 46.064 MHz. Spectra are not folded. **b)** The oriented sample spectra arising from dePaking the spectra shown in **a)**.

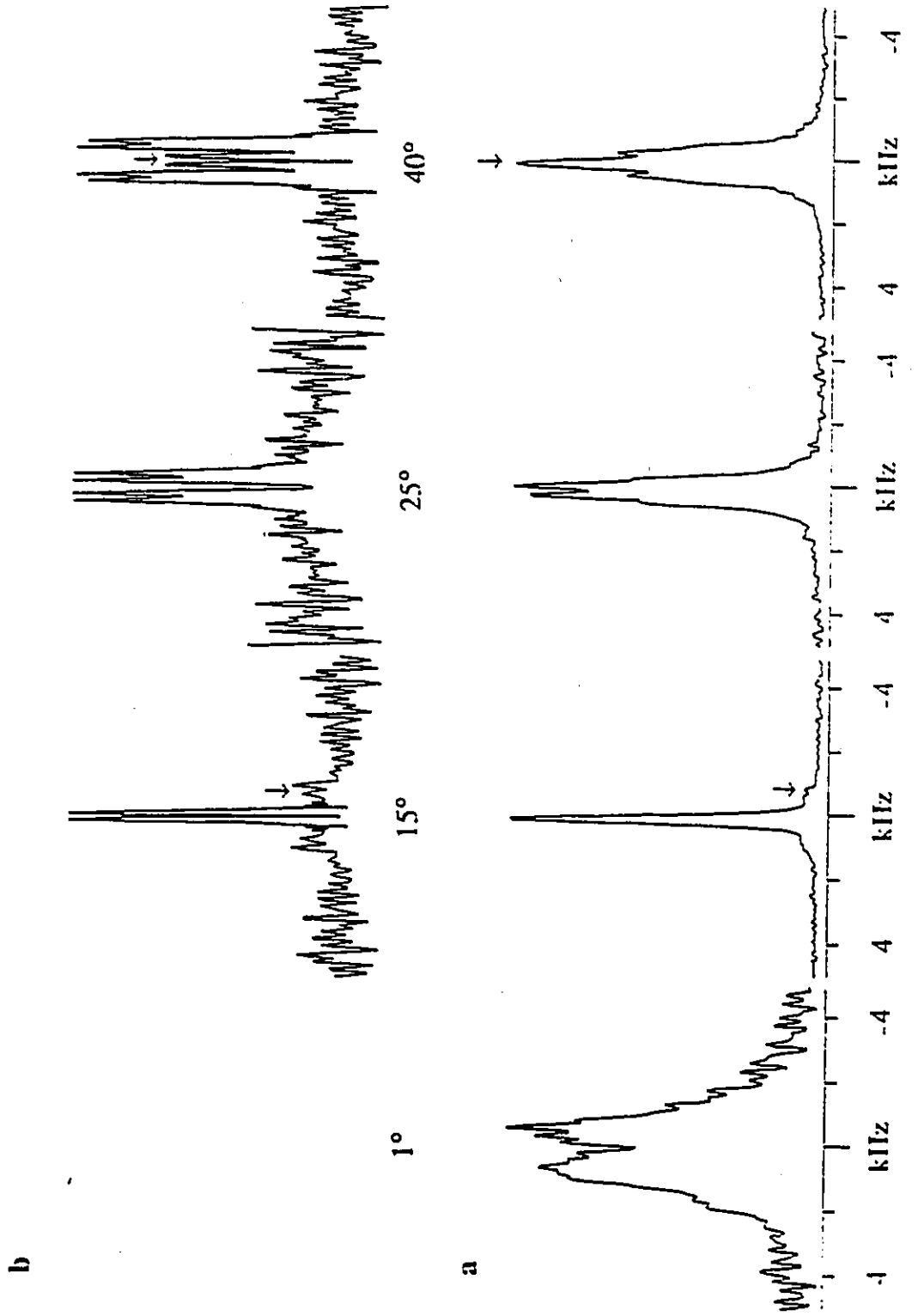
b
1°
15°
25°
40°
a
-1
kHz
-4
4
kHz
-4
4
kHz
-1
4
kHz
-4

temperature indicating that the system becomes more disordered. However, the splittings recorded for several of the deuteriated segments either increase in value with increasing temperature, or remain constant, as can be seen in Figure 4.7. It is unlikely that the ordering of these segments increases with temperature (this would indicate that the amplitudes of motion decrease) and therefore the results must arise from a change in the average orientation of the respective alkene and methylene units.

The temperature dependence of the splittings recorded from the C_6 and C_7, and from the C_9 and C_{10} deuterons confirms that the orientations of both the C_6-C_7 and the C_9-C_{10} double bonds change with temperature. For each double bond, the two deuterium labels are attached to the same rigid unit (ie. the double bond) and their motions are described by the same molecular order parameter, S_{mol}. The values of the two splittings should therefore change proportionally with temperature if the orientation of either double bond remains constant (ie. if both S_{geo}'s remain constant). For the C_9 and C_{10} deuterons, the value of one splitting actually increases with increasing temperature while the other decreases, and for the C_6 and the C_7 deuterons, the value of one splitting decreases with increasing temperature while the other essentially remains constant. A change in orientation of the two double bonds is therefore implied.

The average orientation of the C_8 methylene segment also varies with temperature as is evident by the observation that between 10 °C and 15 °C the splittings essentially collapse to zero and subsequently increase in size. The results also imply that at 15 °C the geometric factors, $(3Cos^2\beta_{8a/b} - 1)/2$ (where β_{8a} and β_{8b} are the angles between the two C-^{2}H bonds and the bilayer normal), for both C_8 deuterium labels are equal to zero. This situation can only occur if both angles, β, are 54.7° and assuming standard bond geometry

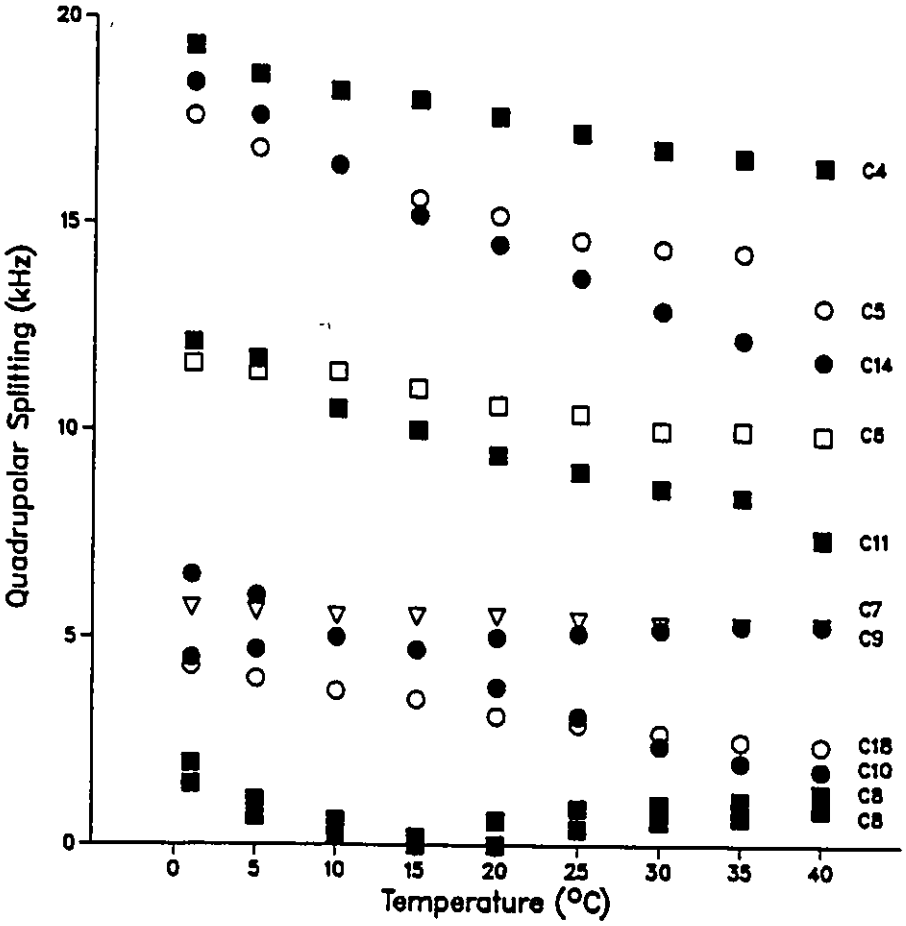

Figure 4.6. A summary of the values of the quadrupolar splittings for each deuteriated position of the isolinoleoyl chain of PiLPC as a function of temperature.

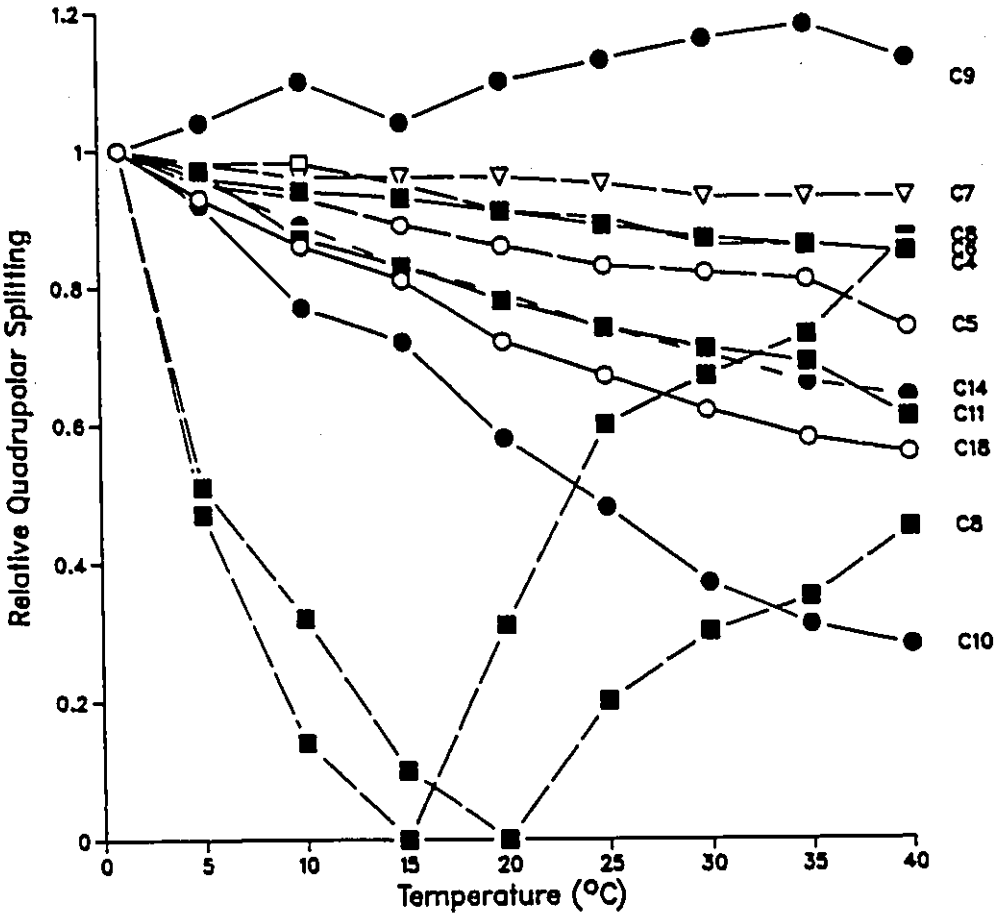

Figure 4.7. A summary of the relative changes in the quadrupolar splittings for each deuteriated position of the isolinoleoyl chain of PiLPC as a function of temperature. The quadrupolar splitting for each labelled position at 1 °C was normalized to a value of 1.0, and the remaining values plotted are the changes in the quadrupolar splittings relative to the values at 1°C.

(tetrahedral bond angles of 109.4°) the average orientation of the methylene unit must be one of those shown in Figure 4.8.

The first is roughly consistent with the angle iron/helical conformation proposed by Applegate and Glomset (see General Introduction, Chapter 1). However, in Chapter 5 it will be shown that the second orientation is the correct one. This orientation of the C_8 methylene segment is clearly inconsistent with the proposed conformation but, as will be discussed, it is an average of two conformations between which the acyl chain undergoes a two-site jump. The principal components of the ordering tensor of the C_8 methylene segment at 40 °C are $S_{11} = -0.089$, $S_{22} = -0.062$, and $S_{33} = 0.150$ (see Chapter 5).

The significance of the changes in orientation of the various segments with changing temperature will be discussed in more detail below, and under "Discussion".

Conformation of the Isolinoleoyl Chain in the Liquid-Crystalline Phase. In principle, the C_6-C_7 and the C_9-C_{10} double bonds of the isolinoleoyl chain can adopt any orientation within the bilayer. However, given the orientation of the C_8 methylene segment specified above, only orientations brought about by rotations about the C_7-C_8 and the C_8-C_9 carbon-carbon single bonds, respectively, are possible. In addition, since the molecular order parameters for the C_6 and the C_7 deuterons, and for the C_9 and the C_{10} deuterons are equivalent, the ratio of their quadrupolar splittings are specified by the ratios of their geometric factors, and only rotations about the respective carbon-carbon single bonds which yield geometric factors consistent with the observed quadrupolar splitting ratios are possible. At 15 °C both ratios are defined as follows:

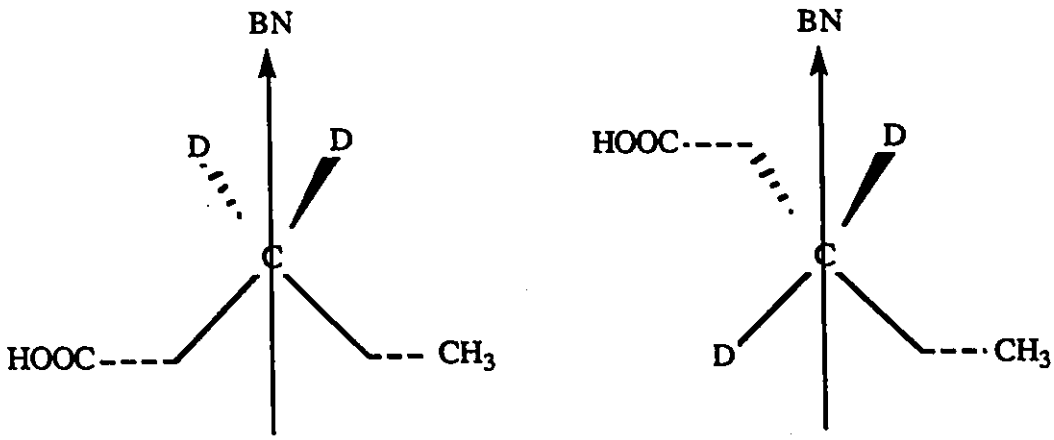

Figure 4.8. The proposed orientations of the C_8 methylene segment at 15 °C. At this temperature both C-^{2}H bonds are oriented at essentially the "magic angle (54.7°)" with respect to the bilayer normal and the methylene segment can therefore adopt one of the two orientations shown. BN shows the direction of the normal to the bilayer surface. For each orientation, however, the aqueous surface of the bilayer can be either above or below the segment so in fact there are four possible orientations.

$$\frac{(3\text{Cos}^2\beta_9 - 1)}{(3\text{Cos}^2\beta_{10} - 1)} = \pm 1.0 \qquad \frac{(3\text{Cos}^2\beta_6 - 1)}{(3\text{Cos}^2\beta_7 - 1)} = \pm 2.0$$

where the angles "β" are between the respective C-^{2}H bond vectors and the axis of motional averaging (usually the bilayer normal). By calculating all possible rotations about the C_7-C_8 and the C_8-C_9 single bonds which satisfy these two ratios, the orientations of the two double bonds can be defined.

One complicating factor arises, however, when the splittings for the C_6 and the C_{10} deuterons are examined. Assuming standard bond geometries, the C_6-$^2H_6$ and the C_{10}-$^2H_{10}$ bond vectors are parallel to the C_7-C_8 and C_8-C_9 bond vectors, respectively, and at 15 °C the latter two are oriented at the "magic angle" with respect to the axis of motional averaging. Consequently, the C_6-$^2H_6$ and the C_{10}-$^2H_{10}$ bonds must also be oriented at the "magic angle" and therefore both should give rise to spectra consisting of an isotropic line with no measurable quadrupolar splittings (as shown below for the C_9-C_{10} double bond).

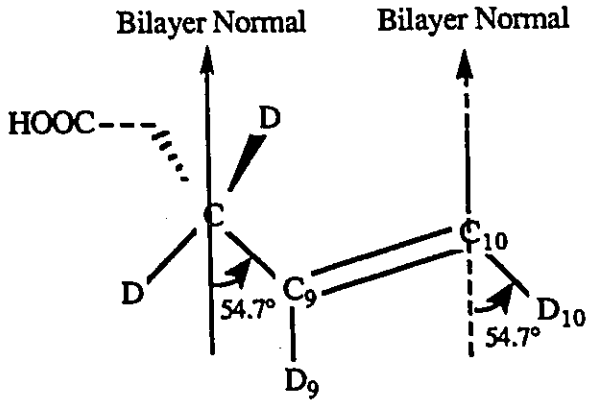

The observation at 15 °C of two powder spectra with splittings of 11.0 kHz and 4.7 kHz for the C_6 and C_{10} deuterons, respectively, suggests that either the orientation of the C_8 methylene unit is specified incorrectly or that the bond angles of the two double bonds deviate significantly from "normal". X-ray crystallography has shown that the bond angles of the two double bonds of linoleic acid deviate by as much as 8.1° from "normal" (see Figure A1, Appendix 1) and therefore the latter conclusion seems likely. All future calculations in this thesis will therefore be performed using the bond angles of the 1,4-pentadiene segment of linoleic acid ($18:2^{\Delta 9,12}$) assigned to the corresponding bond angles of the 1,4-pentadiene segment of isolinoleic acid ($18:2^{\Delta 6,9}$).

All possible orientations of the C_6-C_7 and the C_9-C_{10} double bond at 15 °C were calculated in Appendix 2 using the bond angles of linoleic acid. The angles between the C-^{2}H bond vectors and their double bond axes, however, were not specified in the crystal structure so each of the four C_x-^{2}H bond vectors was assumed to bisect the corresponding $C_{x-1}C_xC_{x+1}$ alkenal bond angle. Each angle was also allowed to vary over a range of 60° to 66° in order to determine the sensitivity of the calculations to such variations. The results summarized in Tables A2.1 and A2.2 of Appendix 2 show that several orientations, for each double bond, are consistent with the quadrupolar splitting ratios. The values of the

molecular order parameter, for each possible orientation, were also calculated from the quadrupolar splitting data and the values range from 0.60 to 0.76 for the C_6-C_7 double bond and from 0.15 to 0.33 for the C_9-C_{10} double bond.

The results were interpreted in terms of a two-site jump model between two conformations in which the double bonds are oriented parallel to the bilayer normal (see Discussion). There are two possible modes, however, of interconverting between the two conformations (see Figure 4.9) and in one case, the path of the C_8 segment passess through an orientation such that the two C-^{2}H bonds extend towards the aqueous interface, whereas in the other the C-^{2}H bonds would be oriented towards the interior of the bilayer. Each is consistent with one of the two orientations proposed for the C_8 methylene unit in Chapter 5, but the first mode would lead to a much smaller angular excursion (a rotation of ~120° as opposed to a rotation of ~240°) and therefore seems likely.

Assignment of the average orientation of the C_8 methylene segment to the orientation shown in Figure 5.10 reduces the number of possible orientations for each double bond and, given the constraints imposed by the parallel packing of acyl chains in the membrane, the average conformation of the 1,4-pentadiene segment of the chain in the liquid crystalline phase was defined. The proposed conformation of the 1,4-pentadiene segment of the isolinoleoyl chain is shown in Figure 4.10. In this conformation, the orientations of the C_6-C_7 and the C_9-C_{10} double bonds arise from rotations about the C_7-C_8 and C_8-C_9 single bonds of ± 120° and ± 25°, respectively, from the starting orientation defined in Appendix 2. The molecular order parameters for the C_6-C_7 and the C_9-C_{10} double bonds were also calculated, assuming axially symmetric ordering, to be roughly 0.60 and 0.15, respectively (for the C_6-C_7 double bond a second orientation arising from a rotation of ± 113° and yielding a molecular order parameter, S_{mol}, of 0.7 is also possible,

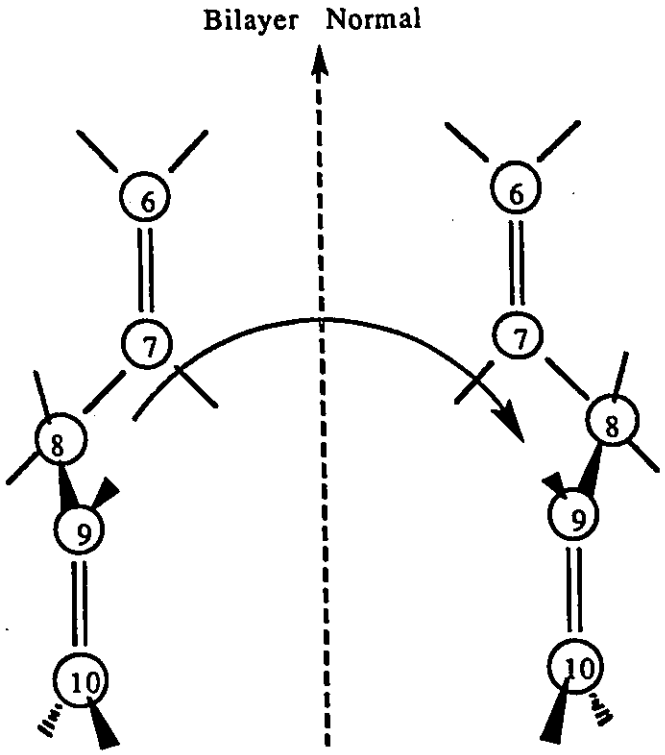

Figure 4.9. The jump model proposed for the motions of the α,4-pentadiene segment of the isolinoleoyl chain of PiLPC. The chain is proposed to exist in one of the two structures shown above, but undergoes a two-site jump between the two conformations in the liquid crystalline phase.

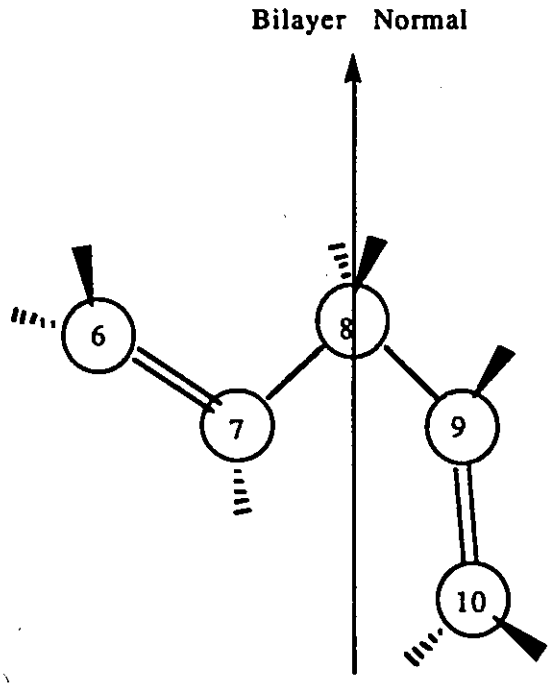

Figure 4.10. The average conformation of the 1,4-pentadiene segment of the isolinoleoyl chain of PiLPC in the liquid crystalline phase at 15 °C. The bilayer normal bisects the two methylene C-^{2}H bonds, the C_6-C_7 double is tilted out of the plane of the paper by a rotation about the C_7-C_8 bond by an angle of $\pm 60^o$, and the C_9-C_{10} double bond is tilted out of the plane of the paper by a rotation about the C_9-C_{10} single bond by an angle of $\pm 25^o$.

see Appendix 2. Intuitively, the former solution is more likely because it would not lead to as drastic a drop in the order parameter from the C_6-C_7 unit to the C_8 unit).

The orientations of the C_8 methylene segment at both 25 °C and 40 °C were defined (Chapter 5) and the analysis described above was performed (Appendix 2) to define the orientations of both double bonds at 25 °C and 40 °C. The results from the calculations are also shown in Tables A2.1 and A2.2 of Appendix 2. The proposed conformation, at 40 °C, arises from rotations of the C_6-C_7 and the C_9-C_{10} double bonds about the C_7-C_8 and C_8-C_9 bond single bonds by angles of $\pm$ 120° and $\pm$ 59°, respectively, from the starting orientation defined in Appendix 2. The molecular order parameters for the two double bonds at 40 °C were also calculated to be 0.56 and 0.08, respectively (see Figure 4.12a).

The calculations show that the changes in the orientation of both the C_8 methylene unit and the C_6-C_7 double bond upon a temperature change from 15 °C to 40 °C are extremely small (for example, the C_8 unit changes its orientation by an angle of only 0.4°), whereas the C_9-C_{10} double bond changes its orientation by a rotation of 35° about the C_8-C_9 bond for the same temperature shift. The results clearly show the sensitivity of the quadrupolar splittings to the orientation of the deuteriated segments, especially when the C-^{2}H bonds are oriented close to the magic angle.

Order Parameter Profile. The quadrupolar splittings are related to the carbon-deuterium bond order parameter, S_{CD}, by the following equation:

$$\Delta\upsilon_Q = \frac{3}{4}\frac{e^2qQ}{h}S_{CD}$$

(equation 7 with $\theta = 90^o$) and the values of S_{CD} versus labeled position are plotted for two temperatures in Figure 4.11. The bond order profile shows a large drop in S_{CD} in the vicinity of the two double bonds of the chain but based upon the results presented above, this decrease can at least be partially attributed to the unique conformation of the isolinoleoyl chain relative to saturated and monounsaturated acyl chains, and not to a low degree of order.

A plot of the molecular order parameters versus temperature for the C_6-C_7, the C_8, and the C_9-C_{10} segments is shown in Figure 4.12a and for comparison, the molecular order parameters observed for the same segments of a saturated chain are plotted in Figure 12b at the same reduced temperature (T_{red}= [T_{obs} - T_c]/ T_c). The results show that the C_6-C_7 double bond is actually more ordered than the same segments of the palmitoyl chain of POPC but that the C_8 and the C_9-C_{10} segments are slightly less ordered (see Discussion).

One final interesting behaviour was noted when the temperature dependence of the various samples was examined. As shown in Figure 4.13 for [$^2H_2$-5]-PiLPC, the intensities of the powder spectra are greatly reduced as the temperature increases, despite the fact that the spectra were acquired at a recycle time of greater than 5 x T_1 (the spin-lattice relaxation time). A reduction in the intensities of the spectra with temperature was noted for several of the samples. However, upon further investigation it was shown that spectral acquisition with a recycle time of slightly greater than 10 x T_1 reduced the decrease in intensity to that expected from a change in the Boltzman distribution of the nuclear spins. It therefore appears that although most workers in the field use a recycle time of 5 x T_1 to

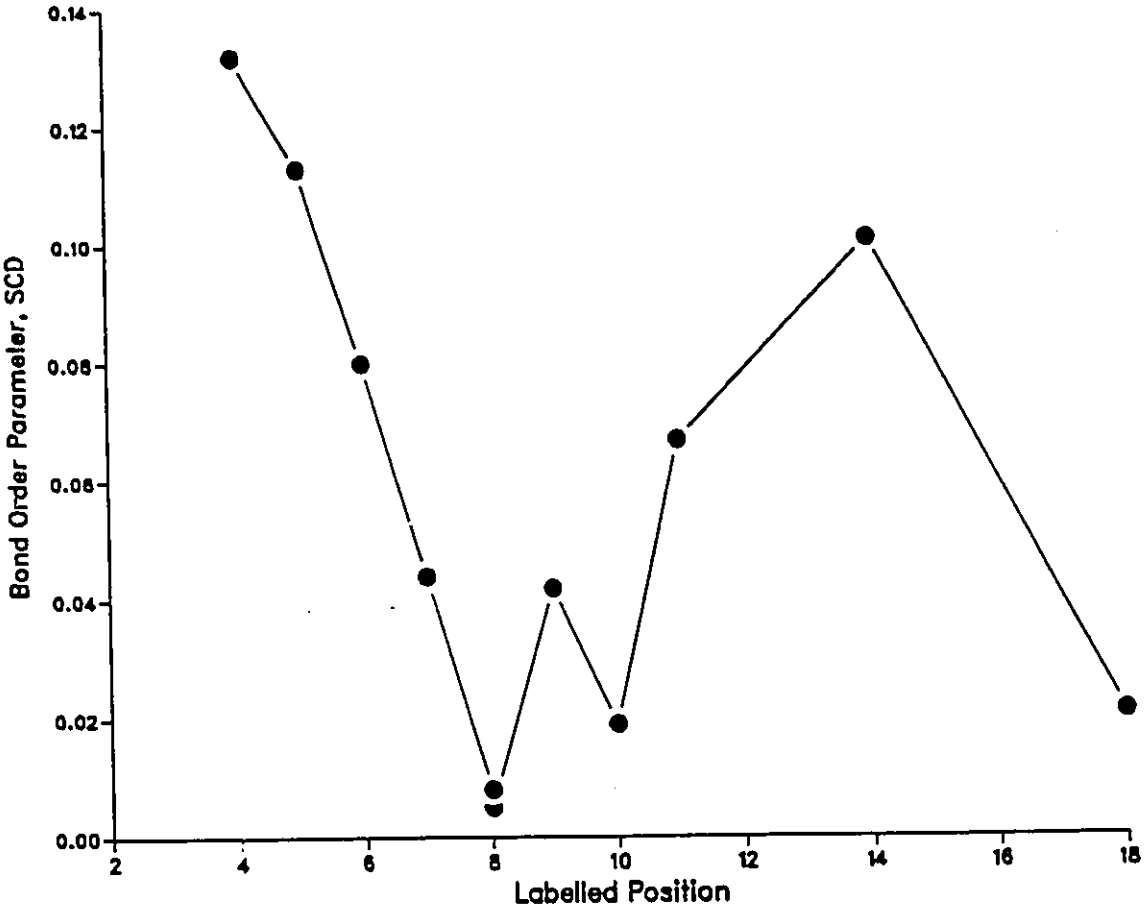

Figure 4.11. A plot of the bond order parameter, S_{CD}, versus labelled position for the isolinoleoyl chain of PiLPC. S_{CD} values were determined from the quadrupolar splittings as indicated in the text, at 30°C.

Figure 4.12.

a) A plot of the molecular order parameter versus reduced temperature (T_{red} = $[T_{obs} - T_c]/T_c$ and T_c = -15 °C) for the C_6-C_7, the C_8, and the C_9-C_{10} segments of the isolinoleoyl chain of PiLPC. The measurement temperatures are 15 °C, 25 °C, and 40 °C. **b)** The same data for POPC deuteriated at similar positions along the palmitoyl chain. The measurement temperatures are 27 °C and 42 °C and the T_c for POPC is -5 °C.

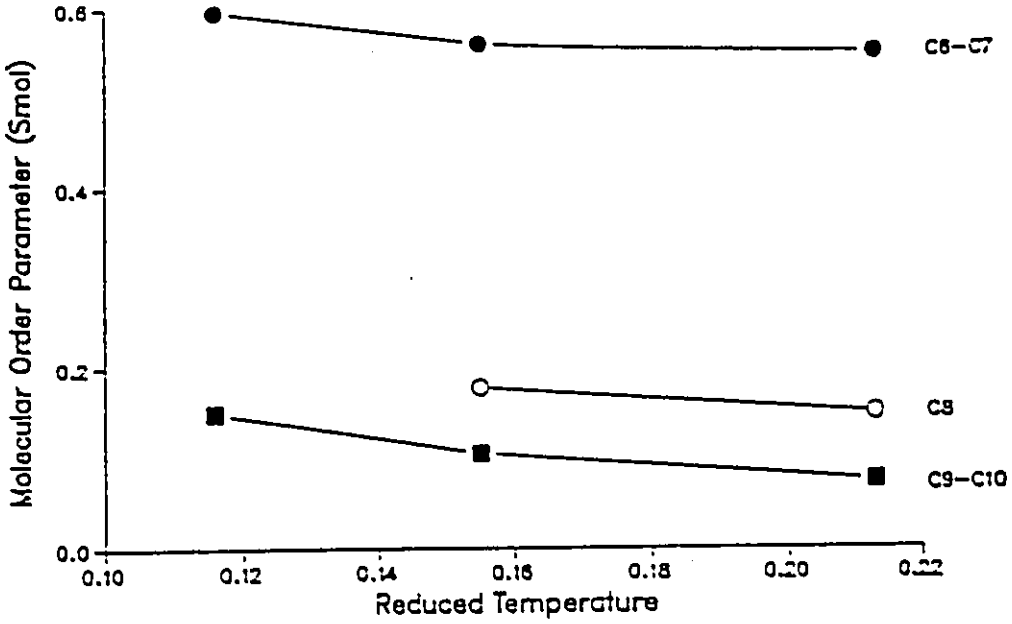
Molecular Order Parameter (Smol)
0.6
0.4
0.2
0.0
0.10
0.12
0.14
0.16
0.18
0.20
0.22
Reduced Temperature
C6–C7
C8
C9–C10

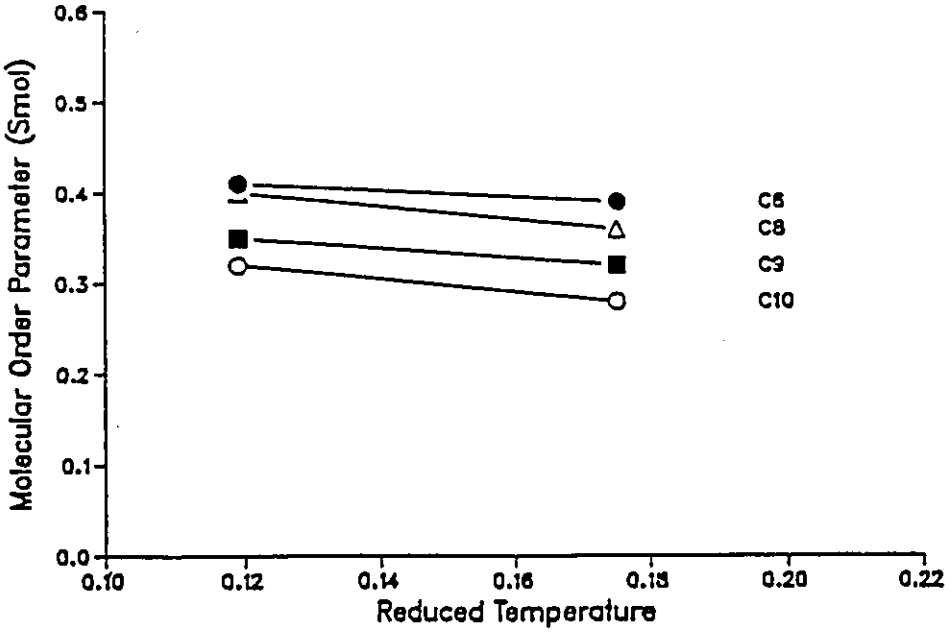
Molecular Order Parameter (Smol)
0.6
0.5
0.4
0.3
0.2
0.1
0.0
0.10
0.12
0.14
0.16
0.18
0.20
0.22
Reduced Temperature
C6
C8
C9
C10

Figure 4.13.

^2H spectra of aqueous dispersions of [$^2H_2$-5']-PiLPC acquired with a recycle time of **a)** 5 x T_1 and **b)** 10 x T_1. The spectra in **a)** show a large decrease in intensity of the spectra with increasing temperature due to incomplete relaxation of the spins back to their Boltzman distributions after each pulse. The spectra in **b)** are permitted to relax fully with a recycle time of 10 x T_1.

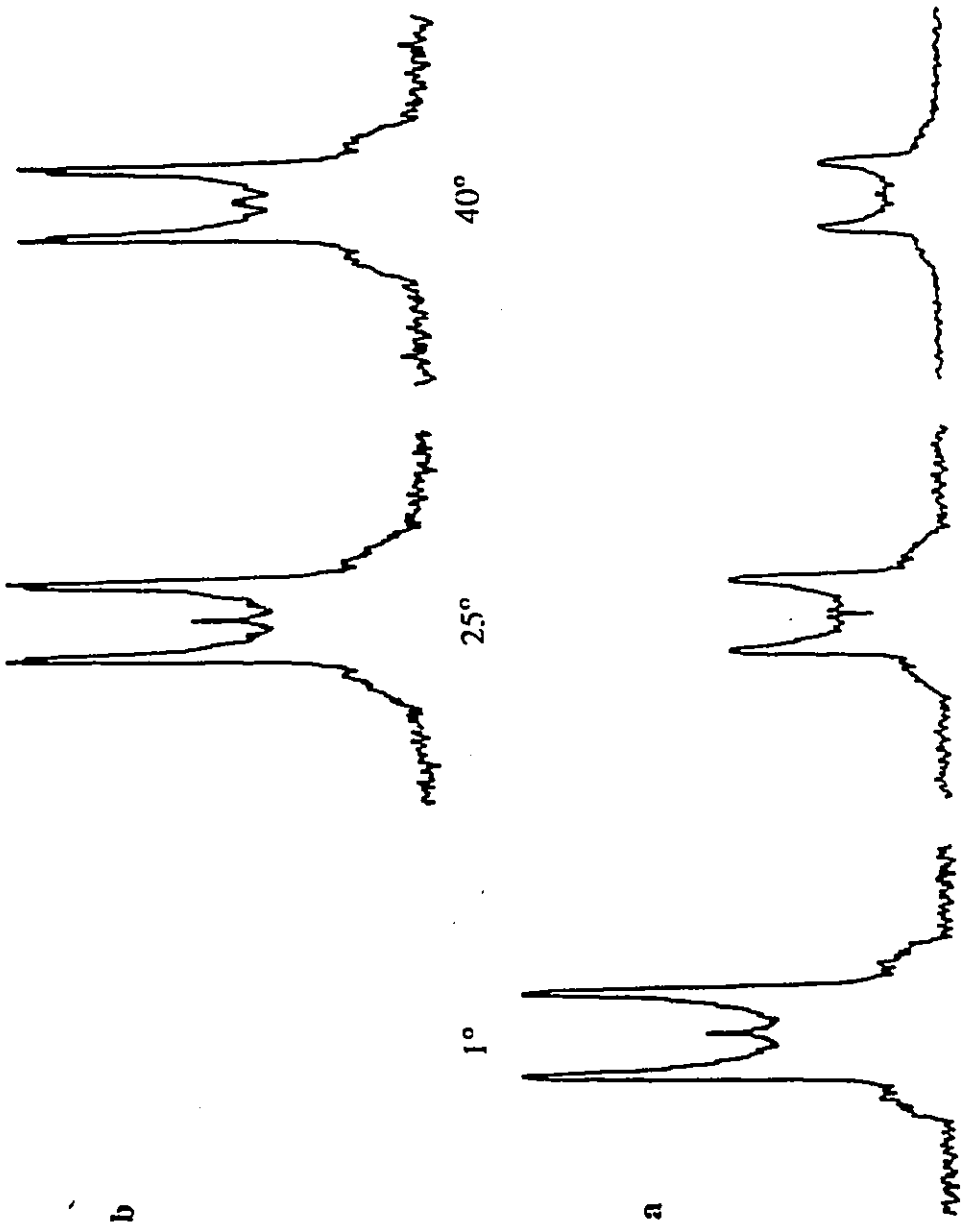
b
a
1°
25°
40°

The Gel Phase

Gel to Liquid-Crystal Transition Temperature. An estimate of the gel-to-liquid crystal phase transition temperature of PiLPC was obtained by acquiring spectra of several samples at low temperatures as is shown in Figure 4.14 for [^{2}H-7']-PiLPC. For all samples, above -5 °C the spectra are characteristic of lipids in the liquid crystalline phase and consist of a well defined powder pattern with distinct peaks and shoulders at twice the quadrupolar splittings. As the temperature is reduced below -5 °C, a broad, featureless component characteristic of lipids in the gel state appears and eventually, dominates the spectra. The existence of two components indicates that both the liquid crystalline and gel phase lipids coexist in the bilayer with an interconversion rate which is less than the difference in the quadrupolar interaction (< 10^5 s^{-1}). This phenomena has also been observed for other lipids.

In order to quantitate the changes occuring in the spectra, the spectral moments were analyzed. The second moment is defined as (Davis, 1983; Jarrell et al., 1981):

$$M_2 = \frac{\int_0^\infty \upsilon^2 F(\upsilon) d\upsilon}{\int_0^\infty F(\upsilon) d\upsilon}$$

where υ is the frequency within the spectrum $F(\upsilon)$. The parameter Δ_2 is defined as:

$$\Delta_2 = \frac{M_2}{1.35 M_1^{\,2}} - 1$$

Figure 4.14.

^2H spectra of aqueous dispersions of [^2H-7']-PiLPC acquired from 25 °C to -25°C.

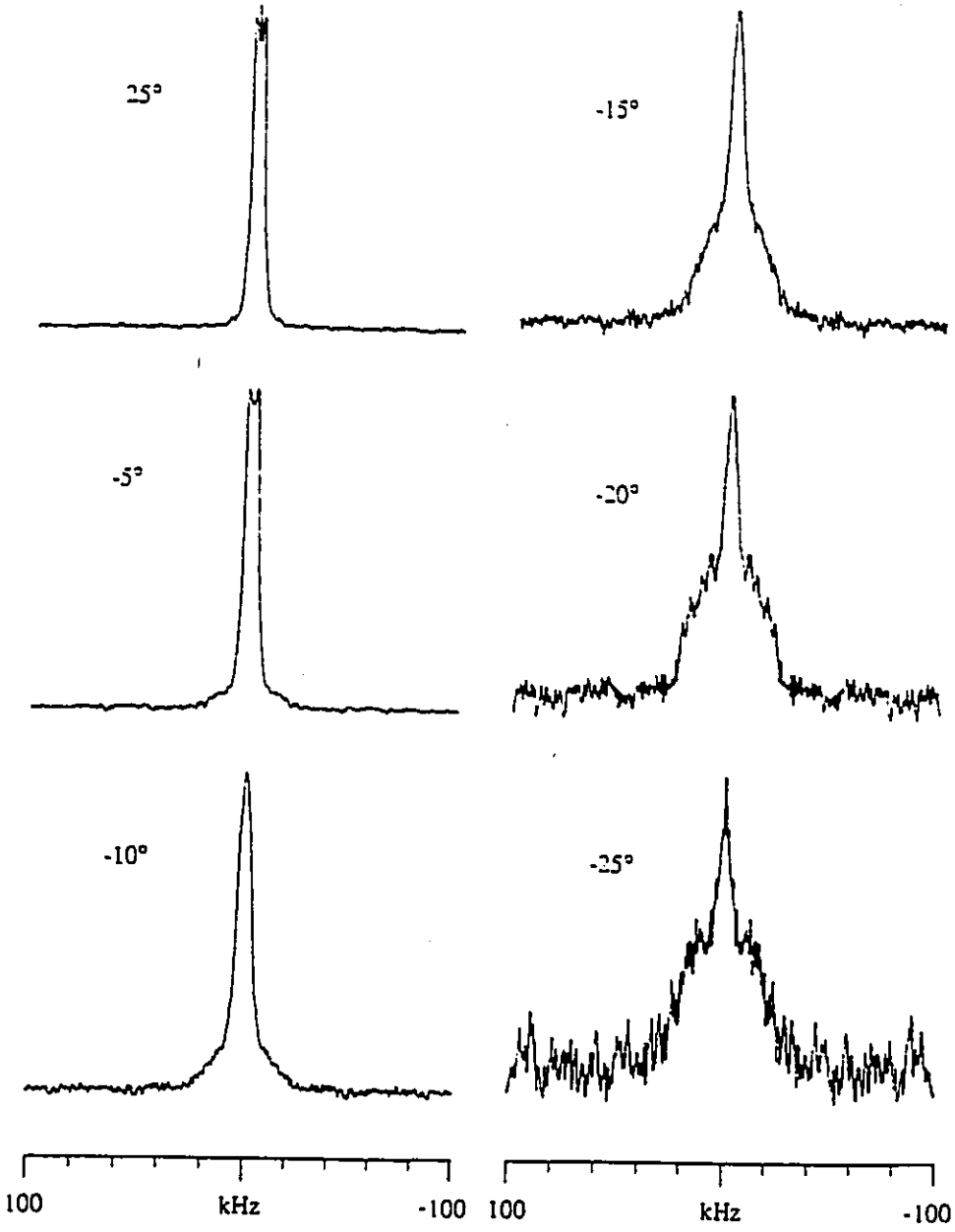
25°
-15°
-5°
-20°
-10°
-25°
100
kHz
-100
100
kHz
-100

M_2 is sensitive to the efficiency of averaging of the magnetic tensor components and a large increase in M_2 indicates that a significant increase in the quadrupolar splittings of the lipids has occured (this will occur if increasing numbers of lipids are found in the gel state). The parameter Δ_2 provides a measure of the fractional mean squared width of the distribution of order parameters; it has been shown that Δ_2 reaches a maximum value at the center of the gel-to-liquid crystal transition temperature of both model and natural membranes (Rance et al., 1980).

Both parameters are plotted as a function of temperature in Figures 4.15 and 4.16, respectively. The steep increase in M_2 below -5 °C reflects an increase in the fraction of the lipid in the gel state but the maximum value of 7.4×10^9 s^{-2} obtained at -25 °C is much less than the rigid lattice value of 1.28×10^{11} s^{-2} (Rance et al, 1980) thus indicating that there is still significant motion occurring in the bilayer (for example, long axis rotation). The Δ_2 function reaches a maximum between -5 °C and -10 °C suggesting that the transition temperature is in this range, however, only a small proportion of the lipid appears to contribute to the gel phase component between these temperatures. The anomaly perhaps arises because the analysis requires spectra with a better signal-to-noise ratio than is obtained in our analysis. Unfortunately, acquisition of spectra with a sufficient signal-to-noise ratio is impratical given the amounts of deuteriated sample available.

A better estimate of the transition temperature of PiLPC was obtained by recording phosphorus spectra of oriented multibilayers of PiLPC at low temperatures. The phosphorus spectra are consistent with the deuterium powder spectra presented above in that the transition region occurs over a temperature range of -5 °C to -25 °C, but the results clearly indicate that the center of the transition occurs at approximately -15 °C (see Chapter 5).

Figure 4.15.

Temperature dependence of the Δ_2 parameter for the ^2H NMR spectra of [^2H-2-7']-PiLPC.

Figure 4.16.

Temperature dependence of the second moment, M_2, for the ^2H NMR spectra of [^2H-2-7']-PiLPC.

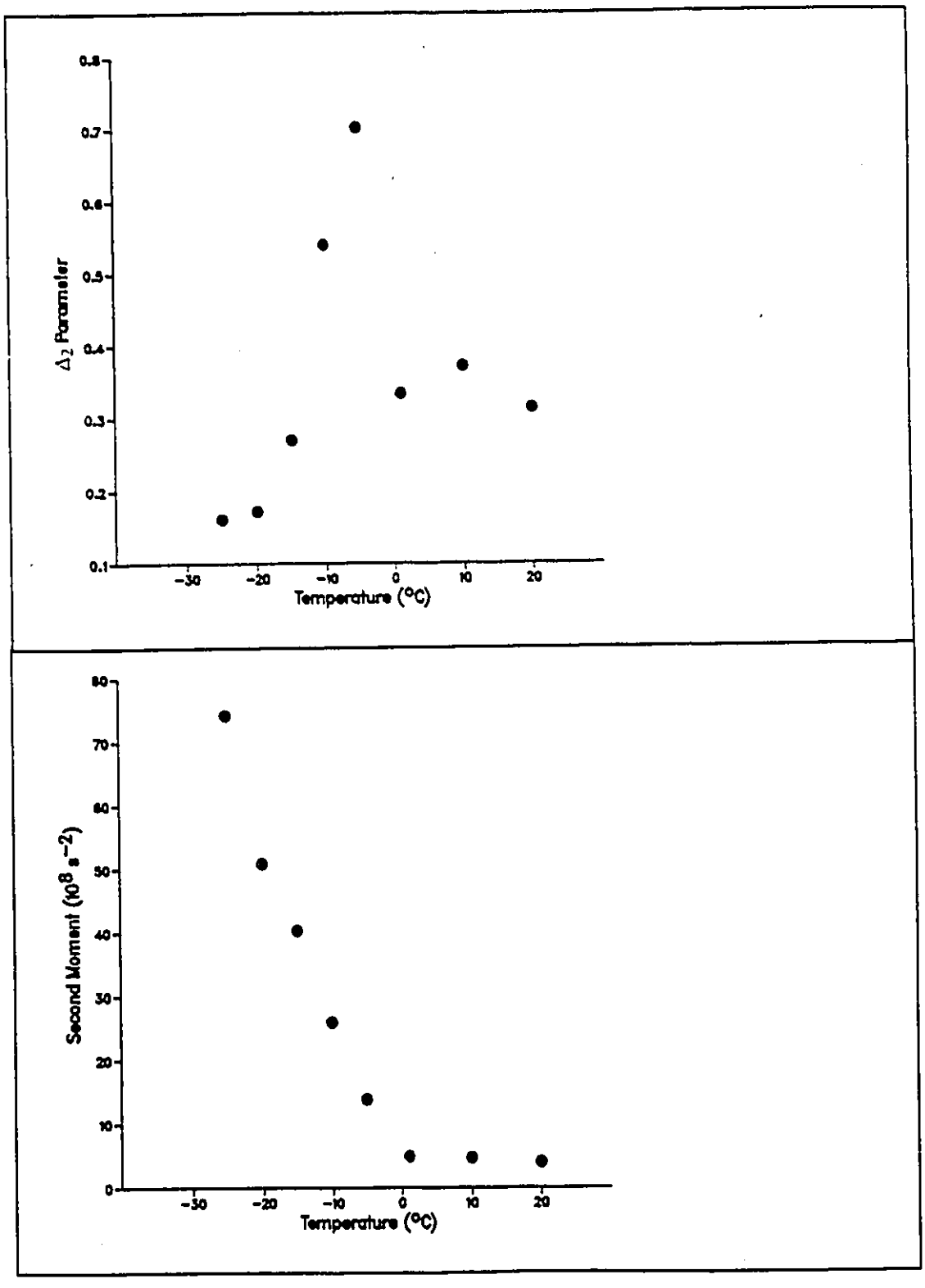
Δ_2 Parameter
0.8
0.7
0.6
0.5
0.4
0.3
0.2
0.1
-30
-20
-10
0
10
20
Temperature (°C)
Second Moment (10^8 s^{-2})
80
70
60
50
40
30
20
10
0
-30
-20
-10
0
10
20
Temperature (°C)

Conformation of Isolinoleic Acid in the Gel Phase. All the spectra acquired at -15 °C consist of a narrow component due to lipids in the liquid crystalline phase and a much broader component due to lipids in the gel phase (Figure 4.17). The spectra are of poor quality due to a low signal-to-noise ratio, but are of interest because of the unique lineshape of the gel-phase component in the spectra of [$^2H_3$-18']-PiLPC. Whereas the other gel phase spectra are broad and featureless (as is the case for most lipids), for [$^2H_3$-18']-PiLPC the spectrum is actually a powder pattern with a quadrupolar splitting of roughly 20 kHz.

The quadrupolar splitting for the terminal methyl group of an acyl chain is defined (assuming fast rotation about the C_{17}-C_{18} single bond) below as:

$$\Delta\upsilon_Q = \frac{3}{2}\frac{e2qQ}{h}\left(\frac{3\mathrm{Cos}^2\delta - 1}{2}\right)\left(\frac{3\mathrm{Cos}^2\omega - 1}{2}\right)\left(\frac{3\mathrm{Cos}^2\theta - 1}{2}\right)S_{mol}$$

where δ is the tetrahedral angle betwen the C-^{2}H bond axis and the C_{17}-C_{18} carbon-carbon bond (109.4°), ω is the angle between the C_{17}-C_{18} bond and the bilayer normal, and θ is as described in Chapter 2. For an acyl chain in the all-trans conformation, ω = 109.4 + 35.25, and with a molecular order parameter, S_{mol}, equal to 1.0, the value of the quadrupolar splitting should be approximately 20 kHz. This is approximately the value observed for the gel phase component of the spectrum of [$^2H_3$-18']-PiLPC and therefore suggests that at -15 °C, PiLPC is undergoing long axis rotation but essentially all other angular fluctuations are absent (ie. S_{mol} = 1.0). At -15 °C, the value of the quadrupolar splittings and thus the width of the gel phase spectra, for each of the deuteriated segments,

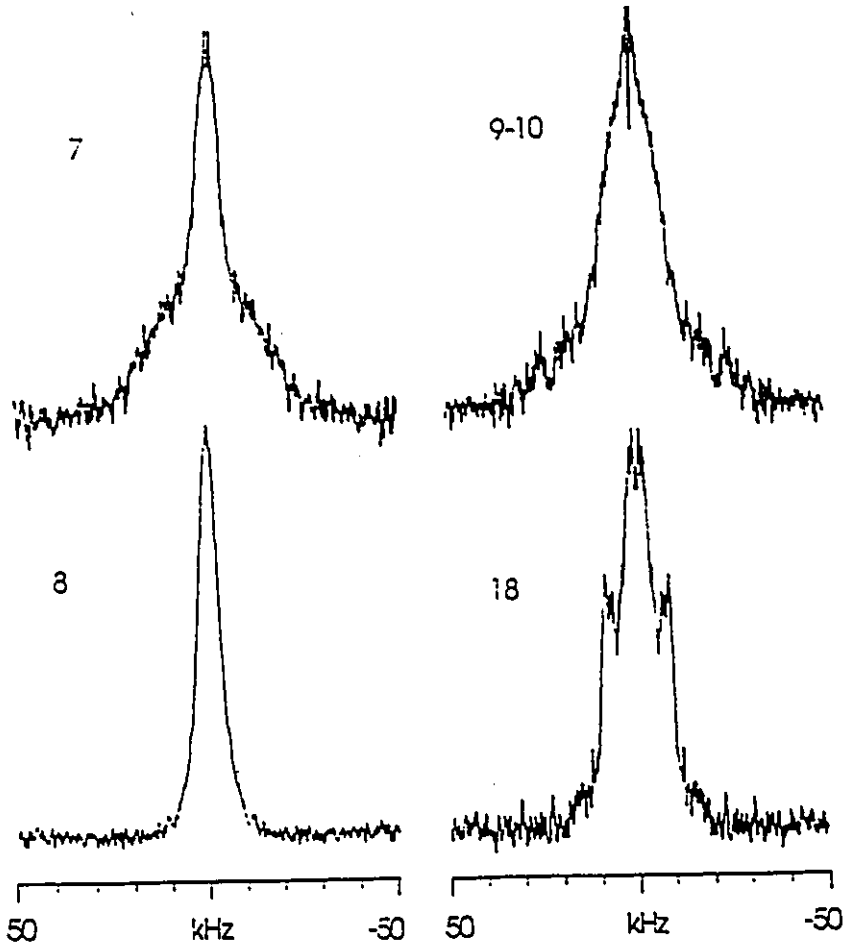

Figure 4.17. Spectra of PiLPC acquired at the center of the phase transition temperature, -15 °C. The spectra of [$^2H_2$-7']-PiLPC and [$^2H_3$-18']-PiLPC clearly show both gel and liquid crystalline phase components in the spectra whereas the spectrum of [$^2H_2$-8']-PiLPC was broadened upon entering the gel phase. The center of the spectrum of [$^2H_2$-9',10']-PiLPC is distorted due to a bad point at the beginning of the FID and the liquid phase component is not clearly evident. All spectra were treated with 500 Hz line broadening and were folded before Fourier Transformation.

is therefore determined (neglecting dipolar broadening) by the geometry of each segment and this provides a means of analyzing whether the conformations proposed above for the liquid crystalline state are evident in the gel phase.

The width of the various gel phase spectra are:

$[^2H\text{-}7']$-PiLPC $\cong$ 50 kHz

$[^2H_2\text{-}8']$-PiLPC $\cong$ 20 kHz

$[^2H_2\text{-}9', 10']$-PiLPC $\cong$ 70 kHz

and a comparison betweeen these values and the values predicted based upon the calculated orientations of the 1,4-pentadiene segment of the isolinoleoyl chain in the liquid crystalline phase is shown in Table 4.1 (see also Appendix 2 and Apendix 3). The comparison suggests that the acyl chain conformations proposed for the liquid crystalline phase do not exist in the gel state.

The spectral widths that one would observe if the isolinoleoyl chain assumed either the angle iron/helical conformation suggested by Applegate and Glomset (1986), or a conformation consistent with the crystal structure of linoleic acid were also calculated in Appendix 3. The results (Table 4.1 and Tables A3.1 and A3.2) show that the experimental data fits the calculated spectral widths for the angle-iron/helical conformation suprisingly well but is clearly inconsistent with a structure similar to the crystal structure of linoleic acid.

Table 4.1

Comparison of the spectral widths[1] observed for PiLPC in the gel phase and those calculated based upon the average conformation defined for the chain at 15 °C, the angle iron/helical conformation proposed by Applegate & Glomset (1986), and a conformation consistent with the crystal structure of linoleic acid (Ernst et al., 1979).

Site of Deuteriation	Observed	Liquid Crystalline Conformation (15°C)	Angle-Iron Conformation	"Linoleic Acid" Conformation
C_7	50	18	55	90
C_8	20	very narrow	15	103
C_9-C_{10}	70	62	64	132

[1] in kHz.

Spectral Simulations and Acyl Chain Migration. Several of the spectra shown in Figures 4.1, 4.2, and 4.5 consist of two or more quadrupolar powder patterns and, in the case of PiLPC deuteriated at each of the C_5, C_7, C_8, and C_{14} positions, one of the powder patterns represents only a small proportion of the total deuterium signal and the value of its splitting is close to the value of the splitting for the more intense ^2H powder. Spectra for two of these samples ([$^2H_2$-5']-PiLPC and [$^2H_2$-14']-PiLPC) were acquired to a higher signal to noise ratio in order to confirm the presence of the second signal and these spectra are plotted in Figure 4.18.

The proportion of the total signal arising from the "second powder" was estimated by simulating the spectra (Figure 4.18) and the results are tabulated in Table 4.2. In each case the amount of the signal giving rise to the "second powder" roughly corresponds to the amount of acyl chain migration that occured during the esterification procedure (Table 4.2) and therefore the additional signals were assigned to 1-isolinoleoyl-2-palmitoyl phosphatidylcholine (iLPPC) with the deuterium labels located at the corresponding position of the *sn*-1 position isolinoleoyl chain.

The temperature dependence of the "minor" splittings and a profile of S_{CD} versus labelled position are shown in Figures 4.19a and 4.19b, respectively, and both correspond closely to the same plots for PiLPC (Figures 4.6 and 4.11, respectively). The results indicate that structural and motional properties of the isolinoleoyl chain in iLPPC are similar to the motions of the acyl chain in PiLPC (see Discussion).

Figure 4.18

Simulations of the powder and the dePaked spectra obtained from aqueous dispersions of **a)** [$^2H_2$-14']-PiLPC (1 °C) and **b)** [$^2H_2$-5']-PiLPC (30 °C). The observed spectra (left) were accumulated for 396,000 and 270,000 scans, respectively, and are plotted without folding. Simulations (right) were performed on the Nicolet 1280E Data Station with the following input parameters: **a)** the two quadrupolar splittings are 18.3 and 16.4 kHz with an intensity ratio of 10.0:3.0, and **b)**, the splittings are 14.39 kHz and 12.93 kHz with an intensity ratio of 10.0:3.75. In both cases, a line width of 850 Hz was assigned to each peak and the 512 data point FID was zero-filled to 1024 data points, and was treated with 200 Hz line broadening before Fourier Transformation.

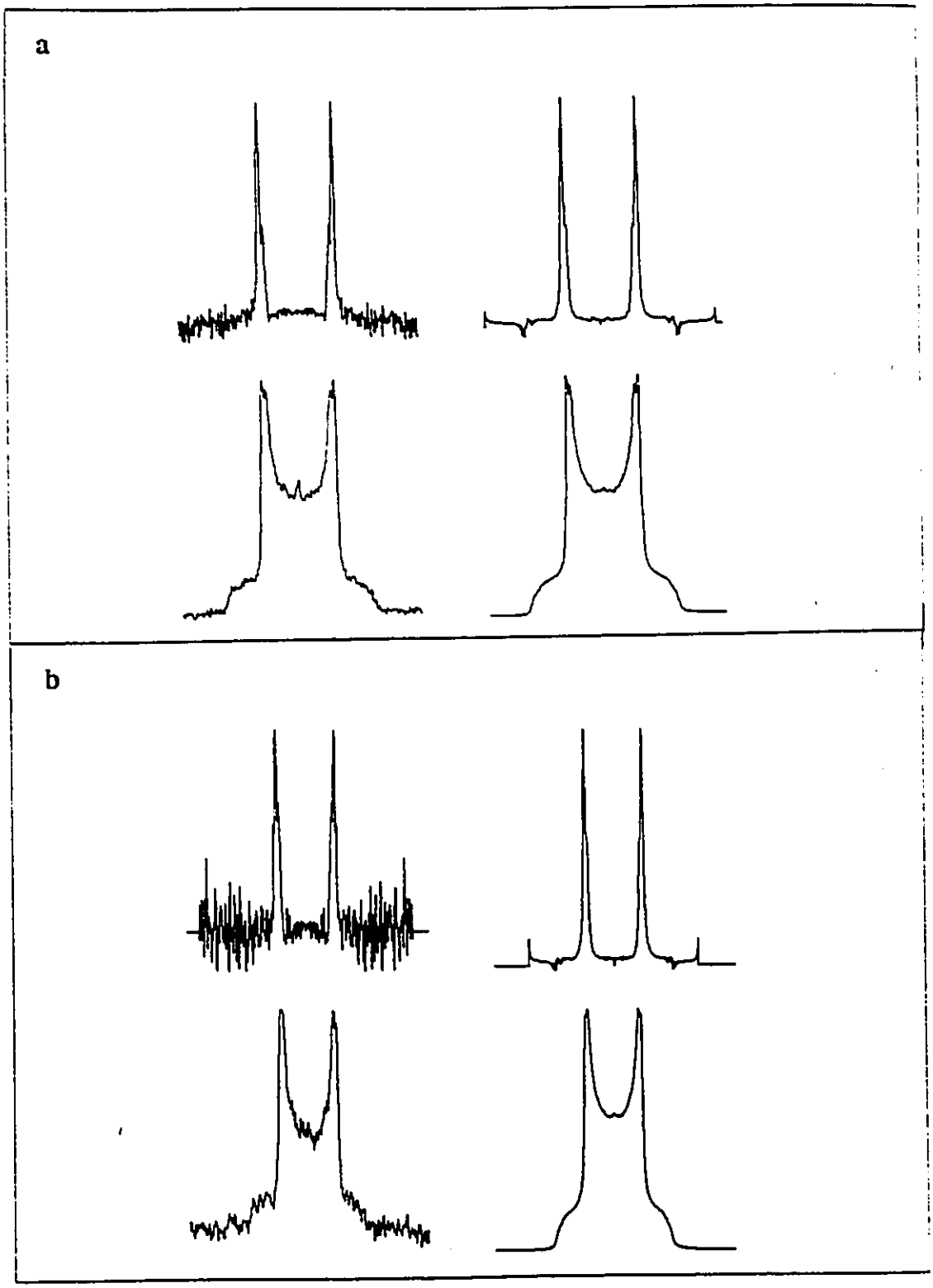
a
b

Table 4.2

Comparison of the relative intensities of the ^2H signals arising from iLPPC to the amount of acyl chain migration in the samples

Position of the label on PiLPC	Percentage of the Powder Pattern Assigned to iLPPC (%)	% Acyl Chain Migration
C_5	27	29
C_7	15	20
C_8	23	18
C_9-C_{10}	—	15
C_{11}	ND	ND
C_{14}	25	23
C_{18}	—	22

Figure 4.19.

a) Summary of the values of the quadrupolar splittings for each deuteriated position of the isolinoleoyl chain of iLPPC and for the C_6 position of the linoleoyl chain of PLPC (C_6*). b) Plot of the S_{CD} bond order parameter as a function of the labelled position along the isolinoleoyl chain of iLPPC, at 30 °C. Filled circles represent S_{CD} values determined from spectra in which a distinct peak was observed for iLPPC. Open circles represent S_{CD} values determined from spectra with only one splitting for both iLPPC and PiLPC.

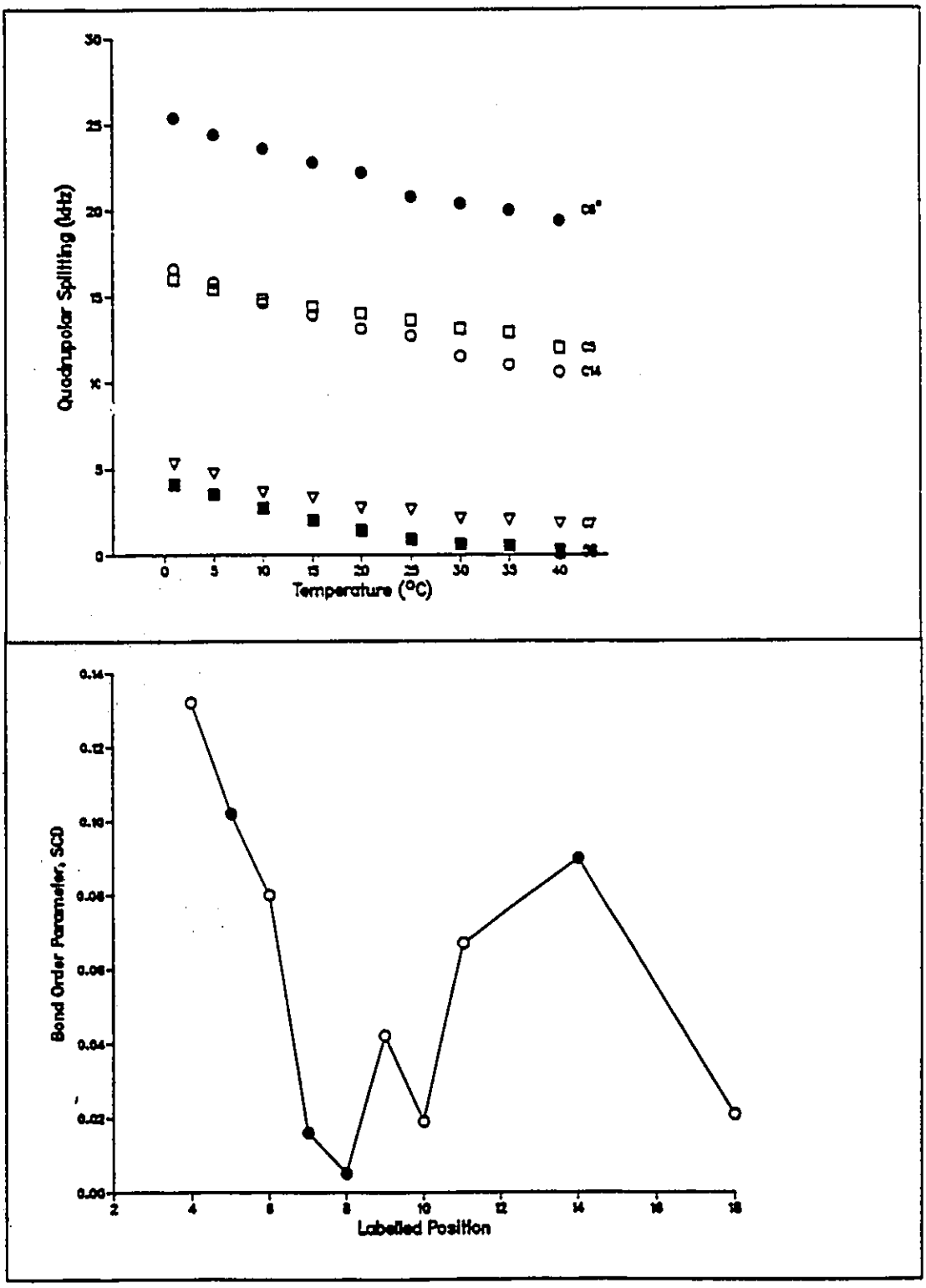
Quadrupolar Splitting (kHz)
Temperature (°C)
Bond Order Parameter, SCD
Labelled Position

The spectra of [^{2}H-6']-PiLPC consist of two overlapping powder patterns, however, both deuterium signals are intense and the values of their splittings are quite different. As illustrated in Chapter 3, the [^{2}H-6]-isolinoleic acid preparation contains some deuteriated linoleic acid and the esterified lipid sample therefore must contain deuteriated 1-palmitoyl-2-linoleoyl PC (PLPC). The relativte intensity of the powder pattern with the largest splitting (determined from the dePaked spectrum) corresponds to the intensity of the deuteriated linoleic acid in the high resolution spectrum of [^{2}H-6']-PiLPC (not shown). The powder pattern with the largest splitting was therefore assigned to [^{2}H-6']-PLPC. The assignment is also supported by calculations of the C_6-C_7 double bond orientation (such as described in Appendix 2) which show that there is no possible mathematical solution for the orientation of the double bond if the larger of the two splittings is assigned to [^{2}H-6']-PiLPC.

The temperature dependence of the quadrupolar splittings recorded for [^{2}H-6']-PLPC (Figure 4.19a) corresponds closely to the temperature dependence of the splittings recorded for oleoyl chains deuteriated at the same position (NB. both chains are saturated at the C_6 position) suggesting that the amplitudes of motion occuring at the C_6 position of the linoleoyl chain are similar to the amplitudes of motion occuring at the C_6 position of the oleoyl chains. Further experimental analysis, however, is needed to determine the geometric contribution to the value of the splittings and thus compare the ordering of the two chains.

Discussion

The goal of the work presented in this chapter was to determine both the average conformation and the molecular order profile of the isolinoleoyl chain in a model membrane, and thus examine how the structural and motional properties of an acyl chain containing two double bonds differ from the corresponding properties of both saturated and monounsaturated chains. To obtain this information, however, one must define both the average orientation and the molecular order parameter, S_{mol}, for each individual segment of the chain. Such an analysis is complicated by the fact that the observed deuterium NMR parameter, the quadrupolar splitting, reflects both the ordering and the time-averaged orientation of each deuteriated segment. In order to interpret the deuterium NMR data explicitly in terms of either parameter, an additional experimental observable, for each deuteriated position, is therefore required.

Conformation of the Isolinoleoyl Chain. The additional information necessary to interpret completely the deuterium NMR data for each deuteriated position of the isolinoleoyl chain could not be obtained. However, as will be described in Chapter 5, acquiring spectra of oriented multibilayers of [$^2H_2$-8']-PiLPC with proton-decoupling led to measurement of the dipolar coupling between the two geminal C_8 deuterons and both the average orientation and the complete ordering tensor for the C_8 methylene segment were therefore determined. Based upon the two orientations shown in Figure 5.10, it was also possible to determine all orientations of each double bond that satisfy the ratio of the quadrupolar splittings observed for the two deuterons attached to each alkene segment, and thus gain some insight into the average conformation and the ordering of the chain.

Several orientations were calculated for each of the two double bonds as shown in Appendix 2, however, none of the orientations or their corresponding molecular order parameters gave the expected results. The double bonds are rigid units and therefore any rotation which brings about motion of the double bonds should also cause a large displacement in the parallel packing of the chain. One would therefore expect the amplitudes of motion to be restricted and the observed order parameters, S_{mol}, to be relatively large. At 15 °C the order parameters calculated for the C_6-C_7 double bond ranged from 0.60 to 0.76,reflecting restricted motion. However, for the C_8 methylene unit and the C_9-C_{10} double bond the calculated order parameters varied from 0.15 to 0.33 indicating considerable motional freedom.

It was also expected that each double bond would adopt an orientation parallel to the bilayer normal, as has been suggested from computer modeling and deuterium NMR studies of lipids containing docosahexaenoyl acyl chains (see Introduction), but none of the double bond orientations are consistent with this hypothesis. In addition, none of the orientations result in an acyl chain conformation consistent with the low energy conformation proposed for the 1,4-pentadiene segment (Applegate & Glomset, 1986), and even the most logical orientations would cause a large kink that would disrupt the parallel packing of the chain. The isolinoleoyl chain, however, can adopt two conformations that allow both double bonds to assume the proposed orientation (see Figure 4.9) and if the chain undergoes a two site jump between these conformations, the calculated orientations would reflect the average of the two conformations as opposed to each individual state. Furthermore, jumping between two conformations could also reduce the order parameters to the values observed for the C_8 and C_9-C_{10} segments.

As the lipid is cooled, one would expect the rate of exchange between the two sites to slow down and eventually the quadrupolar splittings would reflect each individual state as opposed to the average of both. The gel phase component of the spectra recorded from [$^2H_3$-18']-PiLPC at -15 °C is a quadrupolar powder pattern and the value of the splitting is consistent with the lipid undergoing long axis rotation, but with all additional motions absent (ie. S_{mol} = 1.0). In the gel phase at -15 °C, the jumping motion appears to have stopped, and therefore the NMR results should reflect the two individual states described in the model. In addition, the width of the spectra should be determined solely by the geometric factors of the each segment (S_{mol} = 1.0) and are amenable to interpretation in terms of the orientation of the deuteriated segments with respect to the bilayer normal.

The width of the spectra for [^{2}H-7']-PiLPC increases from approximately 12 kHz to 50 kHz upon entering the gel phase. Based upon its orientation in the liquid crystalline phase one would expect a splitting of only 20 kHz (see Table A2, Appendix 2). The width of the gel phase specta recorded for [$^2H_2$-8']-PiLPC is also much broader than expected. Therefore, for both samples the increased spectral width must arise from a change in the average orientation of the deuteriated segments with respect to the bilayer normal upon entering the gel phase.

The spectral widths that one would observe in the gel phase for the angle iron/helical conformation proposed by Applegate and Glomset were also calculated. The results fit the experimental data extremely well (Appendix 3). The gel phase data therefore lend support to an angle iron conformation of the acyl chain in the gel state, and to the proposed two-site jump model for the motion of the acyl chain in the liquid crystalline phase.

Several assumptions were required to perform the above analysis; a brief discussion of the validity of the results,in light of these assumptions is necessary. The first assumption was that the alkenyl bond angles of the 1,4-pentadiene unit of isolinoleic acid correspond to the bond angles of the 1,4-pentadiene unit of crystalline linoleic acid (determined by X-ray crystallography). The quadrupolar splitting data recorded for the C_6 and the C_7 deuterons at 15 °C clearly shows that standard bond geometries are not possible (see Results), so this is likely a reasonable assumption. Unfortunately, the carbon deuterium alkenyl bond angles were not defined in the crystal structure so each C_x-^2H bond was assumed to bisect the corresponding C_{x-1}-C_x-C_{x+1} alkenyl bond angle. This assumption was made solely from geometrical arguments but its validity was tested by allowing the angles to vary over a range of 60° to 66°. As shown in Tables A2.3 and A2.4 (Appendix 2), the variations had little effect on either the calculated double bond orientations in the liquid crystalline phase or their respective molecular order parameters. The spectral widths calculated for the C_7 and the C_9-C_{10} deuterons in the gel phase, based upon the angle iron/helical conformation of Applegate and Glomset, however, were extremely sensitive to this angle. Therefore, although the observed spectral width for the C_8 segment agreed well with the prediction based upon the angle iron conformation, one can only conclude that the results are consistent with the acyl chain adopting this conformation in the gel phase.

The X-ray crystallographic data also suggests that the C_9-C_{10} and the C_{11}-C_{12} double bonds of linoleic acid deviate from planarity by 2.3° and 3.3°, respectively, so the effect of such a deviation on the proposed orientation of the C_9-C_{10} double bond was examined. The results presented in Table A2.5 clearly show that such a deviation also has relatively little effect on the calculated results.

Another assumption was required in order to calculate the molecular order parameters of the two double bonds. In both cases, the segments were assumed to undergo axially symmetric ordering. This assumption may lead to errors because the ordering tensor for the C_8 methylene unit (which was determined witho t any assumptions) indicates that the ordering is not axially symmetric. This assumption, h ever, is inherent in almost all the analyses of acyl chain ordering that have been presented in the literature and is based upon the fact that spectra are indicative of axially symmetric motions. The above assumption could lead to errors in the calculated order parameters.

The molecular order parameter calculated for the C_9-C_{10} double bond is close to the value of the order parameter S_{33} (generally referred to as S_{mol} when axially symmetric ordering is present) calculated for the C_8 segment, suggesting that any errors in the calculations are small. In addition, although the data for the two double bonds strengthens the argument for a two-site jump, the information obtained with regards to the ordering and orientation of the C_8 methylene segment is sufficient to derive the jump model and this data was obtained without assumptions.

In summary, it can be concluded that the assumptions of the geometry and the ordering of the various segments required to perform the analyses presented here are reasonable and do not affect the conclusions as to the structure and motions of the isolinoleoyl chain.

Ordering Profile of the Isolinoleoyl Chain. Although molecular order parameters were not determined for all deuteriated positions along the chain, enough information was obtained to warrant a discussion of the order profile of the diunsaturate relative to monunsaturates and saturates. In the latter two cases, both are relatively ordered for the first 8 to 10 carbons of the chain but the ordering decreases gradually towards the

center of the bilayer (see Figures 2.4 and 2.5 in Chapter 2). In contrast, for the isolinoleoyl chain the order parameter measured for the C_6-C_7 double bond is quite large indicating a high degree of order, but a dramatic decrease to relatively small values for the C_8 methylene segment and the C_9-C_{10} double bonds is observed. The "plateau" region of high order therefore appears to be destroyed by the presence of the second double bond.

Based upon the two-site jump model proposed above, however, the drop in the order parameters of the chain must be interpreted with care. It can be concluded that the "jump" arises mainly from rotations about the C_7-C_8 and the C_8-C_9 single bonds, as the calculated molecular order parameter for the C_8 segment is much lower than that observed for the C_6-C_7 segment, but whether this "jump" should be interpreted as a disordering of the chain is debatable. If, for example, the analysis was performed with an experimental technique that examined motions occuring on a faster time scale (this is analogous to slowing the motions of the jump as occurs in the gel phase) then the jump motion would not average the tensor elements of the electric field gradient and larger order parameters such as those observed for the C_6-C_7 double bond would be observed. In addition, although the proposed jump causes a large drop in the observed order parameters, this jump could result from a highly cooperative motion in contrast to the types of random fluctuations usually associated with a disordered system (Seelig). It would therefore be more desirable to interpret the results in terms of the types of motion and the time scales on which these motions occur, and then compare these properties with the corresponding properties of other acyl chains and correlate them with biological effects. This would avoid the ambiguity that occurs in the order parameter analysis of the results obtained from PiLPC.

The molecular order parameters obtained for the isolinoleoyl chain were also compared to those that have been measured for saturated chains, at the same reduced temperature, T_c. As discussed in the General Introduction and in Chapter 2 (see Applications), the use of reduced temperatures allows one to compare results from different systems at the same thermodynamic state, and at the same T_c, the molecular order parameters calculated for the C_6-C_7 double bond of the isolinoleoyl chain are much higher than those obtained for the same positions of the palmitoyl chain in POPC. One would therefore expect the amplitudes of motion in the plateau region of the isolinoleoyl chain to be restricted relative to those of the saturated chains.

It is also tempting to convert the quadrupolar splitting data for the methylene segments of the chain into molecular order parameters based upon an assumption of an all-*trans* conformation (as is the case in completely saturated systems). This, however, is definitely a poor assumption as the C_4 and C_5 methylene units are likely tilted away from the all-*trans* conformation due to the configuration of the double bonds, and although the C_{14} and the C_{18} segments likely have enough motional freedom to adopt the all-trans conformation, the two site jump that is hypothesized to alter the average conformation of the C_6 to C_{10} segments could also affect the average orientation of the segments further on down the chain. Without additional information, it is therefore unwise to interpret the data obtained for the saturated positions in terms of the molecular order parameters of the segments.

1-Isolinoleoyl-2-Palmitoyl PC (iLPPC) and Acyl Chain Migration. Several of the samples contain measurable amounts of the lipid 1-isolinoleoyl-2-palmitoyl PC (iLPPC) formed by acyl chain migration during the esterification procedure. It has previously been reported that under the esterification conditions used, little (< 5%)

migration occurs (Perly et al., 1984; Dufourc et al., 1987), however, in our case the reactions were performed in the presence of the antioxidant, BHT, which may have an effect on the reaction.

The presence of iLPPC in the samples could, in principle, affect the results obtained for PiLPC by altering the gel-to-liquid crystal phase transition temperature of each individual lipid preparation. Such an effect on the transition temperatures of bilayers has been demonstrated for other similar lipid stereoisomers but in general the differences only occur when the *sn*-1 and *sn*-2 acyl chains differ sustantially in their length. The differences in chain length for the palmitoyl (16 carbons) and the isolinoleoyl (18 carbons) chains are very small and, as only a small amount of acyl chain migration is evident (20 % on average), it likely does not have a large effect on the results or conclusions presented above.

The deuterium data acquired from the deuteriated iLPPCs do, however, provide insight into the motions of the isolinoleoyl chain in iLPPC. It has been suggested that in response to a drastic reduction in the growth temperature, the eukaryote, *Tetrahymena*, forms phospholipids with unsaturated chains in the *sn*-1 position and saturated chains in the *sn*-2 position (this is the reverse of the usual designation) and that these lipids help increase the "fluidity" of the membranes (Muruyama et al., 1982; Dickens & Thompson, 1982; Ramesha et al., 1982; Ramesha & Thompson, 1984). The similarity of the quadrupolar splitting data presented here (see Chapter 5 also) for the isolinoleoyl chain in iLPPC relative to the data for the isolinoleoyl chain in PiLPC, however, indicates that the motions of the diunsaturate are essentially identical in both systems. The results therefore do not support the above hypothesis athough it is possible that larger effects may be observed with acyl chains of higher degrees of unsaturation.

Summary and Conclusions

The analysis presented in this chapter demonstrates the utility of ^2H NMR for obtaining detailed information on the structure and motions of acyl chains in membranes and indicates that both properties of the isolinoleoyl chain differ from those of saturated and monounsaturated acyl chains. Although the quadrupolar splitting data could not be interpreted in terms of the structure and molecular ordering (S_{mol}) of each labelled position, the information provided in Chapter 5 made it possible to define both parameters for the two double bonds and the intervening methylene segment. The results indicate that the chain adopts a conformation in the gel state that is consistent with the structures proposed for highly unsaturated acyl chains by Applegate & Glomset (1986). In the liquid crystalline phase, however, it appears that the chain undergoes a two-site jump between two such conformations. The jump motion represents a clear departure from the types of motion attributed to saturated (Seelig & Seelig, 1974; Schindler & Seelig, 1975), and monounsaturated (Seelig & Waespe-Šarčević, 1978) acyl chains in the liquid crystalline phase and illustrates that the presence of a second double bond has a dramatic effect on the types of motions occuring in a membrane.

The molecular ordering profile (S_{mol} versus labelled position) of the diunsaturate also differs from the profiles of saturated and monounsaturated chains. The isolinoleoyl chain is highly ordered in the plateau region (carbons 2-7) relative to both saturated and monounsaturated chains but becomes highly disordered at the C_8 methylene unit. The apparent disorder occurs as a consequence of the two-site jump, which leads to large amplitudes of motion for the C_8 and C_9-C_{10} segments, and it is not clear whether this jump

motion should be classified as a disordering of the chain. In addition, the jump would likely cause a large displacement in the parallel packing of a chain containing more than two double bonds and therefore, would not likely occur in polyunsaturates. Without the jump, highly unsaturated acyl chains should be highly ordered (as the isolinoleoyl chain is at the C_6-C_7 position) for the length of the chain. A rigid polyunsaturated chain clearly contrasts the accepted concept that polyunsaturates "fluidize" membranes. The implications of this observation will be discussed in more detail in Chapter 6.

Chapter 5

Oriented Multibilayers of 1-Palmitoyl-2-Isolinoleoyl Phosphatidylcholine

---

Chapter 5

Oriented Multibilayers of 1-Palmitoyl-2-Isolinoleoyl Phosphatidylcholine 159

Introduction 161

Materials and Methods 162

Oriented Multibilayers. 162

NMR Spectroscopy. 162

Results.....163

$[^2H_2$-8']-PiLPC. 163

$[^2H_2$ -9',10']-PiLPC. 182

Discussion.....184

Summary and Conclusions.....187

Introduction

In the previous chapter, the ten deuteriated PiLPC's were examined as aqueous dipersions and the quadrupolar splittings were measured for each deuteriated position along the isolinoleoyl chain. As discussed, however, interpretation of the quadrupolar splitting data in terms of either the average structure or the ordering of the chain is not possible without the acquisition of additional experimental information. In this chapter, an analysis of two of the samples ([$^2H_2$-8']-PiLPC and [$^2H_2$-9',10']-PiLPC) as oriented multibilayers will be presented. The results will demonstrate that much more detailed information regarding the structure, motions and ordering of acyl chains can be obtained from oriented systems.

Materials and Methods

Oriented Multibilayers. Under an argon atmosphere, PiLPC deuteriated at either the C_8 or the C_9-C_{10} positions of the isolinoleoyl chain was dissolved in 0.1 - 0.2 mls of $CHCl_3$ and spotted on approximately 40 microscope cover slips (~ 8 mm x 15 mm) with a glass pasteur pipette. In each case, the plates were allowed to dry under argon and then were stacked in a 10 mm NMR tube, lyophilized for at least two hours to ensure the removal of all of the $CHCl_3$ from the sample, and hydrated overnight under an argon atmosphere saturated with deuterium-depleted H_2O at 37 °C. After addition of a drop of deuterium depleted H_2O, the NMR tubes were sealed with epoxy and utilized for NMR.

NMR Spectroscopy. Both oriented samples were examined on a Bruker MSL-300 spectrometer. Phosphorus spectra were recorded for each sample at both the 90° and 0° orientations of the bilayer normal (normal to the glass plates) with respect to the magnetic filed direction to ensure that the lipid molecules were uniformly oriented and then deuterium NMR spectra were recorded either with or without proton decoupling. See Chapter 4 for details.

The orientation of each sample with respect to the magnetic field direction was measured with a small protractor that fitted onto the surface of the NMR probe. The direction of the bilayer normal was taken to be the normal to the glass plates. The angular settings were found to be accurate to ± 3°.

Results

[$^2H_2$-8']-PiLPC. The oriented sample of [$^2H_2$-8']-PiLPC was placed in a horizontal, solenoid coil in the NMR magnet and phosphorus spectra were recorded with the sample oriented such that the normal to the glass plates made an angle of either 0° or 90° with respect to the magnetic field direction. Both spectra shown in Figure 5.1 consist of a single, narrow line (as opposed to a "powder", see Chapter 4) indicating that essentially all the lipid molecules are uniformly aligned. In addition, the chemical shift separation between the two peaks, 48 ppm, is the same as the value of the CSA determined from the phosphorus "powder" recorded from aqueous dispersions of [$^2H_2$-8']-PiLPC (see Chapter 4). The similarity in the two values indicates that the motions of the phospholipid headgroup of PiLPC in the two lipid systems are equivalent.

The deuterium spectra of the aligned sample of [$^2H_2$-8']-PiLPC are narrow and relatively featureles (Figure 5.2a) but as in the case of the spectra acquired from the aqueous dispersions, proton-decoupling narrows the resonances sufficiently that the expected lineshapes are observed (Figure 5.2b). The resulting spectra consist of two quadrupolar doublets of approximately equal intensity. The values of the quadrupolar splittings, and the temperature dependence of each, (Figures 5.3 and 5.4) are similar to the corresponding values determined from the deuterium powder spectra. The splittings are also reduced to zero at 15 °C indicating that both C-^2H bonds of the C_8 methylene segment are oriented at the "magic angle" as is the case in the dispersions. The similarity in the results confirm that the motions of the acyl chains of PiLPC in the two lipid systems are equivalent and, coupled with the phosphorus data it can be concluded that the environment

Figure 5.1

Phosphorus NMR spectra of oriented multibilayers of [$^2H_2$-8']-PiLPC acquired with the sample oriented (the bilayer normal) at an angle of **a)** 90°, and **b)** 0° with respect to the magnetic field direction.

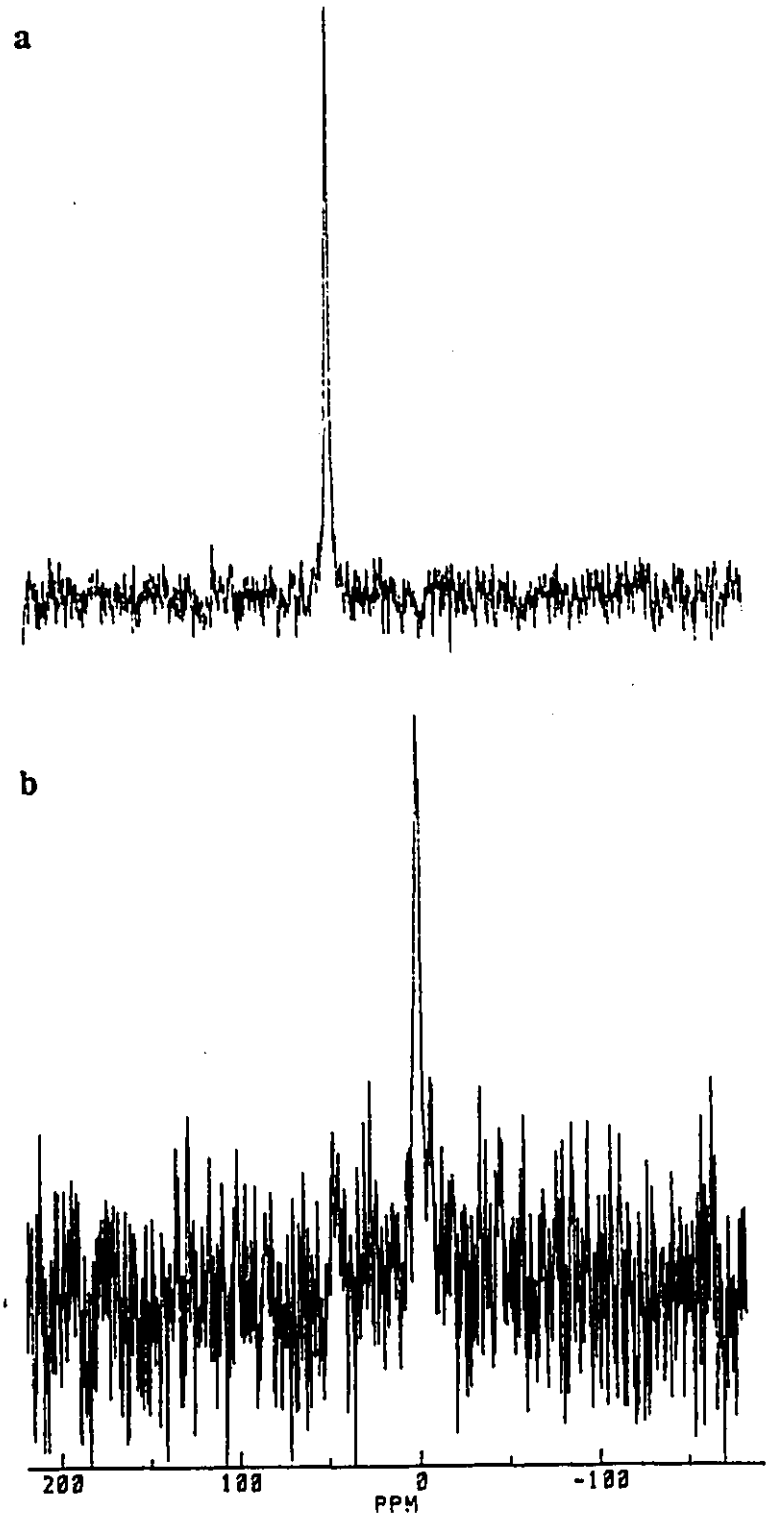
a
b
200
100
0
-100
PPM

Figure 5.2.

^2H spectra of oriented multibilayers of [$^2H_2$-8']-PiLPC acquired **a)** without, and **b)** with proton decoupling. Both were acquired at 25 °C on a Bruker MSL-300 spectrometer operating at 46.064 MHz.

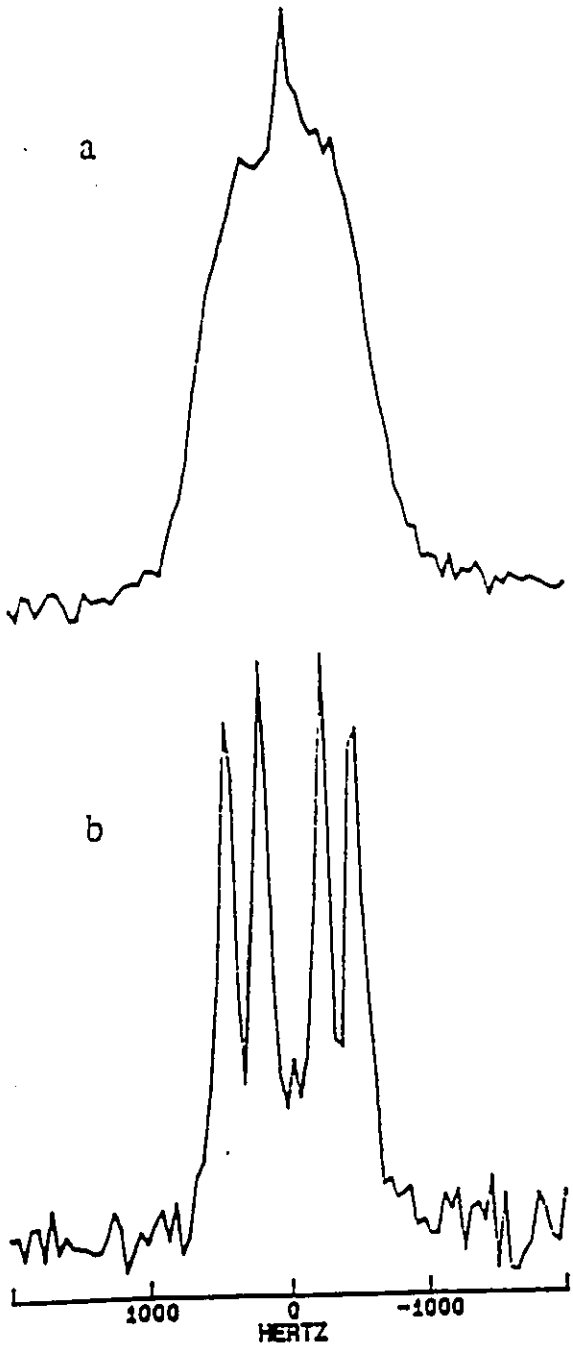
a
b
1000
0
-1000
HERTZ

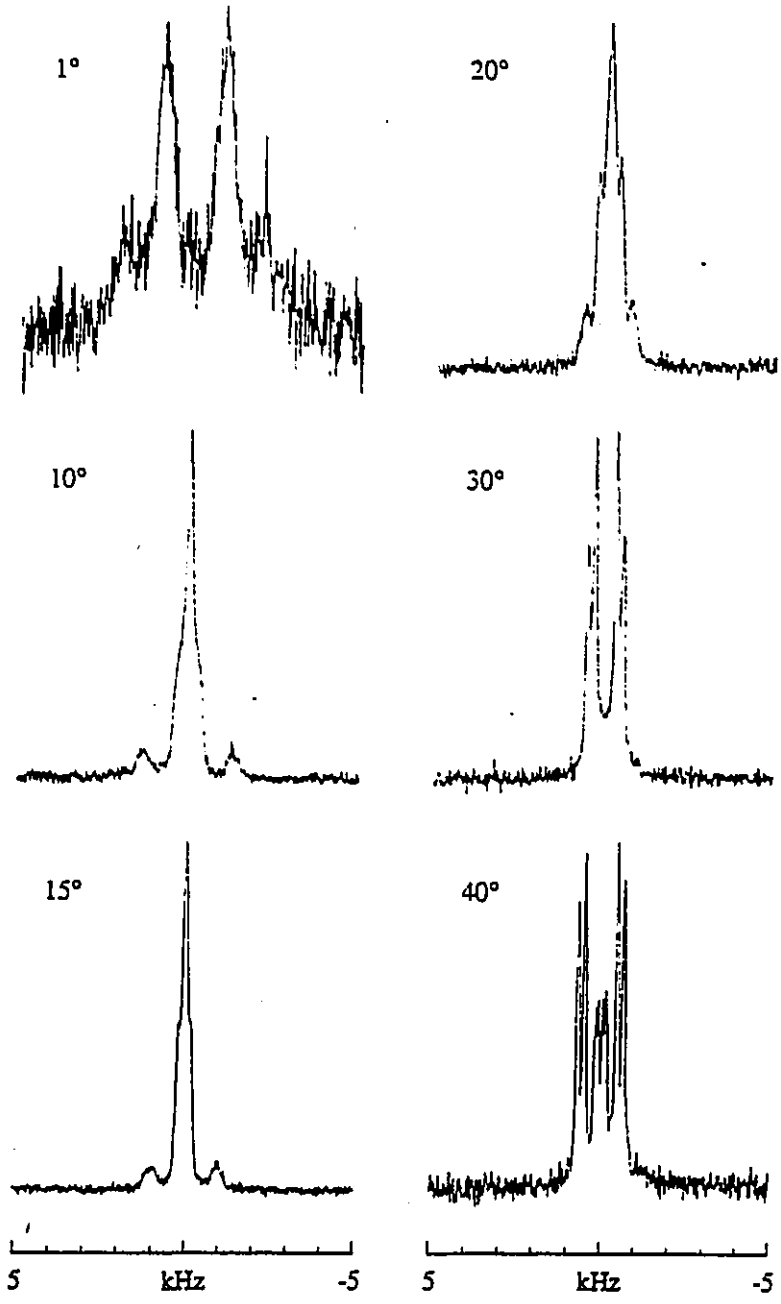
1°
20°
10°
30°
15°
40°
5
kHz
-5
5
kHz
-5

Figure 5.4.

A plot of the temperature dependences of the quadrupolar splittings opbtained from spectra of oriented multibilayers of [$^2H_2$-8']-PiLPC at 25 °C.

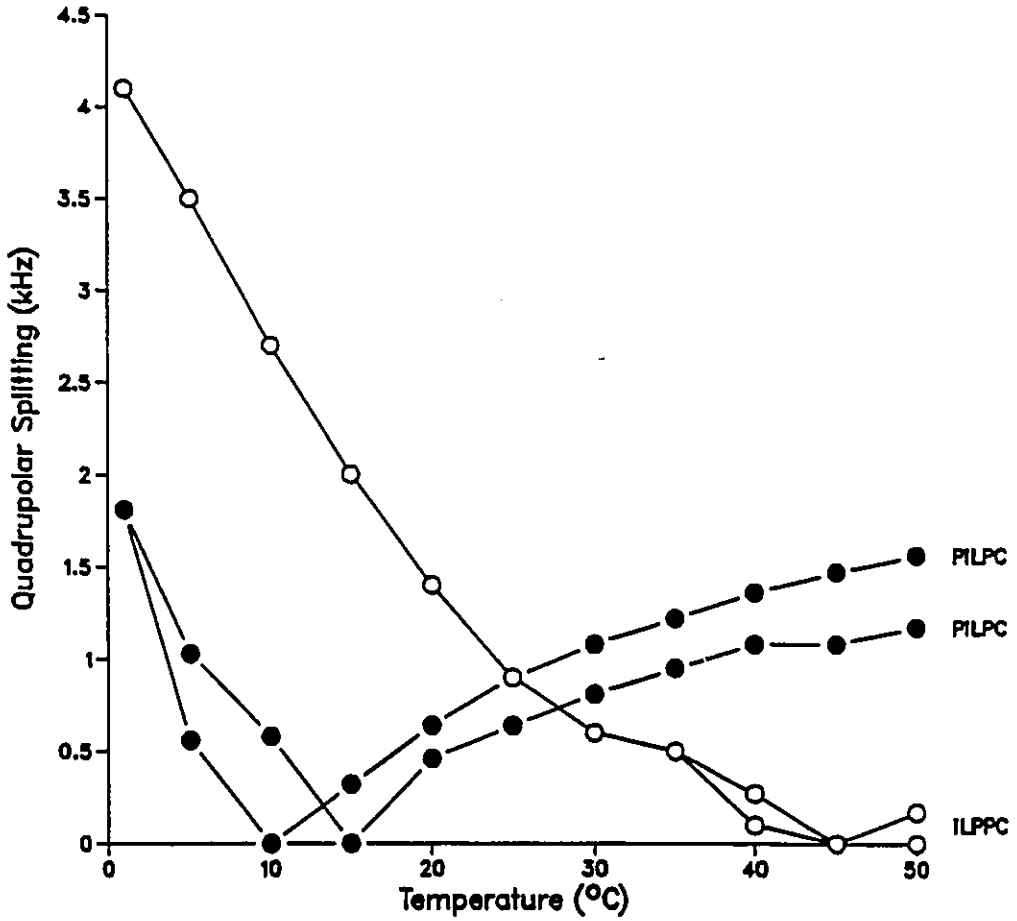
Quadrupolar Splitting (kHz)
4.5
4
3.5
3
2.5
2
1.5
1
0.5
0
0
10
20
30
40
50
Temperature (°C)
PILPC
PILPC
ILPPC

of PiLPC in both systems is identical. The results therefore confirm that application of the data presented here (see below) to the interpretation of the data acquired from the dispersed samples (Chapter 4) is valid.

A third quadrupolar doublet of much lower intensity is also evident in the spectra acquired from the aligned sample of [$^2H_2$-8']-PiLPC (see Figure 5.3). At higher temperatures the third signal is evident in the powder spectra of [$^2H_2$-8']-PiLPC but it is not evident at temperatures below 30 °C. However, as shown in Figure 5.3, at higher temperatures the splitting of the quadrupolar doublet is quite small and the individual peaks of the doublet are relatively narrow, whereas at lower temperatures the splitting is much larger than the splittings of the more intense doublets and the individual peaks of the doublet are very broad. The lack of observation of the signal in the powder spectra below 30 °C is therefore likely due to the breadth and the relatively low intensity of the signal.

The temperature dependence of the quadrupolar splitting of the less intense doublet is also summarized in Figure 5.4; its close similarity to that of the two more intense doublets (arising from PiLPC) suggests that the signal arises from iLPPC as was suggested in Chapter 4. This conclusion is also supported by the fact that there is a correlation between the amount of acyl chain migration and the intensity of the signal, and that at 40 °C the signal is actually resolved into two doublets whose splittings are very close in value (as is the case for PiLPC, see above). In addition, when spectra are acquired with the bilayer normal oriented at the 0^o orientation it is possible to observe the dipolar coupling between the two geminal C_8 deuterons in iLPPC (as is also the case for the spectra of PiLPC; see below), providing further support to this assignment.

The dependence of the quadrupolar splittings upon the orientation of the bilayer normal with respect to the magnetic field direction were examined at 25 °C in order to establish the axis about which the lipid is undergoing axially symmetric motions (Figure 5.5). It is often assumed that lipids undergo fast axial rotation about the bilayer normal and this has been confirmed for many systems by the same approach used here. The values of the quadrupolar splittings for the two most intense peaks are plotted as a function of the angle of orientation, θ, in Figure 5.6a and as a function of $[3Cos^2\theta - 1]/2$ in Figure 5.6b. The results clearly show that the splittings vary as a function of $[3Cos^2\theta - 1]/2$ and that they collapse to zero at an angle of $\theta = 54.7^o$. The axis about which the lipids are undergoing axially symmetric motions (the director) is therefore the bilayer normal, confirming the assumption made in Chapter 4.

The spectra shown in Figure 5.5 also indicate that the individual peaks of the quadrupolar doublets contain additional fine structure. When spectra are acquired with the sample positioned at an angle $\theta = 0^o$, all the spectral parameters achieve their maximum values, thus providing the highest degree of resolution. A spectra of $[^2H_2$-8']-PiLPC acquired at the 0^o orientation with increased digital resolution is shown in Figure 5.7 (at 40 °C). The spectrum clearly indicates that each member of the two most intense quadrupolar doublets is composed of three peaks of unequal intensity, separated by 60 Hz. This triplets are resolved to a greater degree when the FID is subjected to resolution enhancement before Fourier Transformation. As shown in Figure 5.7, each peak is clearly composed of a triplet of uneven intensity.

The fine structure in the spectra is thought to arise from the dipolar coupling between the two geminal C_8 deuterons. In order to confirm this assumption, spectra for

Figure 5.5.

^2H spectra of oriented multibilayers of [$^2H_2$-8']-PiLPC acquired as a function of the angle betweeen the normal to the glass plates (bilayer normal) and the magnetic field direction, H_o. Acquisition temperature was 25 °C.

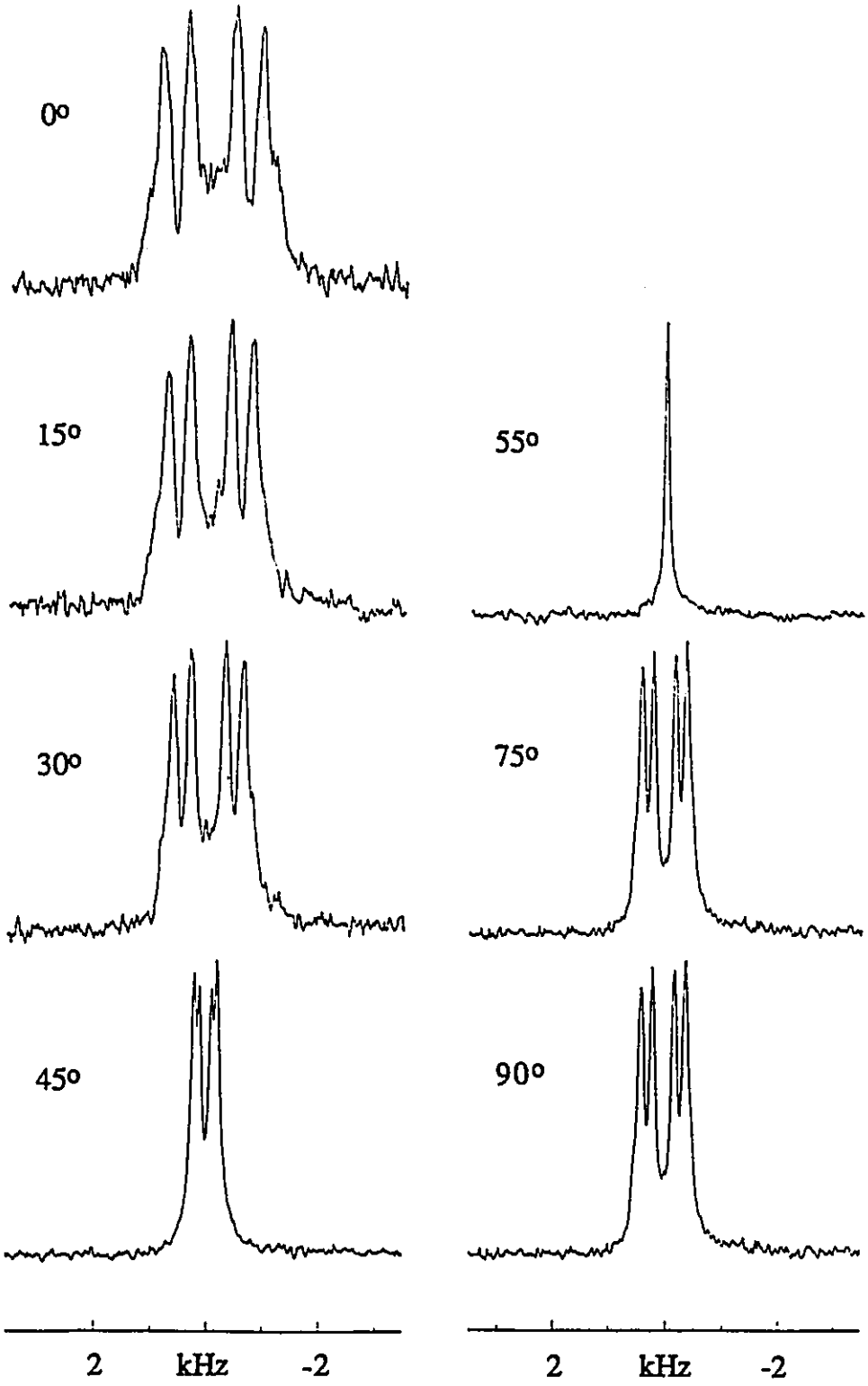
0°
15°
30°
45°
55°
75°
90°
2
kHz
-2
2
kHz
-2

Figure 5.6.

a) Plot of the quadrupolar splittings of [$^2H_2$-8']-PiLPC and [$^2H_2$-8]-iLPPC versus the angle between the bilayer normal and the magnetic field direction (the doubletss corresponding to iLPPC have the same splittings as the doublet with larger splitting of PiLPC). b) Plot of the quadrupolar splittings as a function of $(3Cos^2\theta - 1)/2$, where θ is the angle between the bilayer normal and the magnetic field direction.

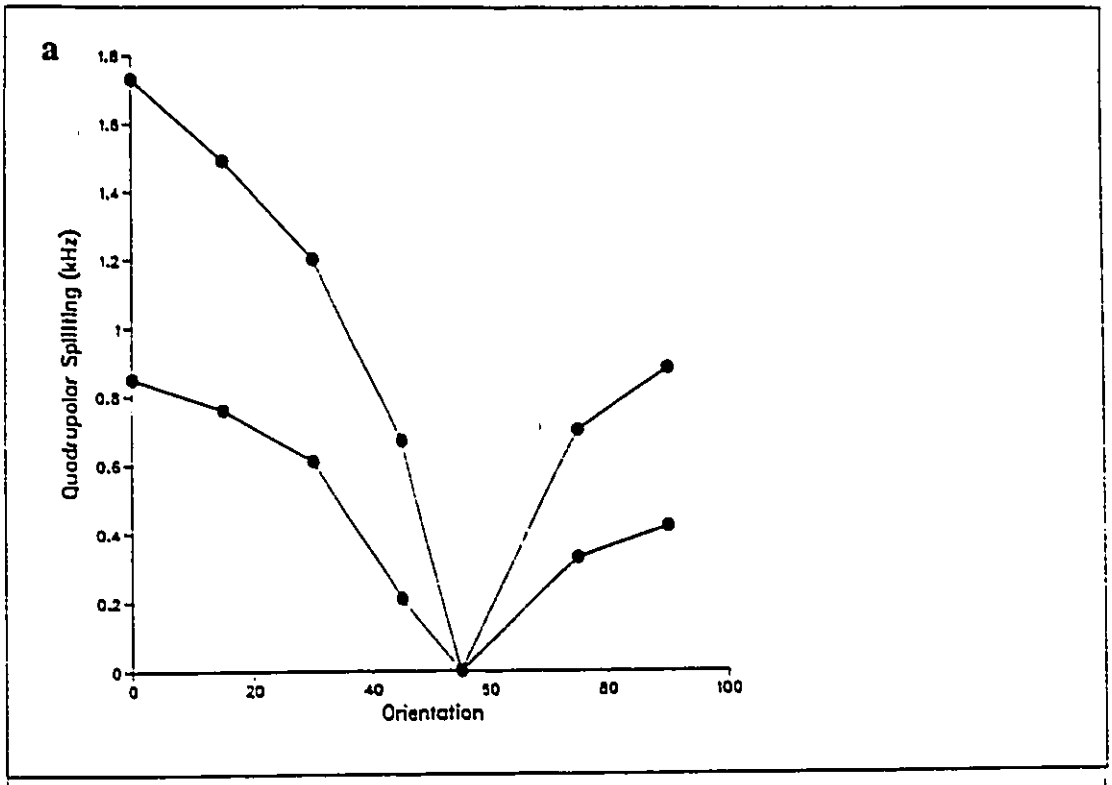
a
Quadrupolar Splitting (kHz)
Orientation
0
20
40
50
60
100
0
0.2
0.4
0.6
0.8
1
1.2
1.4
1.6
1.8

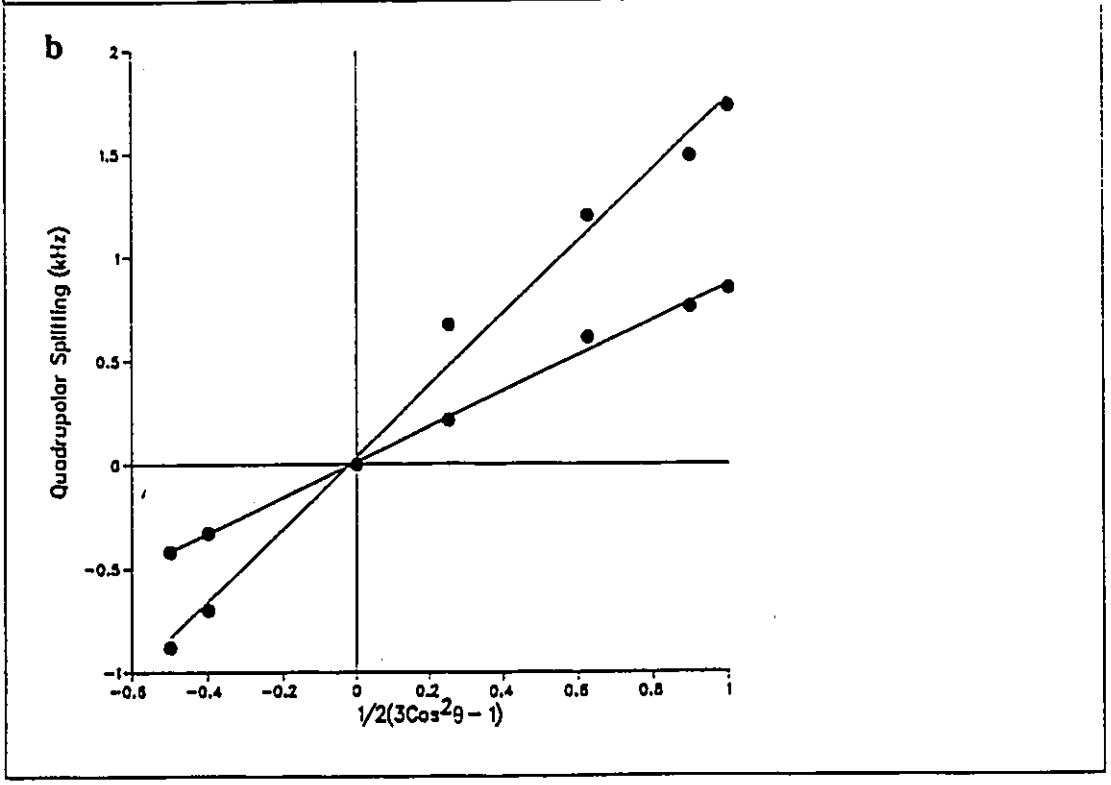
b
Quadrupolar Splitting (kHz)
1/2(3Cos²θ – 1)
-0.6
-0.4
-0.2
0
0.2
0.4
0.6
0.8
1
-1
-0.5
0
0.5
1
1.5
2

Figure 5.7.

Resolution enhancement of the spectrum of [$^2H_2$-8']-PiLPC acquired at 40 °C with the sample oriented such that the bilayer normal is parllel to H_0. The spectrum plotted in **a)** was plotted without resolution enhancement whereas for the remaining spectra, the FIDs were multiplied by an exponential of the form exp (-at - bt^2), where a = π x LB and b = -a/(2 x GB x AQ). AQ is the acquisition time. **b)** GB = 0.3, LB = -50 Hz; **c)** GB = 0.3, LB = -100 Hz; **c)** GB = 0.4, LB = -50 Hz; **d)** GB = 0.4, LB = -100 Hz.

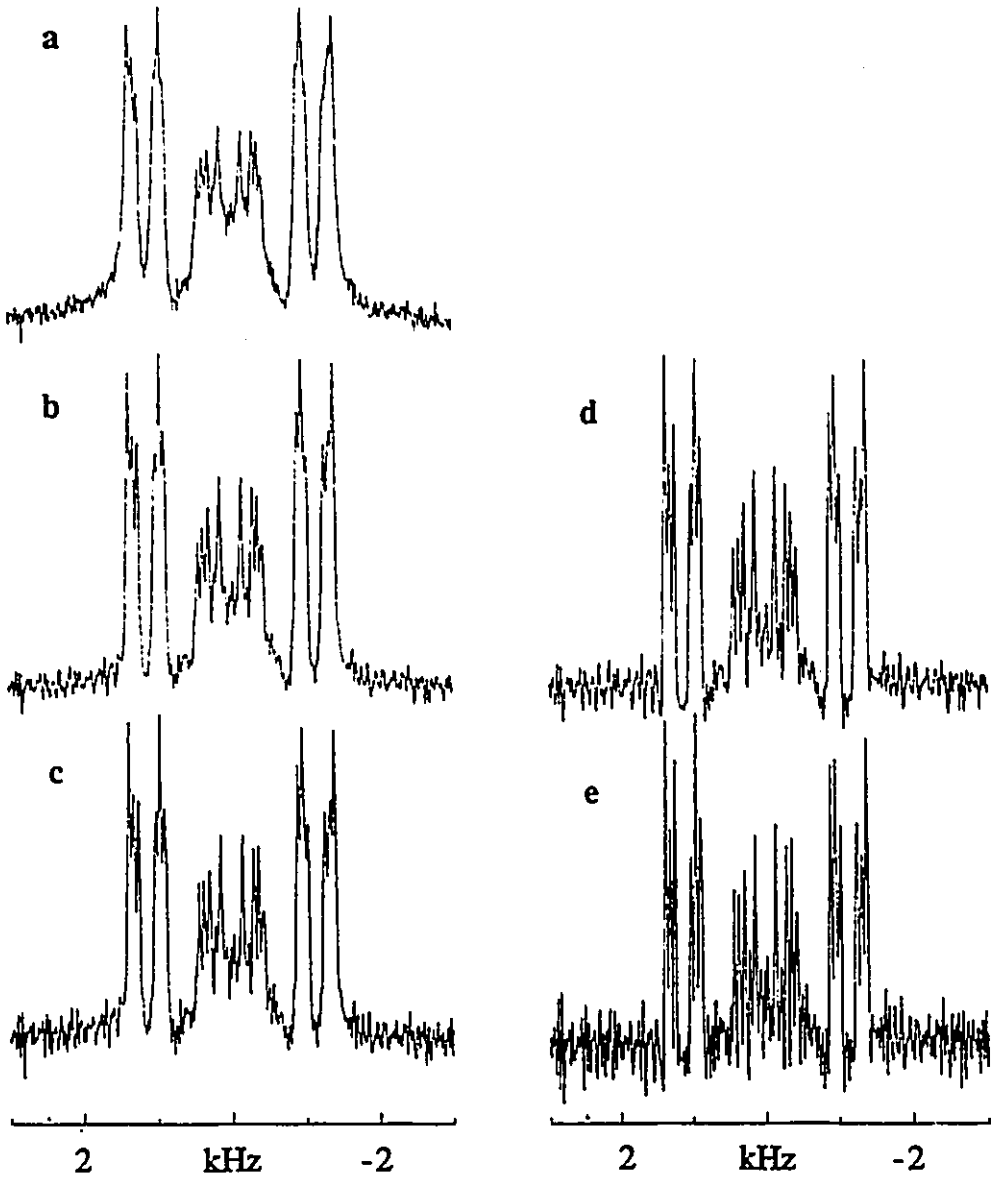
a
b
c
d
e
2
kHz
-2
2
kHz
-2

two dipolar-coupled deuterons were simulated using the PANIC software on the Bruker MSL-300. Input parameters were the values of the two quadrupolar splittings and the deuterium-deuterium dipolar coupling (as estimated from the separation between the individual peaks of the triplets). Several spectra were simulated allowing the relative signs of the splittings and the dipolar couplings to vary (Figure 5.8). The relative signs of the input parameters have a significant effect on the intensity pattern of the triplets, and only when all three parameters are the same sign (ie. all positive or all negative) is the intensity pattern compatible with the observed spectrum .

Spectra were also simulated with increased line width as shown in Figure 5.9. The simulations for both the 0° and the 90° orientation correspond closely to the observed spectra. The line width parameter was adjusted in order to allow the simulated spectra for the 0° orientation to match the experimental spectrum, but the chosen line width is within ± 10 % of the value calculated from the transverse relaxation time, T_2, of the lipid. The simulated spectra provide strong evidence for the assignment of the peak fine structure to the dipolar couplings between the two deuterons. The spectral simulations also confirm that the two most intense doublets are due to the inequivalence of the two C_8 geminal deuterons as opposed to two inequivalent lipid conformations (see Chapter 4).

The dipolar coupling is defined as follows:

$$D_{DD} = \frac{-\gamma_D^2 h}{4\pi r^3} S_{mol} \left(\frac{3\mathrm{Cos}^2\alpha - 1}{2}\right)\left(\frac{3\mathrm{Cos}^2\theta - 1}{2}\right) \qquad (8)$$

Figure 5.8.

Sensitivity of the simulations of the spectrum of [$^2H_2$-8']-PiLPC (40 °C) to the signs of the quadrupolar splittings and the dipolar coupling. **a)** Input parameters were quadrupolar couplings = 1312 and 958 Hz, dipolar coupling = 30 Hz, **b)** -1312 Hz, 958 Hz, 30 Hz, **c)** 1312 Hz, -958 Hz, 30 Hz, and **d)** -1312 Hz, -958 Hz, 30 Hz. In all four cases the digital resolution was 3 Hz/Pt and the line width was negligible.

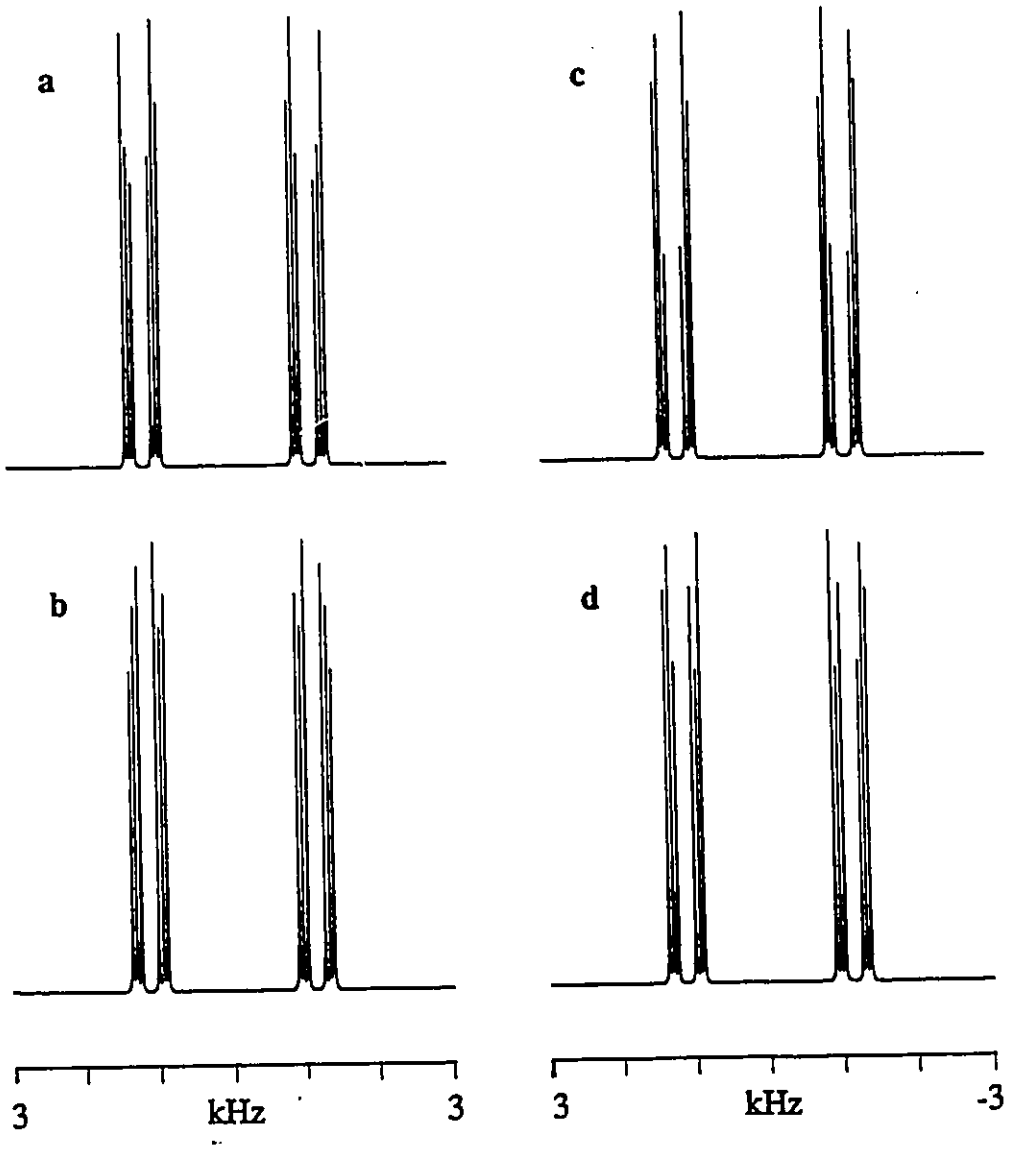
a
c
b
d
3
kHz
3
3
kHz
-3

Figure 5.9.

Simulations of the spectrum of [$^2H_2$-8']-PiLPC (40 °C) acquired at both the 90° and 0° orientations. **a)** Observed spectra, **b)** simulations performed with the same parameters as in Figure 5.8a for the 0° orientation, and **c)** same as in **b)** with 70 Hz Lorentzian line broadening and a digital resolution of 12 Hz/Pt (which corresponds to the observed spectrum). For the simulations of the 90° orientation in **b)** and **c)** the input parameters were halved.

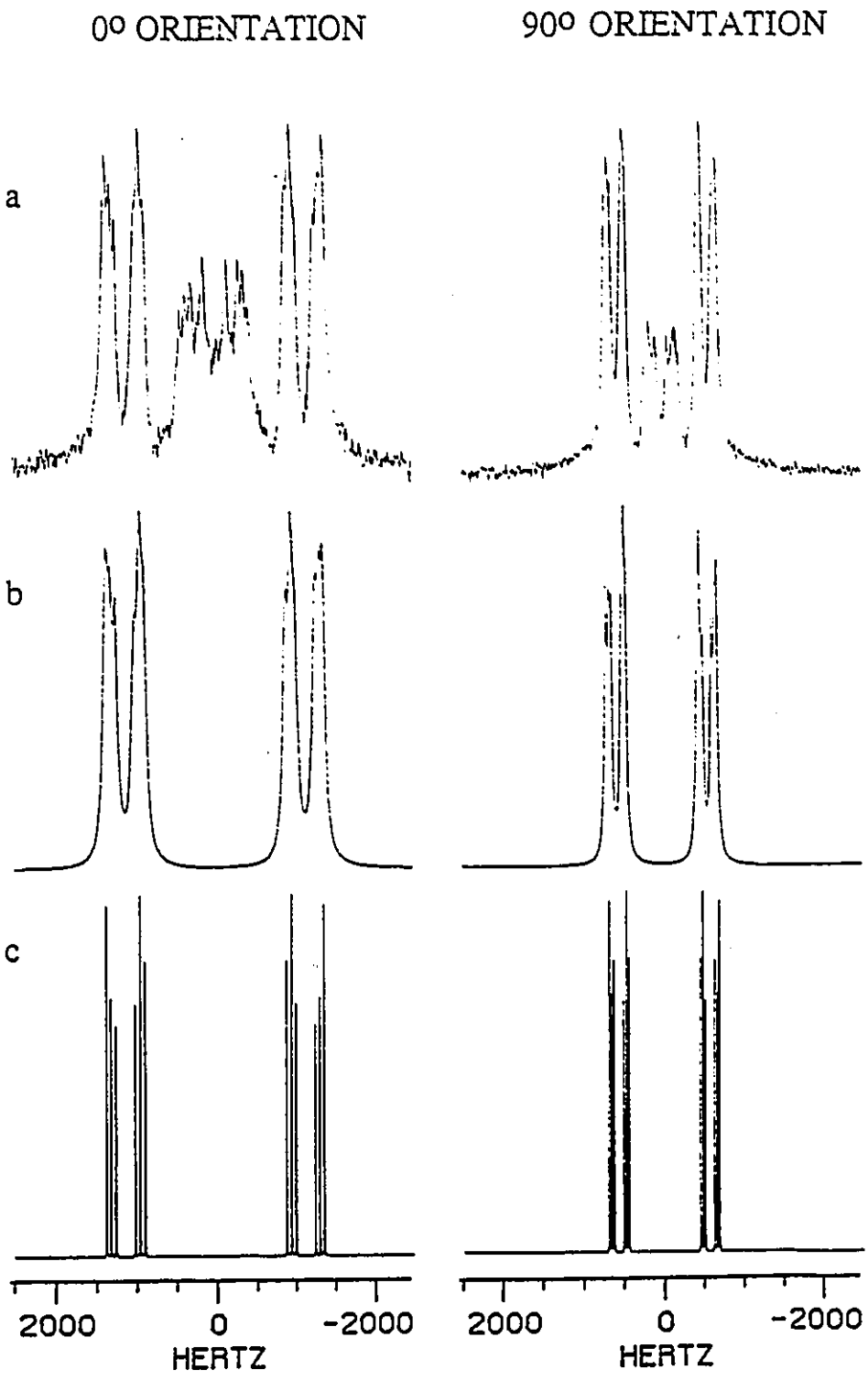
0° ORIENTATION
90° ORIENTATION
a
b
c
2000
0
-2000
HERTZ
2000
0
-2000
HERTZ

where the term involving the angle α is called $S_{DD,}$ and it describes the average orientation and fluctuations of the axis lying along the deuterium-deuterium vector. Order parameters for the carbon-deuterium bonds and for the deuteron-deuteron vector at position C_8 were calculated to be $S_{CD\ (1)} = 7.51 \times 10^{-3}$, $S_{CD\ (2)} = 1.02 \times 10^{-2}$, and $S_{DD} = -6.18 \times 10^{-2}$ (or the reverse sign for all three values) using the above equation and those presented in Chapter 2. As described in Appendix 3, the complete ordering tensor for the methylene unit was defined. The tensor was then diagonalized and the result (S*) indicates that the ordering is not axially symmetric ($S^*_{xx} \neq S^*_{yy}$):

$$S^* = \begin{pmatrix} -0.089 & & \\ & -0.062 & \\ & & 0.150 \end{pmatrix}$$

The methylene unit appears to undergo motions of relatively large amplitude (ie. all three order parameters are smaller than those for saturated systems labeled at the same position) and its average orientation is such that the director (bilayer normal) lies in the ^{2}H-C-^{2}H plane tilted at an angle of $\pm$ 0.4° from the bisector of the ^{2}H-C-^{2}H geminal angle (see Figure 5.10). As discussed in Chapter 4 the unusual order matrix and orientation of the C_8 segment described above are thought to arise because the lipid undergos a two-site jump between conformations in which the double bonds are oriented parallel to the bilayer normal.

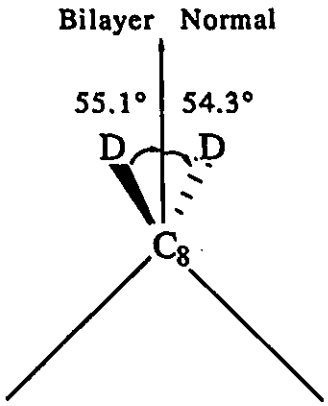

Figure 5.10. Orientation of the C_8 methylene unit of PiLPC at 40 °C as determined in Appendix 4.

Table 5.1

Summary of the tensor components and Euler angles resulting from diagonalization of the ordering matrices for PiLPC and iLPPC[1]

Sample and Temperature	Tensor Components			Euler Angles, °	
	S_{11}	S_{22}	S_{33}	α	β
[$^2H_2$-8']-PiLPC at 40 °C	-0.089	-0.062	-0.150	± 90	± 0.40
[$^2H_2$-8']-PiLPC at 25 °C	-0.096	-0.082	-0.178	± 90	± 0.39
[$^2H_2$-8']-iLPPC at 40 °C	-0.067	-0.062	-0.129	± 90	± 0.29

[1] see Appendix 4 for details.

The resolution enhancement was also applied to spectra acquired at other temperatures and an estimate of the homonuclear dipolar coupling was obtained at 25 °C (at other temperatures, for example 5 °C, the spectra are too noisy to obtain a value for the coupling). The ordering tensor and the average orientation of the segment at 25 °C was calculated, and the results shown in Table 5.1 clearly indicate that the average orientation of the C_8 unit remains essentially constant over the temerature range 25-40 °C. As discussed in Chapter 4, the temperature dependence of the splittings for the C_8unit suggest, however, that the orientation does change with temperature. The anomaly occurs because the C-^{2}H bonds are very close to the magic angle and at this orientation, the splittings are so sensitive to the orientation of the methylene segment that even minor changes in the orientation (ie. a change of 0.2^o) is reflected in the results.

The average orientation and the ordering tensor for the C_8 methylene segment of iLPPC are also summarized in Table 5.1. The results indicate that both properties of the chain, at this position, are similar in both PiLPC and iLPPC (see Chapter 4).

The proton-coupled and decoupled spectra of [$^2H_2$-8']-PiLPC acquired with the sample oriented at the 90^o orientation with respect to the magnetic field direction were simulated using the available values of the quadrupolar splittings and the total contribution of proton-deuteron dipolar coupling to the widths of the resonances was thus determined to be roughly 650 Hz (Figure 5.11). Although this value can not be used to interpret the data explicitly in terms of chain structure, when compared to the corresponding parameter for [$^2H_2$ -9',10']-PiLPC the value does support the jump model proposed in Chapter 4. This parameter could also be used in spectra simulations which would help confirm the jump hypothesis (see Discussion).

Figure 5.11.

Simulations of the proton coupled and proton decoupled spectra of oriented multibilayers of [$^2H_2$-8']-PiLPC acquired at 25 °C. **a)** the observed proton-coupled (top) and proton-decoupled (bottom) spectra; ; **b)** simulations using 90 Hz (top) and 800 Hz (bottom) Lorentzian line broadening; **c)** simulation using 750 Hz Gaussian line broadening. In **b)** and **c)** the input parameters to the PANIC software were the two quadrupolar splittings, 220 and 464 Hz, and the digital resolution, 12 Hz/Pt.

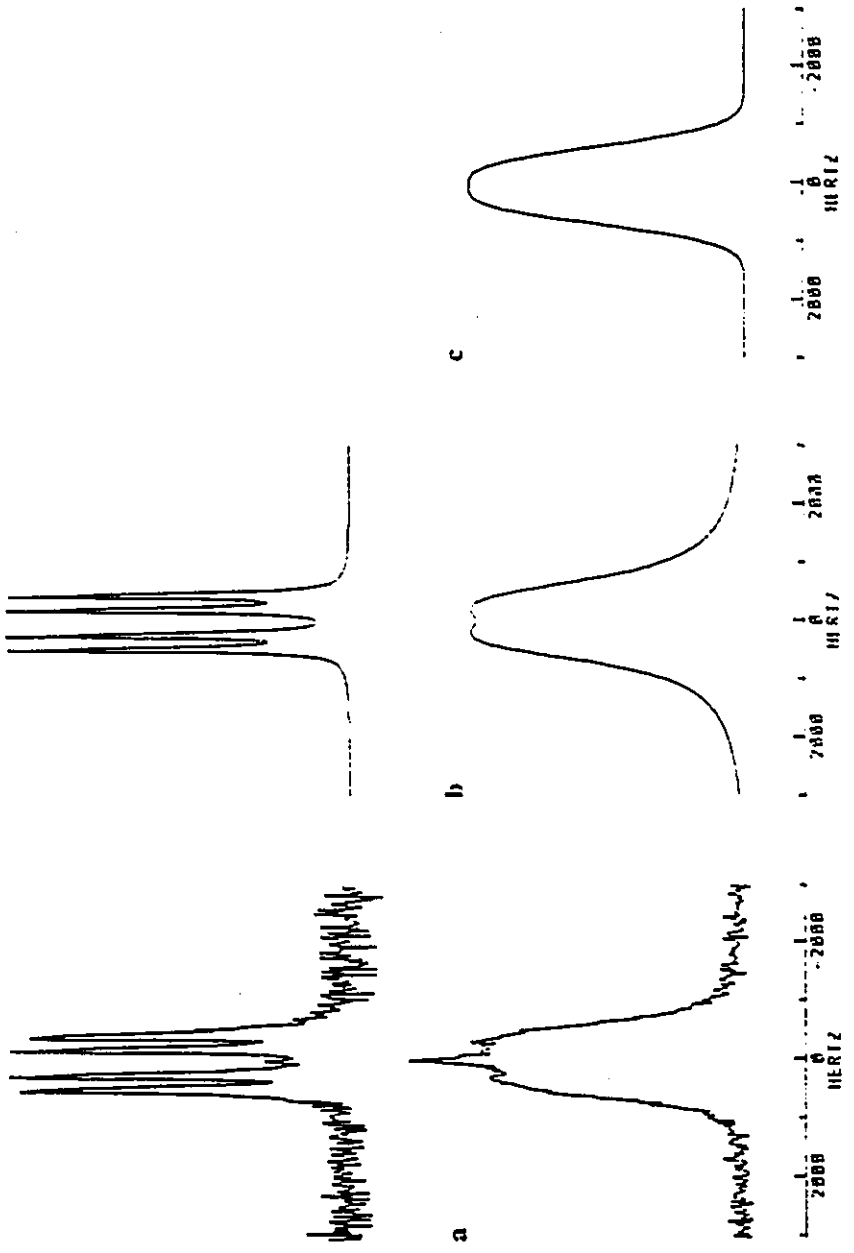
a
b
c
2000
0
-2000
HERTZ

Figure 5.12

^2H spectra of oriented multibilayers of [$^2H_2$-9',10']-PiLPC acquired **a)** with proton decoupling, and **b)** without proton decoupling.

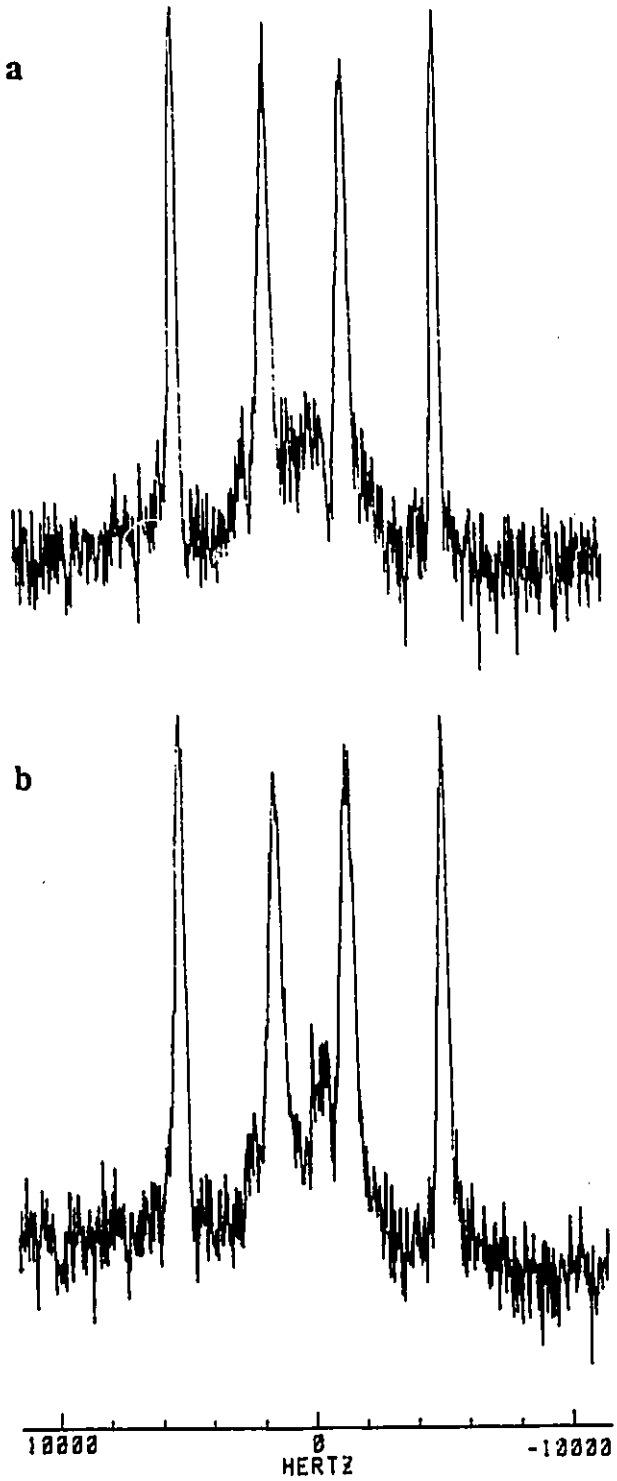
a
b
10000
0
HERTZ
-10000

[$^2H_2$ -9',10']-PiLPC. ^{2}H NMR spectra of oriented multibilayers of [$^2H_2$ -9',10']-PiLPC were acquired with and without proton decoupling. In contrast to the dramatic effects of proton-decoupling on the spectra of [$^2H_2$-8']-PiLPC, proton decoupling had almost no effects upon the spectra of [$^2H_2$ -9',10']-PiLPC (Figure 5.12). The size of the proton-deuteron dipolar couplings for the C_9-C_{10} segment is therefore essentially zero. Unfortunately, even with proton decoupling it was not possible to observe the dipolar couplings between the C_9 and C_{10} deuterons.

In order to estimate the gel-to-liquid crystal phase transition of PiLPC, phosphorus spectra were acquired from -20 °C to 25 °C (Figure 5.13; Hemminga & Cullis, 1982). At 25 °C, the sample consists almost entirely of a narrow peak (a small amount of the signal corresponding to unaligned lipid is evident) but below -5 °C the spectra are broadened significantly due to the appearance of lipids in the gel phase (the spectra are broadened due to dipolar interactions; Hemminga & Cullis, 1982). The s pectra change rapidly between -10 °C and -20 °C suggesting that the center of the transition is -15 °C.

Figure 5.13

Phosphorus spectra of oriented multibilayers of [$^2H_2$-9',10']-PiLPC acquired as a function of temperature. The spectrum at 25 °C was acquired first, and then the sample was cooled to -20 °C and the remaining spectra acquired sequentially. The assymmetry in the spectra is most likely due to a small amount of unoriented lipid which was formed at low temperatures due to dehydration of the sample.

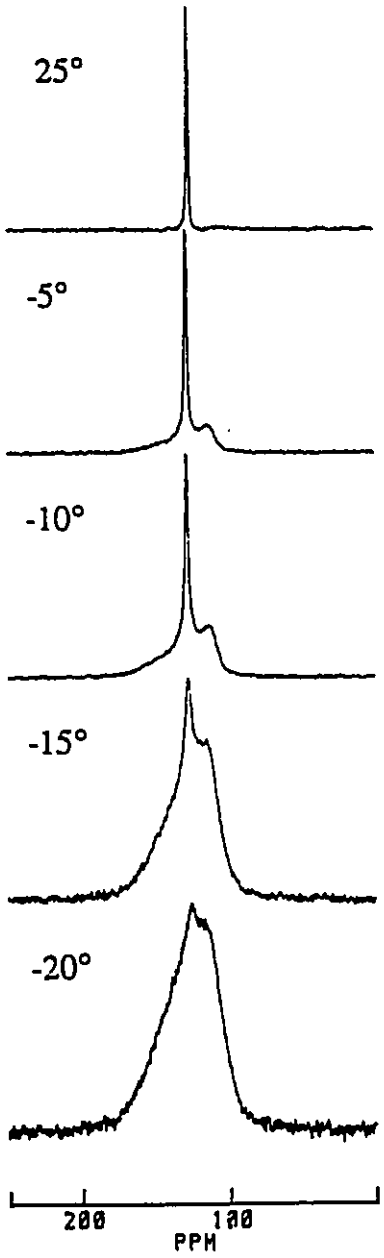
25°
-5°
-10°
-15°
-20°
200
100
PPM

Discussion

In recent years, oriented multibilayers of lipids have been used to examine the structural and motional properties of lipids in bilayers, and these experiments have provided more detailed information than is usually obtainable by conventional ^2H NMR analyses. The oriented system allows the examination of the orientational dependence of many spectroscopic properties such as the quadrupolar splittings (Seelig & Niederberger, 1974; Jarrell et al., 1987) and spin-lattice relaxation times (Bonmatin et al., 1987; Jarrell et al., 1987), and as shown here, the combination of oriented multibilayers and proton-decoupling increases the resolution of the spectra and makes it possible to gain access to otherwise inaccessible NMR parameters (ie. the ^2H-^2H dipolar couplings).

It had previously been reported that proton-decoupling has little effect on the deuterium powder spectra of deuteriated lipids (Seelig, & Seelig, 1974). In our case, the spectra of [$^2H_2$-8']-PiLPC show a dramatic effect and with the decrease in the line width of the peaks, it was possible to measure directly both the magnitude and the sign of the dipolar coupling between the two geminal C_8 deuterons. The line widths were also sufficiently narrow to allow the use of resolution enhancement techniques which assisted the interpretation of the spectra. The proton decoupling experiments permit analysis of the deuterium NMR data at a level of detail comparable to that of a high resolution NMR experiment.

Observation of the magnitude and the relative signs of the dipolar couplings between the two C_8 deuterons provided the additional parameter necessary for determine the completer ordering tensor and the orientation of the C_8 methylene unit as described in Appendix 4. Of greatest importance, however, is the fact that both parameters were determined without assumptions, which is not the case in most analyses of lipid acyl chain ordering. Clearly, any assumptions as to the average orientation of the chain based upon either the computer modeling studies of Applegate & Glomset (1986) or the crystal structure of linoleic acid determined by Ernst & Sheldrick (1979) would have led to large errors in the analysis. Observation of the dipolar couplings was therefore essential in order to draw any concrete conclusions about either the ordering or the structure of the diunsaturated chain.

The data was interpreted in terms of a model in which the acyl chain undergoes a two-site jump between two angle iron/helical conformations (Chapter 4). To gain further support for the jump motion, oriented samples of [$^2H_2$-9',10']-PiLPC were examined by acquiring ^2H spectra with and without proton decoupling. Unfortunately, the dipolar coupling between the C_9 and C_{10} deuterons could not be measured from the spectra (even when acquired with proton-decoupling) and therefore the analysis describedin Appendix 4 for the C_8 methylene unit could not be extended to the C_9-C_{10} segment. Lack of observation of the coupling is not suprising given its low order parameter and the increased distance between the two alkene deuterons relative to the distance between the two C_8 methylene deuterons (the magnitude of the interaction is scaled by $1/r^3$; equation 8, Chapter 2).

In principle, the proton-deuteron dipolar couplings can also provide information on the structure and motions of the chain. The couplings of the C_9 and C_{10} deuterons with

adjacent protons did not contribute to the line widths of the ^2H resonances whereas the couplings contribute roughly 650 Hz line broadening to the C_8 deuteron resonances . If the 1,4-pentadiene unit of the acyl chain was a rigid segment, the proton-deuteron couplings could be used via equation 9 (Chapter 2) to gain insight into the orientation and the order parameters for the proton-deuteron internuclear vectors. The molecular order parameters calculated in Chapter 4 suggest that the three-carbon unit is not rigid and therefore such an analysis is not possible. However, the results are consistent with the jump model in that the couplings between the C_8 deuterons and adjacent protons are much larger than the couplings for the C_9 and C_{10} deuterons. In the jump model, the C_6-C_7 segment is relatively immobile and therefore the C_8 deuterons should couple with the protons attached to the C_6-C_7 double bond. The C_9-C_{10} unit is surrounded on both sides by segments undergoing large amplitudes of motion and therefore the couplings between the C_9 and C_{10} deuterons and adjacent protons should be averaged to very small values.

The jump model is therefore consistent with all the data presented in this and the preceding chapter, for both the liquid-crystalline and the gel phase. Recent advances in the interpretation of ^2H NMR relaxation behaviour have enabled the testing of models for the motions of both lipids (Bonmatin et al., 1987; Auger et al., *in press*) and proteins (Torchia & Szabo, 1982) and via such an approach more insight into jump motion could be obtained. Deuterium NMR spectroscopy therefore provides a means for obtaining detailed information on the structural and motional properties of polyunsaturated acyl chains.

Summary and Conclusions

The results presented in Chapter 5 demonstrate that more detailed information on the structure and ordering of lipids in membranes can be obtained by ^2H NMR if the lipids are examined as oriented multibilayers as opposed to aqueous dispersions. The axis of motional averaging for the isolinoleoyl chain was defined as the bilayer normal by examining the orientation dependence of the quadrupolar splittings of [$^2H_2$ -8'] - PiLPC, and acquiring spectra of [$^2H_2$ -8'] - PiLPC with proton-decoupling also narrowed the line widths sufficiently to permit a direct measurement of the relative sign and magnitude of the dipolar coupling between the two C_8 geminal deuterons. The dipolar couplings were utilized to define the average orientation and the ordering tensor for the C_8 methylene unit. These calculations were essential to the analysis presented in Chapter 4 and, without this information concrete conclusions regarding the structure or motions of the isolinoleoyl chain would not have been possible.

Chapter 6

General Summary and Conclusions

Chapter 6

General Summary and Conclusions.....188

Despite increasing evidence that polyunsaturated fatty acyl chains play an essential role, there still remains a lack of understanding of the function of polyunsaturates in biological membranes. The generally accepted concept is that highly unsaturated lipids lower the phase transition temperature and thus "fluidize" membranes. However, this has recently been challenged (Coolbear et al., 1983; Deese et al., 1981), and until detailed information concerning the physico-chemical properties of polyunsaturates in the liquid crystalline phase of membranes can be obtained, the issue will remain unresolved.

Deuterium NMR spectroscopy can provide detailed information on the physico-chemical properties of acyl chains in membranes and as a non-perturbing technique is the method of choice for examining polyunsaturated acyl chains. However, the analysis of polyunsaturates has been hampered by two factors; 1) specifically deuteriated lipids are necessary in order to perform the NMR experiment and routes to the chemical synthesis of specifically deuteriated polyunsaturates have not been developed, and 2) although a deuterium NMR analysis can provide information on the both the average orientation and the amplitudes of motion (the ordering) of a deuteriated segment, the analysis is ambiguous in that the measured parameter (the quadrupolar splitting) reflects both parameters (Figure 6.1). For saturated chains, the deuteriated segments are assumed to adopt the all-*trans* conformation and the splittings can be interpreted directly in terms of the ordering of the chain. For polyunsaturates, both parameters are of interest, but neither can be accessed by the conventional ^2H NMR experiment without obtaining additional experimental observables. A large proportion of this thesis therefore was concerned with addressing the **two major technical problems** associated with a dueterium NMR analysis of unsaturated acyl chains.

The requirement for deuteriated lipids was overcome by developing a biological approach to their synthesis using the protozoan, *Tetrahymena* , and a series of isolinoleic acids specifically labelled at ten different positions along the chain were produced. Characterization of the products clearly established the utility of the biological approach, and as discussed in Chapter 3, the protocol could be improved and expanded in order to produce fatty acids with increasing numbers of double bonds.

The biosynthetic work also demonstrates that eukaryotic organisms will incorporate deuteriated fatty acids directly into their membranes and thus analyses of the physico-chemical properties of lipids in eukaryotic membranes are possible. Given the specificity in channeling polyunsaturates into the membranes of the eye and nerves in mammalian tissues, it may also be possible to incorporate specifically deuteriated polyunsaturates into the membranes of mice or rats and perform *in vivo* deuterium NMR spectroscopy. Considerable avenues in this area are possible.

The second technical obstacle was overcome by examining lipids as oriented multibilayers as opposed to aqueous dispersions. As shown in Chapter 5, additional observables can be obtained from the oriented samples which allow the data to be interpreted unambiguously in terms of both the structure and the molecular order of the deuteriated segment. Combined with the advantageous increase in the signal-to-noise ratio obtained by concentrating the ^2H signals into two narrow peaks, as opposed to spreading the signal out over the entire powder spectrum, analysis of the structure and order of highly unsaturated acyl chains in oriented systems should also be possible.

The analysis presented here for isolinoleic acid provides insight into the physico-chemical properties of polyunsaturated acyl chains in membranes. The diunsaturated chain

adopts a conformation in the gel state that is consistent with the angle iron/helical conformation proposed by Applegate and Glomset (1986), but in the liquid crystalline phase appears to undergo a two site jump between two such conformations. The results therefore support the proposed existence of angle iron or helical conformations for highly unsaturated acyl chains and suggest that these structures could play a role in the bilogical function of polyunsaturates. However, more work must be performed to investigate this latter hypothesis.

The analysis also shows that the motions of the diunsaturated acyl chain differ significantly from the same properties of saturated and monounsaturated chains. The motional differences are reflected in the order parameter profiles which are plotted in Figure 6.1. In Figure 6.1a, the bond order parameters, S_{CD}, are plotted as a function of labelled position and for comparison the same profiles for saturated and monounsaturated acyl chains are shown. The molecular order parameter profiles (S_{mol} versus labelled position) are plotted for the same three acyl chains in Figure 6.1b, and the values shown reflect the amplitudes of fluctuations occuring at each segment (the values of S_{CD}, in contrast, contain a geometrical contribution as well). The results clearly indicate that the presence of a second double bond in the isolinoleoyl chain has a definite effect on the motions of the chain in a bilayer.

The C_6-C_7 double bond has a large order parameter suggesting that the isolinoleoyl chain is relatively ordered in the plateau region, but the C_8 and C_9-C_{10} segments become relatively disordered due to the proposed two-site jump. The increased motional restrictions imposed by additional double bonds, however, would likely make it very difficult for a chain containing three or more double bonds to undergo such a two-site jump between angle iron or helical conformations. Without the jump motion, one would

Figure 6.1

Comparison of the bond order parameter, S_{CD}, and the molecular order parameter, S_{mol}, profiles for saturated, monounsaturated, and diunsaturated fatty acyl chains. The data in a) is plotted at a reduced temperature of 0.05 and in b) at 0.13. The data for the saturated and monunsaturated chains are for the palmitoyl and oleoyl chains of POPC and are from Figure 4.5

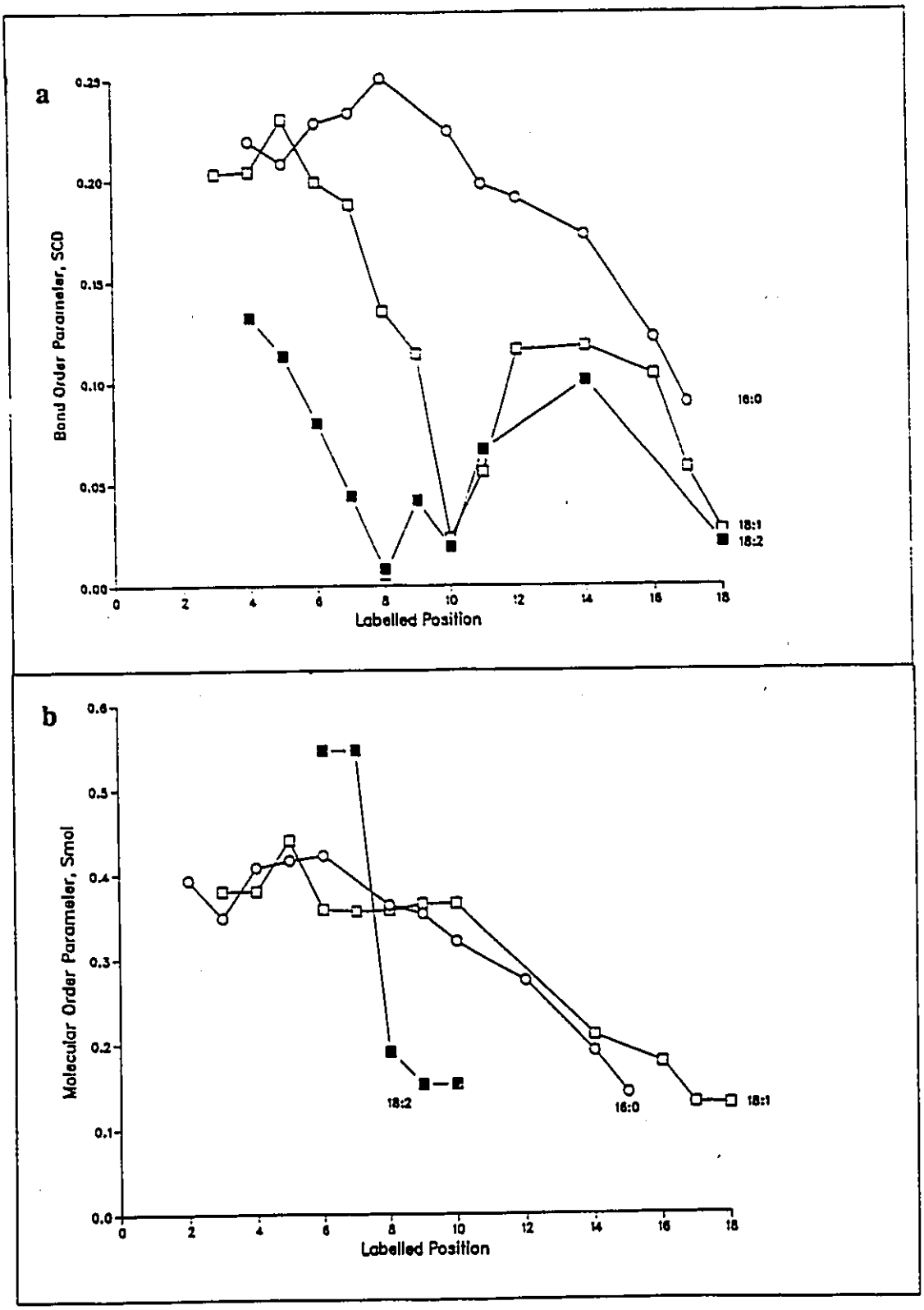
a
Bond Order Parameter, SCD
0.25
0.20
0.15
0.10
0.05
0.00
0
2
4
6
8
10
12
14
16
18
Labelled Position
16:0
18:1
18:2
b
Molecular Order Parameter, Smol
0.6
0.5
0.4
0.3
0.2
0.1
0.0
0
2
4
6
8
10
12
14
16
18
Labelled Position
18:2
16:0
18:1

therefore expect that highly unsaturated chains would be highly ordered for the length of the chain (as the isolinoleoyl chain is for the C_6-C_7 segment). This is intuitively obvious because the source of disordering of saturated lipids, *trans-gauche* isomerizations (Seelig & Seelig, 1974; Schindler & Seelig, 1975; Marcelja, S., 1974; Israelachvilli et al., 1980), cannot occur in highly unsaturated chains and therefore one would not expect the same orering profile for highly unsaturated chain that one observes for saturates.

However, it is generally assumed that the hydrophobic interiors of biological membranes are relatively homogenious regions of flexible hydrocarbon chains (Seelig & Browning, 1980; Israelachvilli et al., 1980) and that the flexibility or "fluidity" is important for accomadating rigid molecules such as cholesterol and proteins (Israelachvilliet al., 1980). Indeed, all acyl chains that have been examined by deuterium NMR to date have shown order profiles that are essentially identical without any dependence upon the length of the acyl chains, type of headgroup, etc. (Seelig & Browning, 1980). The results presented here clearly indicate that not all hydrophobic regions of biological membranes are homogeniously "fluid", and that the interiors of membranes rich in polyunsaturated lipids are in fact relatively rigid. The concept of a "rigid" hydrophobic interior therefore must be taken into account when one examines the role of lipids in membrane function.

References.

Abragam, A. (1961) *The Principles of Nuclear Magnetism* Oxford University Press, London.

Anderson, R.E. & Maude, M.B. (1972) "The Effects of Essential Fatty Acid Deficiency on the Phospholipids of the Photoreceptor Membranes of Rat Retina" *Arch. Biochem. Biophy.* **151**, 270-276.

Applegate, K.R. & Glomset, J.A. (1986) "Computer-based Modeling of the Conformation and Packing Properties of Docosahexaenoic Acid" *J. Lipid Res.* **27**, 658-680.

Aveldano, M.I., Van Rollins, M. & Horrocks, L.A. (1983) "Separation and Quantitation of Free Fatty Acid Methyl Esters by Reverse Phase High Pressure Liquid Chromatography" *J. Lipid Res.* **24**, 83-93.

Barton, P.G. & Gunstone, F.D. (1975) Hydrocarbon Chain Packing and Molecular Motion in Phospholipid Bilayers Formed from Unsaturated Lecithins"*J. Biol. Chem.* **250**, 4470-4476.

Batchelor, J.G., Cushley, R.J., Prestegard, J.H. & Lipsky, S.R. (1974) "Carbon-13 Fourier Transform Nuclear Magnetic Resonance. VIII. Role of Steric and Electrical Field Effects in Fatty Acid spectra" *J. Org. Chem.* **39**, 1698-1705.

Batchelor, J.G., Prestegard, J.H., Cushley, R.J. & Lipsky, S.R. (1973) "Electric Field Effects in the ^{13}C Nuclear Magnetic Resonance Spectra of Unsaturated Fatty Acids. A Potential Tool for Conformational Analysis" *J. Am. Chem. Soc.* **95**, 6358-6364.

Benolken, R.M., Wheeler, T.G., & Anderson, R.E. (1973) ""Membrane Fatty Acids Associated with the Electrical Response in Visual Excitation" *Science* **182**, 1253-1254.

Bitman, J. & Wood, D.L. (1982) "An Improved Copper Reagent for Quantitative Densitometric Thin-Layer Chromatography"*J. Liq. Chromatogr.* **5**, 1155-1162.

Bonmatin, J-M., Smith, I.C.P., Jarrell, H.J. & Siminovitch, D.J. (1987) "Orientation Dependence of ^2H NMR Spin-Lattice Relaxation Rates for Cholesterol in Macroscopically Oriented Multibilayers" *J. Am. Chem. Soc.* **110**, 8693-8695.

Boggs, J.M. "Intermolecular Hydrogen Bonding between Membrane Lipids" (1984) in *Membrane Fluidity* (Kates, M. & Manson, L.A., eds.) pp 3-53, Plenum Pub. Co., N.Y.

Borch, R.F. (1975) "Seperation of Long Chain Fatty Acids as Phenacyl Esters by HighPressure Loquid Chromatography" *Anal. Chem.* **47**, 2437-2439.

Breckenridge, W.C., Morgan, I.G., Zanetti, J.P., & Vindendon, G. (1973) "Adult Rat Brain Synaptic Vesicles. II Lipid "Composition" *Biochim. Biophys. Acta* **320**, 681-686.

Brown, P.K. (1972) "Rhodopsin Rotates in the Visual Receptor Membrane" *Nature, New Biol.* **236**, 35-38.

Browning, J.L. (1981) "NMR Studies of the Structural and Motional Properties of Phospholipids in Membranes" in *Liposomes: From Physical Structure to Therapeutic Applications* pp 189-242, Elsevier/North-Holland Biomedical Press, Amsterdam.

Chin, J.H. & Goldstein, D.B. (1977) "Drug Tolerance in Biomembranes: a Spin Label Study of the Effects of Ethanol" *Science* **196**, 684-685.

Christie, W.W. & Holman, R.T. (1966) "Synthesis and Characterization of the Complete Series of Methylene-Interrupted *cis*, *cis*-Octadecadienoic Acids" *Chem. Phys. Lipids* **1**, 407-423.

Cone, P.K. (1972) "Rotational Diffusion of Rhodopsin in the Visual Receptor Membrane" *Nature, New Biol.* **236**, 39-43.

Conner, R.L., Burtness, B. & Ferguson, K.A. (1984) "Fatty Acid Desaturase Specificity in *Tetrahymena*" *Lipids* **19**, 285-288.

Coolbear, K.P., Berde, C.B., & Keough, K.M.W. (1983) "Gel to Liquid-Crystalline Phase Transitions of Aqueous Dispersions of Polyunsaturated Mixed-Acid Phosphatidylcholines" *Biochemistry* **22**, 1466-1473.

Cotman, C., Blank, M.L., Moehl, A., & Snyder, F. (1969) "Lipid Composition of Synaptic Plasma Membranes Isolated from Rat Brain by Zonal Centrifugation" *Biochemistry* **8**, 4606-4612.

Crawford, M.A., Hassam, A.G., Williams, G., & Whitehorse, W. (1973) "Fetal Accumulation of Long-Chain Polyunsaturated Fatty Acids" *Adv. Exp. Med. Bio.* **83**, 135-143.

Davis, J.H. (1983) "Description of Membranes Lipid Conformation, Order and Dynamics by ^2H NMR" *Biochim. Biophys. Acta.* **737**, 117-171.

Deese, A.J., Dratz, E.A., Dahlquist, F.W. & Paddy, M.R. (1981) "Interactions of Rhodopson with two Unsaturated Phosphatidylcholines: a Deuterium NMR Study" *Biochemistry* **22**, 1466

Deinum, G., van Langen, H., von Ginkel, G., & Levine, Y.K. (1988) "Molecular Order and Dynamics in Planar Lipid Bilayers: Effects of Unsaturation and Sterols" *Biochemistry* **27**, 852-860.

Dickens, B.F. & Thompson, G.A. Jr. (1981) "Rapid Membrane Response During Low-Temperature Acclimation. Correlation of Early Changes in the Physical Properties and Lipid Composition of Tetrahymena Microsomal Membranes" *Biochim. Biophys. Acta* **644**, 211-218.

Dickens, B.F. & Thompson, G.A. Jr. (1982) "Phospholipid Molecular Species Alterations in Microsomal Membranes as an Initial Key Step during Cellular Acclimation to Low Temperature" *Biochemistry* **21**, 3604-3611.

Dommes, V., Wirtz-Pietz, F. & Kunau, W.H. (1976) "Structure Determination of Polyunsaturated Fatty Acids by Gas Chromatography-Mass Spectrometry-A Comparison of Fragmentation Patterns of Various Derivatives" *J. Chromatogr. Sci.* **14**, 360-366.

Dratz, E.A. & Deese, A.J. (1986) "The Role of Docosahexaenoic Acid (22:6 w-3) in Biological Membranes: Examples From Photoreceptors and Model Membrane Bilayers" in *Health Effects of Polyunsaturated Fatty Acids in Seafoods*. (Simopoulos, A.P., Kifer, R.R., & Martin, R.E. Eds.) pp 319-351, Academic, N. Y.

Drenthe, E.H.S., Klompmakers. A.A., Bonting, S.L., & Daemen, F.J.M. (1981) "Transbilayer Distribution of Phospholipid Fatty Acyl Chains in Photoreceptor Membrane" *Biochim. Biophys. Acta* **641**, 377-385.

Dufourc. E.J., Smith, I.C.P, & Jarrell, H.C. (1983) "A 2H NMR Analysis of Dihydrosterculoyl-Containing Lipids in Model Membranes: Structural Effects of a Cyclopropane Ring" *Chem. Phys. Lipids* **33**, 153-177.

Ernst, J., Sheldrick, W.S. & Furrhop, J.-H. (1979) "The Structures of the Essential Unsaturated Fatty Acids. Crystal Structures of Linoleic Acid and Evidence for the Crystal Structures of α-Linolenic Acid and Arachidonic Acid" *Naturforsch* **34**, 706-711.

Emsley, J.W. & Lindon, J.C. (1975) *NMR Spectroscopy Using Liquid Crystals Solvents* Pergamon Press Ltd., Oxford.

Evans, R.W. & Tinoco, J. (1978) "Monolayers of Sterols and Phosphatidylcholines Containing a 20-Carbon Chain" *Chem. Phys. Lipids* **22**, 207-220.

Ferguson, K.A., Davis, F.M., Conner, R.L., Landrey, J.R. & Mallory, F.B. (1975) "Effects of Sterol Replacement in Vivo on the fatty acid composition of Tetrahymena" *J. Biol. Chem.* **250**, 6998-7005.

Fleisher, S. & Rouser, G. (1965) "Lipids of Subcellular Particles" *J. Am. Oil Chem. Soc.* **42**, 588-607.

Fukushima, E.L. & Roeder, S.B. (1981) *Experimental Pulse NMR. A Nuts and Bolts Approach*, Reading Addison-Wesley Publishing Co. Inc., M.A.

Futterman, S., Downer, J.L., & Hendrickson, A. (1971) "Effect of Essential Fatty Acid Deficiency on the Fatty Acid Composition, Morphology, and Electroretinographic Response of the Retina" *Invest. Opthamol.* **10**, 151-156.

Frye, C.D. & Edidin, M. (1970) "The Rapid Intermixing of Cell Surface Antigens After Formation of Mouse-Human Heterokaryons" *J. Cell Sci.* **7**, 319-335.

Gally, H.U., Pluschke, G., Overath, P. & Seelig, J. (1980) "Structure of Esherichia coli Membranes. Fatty Acyl Chain Order Parameters of Inner and Outer Membranes and Derived Liposomes" *Biochemistry* **19**, 1638-1643.

Granstrom, E. & Hedquist, P. (1982) in *Patholbiology of the Endothelial Cell* , Academic Press.

Gruen, D.W.R. (1980) "A Statistical Mechanical Model of the Lipid Bilayer Above its Phase Transition" *Biochim. Biophys. Acta* **595**, 161-183.

Gunstone, H.U. & Ismail, I.A. (1967) "The Conversion of the *Cis* Octadecenoic Acids to their T*rans* Isomers" *Chem. Phys. Lipids* **1**, 264-269.

Hahn, E.L. (1950) "Spin Echoes" *Phys. Rev.* **80**, 580-594.

Hare, F.,& Lussan, C. (1977) "Variations in Microviscosity Values Induced by Different Rotational Behaviour of Fluorescent Probes in Some Aliphatic Environments" *Biochim. Biophys. Acta* **467**, 262-272.

Harris, R.K. (1983) *Nuclear Magnetic Resonance Spectroscopy*, Pitman Publishing Co., London.

Hemminga, M.A. & Cullis, P.R. (1982) "^{31}P NMR Studies of Oriented Phospholipid Multibilayers" *J. Mag. Reson.* **47**, 307-323.

Higgs, T.P. & Mackay, A.L. (1977) "Determination of the Complete Order Parameter Tensor for a Lipid Methylene Group from ^{1}H- and ^{2}H-NMR Spin Labels" *Chem. Phys. Lipids* **20**, 105-114.

Hill, R.J., Prescott, D.J., Spence, S.L. & Conner, R.L. (1983) "Characterization of an Unsaturated Fatty Acid Auxotroph of *Tetrahymena*" *Biochim. Biophys. Acta* **754**,150-158.

Hope, M.J., Bally, M.B., Mayer, L.D., Janoff, A.S. & Cullis, P.R. (1986) "Generation of Multilamellar and Unilamellar Phospholipid Vesicles" *Chem. Phys. Lipids* **40**, 89-107.

Hsung, J.C., Huang, L., Hoy, D.J., & Haug, A. (1974) "Lipid and Temperature Dependence of Membrane-Bound ATPase activity of *Acholeplasma laidlawii*" *Can. J. Biochem.* **52**, 974-980.

Huang, L., Lorch, S.K., Smith, C.G., & Haug, A. (1974) "Control of Membrane Lipid Fluidity in *Acholeplasma laidlawii*" *FEBS Lett*. **43**, 1-5.

Israelachvilli, J.N., Marcelja, S. & Horn, R.G. (1980) "Physical Principles of Membrane Organization" *Quart. Rev. Biophys.* **13**, 121-200.

Jarrell, H.J., Byrd, R.A. & Smith, I.C.P. (1981) "Analysis of the Composition of Mixed Lipid Phases by the Moments of ^{2}H NMR Spectra" *Biophys. J.* **34**, 451-463.

Jarrell, H.J., Jovall, P.Å, Giziewicz, J.B., Turner, L.A. & Smith, I.C.P. (1987) "Determination of Conformational Properties of Glycolipid Head Groups by ^{2}H NMR of Oriented Multibilayers" *Biochemistry* **26**, 1805-1811.

Jarrell, H.C., Smith, I.C.P., Jovall, P.A., Mantsch & Siminovitch, D.J. (1988) *J. Chem. Phys.* **88**, 1260-1263.

Kates, M. (1972) *Techniques of Lipidology Isolation, Analysis and Identification of Lipids*, North Holland Publishing Co., Amsterdam.

Keough, K.M.W. & Davis, P.J. (1979) "Gel to Liquid-Crystalline Transitions in Water Dispersions of Saturated Mixed-Acid Lecithins" *Biochemistry* **18**, 1453-1459.

Lamptey,M.S. & Walker, B.L. (1976) "A Possible Essential Role for Dietary Linolenic Acid in the Development of teh Young Rat" *J. Nutr.* **106**, 86-93.

Lands, W.E.M. & Davis, F.S. (1984)"Fluidity of Membrane Lipids" in *Membrane Fluidity* (Kates, M. & Manson, L.A., eds.) pp. 475-517, Plenum Pub. Co., N.Y.

Marcelja, S. (1974) "Chain Ordering in Liquid Crystals II. Structure of Bilayer Membranes" *Biochim. Biophys. Acta* **367**, 165-176.

Martin, C.E., Hiramitsu, K., Kitajima, Y., Nozawa, Y., Skriver, L. & Thompson, G.A. Jr. (1976) "Molecular Control of Membrane Properties During Temperature Acclimation. Fatty Acid Desaturase Regulation of Membrane Fluidity in Acclimating *Tetrahymena* Cells" *Biochemistry* **15**, 52185233.

Maruyama, H., Banno, Y., Watanabe, T & Nozawa, Y. (1982) "Studies of Thermal Adaptation in Tetrahymena Membrane Lipids. Modification of Positional Distribution of Phospholipid Acyl Chains in Plasma Membranes, Mitochondria, and Microsomes" *Biochim. Biophys. Acta* **711**, 229-244.

Miljanich, G.P., Sklar, L.A., White, D.L., & Dratz, E.A. (1979) "Disaturated and Dipolyunsaturated Phospholipids in the Bovine Retinal Rod Outer Segment Disk Membrane" *Biochim. Biophys. Acta* **552**, 294-306.

Millet, F., Hargrave, P.A., Raftery, M.A. (1973) "Natural Abundance ^{13}C Nuclear Magnetic Resonance Spectra of the Lipid in Intact Bovine Retinal Rod Outer Segment Membranes" *Biochemistry* **12**, 35913592.

Morrison, W.R. & Smith, L.M. (1964) "Preparation of Fatty Acid Methyl Esters and Dimethyl Acetals from Lipids with Boron Fluoride-Methanol" *J. Lipid Res.* **5**, 600-608.

Neuringer, M., Connor, W.E., Van Petton, D., & Barstad, L. (1984) "Dietary Omega -3 Fatty Acid Deficiency and Visual Loss in Infant Rhesus Monkeys" *J. Clin. Invest.* **73**, 272-276.

Nozawa, Y., Iida, H., Fukishimal, H., Ohki, K. & Ohnishi, S. (1974) "Studies on *Tetrahymena* Membranes: Temperature Induced Alterations in Fatty Acid Composition of Various Membrane Fractions in *Tetrahymena pyriformis* and its Effects on Membrane Fluidity as Inferred by Spin Label Study" *Biochim. Biophys. Acta* **367**, 134-147.

Oldfield, E., Meadows, M., Rice, D. & Jacobs, R. (1978) "Spectroscopic Studies of Specifically Deuterium Labeled Membrane Systems. Nuclear Magnetic Resonance

Investigation of the Effects of Cholesterol in Model Systems" *Biochemistry* **17**, 2727-2740.

Paddy, M.R., Dahlquist, F.W., Dratz, E.A., & Deese, A.J. (1985) "Simultaneous Observation of Order and Dynamics at Several Defined Positions in a Single Acyl Chain using ^2H NMR of Single Acyl Chain Perdeuterated Phosphatidylcholines" *Biochemistry* **24**, 5988-5995.

Perly, B., Dufourc, E.J. & Jarrell, H.C. (1984) *J. Labelled Compd. Radiopharm.* **21**, 1-13.

Pierce, D.M. (1981) "Selection of Solvents for Thin-Layer Chromatography by Means of a Simple Ranking System Based on Dielectric Constants" *Nenobiotica* **11**, 857-862.

Porter, N.A. (1986) *Acc. Chem. Res.* **19**, 262-268.

Ramesha, C.S. & Thompson, G.A. Jr. (1982) "Changes in the dLipid Composition and Physical Properties of *Tetrahymena* Ciliary Membranes following Low-Temperature Acclimation" *Biochemistry* **21**, 3612-3617.

Ramesha, C.S. & Thompson, G.A. Jr. (1983) "Cold Stress Induces *in Situ* Phospholipid Molecular Species Changes in Cell Surface Membranes" *Biochim. Biophys. Acta* **731**, 251-260.

Ramesha, C.S. & Thompson, G.A. Jr. (1984) "Effect of Temperature on Phospholipid Deacylation and Reacylation Reactions in the Cell Surface Membrane" *J. Biol. Chem.* **259**,8706-8712.

Ramesha, C.S., Dickens, B.F. & Thompson, G.A. Jr. (1984) "Phospholipid Molecular Species Alteration in *Tetrahymena* Ciliary Membranes following Low-Temperature Acclimation" *Biochemistry* **21**, 3618-3622.

Rance, M. & Bird, A. (1983) "Obtaining High Fidelity Spin-1/2 Powder Spectra in Anisotropic Media: Phase-Cycled Hahn-Echo Spectroscopy" *J. Magn. Res.* **52**, 221-240.

Rance, M., Jeffrey, K.R., Tulloch, A.P., Butler, K.W. & Smith, I.C.P. (1980) "Orientational Order of Unsaturated Lipids in the Membranes of *Acholeplasma laidlawii* as Observed by ^{2}H-NMR" *Biochim. Biophys. Acta* **600**, 245-262.

Rutledge, R.G., Neelin, J.M. & Seeligy, V.L. (1984) "Uncoupled Synthesis of H1^o-like Histone H1^s During Late Erythropoiesis in *Xenopus laevis*" *Eur. J. Biochem.* **144**, 191-198.

Salem, N. Jr., Kim, H-Y., & Yergey, J.A. (1986) "Docosahexaenoic Acid: Membrane Function and Metabolism" in *Health Effects of Polyunsaturated Fatty Acids in Seafoods* (Simopoulos, A.P., Kifer, R.R., & Martin, R.E. Eds.) pp. 263-317, Academic, N.Y.

Salmon, A., Dodd, S.W., Williams, G.D., Beach, J.M., & Brown, M.F. (1987) "Configurational Statistics of Acyl Chains in Polyunsaturated Lipid Bilayers from ^{2}H NMR" *J. Amer. Chem. Soc.* **109**, 2600-2609.

Sandermann, H. Jr. (1978) "Regulation of Membrane Enzymes by Lipids" *Biochim. Biophys. Acta* **515**, 209-237.

Schindler, H. & Seelig, J. (1975) "Deuterium Order Parameters in Relation to Thermodynamic Properties of a Phospholipid Bilayer. A Statistical Mechanical Interpretation" *Biochemistry* **14**, 2283-2287.

Schmitz, B. & Egge, H. (1979) "Determination of Double Bond Position in Tri-Hexaenoic Fatty Acids by Mass Spectrometry" *Chem Phys. Lipids* **25**, 287-298.

Seelig, A & Seelig J. (1974) "The Dynamic Structure of Fatty Acyl Chains in a Phospholipid Bilayer Measured by Deuterium Magnetic Resonanc" *Biochemistry* **13**, 4839-4845.

Seelig, A & Seelig J.a (1977) "Effect of a Single *Cis* Double Bond on the Structure of a Phospholipid Bilayer" *Biochemistry* **16**, 45-50.

Seelig, J. (1977) "Deuterium Magnetic Resonance: Theory and Application to Lipid Membranes" *Q. Rev. Biophys.* **10**, 353-418.

Seelig, J. & Browning, J.L. (1978) "General Features of Phospholipid Conformation in Membranes" *FEBS Lett.* **92**, 41-44.

Seelig, J. & Niederberger, W. (1974) "Deuterium Labeled Lipids as Structural Probes in Liquid Crystalline Bilayers" *J. Am. Chem. Soc.* **96**, 2069-2073.

Seelig, J. & Waespe-Sarcevic, N. (1978) "Molecular Order in *Cis* and *Trans* Unsaturated Phospholipid Bilayers" *Biochemistry* **17**, 3310-3315.

Shaka, A.J., Keeler, J., Frenkiel, T. & Freeman, R. (1983) "An Improved Sequence for Broadbond Decoupling: Waltz-16" *J. Magn. Reson.* **52**, 335-341.

Shinitzky, M. & Barenholtz, Y. (1974) "Dynamics of the Hydrocarbon Layer in Liposomes of Lecithin and Sphingomyelin Containing Dicetylphosphate"*J. Biol. Chem.* **249**, 2652-2657.

Singer, S.J. & Nicolson, G.L. (1972) "The Fluid Mosaic Model of the Strucure of Cell Membranes" *Science* **175**,720-731.

Skipski, V.P. & Barclay, M. (1969) ""Thin-Layer Chromatography of Lipids" *Methods Enzymol.* **8**, 530-598.

Smith, I.C.P., Butler, K.W., Tulloch, A.P., Davis, J.H. & Bloom, M. (1979) "The Properties of Gel State Lipids in Membranes of *Acholeplasma laidlawii* as Observed by ^{2}H NMR" *FEBS Lett.* **100**, 57-61.

Smith, I.C.P. & Ekiel, I.H. (1984) "Phosphorus-31 NMR of Phospholipids in Membranes, in *Phosphorus-31 NMR Principles and Applications* (Gorenstein, D.G. ed.) pp. 447-475, Academic Press, Inc., Toronto.

Smith, I.C.P. & Mantsch, H.H (1982) "Deuterium NMR Spectroscopy" in *NMR Spectroscopy: New Methods and Applications* (George C. Levy, Ed.) pp. 97-117, American Chemical Society.

"Spector, A.A. & Yorek, M.A. (1985) "Membrane Lipid Composition and Cellular Function" *J. Lip. Res.* **26**, 1015-1035.

Sternin, E., Bloom, M. & Mackay, A.L. (1983) "De-Pake-ing of NMR Spectra" *J. Mag. Res.* **55**, 274-282.

Stockton, G.W., Johnson, K.G., Butler, K.W., Tulloch, A.P., Boulanger, Y., Smith, I.C.P., Davis, J.H. & Bloom, M. (1977) "Deuterium NMR Study of the Lipid Organisation in Acholeplasma laidlawii membranes" *Nature* **269**, 266-267.

Stone, W.L., Farnsworth, C.C. & Dratz, E.A. (1979) "A Re-Investigation of of the Fatty Acid Content of Bovine, Rat, and Frog Retinal Rod Outer Segments" *Exp. Eye Res.* **28**, 387-397.

Stubbs, C.D., Kouyama, Y., Kinosita, K., & Ikegami, A. (1981) "Effect of Double Bonds on the Dynamic Properties of the Hydrocarbon Region of Lecithin Bilayers" *Biochemistry* **20**, 4257-4262.

Stubbs, C.D. & Smith A.D. (1984) "The Modification of Mammalian Membrane Polyunsaturated Fatty Acid Composition in Relation to Membrane Fluidity and Function" *Biochim. Biophys. Acta* **779**, 89-137.

Taylor, M.G., Akiyama, T. & Smith, I.C.P. (1981) "The Molecular Dynamics of Cholesterol in Bilayer Membranes: a Deuterium NMR Study" *Chem. Phys. Lipids* **29**, 327-339.

Torchia, D.A. & Szabo, A.J. (1982) "Spin-Lattice Relaxation inSolids" *J. Magn. Reson.* **49**, 107-121.

Tinoco, J., Babcock, R., Hincenbergs, I., Medwadowski, B., Miljanich, P. & Williams, M.A. (1978) "Linolenic Acid Deficiency" *Lipids* **14**, 166-173.

Tulloch, A.P. (1979) "Synthesis of Deuterium and Carbon-13 Labelled Lipids" *Chem. Phys. Lipods* **24**, 391-406.

Viret, J. & Leterrier, F. (1976) "A Spin Label Study of Rat Brain Membtanes. Effects of Temperature and Divalent Cations" *Biochim. Biophys. Acta* **436**, 811-824.

Wheeler, T.G., Benolken, R.M., & Anderson, R.E. (1975) "Visual Membranes: Specificity of Fatty Acid Precursors for the Electrical Response to Illumination" *Science* **188**, 1312-1313.

Whitting, L.A., Harvey, C.C., Century, B. & Horwitt, M.K. (1961) "Dietery alterations of Fatty Acids of Erythrocytes and Mitochondria of Brain and Liver" *J. Lipid Res.* **2**, 412-418.

Wolber, P.K. & Hudson B.S. (1981) "Fluorescence Lifetime and Time-resolved Polarization Anisotropy Studies of Acyl Chain Order and Dynamics in Lipid Bilayers" *Biochemistry* **20**, 2800-2810.

Yeagle,P.L. & Frye, J. (1987) "Effects of Unsaturation on ^{2}H NMR Quadrupole Splittings and ^{13}C NMR Relaxation in Phospholipid Bilayers" *Biochim. Biophys. Acta* **899**, 137-142.

Appendices

Appendices.....206

Appendix 1:

Alkenyl Bond Angles and Torsion Angles of the 1,4-Pentadiene Unit of Linoleic Acid.....208

Appendix 2:

Orientations of the C_6-C_7 Double Bonds in the Liquid Crystalline Phase.....209

Double Bond Orientations.....209

Sensitivity of the Calculations to the Angle ψ.....216

Sensitivity of the Calculation to the Double Bond Torsion Angles.....216

Sensitivity of the Calculation to the Double
Bond Torsion Angles 216

Appendix 3:

**Orientations of the Isolinoleoyl
Chain in the Gel Phase 222**

Angle Iron Conformation 222

C_7 Deuteron 222

C_8 Methylene Deuterons 223

C_9-C_{10} Double Bond 224

Linoleic Acid Crystal Structure 228

Appendix 4:

**Calculation of the Orientation and Order Matrix for the
C_8 Methylene Segment in the Liquid Crystalline Phase 231**

Appendix 1

Alkenyl Bond Angles and Torsion Angles of the 1,4-Pentadiene Unit of Linoleic Acid

Torsion Angles

C8-C9-C10-C11 = 2.3°

C9-C10-C11-C12 = 122.7°

C10-C11-C12-C13 = 123.5°

C11-C12-C13-C14 = 3.3°

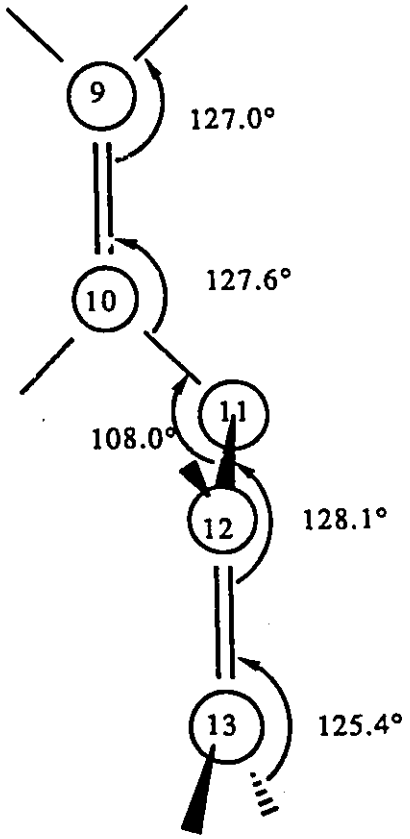

Figure A1.1 Bond angles of the 1,4-pentadiene segment of linoleic acid as determined by X-ray crystallography (Ernst & Sheldrick, 1979).

Appendix 2

Orientations of the C_6-C_7 and the C_9-C_{10} Double Bonds in the Liquid-Crystalline Phase

Double Bond Orientations. The average orientation of each double bond with respect to the bilayer normal was calculated as follows. A right handed cartesian coordinate system (X-Y-Z) was attached to both the C_6-C_7 and the C_9-C_{10} double bonds as shown in Figure A2.1 and the coordinates of all four deuterons in their respective axis system were specified:

$$P_6 = (0, \text{Cos}\phi_6, \text{Sin}\phi_6); \qquad \phi_6 = \psi_6 - 52.4^o$$
$$P_7 = (0, \text{Sin}\phi_7, \text{Cos}\phi_7); \qquad \phi_7 = \psi_7 - 37.6^o$$
$$P_9 = (0, \text{Sin}\phi_9, \text{Cos}\phi_9); \qquad \phi_9 = \psi_9 - 38.1^o$$
$$P_{10} = (0, \text{Cos}\phi_{10}, \text{Sin}\phi_{10}); \qquad \phi_{10} = \psi_{10} - 51.9^o$$

The angles ψ are between the respective carbon deuterium bond vectors and their double bond axis ($\psi_6 = 63.5^o$, $\psi_7 = 63.8^o$, $\psi_9 = 64.1^o$, and $\psi_{10} = 62.7^o$; see below) and the angles ϕ were calculated, as shown above and in Figure A2.1, using the bond angles determined for the 1,4-pentadiene segment of linoleic acid (Figure A1.1).

Each double bond was then allowed to adopt any orientation consistent with the specified average orientation of the C_8 methylene segment with respect to the bilayer normal (Chapter 5 and Appendix 4) by rotating each bond by an angle θ about either the

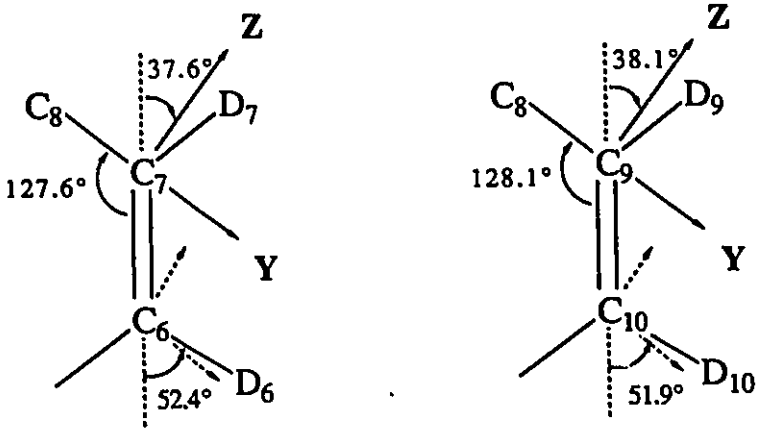

Figure A2.1. The X-Y-Z axis systems attached to the C_6-C_7 and the C_9-C_{10} double bonds. In both cases the Z axes are in the plane of the double bond and the X axes are projected straight out of the plane of the paper. The two Y axes are coincident with the C_7-C_8 and the C_8-C_9 carbon-carbon single bonds, respectively.

C_7-C_8 or the C_8-C_9 single bonds, respectively (this corresponds to a rotation about the Y axis in each coordinate system). All four deuteron coordinates were then referred to a newaxis system X'-Y'-Z' by rotating the old axis X-Y-Z counterclockwise about the X axis by an angle $\eta = 36.0^{o}$, in this new coordinate system the Z' axis is coincident with the bilayer normal (see Figure A3). Both rotations were accomplished using transformation matrices as shown below for the point P_9:

$$\begin{matrix} & & & & & & P_9 & & P'_9 \end{matrix}$$

$$\begin{pmatrix} 1 & 0 & 0 \\ 0 & \text{Cos}\eta & \text{Sin}\eta \\ 0 & -\text{Sin}\eta & \text{Cos}\eta \end{pmatrix} \begin{pmatrix} \text{Cos}\theta & 0 & -\text{Sin}\theta \\ 0 & 1 & 0 \\ \text{Sin}\theta & 0 & \text{Cos}\theta \end{pmatrix} \begin{pmatrix} 0 \\ \text{Sin}\phi_9 \\ \text{Cos}\phi_9 \end{pmatrix} = \begin{pmatrix} -\text{Sin}\theta\text{Cos}\phi_9 \\ \text{Cos}\eta\text{Sin}\phi_9 + \text{Sin}\eta\text{Cos}\theta\text{Cos}\phi_9 \\ -\text{Sin}\eta\text{Sin}\phi_9 + \text{Cos}\eta\text{Cos}\theta\text{Cos}\phi_9 \end{pmatrix}$$

In X'-Y'-Z', the Z component of each vector P'_x corresponds to the cosine of the angle between the respective C_x-^{2}H bond vector and the Z'-axis or bilayer normal (angle β, see equation 7, Chapter 2) and therefore the geometric factors for each deuteron can be obtained directly from the coordinate vectors. At 15 °C, the geometric factors must satisfy one of the following conditions (see Chapter 4):

For the C_6-C_7 double bond:

$$\frac{(3\text{Cos}^2\beta_6 - 1)}{(3\text{Cos}^2\beta_7 - 1)} = \pm 2$$

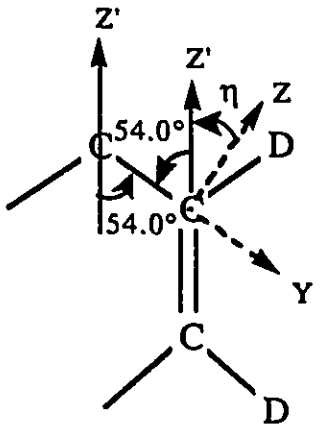

Figure A2.2. The two coordinate transformations performed to calculate the geometric factors for each double bond, given any orientation of each consistent with the specified orientation of the C_8 methylene segment. The angle $\eta = 90^o - 54^o = 36^o$.

and for the C_9-C_{10} double bond:

$$\frac{(3\text{Cos}^2\beta_9 - 1)}{(3\text{Cos}^2\beta_{10} - 1)} = \pm 1$$

For each double bond, substituting the two Z-components into the appropriate equation leads to an new equation that can be solved to yield all possible rotations θ (and thus all possible double bond orientations) consistent with the quadrupolar splitting ratios observed for the two deuterons of each alkene segment.

Several possible orientations for each double bond were determined at 15 °C (Tables A2.1 and A2.2), and for each solution, the C_8 methylene unit (and thus the double bond) can actually adopt two orientations. In one, the C-^{2}H bond vectors of the C_8 unit are oriented towards the aqueous interface, whereas in the other they are oriented towards the center of the bilayer normal. However, as discussed in Chapter 4, only one orientation of the C_8 methylene unit is likely, and for this orientation only one orientation of the C_9-C_{10} double bond is consistent with the parallel packing of the acyl chain (bold face in Table A2.2). Although there are two possible orientations for the C_6-C_7 double bond, both are similar with order parameters i the same range.

The same calculations were performed at both 25 °C and 40 °C and the results are tabulated in Tables A2.1 and A2.2. Due to the ambiguity in the assignment of the quadrupolar splittings recorded for [$^2H_2$-9',10']-PiLPC to the C_9 or the C_{10} deuteron, however, the number of possible solutions for the orientation of the C_9-C_{10} double bond actually increases. For example, at 40 °C the ratios of the splittings and thus the ratio of the geometric factors is one of the following:

Table A2.1

Orientation of the C_6-C_7 Double Bond

Temperature (°C)	Rotation Angle, θ,°	β_6,°	β_7,°	S_{mol}[1]	Maximum[1,2] Spectral Width
15	± 120	130	128	0.596	18
	± 113	130	123	0.757	15
25	± 120	131	128	0.559	20
	± 113	130	123	0.721	15
40	± 120	131	128	0.546	20
	± 113	130	123	0.708	16

[1] the absolute values of the data are listed.

[2] calculated for a value of $S_{mol} = 1.0$, see Appendix 3.

Table A2.2

Orientation of the C_9-C_{10} Double Bond

Temperature (°C)	Rotation Angle, θ,°	β_9,°	β_{10},°	S_{mol}[1]	Maximum[1,2] Spectral Width
15	± 25.3	65.1	115	0.152	62
	± 126	132	132	0.197	48
	± 111	121	130	0.333	28
25	± 39.0	71	116	0.105	89
	± 134	139	134	0.098	96
	± 109	119	129	0.232	41
40	± 59.3	82.5	119	0.075	125
	No comparable solution				
	± 104	115	128	0.155	61

[1] the absolute values of the data are listed.

[2] calculated for a value of $S_{mol} = 1.0$, see Appendix 3.

$$\frac{(3\text{Cos}^2\beta_9 - 1)}{(3\text{Cos}^2\beta_{10} - 1)} = \pm 3.31 \text{ or}$$

$$\frac{(3\text{Cos}^2\beta_9 - 1)}{(3\text{Cos}^2\beta_{10} - 1)} = \pm 1 / 3.31$$

The only solution for the orientation of the double bond that is consistent with its orientation at 15 °C (see Discussion Chapter 4) arises if the ratio of the splittings is 3.31. The larger of the two splittings above 15 °C was therefore assigned to the C_9 deuteron. Only the results from the calculations performed using this ratio are shown in Table A2.2.

Sensitivity of the Calculations to the Angle ψ. In the calculations performed above, the angles ψ for each deuteron were calculated assuming that each carbon-deuterium bond vector (C_x-^{2}H) bisects the C_{x-1}-C_xC_{x+1} alkenyl bond angle. This assumption is based solely upon geometrical arguments and to determine the effect of this assumption and hence the accuracy of the results, the calculations were performed varying the angles ψ_x over the range of 60 to 66°. The effect of the angular variations on the proposed orientation of each double bond at 15 °C are shown in Tables A2.3 and A2.4 and, in general, the variations in the results are relatively small.

Sensitivity of the Calculations to the Double Bond Torsion Angles. The crystal structure also indicates that the two double bonds of linoleic acid are not planar and exhibit torsion angles of 2.3° and 3.3° for the C_8-C_9-C_{10}-C_{11} and the C_{11}-C_{12}-C_{13}-C_{14} bonds. The effects of such torsion angles upon the calculations presented above were also examined as shown for the chosen orientation of the C_9-C_{10} double bond at 15 °C. The general approach was identical to that presented above, except that the coordinates of

Table A2.3

Orientation of the C_6-C_7 Double Bond at 15°C:
Sensitivity to Variations in the Angles ψ_6 and ψ_7

C-^{2}H Bond Angles, ψ,°	Rotation Angle, θ,°	S_{mol}[1]	Maximum[1,2] Spectral Width
60	±121	0.762	14
	±116	0.892	12
62	±120	0.650	17
	±114	0.796	14
64	±120	0.577	19
	±113	0.741	15
66	±119	0.527	39
	±112	0.713	15

[1] the absolute values of the data are listed.

[2] calculated for a value of S_{mol} = 1.0, see Appendix 3.

the C_{10} deuteron in the X-Y-Z coordinate system had to be calculated allowing for the torsion angle of 3.3°. The coordinates for P_{10} in X-Y-Z are:

$$\begin{pmatrix} -\mathrm{Sin}\alpha\mathrm{Sin}\phi_{10} \\ \mathrm{Cos}\beta\mathrm{Cos}\alpha\mathrm{Sin}\phi_{10} + \mathrm{Sin}\beta\mathrm{Cos}\phi_{10} \\ \mathrm{Sin}\beta\mathrm{Cos}\alpha\mathrm{Sin}\phi_{10} - \mathrm{Cos}\beta\mathrm{Cos}\phi_{10} \end{pmatrix}$$

where the angles $\alpha = \pm 3.3^{o}$ (the torsion angle) and $\beta = 38.1^{o}$ (a coordinate transformation). The results from the calculations are shown in Table A2.5 and Figure A2.3.

Table A2.4

Orientation of the C_9-C_{10} Double Bond at 15°C:
Sensitivity to Variations in the Angles ψ_9 and ψ_{10}

C-^{2}H Bond Angles, ψ	Rotation Angle, θ	S_{mol}[1]	Maximum[1,2] Spectral Width
60	± 22.1	0.224	42
	± 125	0.280	34
	± 114	0.391	24
62	± 22.1	0.179	53
	± 125	0.280	34
	± 112	0.360	26
64	± 22.1	0.145	63
	± 125	0.203	46
	± 111	0.343	27
66	± 22.1	0.130	72
	± 125	0.180	52
	± 109	0.338	28

[1] the absolute values of the data are listed.

[2] calculated for a value of $S_{mol} = 1.0$, see Appendix 3.

Figure A2.3.

A schematic representation of the effect of the torsion angle on the calculated orientation of the C_9-C_{10} double bond. The diagram represents the solutions arising from a torsion angle of +3.3°, which gives a rotation angle θ of 22.7 about the C_8-C_9 bond, and a torsion angle of -3.3°, which gives a rotation angle θ of 27.5°.

Table A2.5.

Effect of the torsion angle on the calculated orientation of the C_9-C_{10} double bond.

Figure A2.3

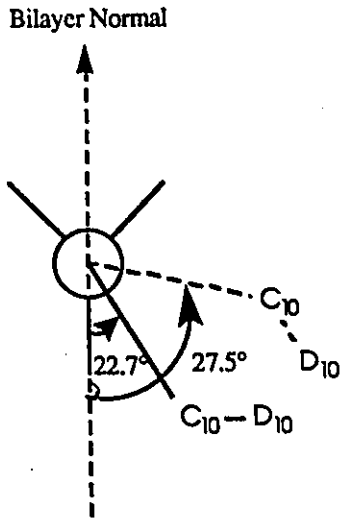

Table A2.5

Torsion Angle,°	Rotation Angle, θ,°	S_{mol}	Maximum Spectral Width (Hz)
+ 3.3	+ 22.7	0.164	57
	- 27.5	0.140	67
- 3.3	- 22.7	0.164	57
	+ 27.5	0.140	67

Appendix 3

Orientations of the Isolinoleoyl Chain in the Gel Phase

The maximum spectral widths for several deuteriated segments of the isolinoleoyl chain that would occur if the chain adopts the same conformation in both the gel phase and the liquid crystalline phase at 15 °C are tabulated in Tables A2.1 and A2.2 of Appendix 2. They were calculated directly from the geometric factors (the angles β are tabulated in Tables A2.1 and A2.2) using equation 6 and 7, of Chapter 2, with S_{mol} equal to 1.0 (see also Tables A2.3 and A2.4 for the sensitivity of the calculations to the angles ψ). The spectral widths for several deuteriated segments in the gel phase given either an angle iron/helical conformation or a structure consistent with the crystal structure of linoleic acid were calculated by determining the geometric factors for each C-^{2}H bond vector and then substituting these values into equations 6 and 7 (the calculations neglect the effects of line broadening due to dipolar interactions, etc.).

Angle Iron Conformation

C_7 Deuteron. For the angle iron/helical conformation, the bilayer normal is essentially coincident with both double bond axes. As a starting point it was assumed that

the bilayer normal is coincident with the C_6-C_7 bond axis and for the C_7 deuteron the geometric factor can therefore be calculated directly from the angle between the C-^{2}H bond vector and the double bond axis. Using the angles ψ described in Appendix 2, the maximum spectral widths were calculated and tabulated as shown in Table A6

C_8 Methylene Deuterons. A right-handed coordinate system X-Y-Z was attached to the C_7-C_8 single bond as shown in Figure A3.1 and a given orientation of the C-^{2}H bond vector specified in this figure. Its coordinates are:

$$P_{D8} = (0, \text{Cos}70.6, \text{Sin}70.6)$$

There are in fact two C_8 deuterons. The coordinates of each in X-Y-Z given the C_6-C_7-C_8-C_9 torsion angle, were calculated by rotating the C-^{2}H vector by an angle of 2.7°, for D_{8a} and by -117.3° for D_{8b}. The new coordinates were then referred to an axis system X'-Y'-Z', in which the Z' axis is coincident with the bilayer normal, by rotating the X-Y-Z axis system about the X axis by an angle of 37.6°. Both rotations were accomplished using transformation matrices as shown below for P_{D8a}:

$$\begin{pmatrix} 1 & 0 & 0 \\ 0 & \text{Cos}37.6 & \text{Sin}37.6 \\ 0 & -\text{Sin}37.6 & \text{Cos}37.6 \end{pmatrix} \begin{pmatrix} \text{Cos}2.7 & 0 & \text{Sin}2.7 \\ 0 & 1 & 0 \\ -\text{Sin}2.7 & 0 & \text{Cos}2.7 \end{pmatrix} \begin{pmatrix} 0 \\ \text{Cos}70.6 \\ \text{Sin}70.6 \end{pmatrix} =$$

P_{D8a} $\qquad$ P'_{D8a}

$$\begin{pmatrix} \text{Sin}2.7\text{Sin}70.6 \\ \text{Cos}37.6\text{Cos}70.6 + \text{Sin}37.6\text{Cos}2.7\text{Cos}70.6 \\ -\text{Sin}37.6\text{Cos}70.6 + \text{Cos}\ 37.6\text{Cos}2.7\text{Sin}70.6 \end{pmatrix}$$

Figure A3.1

The right-handed coordinate system attached to the C_7-C_8 single bond. The X-axis is projected out of the plane of the paper.

Figure A3.2

The right-handed coordinate system attached to the C_9-C_{10} single bond. The Z-axis is projected out of the plane of the paper

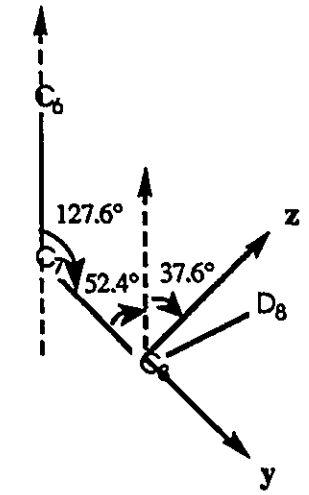
C6
127.6°
C7
52.4°
37.6°
z
D8
C8
y

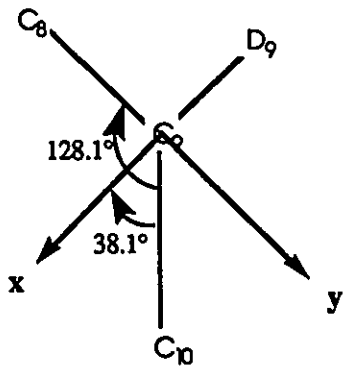
C8
D9
128.1°
C9
38.1°
x
y
C10

Table A3.1

Maximum spectral widths for the deuteriated segments of the isolinoleoyl chain calculated assuming an angle iron/helical conformation.

Segment	Angle ψ	Maximum Spectrai Width (kHz)
C_6-C_7	60	33
	62	45
	64	56
	66	66
	63.5 ($^2H_6$), 63.8 ($^2H_7$)	55
C_8	NA	15
C_9-C_{10}	60	42
	62	53
	64	64
	66	74
	62.7 ($^2H_9$), 64.05 ($^2H_{10}$)	64

The Z component of each vector P'_{D8} is the cosine of the angle between the respective C-^{2}H bond and the bilayer normal. The two Z components were therefore substituted into equations 6 and 7 of Chapter 2 to calculate the spectral widths (Table A3.1).

C_9-C_{10} Double Bond. A right handed cartesian coordinate system was attached to the C_8-C_9 single bond as shown in Figure A3.2 and the coordinates of the C_9 and C_{10} deuterons in this axis system were defined as follows:$P_{D9} = (Cos\phi_9, Sin\phi_9, 0)$

$$P_{D10} = (Cos\phi_{10}, Sin\phi_{10}, 0)$$

Each of the deuteron coordinates was then submitted to four coordinate transformations as defined below:

1) Rotate each point counter clockwise about the Y axis by an angle of $\alpha = 123.5^o$ to account for the C_7-C_8-C_9-C_{10} torsion angle.

2) Rotate the X-Y-Z axis system by an angle of $\beta = 72^o$ about the Z axis to create the new axis system X'-Y'-Z' in which the Y' axis is coincident with the C_7-C_8 single bond.

3) Rotate the X'-Y'-Z' axis system clockwise about the Y' axis by an angle of $\gamma = 122.7^o - 90^o = 32.7^o$ to create the axis system X"-Y"-Z" bring the Z" axis is in the C_6-C_7-C_8 plane, and finally

4) Rotate the X"-Y"-Z" axis system counterclockwise about the X" axis by an angle of $\delta = 37.6^o$ to bring the Z" axis coincident with the bilayer normal.

The tranformations were performed using transformation matrices as shown below for the point P_{D9}:

$$\begin{pmatrix} 1 & 0 & 0 \\ 0 & \text{Cos}\delta & \text{Sin}\delta \\ 0 & -\text{Sin}\delta & \text{Cos}\delta \end{pmatrix} \begin{pmatrix} \text{Cos}\gamma & 0 & \text{Sin}\gamma \\ 0 & 1 & 0 \\ -\text{Sin}\gamma & 0 & \text{Cos}\gamma \end{pmatrix} \begin{pmatrix} \text{Cos}\beta & \text{Sin}\beta & 0 \\ -\text{Sin}\beta & \text{Cos}\beta & 0 \\ 0 & 0 & 1 \end{pmatrix} \begin{pmatrix} \text{Cos}\alpha & 0 & \text{Sin}\alpha \\ 0 & 1 & 0 \\ -\text{Sin}\alpha & 0 & \text{Cos}\alpha \end{pmatrix} \begin{pmatrix} \text{Cos}\phi_9 \\ \text{Sin}\phi_9 \\ 0 \end{pmatrix} = P_{D9}$$

$$P'_{D9}$$

$$\begin{pmatrix} \text{Cos}\gamma\text{Cos}\beta\text{Cos}\alpha\text{Cos}\phi_9 + \text{Cos}\gamma\text{Sin}\beta\text{Sin}\phi_9 - \text{Sin}\gamma\text{Sin}\alpha\text{Cos}\phi_9 \\ \text{Sin}\beta\text{Cos}\alpha\text{Cos}\phi_9 + \text{Cos}\beta\text{Sin}\phi_9 \\ -\text{Sin}\gamma\text{Cos}\beta\text{Cos}\alpha\text{Cos}\phi_9 - \text{Sin}\gamma\text{Sin}\beta\text{Sin}\phi_9 - \text{Cos}\gamma\text{Sin}\beta\text{Sin}\phi_9 \end{pmatrix}$$

and the Z component of the vectors was then used with equation 7, Chapter 2 to determine the spectral width, with $S_{mol} = 1.0$ (Table A3.1).

Linoleic Acid Crystal Structure

The coordinates of all the deuterons of interest, with respect to an axis system X'-Y'-Z' in which the Z' axis is coincident with the bilayer normal, were calculated for the "angle iron/helical" conformation. The coordinate system X'-Y'-Z' was then transformed into a new coordinate system in order to orient the 1,4-pentadiene segment of the chain at an angle with respect to the bilayer normal that is consistent with the linoleic acid crystal structure. This was accomplished by performing three coordinate transformations:

1) Rotate the axis system clockwise about the X' axis by an angle of 37° to create the new axis system X"-Y"-Z".

2) Rotate all points counterclockwise about the Y" axis by 60.6° to account for the C_4-C_5-C_6C_7 torsion angle.

3) Rotate the axis system counterclockwise about the X" axis by 54.7° to bring the Z" axis coincident with the bilayer normal.

The geometric factors were then calculated for each C-^{2}H bond from the Z components of each coordinate vector and the maximum splittings determined (assuming $S_{mol} = 1.0$) as was done above. The results are tabulated in Table A3.2

Table A3.2

Maximum spectral widths for the deuteriated segments of the isolinoleoyl chain calculated assuming a conformation consistent with the crystal structure of linoleic acid.

Segment	Angle ψ,°	Maximum Spectral Width (kHz)
C_6-C_7	60	106
	62	97
	64	89
	66	80
	63.5 ($^2H_6$), 63.8 ($^2H_7$)	**90**
C_8	NA	103
C_9-C_{10}	60	158
	62	145
	64	132
	66	119
	62.7 ($^2H_9$), 64.05 ($^2H_{10}$)	**132**

Appendix 4

Calculation of the Orientation and Order Matrix for the C_8 Methylene Segment in the Liquid Crystalline Phase

Following the approach of Seelig (1977) and Seelig & Waespe-Šarčevič (1978), a right handed cartesian coordinate system was attached to the C_8 methylene segment as shown in Figure A4.1. The two irreducible tensor componenets, $V^{(2,0)}$, of the electric field gradient tensor (one for each deuteron) were then defined in X-Y-Z by performing a series of molecular transformations from the principal axis system (the C-^{2}H bond vector) into X-Y-Z. Substitution of the resulting $V^{(2,0)}$ terms into equation 2.5, Chapter 2, leads to the following expression for the S_{CD} bond order parameters:

$$S_{CD} = \left(\frac{3\mathrm{Cos}^2\beta - 1}{2}\right)\left(\frac{3\mathrm{Cos}^2\beta' - 1}{2}\right) \pm 3/4\ \mathrm{Sin}2\beta\ \mathrm{Sin}2\beta'\ \mathrm{Cos}\alpha' + 3/4\mathrm{Sin}^2\beta\mathrm{Sin}^2\beta'\mathrm{Cos}\alpha' \qquad (11)$$

where the angle $\beta = 54.7^o$ (see Figure A7), and β' and α' are the Euler angles θ and ϕ, respectively. This expression can be simplified to give the following:

$$S_{CD} = \left(\frac{3\mathrm{Cos}^2\beta - 1}{2}\right) S_{33} \pm \mathrm{Sin}2\beta\ S_{13} + 1/2\ \mathrm{Sin}^2\beta\ (2S_{11} - S_{33}) \qquad (12)$$

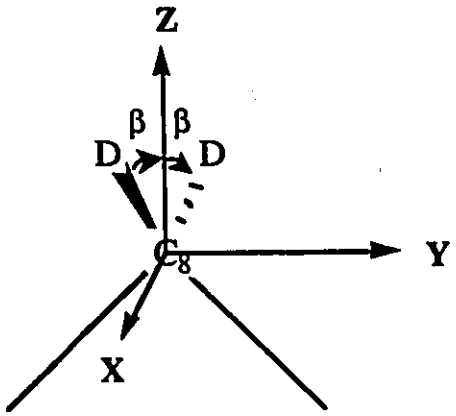

Figure A.4.1. The cartesian coordinate system attached to the C_8 methylene segment in Appendix 4.

where the terms S_{11}, S_{22}, and S_{33} are order parameters describing the fluctuations of the three segment-fixed axes X, Y, Z, respectively. The following can be defined directly from the deuterium spectra in Figure 5.8:

$$S_{CD}\,(a) = 0.0103$$
$$S_{CD}\,(b) = 0.0075 \qquad S_{DD} = -0.0618,$$

where S_{DD} describes the fluctuations of the X axis and therefore can be referred to as S_{11}

Substituting these values into equation 12 leads to definition of the complete ordering tensor for the C_8 segment:

$$S = \begin{pmatrix} -0.062 & & 0.002 \\ & -0.089 & \\ 0.002 & & 0.150 \end{pmatrix}$$

which can be diagonalized by rotations about the angles α and β to give the following:

$$S^* = \begin{pmatrix} -0.089 & & \\ & -0.062 & \\ & & 0.150 \end{pmatrix}$$

The calculated orientation of the C_8 methylene unit at 40 °C is shown in Figure 5.10 of Chapter 5 and arises by a rotation of $\beta = \pm 0.4^o$ about the Y axis followed by a rotation of $\alpha = \pm 90^o$ about the Z axis. The parameter S_{mol} quoted in the text refers to the order parameter, S_{33} (in this case $S_{33} = 0.150$).